Development and Application of Rhodium(III)-Catalysed C-H Activation Methodologies

Nicola Jayne Webb

Submitted in accordance with the requirements for the degree of
Doctor of Philosophy

The University of Leeds
School of Chemistry

December 2014

The candidate confirms that the work submitted is his/her own, except where work which has formed part of or jointly-authored publications has been included. The contribution of the candidate and the other authors to this work has been explicitly indicated below. The candidate confirms that appropriate credit has been given within the thesis where reference has been made to the work of others.

References for the jointly authored papers include:

N. J. Webb, S. P. Marsden and S. A. Raw, 'Rhodium(III)-Catalyzed C–H Activation/ Annulation with Vinyl Esters as an Acetylene Equivalent', *Org. Lett.* 2014, **16**, 4718-4721.

The experimental work, supporting information and initial draft of the manuscript were completed by the candidate. Stephen Marsden and Steven Raw supervised the research. Stephen Marsden prepared the final version of the manuscript for publication.

This copy has been supplied on the understanding that it is copyright material and that no quotation from the thesis may be published without proper acknowledgement.

The right of Nicola Jayne Webb to be identified as Author of this work has been asserted by her in accordance with the Copyright, Designs and Patents Act 1988.

©2014 The University of Leeds and Nicola Jayne Webb

Acknowledgements

First and foremost, I would like to thank Steve for his invaluable guidance and support with all aspects of this project. I am extremely grateful for the training I have received over the past three and a half years. Additionally, I'd like to say thanks for the numerous treats the group has received, including evenings out and foreign goodies (although I think we could have done without those durian fruit biscuits). I must also thank my industrial supervisor, Steve Raw, for his enthusiasm and ideas during our meetings, many of which went on to be realised in the laboratory.

I'd like to thank the technical staff at Leeds, particularly the crystallographers Chris Pask, Jonny Loughrey and my personal crystallographic consultant, James for help with the collection and elucidation of my X-ray crystal structures. I would like to thank Carlo Sambiagio and Mike Chapman for their help with the cyclic voltammetry studies. I must also thank all the MChems and summer students, Mike, Brit, Reuven and Alex for all of their hard work.

For funding, I would like to thank AstraZeneca and the EPSRC.

Now to thank the rabble who have made the last three years so enjoyable. Massive thanks go to: Dan 'woodlouse to winner', I'm so sad that I will miss your Shawshank moment on your viva day. I want to thank the infectiously happy running squad, Seb and Tony; fantastiche Sebo must be thanked for his never-ending supply of entertainment and for accepting me as a token northerner. On we go to the mad French man, who has meticulously proof read so much of this thesis. I want to thank MD for introducing me to the watermelon catapult and for our mutual love of Apple products – I will miss putting my headphones on to ignore you. Now to the chocolate-addicted, vegetable-fearing Martarn, thank you for being there to witness the four o'clock meltdowns and for generally occupying the party spot. Thank you to the original crew, John 'Flaming' Li, David, James, Mary and Roberta for our wonderful tea break discussions and the cheese and wine nights, and to the new team Marsden members for making these three years so fantastic. You will all be missed.

Thank you to my family for their never-ending support, despite not having a clue what I do or wondering if I will ever leave University and get a 'real job'. Finally, and most importantly, thank you to my best friend and husband-to-be, James. Without his support and encouragement I'm sure I would be completely lost. I'm looking forward to our USA adventure. This thesis is dedicated to you.

Abstract

In recent years, rhodium(III)-catalysed C-H activation methodologies have come to the fore and proved to be an invaluable and powerful synthetic tool for the preparation of heterocycles. C-H activation using rhodium(III)-catalysed processes with internal oxidants has considerably improved the accessibility of these scaffolds. Furthermore, the alkynes and alkenes used to intercept the arylmetal species in the aforementioned systems have been either electronically neutral or electron-deficient.

Chapter 1 outlines the investigation of electron-rich substrates, using vinyl esters as acetylene synthons and vinyl ethers as acetaldehyde enolate/acyl anion equivalents. From this study, a competing rhodium-catalysed Lossen rearrangement was identified and the regiochemical preference of vinyl ether substrates was determined. The preliminary screening identified the formation of a 3,4-unsubstituted isoquinolone from the reaction of vinyl acetate with the acyl hydroxamates.

As a result, the synthesis of 3,4-unsubstituted isoquinolones, using vinyl acetate, a cheap bulk chemical, as an acetylene equivalent was explored. The procedure works well for a range of substituted *N*-(pivaloyloxy)benzamide derivatives; in total, 17 examplar 3,4-unsubstituted isoquinolones were prepared with an average yield of 75%. Heterocyclic pivaloyl hydroxamates were also tolerated in the reaction. These conditions offer distinct advantages over traditional methods. The utility of the procedure was demonstrated in the synthesis of two intermediates towards hepatitis C virus inhibitors. The ensuing chapter describes the optimization of this methodology using aryl ketoximes for the synthesis of 3,4-unsubstituted isoquinolines.

To conclude, the final chapter describes the isolation and attempted optimisation of a highly fluorescent tetracyclic imide. Mechanistic studies used to determine the formation of the imide identified putative intermediates, however the synthetic procedure could not be optimised further. Using a novel strategy, *via* a key C-H activation/annulation reaction of a range of bespoke alkynes and *N*-(pivaloyloxy)benzamides, a library of nine imides was prepared.

Contents

Abbreviations

α	*alpha*
Å	angstrom
β	*beta*
γ	*gamma*
Δ	heat
δ	chemical shift
ε	molar absorption coefficient
Φ_F	fluorescence quantum yield
λ	wavelength
λ_{abs}	wavelength at absorption maxima
λ_{emis}	wavelength at emission maxima
A	ampere
A	absorbance
Ac	acetyl
atm	atmospheres
Bn	benzyl
Boc	*tert*-butyloxycarbonyl
BocValOH	(*S*)-2-(Boc-amino)-3-methylbutyric acid
BQ	1,4-benzoquinone
^{t}Bu	*tert*-butyl
Bz	benzoyl
c	concentration
Cbz	carboxybenzyl
CDI	1,1'-carbonyldiimidazole
CMD	concerted metallation-deprotonation
cod	1,5-cyclooctadiene
COSY	correlated spectroscopy
Cp	cyclopentadienyl
Cp^t	di-*tert*-butylcyclopentadienyl
Cp*	pentamethylcyclopentadienyl
Cy	cyclohexyl
dba	*trans,trans*-dibenzylideneacetone
DCE	1,2-dichloroethane
DCM	dichloromethane

DEPT	distortionless enhancement by polarisation transfer
DFT	density functional theory
DG	directing group
DIAD	diisopropyl azodicarboxylate
DKIE	deuterium kinetic isotope effect
DMF	*N*,*N*-dimethylformamide
DMA	*N*,*N*-dimethylacetamide
DMAP	*N*,*N*-dimethylaminopyridine
DMP	Dess-Martin periodinane
DMPU	1,3-dimethyltetrahydropyrimidin-2(*1H*)-one
DMSO	dimethylsulfoxide
DPPA	diphenylphosphoryl azide
dppf	1,1'- bis(diphenylphosphino)ferrocene
E	entgegen
EDG	electron-donating group
Et	ethyl
er	enantiomeric ratio
E_{pA}	potential of the anodic peak current
E_{pC}	potential of the cathodic peak current
eq.	equivalent
ESI	electrospray ionisation
EWG	electron-withdrawing group
Fc	ferrocene
Fmoc	fluorenylmethyloxycarbonyl
h	hour
het	heterocycle
hex	*n*-hexyl
HPLC	high-performance liquid chromatography
HRMS	high-resolution mass spectrometry
i_{pA}	anodic peak current
i_{pC}	cathodic peak current
K	Kelvin
KHMDS	potassium *bis*(trimethylsilyl)amide
l	path length
LA	Lewis-acid
LCMS	Liquid chromatography-mass spectrometry
M	molar
Me	methyl

MIDA	*N*-methyliminodiacetic acid
MOM	methoxymethyl ether
MOPS	3-(*N*-morpholino)propanesulfonic acid
NMP	1-methyl-2-pyrrolidinone
NMR	nuclear magnetic resonance
NOESY	nuclear Overhauser effect spectroscopy
o-	*ortho*-
[O]	oxidation
oLED	organic light emitting diodes
PCC	pyridinium chlorochromate
Ph	phenyl
PhMe	toluene
Piv	pivaloyl
pka	acid dissociation constant
ppm	parts per million
Pr	propyl
R	molar gas constant
R_F	retention factor
rt	room temperature
sec	secondary
SCE	saturated calomel electrode
S_EAr	electrophilic aromatic substitution
S_N2	bimolecular nucleophilic substitution
S_NAr	nucleophilic aromatic substitution
SPhos	2-dicyclohexylphosphino-2′,6′-dimethoxybiphenyl
T	temperature
TBAF	tetrabutylammonium fluoride
TBS	*tert*-butyldimethylsilyl
tert	tertiary
Tf	trifluoromethanesulfonyl
TFE	2,2,2-trifluoroethanol
THF	tetrahydrofuran
TLC	thin layer chromatography
TMB	trimethoxybenzene
TMEDA	*N,N,N',N'*-tetramethylethylenediamine
TMS	trimethylsilyl
TON	turn over number
TPAP	tetrapropylammonium perruthenate

Ts	tosyl
UV	ultraviolet
V	voltage
Vis	visable
wt	weight
Z	zusammen

Chapter 1

Introduction

1.1 C-H Activation

Transition metal-catalysed cross-coupling methodologies represent one of the most powerful classes of chemical reactions in organic chemistry. Recognised by the scientific community as a highly versatile tool in synthetic disconnections, Heck, Negishi and Suzuki were awarded the Nobel prize for their contribution to the field for the development of palladium-catalysed cross-coupling reactions.[1–7] As the field has matured, new disconnections and novel catalysts have been identified for a variety of systems. Despite these well-established and robust protocols, the influence of economic and environmental factors has intensified the search for atom-efficient and environmentally green protocols. The advent of novel C-H activation methodologies, whereby the typically inert and ubiquitous C-H bond can be utilised instead of either an organometallic coupling partner or an aryl halide, has identified a powerful alternative. This emerging field is constantly evolving to encompass new areas that include heterocyclic synthesis, chiral C-H activation, *sp*, sp^2 and sp^3 hybridised systems, double C-H activation (C-H to C-H coupling) and many more. The aim of this introduction is to outline the origin of C-H activation in reference to the oxidative Heck reaction, to highlight examples of heterocyclic synthesis based on rhodium catalysis and finally, to discuss the recent developments of redox-neutral systems.

1.2 The oxidative Heck reaction

In 1967, Fujiwara and Moritani discovered the oxidative Heck reaction from the coupling of styrene **4** with benzene **3** in acetic acid using a styrene-palladium chloride complex **2**[8] to give *trans*-stilbene **1** (Scheme 1.1).[9] This was the first reaction of its kind that utilised a C-H bond in a cross-coupling reaction with an alkene. The reaction highlighted the potential to streamline target-orientated synthesis by obviating the requirement to prefunctionalise starting materials. In order to reduce the stoichiometric palladium loading, investigation of suitable co-oxidants were undertaken. Fujiwara and Moritani found that addition of copper(II) acetate or silver(I) acetate under an oxygenated atmosphere would allow the reaction of styrene **4** and benzene **3** to proceed catalytically with respect to both palladium and copper/silver (Scheme 1.1).[10]

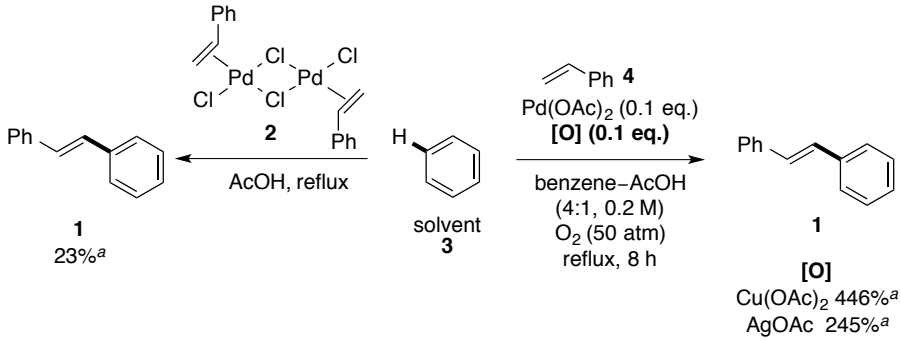

Scheme 1.1. [a]*Yields with respect to the palladium catalyst.*

Shue published a communication on the coupling of benzene **3** and styrene **4** using oxygen as the sole oxidant, which effectively reduced the catalyst loading to one mol% (Scheme 1.2).[11] Following optimisation studies on a number of oxidation systems, Fujiwara *et al*. identified *tert*-butyl peroxide with benzoquinone as the ideal system (Scheme 1.2).[12] The reaction of benzene **3** with various cinnamates **5** proceeded to give good yields of the unsaturated products **6** and **7**. The increase in the catalytic turnover number was attributed to the dual role of benzoquinone as an oxidant to regenerate palladium(II) from palladium(0) and to prevent palladium(0) nanoparticle aggregates forming in the reaction by coordination.[13]

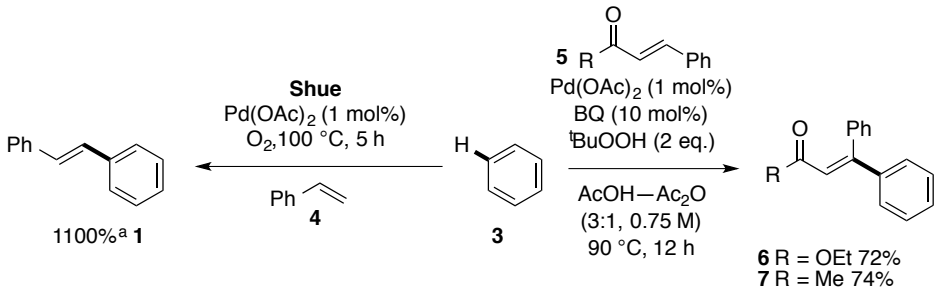

Scheme 1.2. [a]*Yield with respect to the palladium catalyst.*

1.3 Catalytic cycles

The classic Heck reaction proceeds *via* the coupling of an aryl/vinyl halide with an alkene to furnish an alkenylated aromatic. The catalytic cycle proceeds by the oxidative insertion of a palladium(0) species **I** into the aryl/vinyl halide (or pseudohalide) C-X bond to give a palladium(II) salt **II**. Coordination of the alkene substrate **III** followed by *syn*-addition results in the alkylated palladium complex **IV**. Subsequent *syn*-*β*-hydride elimination releases the coupled alkene (typically the *trans*-alkene is favoured) and the palladium(II) salt **V**, which can undergo reductive elimination to regenerate the active palladium(0) catalyst **I** (Pathway A, Scheme 1.3).

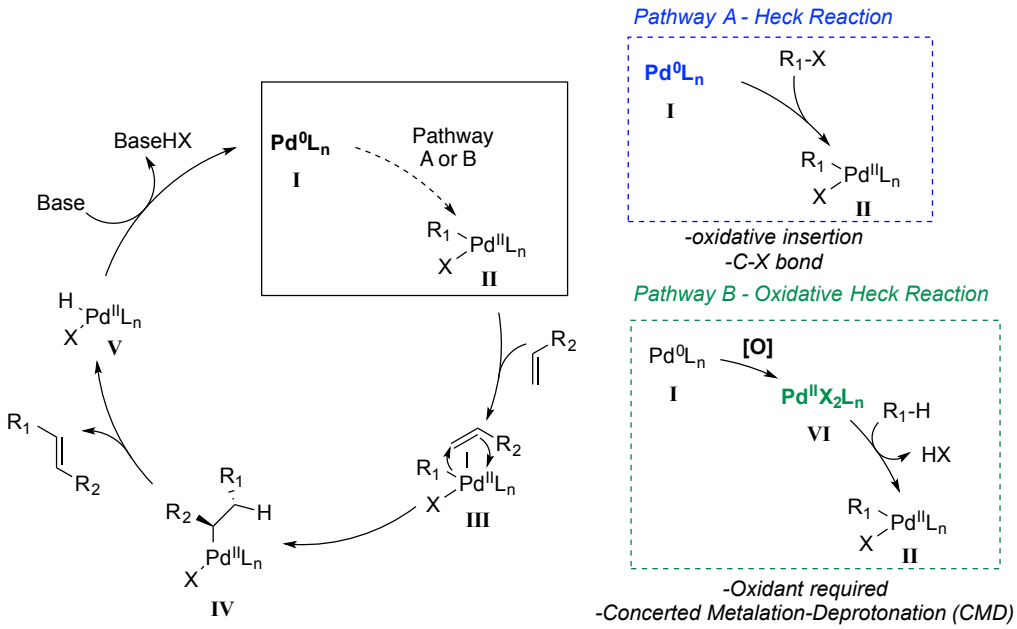

Scheme 1.3

The oxidative Heck reaction follows the same reaction pathway with two exceptions. The active palladium(II) catalyst **VI** oxidatively inserts into the C-H bond *via* a base-promoted concerted metallation-deprotonation (CMD) pathway, using one of the σ-donor ligands, to generate the intermediate **II**.[14] At this stage the cycle mimics the catalytic cycle of the Heck reaction until the palladium(0) species **I** forms. In order to complete the catalytic cycle an oxidant is required to reoxidise the palladium(0) **I** to palladium(II) **VI** (Pathway B, Scheme 1.3).

The key challenge in the design of an oxidative Heck system lies in selecting a single C-H bond and identifying an oxidant that is suitable to use in conjunction with the substrates and metal-catalyst. The metal catalyst can be influenced to insert into a specific C-H bond by means of a directing group, i.e. one that is capable of coordinating to the metal. This interaction guides the catalyst into the proximity of the desired C-H bond, ensuring that this position is kinetically favoured. This interaction can be used to achieve excellent regioselectivity in reactions. In comparison to the broad range of directing groups available, the oxidant selection is somewhat limited, with optimised systems having been identified for palladium, rhodium and ruthenium catalysts.

1.4 Rhodium-mediated oxidative Heck reactions

Over the past decade there have been numerous reports of rhodium(III)-mediated oxidative Heck reactions with particular emphasis on one precatalyst, pentamethylcyclopentadienylrhodium(III) chloride dimer ($[Cp^*RhCl_2]_2$). Associated benefits over the existing palladium catalysts included lower catalyst loadings, higher selectivity for the mono-olefinated *versus* the bis-olefinated products and broader alkene scope. Glorius *et al*. have used this catalyst to couple acetanilide derivatives **8** to a number of electron-rich and poor styrene derivatives, resulting in a variety of *trans*-stilbene type products.[15] A comparison of the rhodium and the palladium-catalysed coupling of 3-methylacetanilide **8a** to *n*-butyl acrylate reveals an increase in the yield of the stilbene derivative **9** to 98% from the 91% previously reported by de Vries using their optimised palladium system (Scheme 1.4).[16] The rhodium complex $[Cp^*RhCl_2]_2$ was used sparingly (0.5 mol%) with two equivalents of copper(II) acetate oxidant and silver hexafluoroantimonate ($AgSbF_6$, 2 mol%) as a chloride ion scavenger. Under these reaction conditions a range of alkenes were coupled to substituted acetanilides **8** to afford excellent yields of the *ortho*-alkenylated products **9-13** (48-98%).

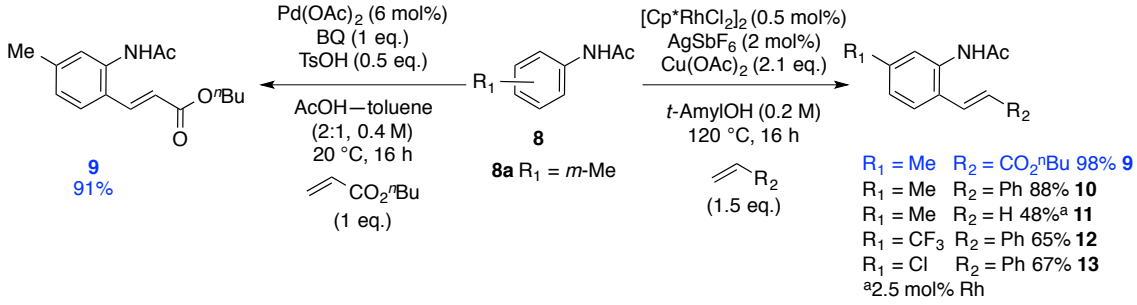

Scheme 1.4

Lower yields were observed when sterically encumbered olefins were chosen. Halide functional groups were tolerated, both in the acetanilide and the styrene substrates; proto-debromination products or Heck products (from the reaction of the aryl halide) were not detected in the reactions. This can often be an issue when using palladium catalysts. Under a mild pressure (2 bar), ethylene was coupled to **8a** to give the styrene derivative **11** (48% yield), although a higher catalyst loading was required (2.5 mol%). The preparation of styrenes *via* the palladium(II)-catalysed oxidative Heck reaction had previously been acknowledged to be challenging, poorly selective and only feasible under harsh conditions.[10,17,18]

1.5 Heterocycle formation using C-H activation with alkynes

The rhodium-catalysed oxidative Heck reaction has been thoroughly exemplified with a range of directing groups, including ureas, carbamates, ketones and amides, to prepare unsaturated products from a range of alkenes.[19] Using similar conditions, C-H annulation protocols were developed for the synthesis of heterocyclic scaffolds, using internal alkynes. For example, Glorius *et al.* utilised primary benzamides **15** to direct the insertion of styrene derivatives to afford a range of *trans*-stilbene products **17** (Scheme 1.5).[20] Using similar conditions, Rovis *et al.* prepared 12 exemplar isoquinolones **14** from the C-H activation/annulation of secondary benzamides **16** with diphenyl acetylene (Scheme 1.5).[21]

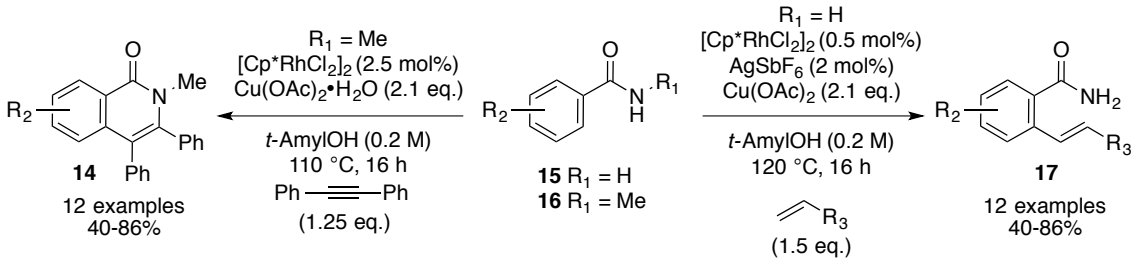

Scheme 1.5

Fagnou[22] *et al.* reported the synthesis of acetyl-protected indoles **19** from acetanilide **8** and a range of unsymmetrical internal alkynes. Excellent regioselectivity was observed for installation of the aromatic at the 2-position, for example with 1-phenyl-1-propyne **18** (Scheme 1.6). Electron-donating and withdrawing groups were tolerated on the acetanilide **8**, with the corresponding indoles **19** isolated in high yields.

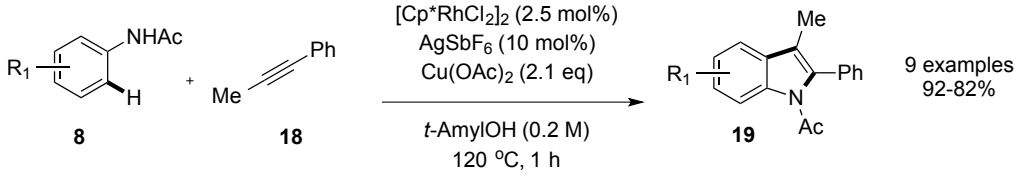

Scheme 1.6

Glorius[23] *et al.* were able to prepare penta- and tetra-substituted pyrroles, **20** and **22**, from enamine derivatives **21** (Scheme 1.7). Interestingly, the nature of the proximal directing group was observed to influence product formation. Substituting the ester for the nitrile resulted in α-functionalisation of the enamine, opposed to the γ-selectivity observed with the ester. Further investigation identified the ester as a crucial factor to achieve allylic sp^3 C-H bond activation.

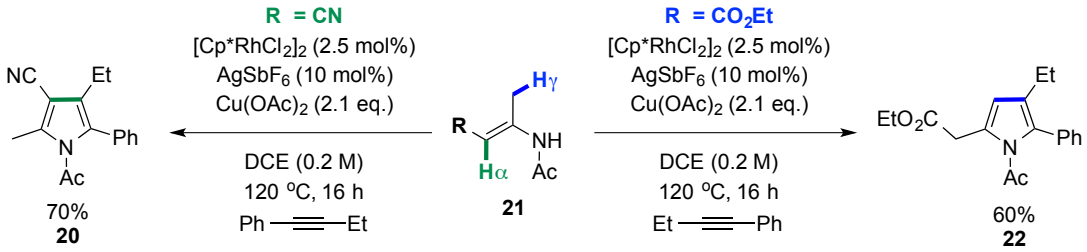

Scheme 1.7

Fagnou[24] and Miura[25] have each published similar work on the oxidative coupling of aryl aldimines **23** and ketimines **26** with symmetrical and unsymmetrical alkynes furnishing isoquinolines **24** and **27** (Scheme 1.8). The reaction of *N*-*tert*-butylbenzaldimine derviatives **23** resulted in the loss of isobutylene *via* the isoquinolinium salt **25** formed post-cyclisation. Li *et al*. expanded the scope to include *N*-substituted benzamidines **28** and alkynes, leading to 1-(alkylamino)- and 1-(arylamino)-isoquinolines **29** with yields ranging from 38-97%. These C-H activation protocols provide an attractive route for the synthesis of substituted isoquinolines, a ubiquitous motif found in natural products and pharmaceutical/agrochemical compounds.[26]

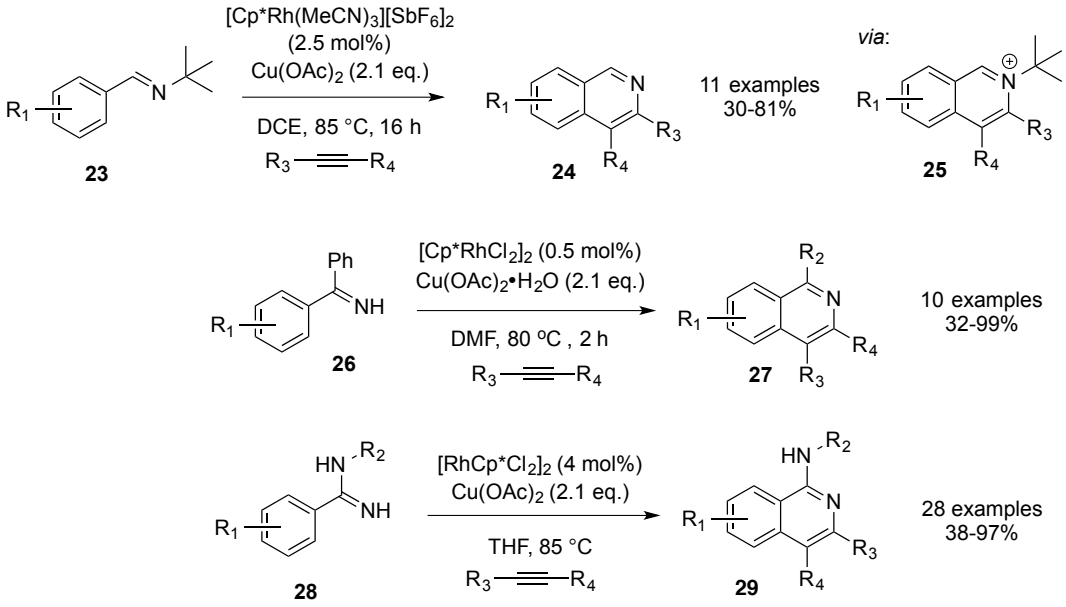

Scheme 1.8

The oxidative Heck reaction, and the variants based on these systems, has been shown to tolerate a wide substrate scope, both in terms of the directing groups used and suitable coupling partners. Systems using ruthenium, palladium and rhodium have been developed, however these systems rely on stoichiometric oxidants, which are typically metal-based. This leads to the generation of expensive, environmentally unfriendly waste streams. Often high temperatures, achieved by super heating solvents in sealed tubes, are required for reaction completion. These factors inherently limit this methodology to small-scale synthesis.

1.6 Redox-neutral C-H activation

The discovery and development of redox-neutral systems using 'internal oxidants' has had a significant impact on the field of C-H activation chemistry.[19,27–29] The internal oxidant refers to a cleavable bond in the starting material which can act as an oxidant for the metal catalyst. Significant benefits include: mild and simple reaction conditions, no external oxidants, which avoids the use of stoichiometric copper acetate and silver salts,[30–32] excellent functional group tolerance, high regioselectivity and low catalyst loadings.

Wu and Cui *et al.* were the first to identify the potential in using the cleavage of an N-O bond to provide an oxygen atom transfer reagent.[33] Using a palladium-catalysed system, quinoline-*N*-oxides **30** were used to simultaneously direct C-H activation in the C_2-position and provide an oxidant for the catalytic cycle, to furnish twelve alkenylated quinolines **32** (27-95% yields) using ethyl acrylate **31** in the oxidative Heck reaction (Scheme 1.9). Based on this concept, Harwig *et al*. have subsequently used oxime esters **33** to prepare a series of substituted indoles **34** *via* an intramolecular C-H amination.

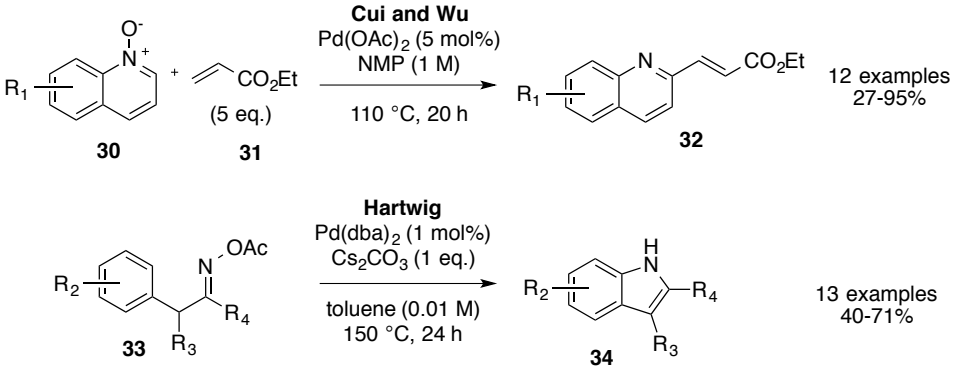

Scheme 1.9

In rapid succession, the groups of Fagnou[34,35] and Glorius[36] reported a rhodium-catalysed system using internal oxidants, treating benzhydroxamic ethers with alkenes and alkynes to afford *ortho*-alkenylated benzamides **17** and isoquinolones **35**, respectively (Scheme 1.10). Using electron-rich and electron-deficient *N*-methoxybenzamide derivatives **36**, Fagnou exemplified the synthesis of substituted isoquinolones **35**. Unsymmetrical alkynes reacted with good regioselectivity in favour of the sp^2 group adopting the 3-position; for example, treatment of the *N*-methoxybenzamide **36** with 1-phenyl-1-propyne furnished 4-methyl-3-phenylisoquinolone as the single regioisomer. Using the same hydroxamate ether **36**, with a lower catalyst loading of 1 mol% (compared with 2.5 mol% required with the alkynes), Glorius reported the synthesis of thirty-five exemplar 2-alkenylbenzamides **17**, using substrates that included styrene derivatives, a ferrocenyl-substituted alkene, butyl acrylate and ethylene. The

added advantage of these systems was the control over mono- *versus* disubstitution. Previously, a carefully selected substitution pattern using steric shielding would have been required to suppress the double olefination.[36]

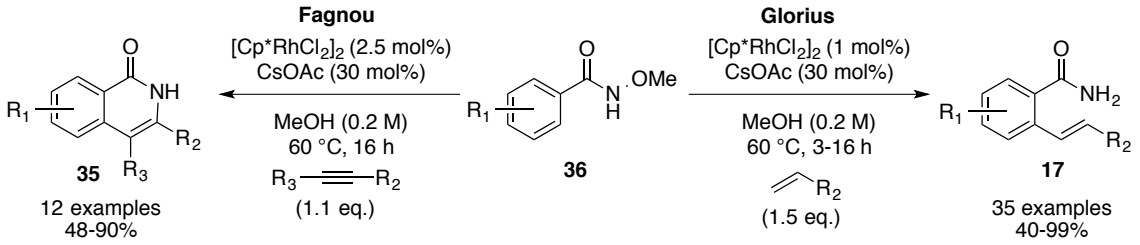

Scheme 1.10

During their mechanistic studies, Glorius *et al.* postulated a seven-membered rhodacycle intermediate **37** that underwent a *β*-hydride elimination, *via* **II**, to afford the alkenylated benzamides **17** (Scheme 1.11). Based on this hypothesis they reasoned that coordination saturation of the rhodium catalyst, *via* **I**, could divert the reaction pathway away from the *β*-hydride elimination and towards reductive elimination of the C-N bond.

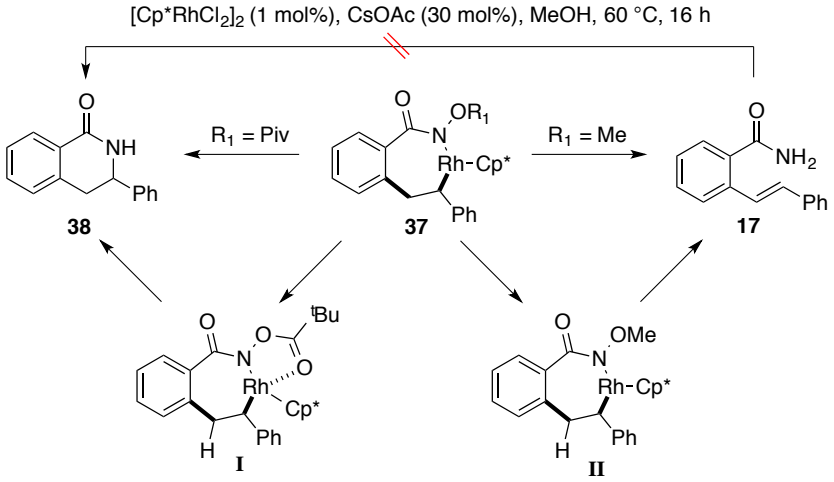

Scheme 1.11

By exchanging the methoxy group with a pivaloyl group the reactions of *N*-(pivaloyloxy)benzamide derivatives **39** with a range of alkenes furnished the dihydroisoquinolones **38**, supporting their hypothesis (Scheme 1.12). To unambiguously rule out the stilbene **17** as an intermediate in the cyclisation reaction, a control experiment was carried out. Treatment of **17** under the standard reaction conditions did not form the dihydroisoquinolone **38** (Scheme 1.11).

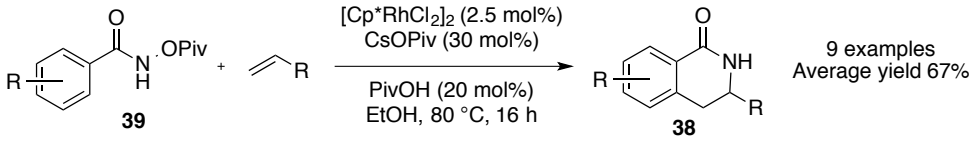

Scheme 1.12

A comprehensive optimisation study of the internal oxidant was subsequently reported by Fagnou *et al.* (Figure 1.1).[34] The rationale behind the substrate selection was two-fold; to investigate internal oxidants bearing better leaving groups, and to use groups that could stabilise intermediates in the catalytic cycle.[34] In order to standardise the reactions, a diaryl alkyne (diphenylacetylene **40**) and a dialkyl alkyne (4-octyne **41**) were screened against a number of substrates (entries 1-11) using the standard reaction conditions. A marked increase in reactivity was observed with carbonyl-containing internal oxidants (entries 4-8), particularly in the reactions using 4-octyne **41** as the substrate. The reactions of the dialkyl alkyne showed a marked improvement in yield compared to their previous system using stoichiometric copper acetate as an external oxidant.[35] Nitrogen-containing leaving groups (entries 10 and 11) failed as internal oxidants.[34]

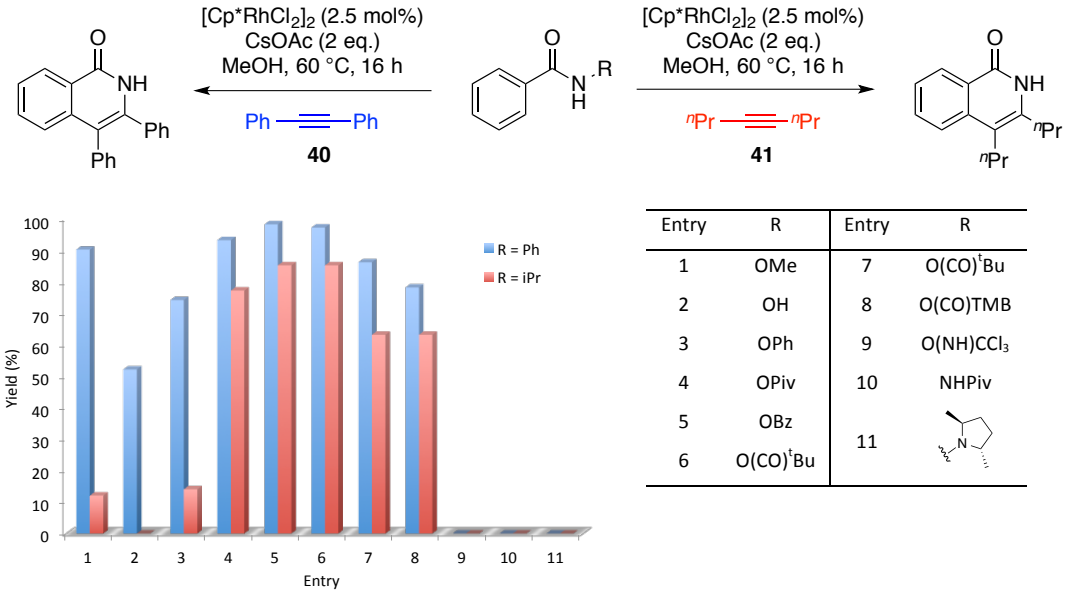

Entry	R	Entry	R
1	OMe	7	O(CO)^{t}Bu
2	OH	8	O(CO)TMB
3	OPh	9	O(NH)CCl$_3$
4	OPiv	10	NHPiv
5	OBz	11	
6	O(CO)^{t}Bu		

Figure 1.1

Continuing with their optimal substrate, *N*-(pivaloxyloxy)benzamide **43**, Fagnou *et al.* repeated their previous reactions where they had used *N*-methoxybenzamide **42** to illustrate the superior activity of this new substrate in redox-neutral systems (Table 1.1).[34] The optimised conditions improved upon those previously reported by Glorius *et al.*,[36] (*cf.* Scheme 1.12) by reducing the catalyst loading (from 2.5 to 0.5 mol%) and the temperature (from 80 °C in ethanol to room temperature in methanol). Fagnou *et al.* compared their previous results using

N-methoxybenzamide **42** to those using *N*-(pivaloyloxy)benzamide **43**, which showed a marked improvement on the reaction yields with less reactive dialkylsubstituted alkynes, for example 1-phenyl-1-propyne and 4-octyne (entries 1-4, Table 1.1). Increasing the catalyst loading to 2.5 mol% facilitated the coupling of terminal alkynes with *N*-(pivaloyloxy)benzamide **43**, a result which had previously been unachievable using external oxidant based systems. Previous to this report, examples of annulation protocols using copper acetate as an oxidant were limited to internal alkynes, resulting in disubstituted heterocycles. The restriction stems from the copper(I)-catalysed Glaser coupling, whereby terminal alkynes preferentially dimerize than react to afford a mono-substituted heterocycle.[34] Fagnou *et al.* utilised their copper-free conditions with terminal alkynes, which gave the corresponding 3-substituted isoquinolones **35**, as single regioisomers, albeit using a higher catalyst loading of 2.5 mol% (entries 6-9). These systems have now become the archetype for many rhodium based redox-neutral strategies.[29]

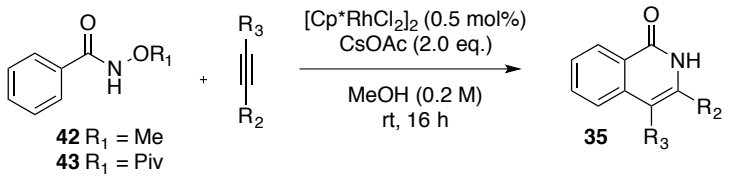

Entry	R1	R2	R3	Temp (°C)	Cat. Loading (mol%)	Yield
1	Me	Ph	Me	60	2.5	61[a]
2	Piv	Ph	Me	rt	0.5	92
3	Me	^{n}Pr	^{n}Pr	60	2.5	12[a]
4	Piv	^{n}Pr	^{n}Pr	rt	0.5	70
5	Piv	^{n}hex	H	rt	0.5	92
6	Piv	$(CH_2)_2OH$	H	60	2.5	85
7	Piv	CO_2Me	H	60	2.5	49
8	Piv	TMS	H	rt	2.5	75
9	Piv	cyclopropane	H	rt	2.5	95

[a]*CsOAc (0.3 eq.)*

Table 1.1

1.7 Mechanistic studies

1.7.1 Experimental data

To investigate the true role of the internal oxidant, Glorius *et al.* used a competition experiment to determine whether the reaction proceeded *via* an intra or intermolecular oxidation (Scheme 1.13).[36] Under the standard conditions, using equimolar amounts of two distinct *N*-methoxybenzamide derivatives **44** and **45** with 1-methyl-4-vinylbenzene **46**, the observed high recovery of **45** was indicative that the N-OMe bond acts as an internal oxidant.

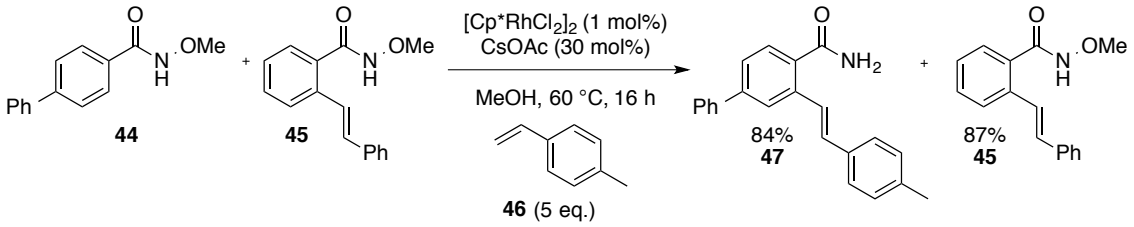

Scheme 1.13

Fagnou *et al.* highlighted the superiority of *N*-methoxybenzamide **42** as a directing group compared with benzamide **48** through a deuterium incorporation study (**A** and **B**, Scheme 1.14).[35] Only 25% deuterium incorporation was identified using benzamide **48** compared with 90% with *N*-methoxybenzamide **42**, indicating higher rhodation of the C-H bond. On addition of diphenylacetylene **40**, no deuterium was incorporated in the recovered starting material **42** or product **49**, thus signifying an irreversible C-H insertion in the presence of the alkyne **40** (**C**), compared with reversible rhodation in its absence (**B**).[35]

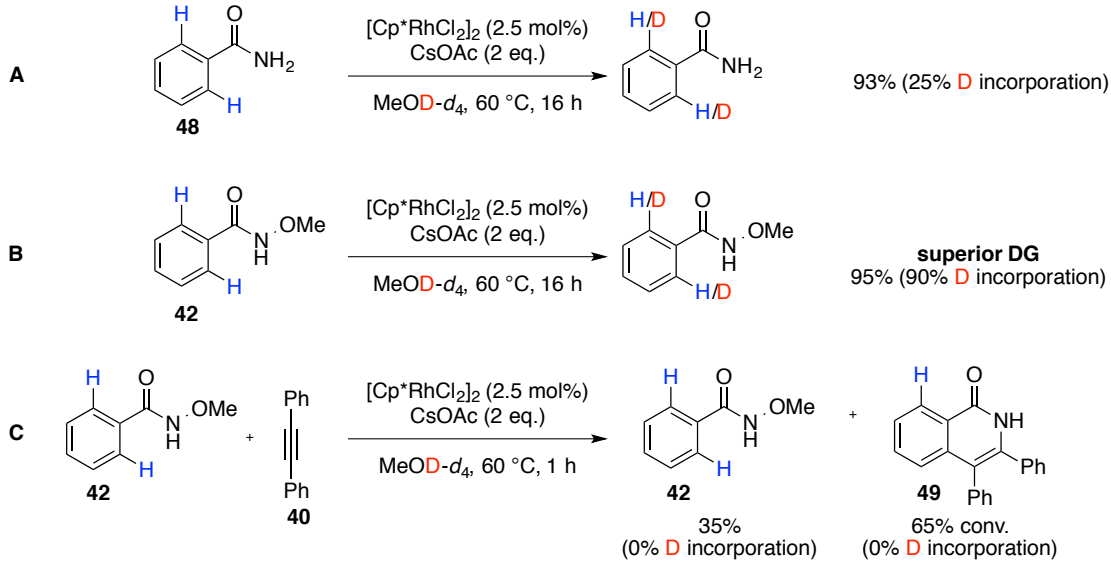

Scheme 1.14

The availability of a coordinating nitrogen in the directing group proved to be crucial in order to facilitate C-H insertion. A trial reaction, using standard conditions, with *N*-methyl-*N*-methoxybenzamide and styrene resulted in unreacted starting material.[36] Furthermore, all attempts using rhodium(I) catalysts, $RhCl(PPh_3)_3$ and $[RhCl(cod)]_2$, in place of $[Cp^*RhCl_2]_2$ were unsuccessful.[36]

Both Fagnou and Glorius conducted deuterium kinetic isotope effect (DKIE) studies to determine the rate-limiting step in the C-H activation mechanism (Scheme 1.15). For *N*-methoxybenzamide **42** a primary DKIE of 1.0 ±0.1 was found. In contrast, *N*-(pivaloyloxy)-benzamide **43** was found to have a DKIE of 14.6 ±0.1, suggesting that C-H insertion is the rate determining step with this substrate.[34,36]

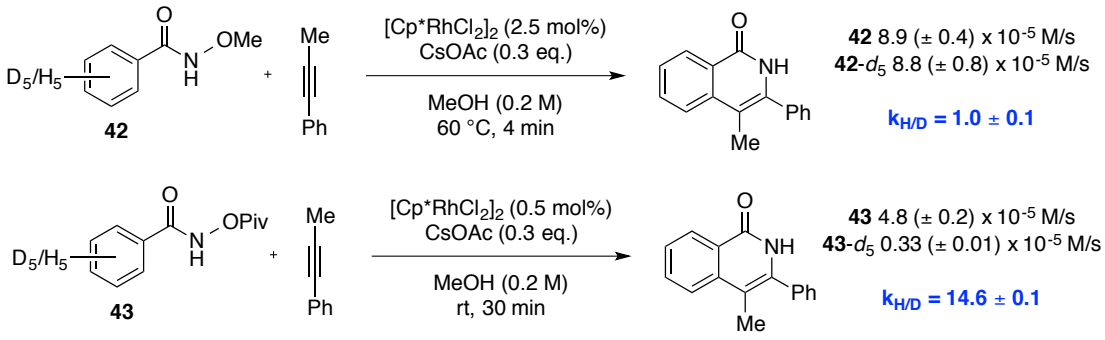

Scheme 1.15

1.7.2 Computational data

In an attempt to rationalise the difference in reactivity the *N*-methoxy- and *N*-(pivaloyloxy)-benzamide, **42** and **43**, Xia *et al.* reported a computational elucidation of the divergent reaction pathways of the –OMe and –OPiv catalytic cycles.[37] Using density functional theory (DFT) calculations, reaction pathways of *N*-methoxybenzamide **42** and *N*-(pivaloyloxy)benzamide **43** were calculated, using ethylene as a model substrate. The initial N-H deprotonation, C-H activation and olefin insertion steps were observed as the same for both substrates **42** and **43**. Xia's report describes the formation of the active catalyst, $Cp^*Rh(OAc)_2$, from the dimer $[RhCp^*Cl_2]_2$ and CsOAc, followed by deprotonation of the NH bond **I** by one of the acetate ligands, leading to the displacement of one molecule of acetic acid **II** (Scheme 1.16). Previous reports had postulated $[Cp^*RhOAc]^+$ as the active catalyst, however Xia *et al.* claim their calculations eliminate this complex as the reactive catalyst and additionally rule out C-H cleavage prior to the N-H deprotonation.

The C-H insertion proceeds *via* a concerted-metallation deprotonation mechanism (CMD).[14,38] The C-H bond is polarised as a result of an agostic interaction, which consequently increases the

acidity of the proton. The C-H bond is then deprotonated by the resting acetate ligand to give **III**. Release of acetic acid from the rhodium complex **III** reveals a vacant site for coordination of the olefin substrate **IV**. From their calculations, the intermediate **III** was slightly higher in energy that the free substrate and catalyst, indicating the reversibility of the NH deprotonation/C-H activation processes for substrates **42** and **43**. On insertion of the rhodium into the alkene, Xia *et al.* calculated the formation of the puckered intermediate **VI**, formed as a result of weak coordination with the π-electrons of the C_1 and C_2 aryl ring. Dissociation from the aryl ring from the rhodium centre alleviates the bond strain to form a seven membered intermediate **VII**. The calculated intermediate **VI** from the mechanistic pathway of *N*-methoxybenzamide **42** was shown to be more stable than the resultant seven-membered ring **VII**, which is possibly a result of the unsaturated coordination of the rhodium centre.[37] In comparison, the intermediate **VII** is more stable than **VI**, with the *N*-(pivaloyloxy)benzamide **43**, due to the stabilising interaction of the pendent carbonyl (in the pivaloyl group) with the rhodium centre.

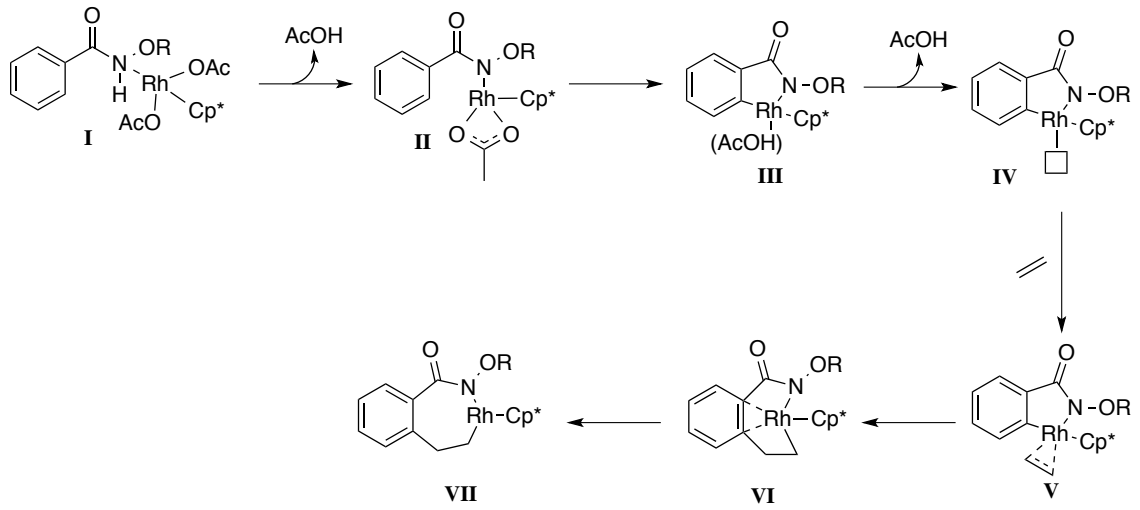

Scheme 1.16

The seven-membered rhodacycle **VII**, formed after the olefin insertion, represents a key intermediate. At this stage the internal oxidant directs the reaction pathway. The *N*-(methoxy)benzamide continues through a *β*-hydride elimination step **VIII** *via* a rhodium-hydride intermediate **IX** (Scheme 1.17). Transfer of the hydride to the nitrogen results in the rhodium(I) species **X**. In order to regenerate the catalyst, their calculations suggest the assistance of a molecule of acetic acid drawing the methoxy group away from the nitrogen **XI**, causing a formal covalent bond to form between the rhodium catalyst **XII** and the nitrogen, resulting in a cationic rhodium(III) species **XIII**. Their calculations eliminated the possibility of a formal 1,2-migration of the methoxy from the nitrogen to rhodium from the intermediate **X**, due to a large activation barrier.

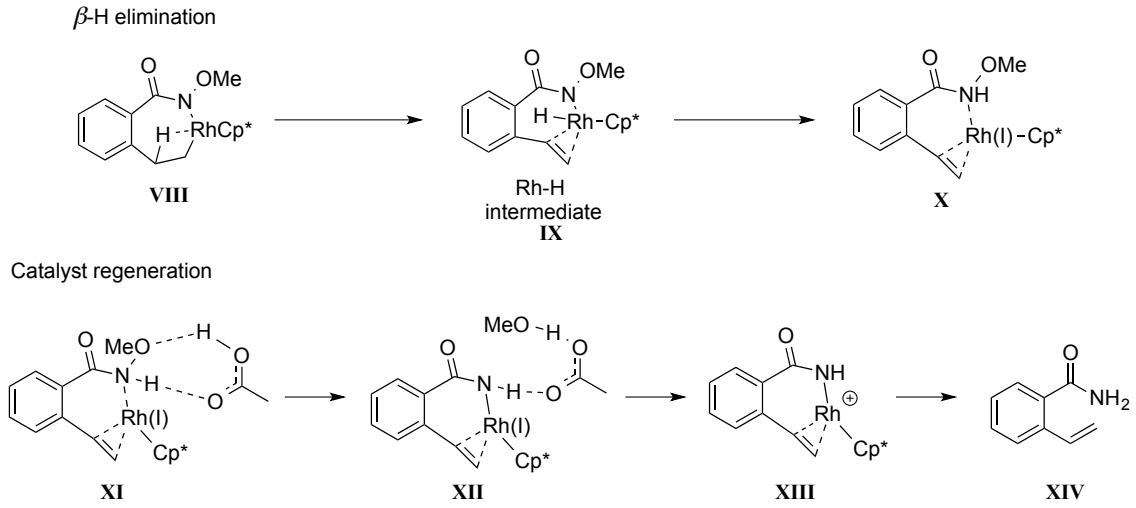

Scheme 1.17

As Fagnou[34] and Glorius[36] had postulated, the *N*-(pivaloyloxy)benzamide is able to stabilise the seven-membered rhodacycle **XV** through weak coordination of the carbonyl group (Scheme 1.18). Xia *et al.* postulated that an acyloxy transfer *via* the transition state **XVI** affords a rhodium(V)-nitrene intermediate **XVII**. Empirically, a rhodium(V) oxidation state has not been observed, only the more common rhodium(I) and rhodium(III) states. Subsequent C-N bond formation (reductive elimination) leads to regeneration of the rhodium(III) species **XVIII**.

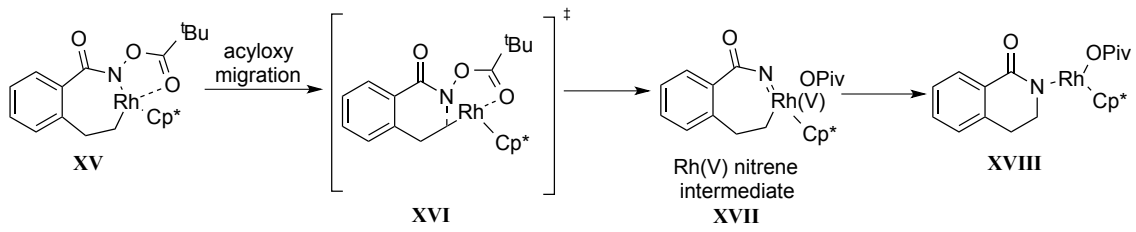

Scheme 1.18

1.8 Redox-neutral strategies

These seminal reports by Glorius[36] and Fagnou[34,35] laid the foundations for redox-neutral strategies and have since spurred a plethora of C-H activation systems for the synthesis of diverse heterocycles and functionalised aromatics.[29] These systems have now been developed for ruthenium catalysts,[39,40] using similarly mild conditions in solvents including water.[41] Strategies have been developed based on a tethered internal oxidant-directing group motif, whereby examples using RN-O, RO-N and RN-N bonds have been exemplified (**A**, Scheme 1.19). Furthermore, the methodology has been extended to external oxidants, based on N-N and N-O substrates (**B**, Scheme 1.19), as milder oxidants, compared with copper(II) acetate. These approaches have been outlined accordingly.

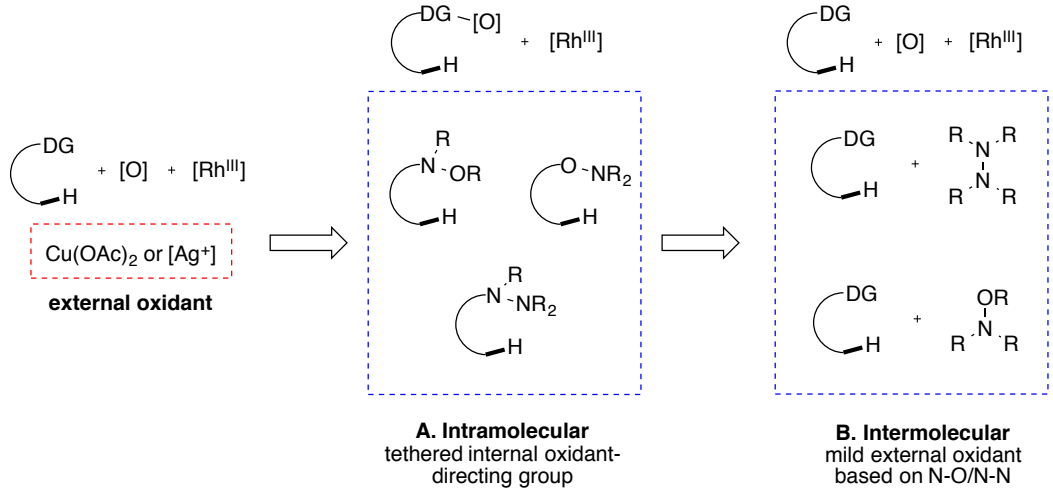

Scheme 1.19

1.9 Ligand and directing group modification for control of stereoselectivity and regioselectivity

The groups of Cramer[42] and Rovis[43] independently reported asymmetric variants of the annulation protocol using modified cyclopentadienyl ligands to effectively bias the coordination sphere (Scheme 1.20). These elegant strategies rely on the fixed Cp ligand controlling the arrangement of the substrates and other ligands around the metal centre, which makes the development of catalytic asymmetric variants enormously challenging. Cramer *et al.* developed a series of modified Cp-ligands **50** incorporating three key features: a) a steric shield to control positional selectivity of the incoming reactant (R_C); b) a position lock to ensure stable conformation of the Cp-ligand; and c) a large pendent group to control the orientation of the substrates on the metal centre.[42] Using benzoyl peroxide to generate the rhodium(III) catalyst *in situ,* they were able to catalyse the annulation of *N*-(pivaloyloxy)benzamide derivatives **39** with terminal or cyclic alkenes to prepare a range of dihydroisoquinolones **38** with excellent enantioselectivity (89:12-97:3 er).

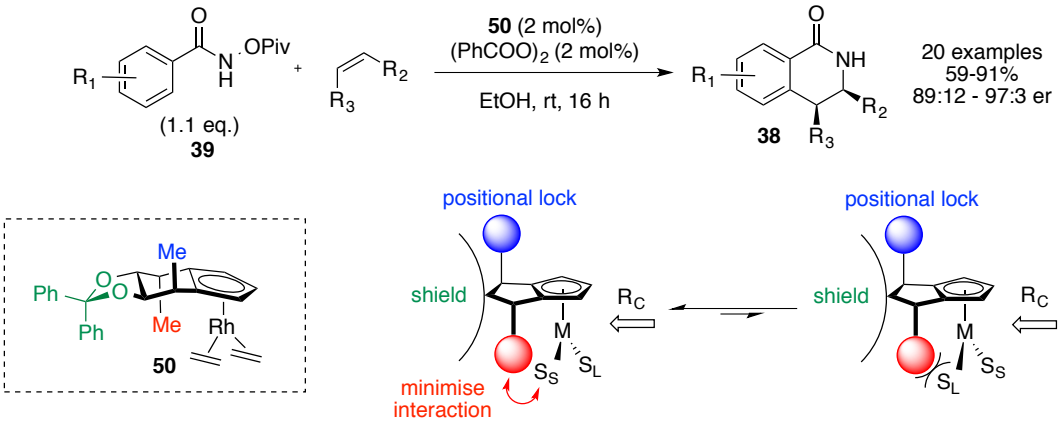

Scheme 1.20

Evolution of this strategy led to the development of a second-generation catalyst **53**, used for the intramolecular asymmetric hydroarylation of 1,1-disubstituted alkenes tethered to a phenolic *N*-methoxybenzamide derviative **51** to create quaternary stereogenic centres (Scheme 1.21).[44] Typically *N*-methoxybenzamide derivatives react with alkenes to produce the unsaturated product *via* β-elimination (*cf.* Scheme 1.11), however in this system, the lack of β-hydrogens resulted in a mixture of the isoquinolone **54** (*via* cyclisation) and the dihydrobenzofuran **52** (*via* protonolysis); the latter was accelerated by the addition of pivalic acid. Cramer *et al.* exemplified this strategy with 15 illustrative examples, each with excellent enantiomeric control (91:9-96:4 er).

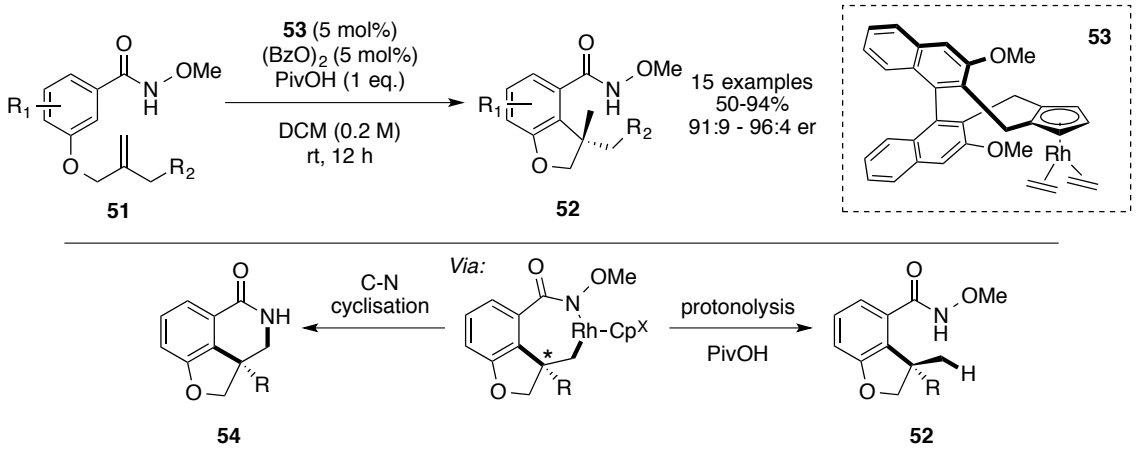

Scheme 1.21

Using a different strategy, Rovis *et al.* exploited the inherent chiral environment of the protein Streptavidin to foster their C-H activation protocol. Since the advent of bioengineering, metalloenzymes (enzymes that incorporate metal co-factors) have become powerful hosts for a wide range of chemical transformations, particularly in asymmetric catalysis,[45] owing to their intricately tailored chiral environment. Amino acid residues that are not directly coordinated to the metal co-factor are available to interact with other substrates through non-covalent

interactions, this is defined as the second coordination sphere.[46] These dormant residues can be employed to alter the active site in order to meet the transformations requirements. Rovis and Ward *et al.,* employed this strategy in the design of their bifunctional engineered Streptavidin using the biotinylated rhodium(III) complex, $[RhCp^{*biotin}Cl_2]_2$, for asymmetric C-H activation (Scheme 1.22).[43] Having successfully docked the rhodium catalyst to the protein, using a biotin tether, the catalytic activity was optimised using a proximal glutamate residue (installed by site-specific mutagenesis of Streptavadin (SavMutant), whose activity was accelerated by addition of a proximal lysine residue to ensure full deprotonation of the glutamic carboxylate. The carboxylate ligand significantly reduces the activation energy of the concerted metalation-deprotonation mechanism by stabilising the transition state, compared with the system using an exogenous acetate. Treatment of *N*-(pivaloyloxy)benzamide **43** with acrylates in a 3-morpholinopropane-1-sulfonic acid buffer solution (MOPS) in MeOH furnished the corresponding dihydroisoquinolones **38** with good enantiomeric ratios (61-95%, er 73:27 – 93:7). Both Rovis and Cramer's approaches require highly specialised ligands to achieve intricate control of the coordination sphere, which reflects the difficulty involved in chiral C-H activation.

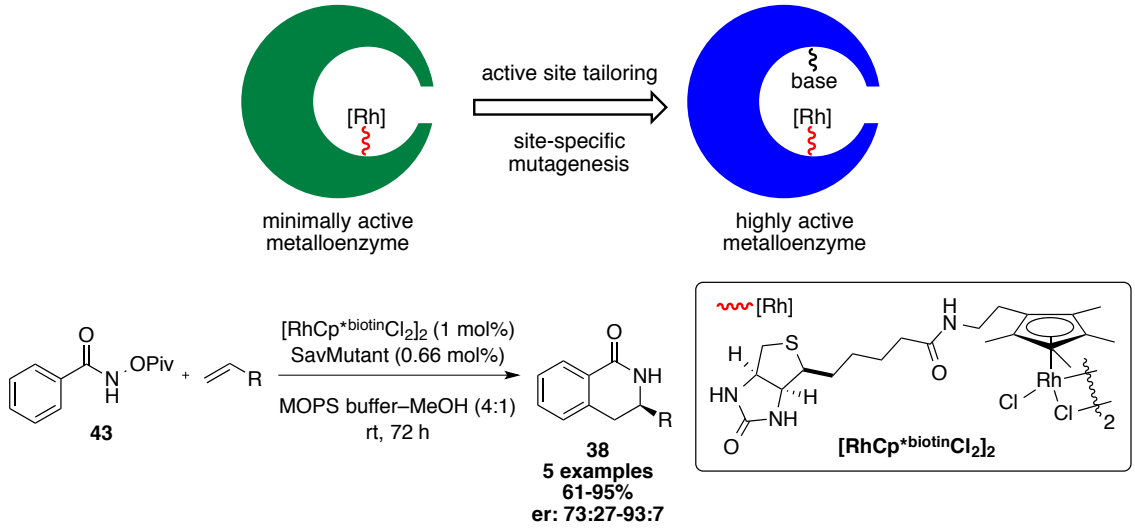

Scheme 1.22

Regioselectivity is determined by the balance of three factors including the steric environment of the activated C-H bond (**A**, Scheme 1.23), the electronics and the size of the groups on the reacting alkene/alkyne. Typically, non-symmetrical alkenes/alkynes prefer to coordinate to rhodium with the larger group occupying the α-position in the rhodacycle (**B**). When electronics govern the system, the electron-donating group prefers to be β-substituted to rhodium in the metallocycle, presumably to stabilise the electron-poor metal (**C**).[47]

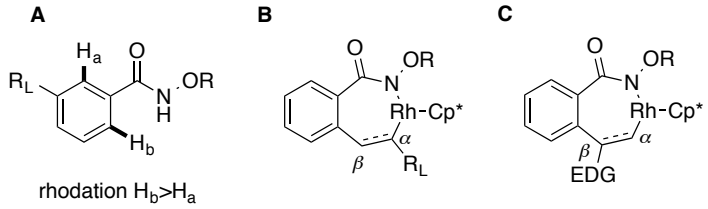

Scheme 1.23

Rovis *et al.* developed a sterically bulky di-*tert*-butylcyclopentadienyl ligand (Cp^t) **55** to enhance the regioselectivity of alkene and alkyne migratory insertion events, delivering regioselectivities (generally >10:1) modestly above those achievable by Cp* ligated Rh complexes (<6:1) with alkyne substrates (Table 1.2).[48,49] The Cp^t ligand was particularly effective for regiocontrol over alkene substrates, which typically react with poor regioselectivitiy, possibly due to competing electronic and steric effects. Using their modified catalyst **55** with *N*-(pivaloyloxy)benzamide **43**, Rovis *et al.* were able to control the migratory insertion step with enhanced regioselectivity compared with the Cp* system, furnishing 3-substituted dihydroisoquinolones as the major isomer.

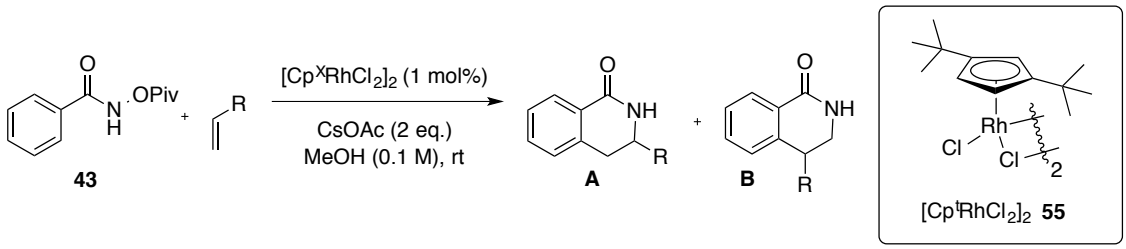

Entry	Alkene	Yield % (Cp^t)	Cp* A:B	Cp^t A:B
1	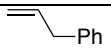	85	1.6:1	5.1:1
2	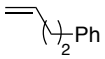	95	2.3:1	14:1
3	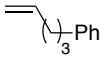	85	1.6:1	8:1
4	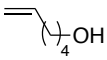	80	1.4:1	12:1
5	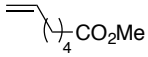	89	2:1	14:1
6	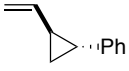	93	1:1	11:1

Table 1.2

Previous attempts to use nicotinamide derivatives in rhodium-catalysed C-H activation/annulation have resulted in low yields, due to the electron-poor nature of the ring,[21] and poor regioselectivity for the C_2 and C_4 positions.[50,51] Huckins and Bercot utilised the nicotinamide *N*-oxide derivative **56** to simultaneously improve the C_2 selectivity on the pyridine ring and to increase the electron density in the ring system (Scheme 1.24).[52] This dual activation

generally improved the reaction yields and significantly improved the C_2:C_4 (**A:B**, Scheme 1.24) regioselectivity of the reaction compared with the 3-*N*-(pivaloyloxy)nicotinamides **57** e.g. from 1.9:1 to >20:1 (**A**:**B**) of **58** and **59** using norbornadiene and 1.7:1 to 17:1 of **60** and **61** using 4-octyne.

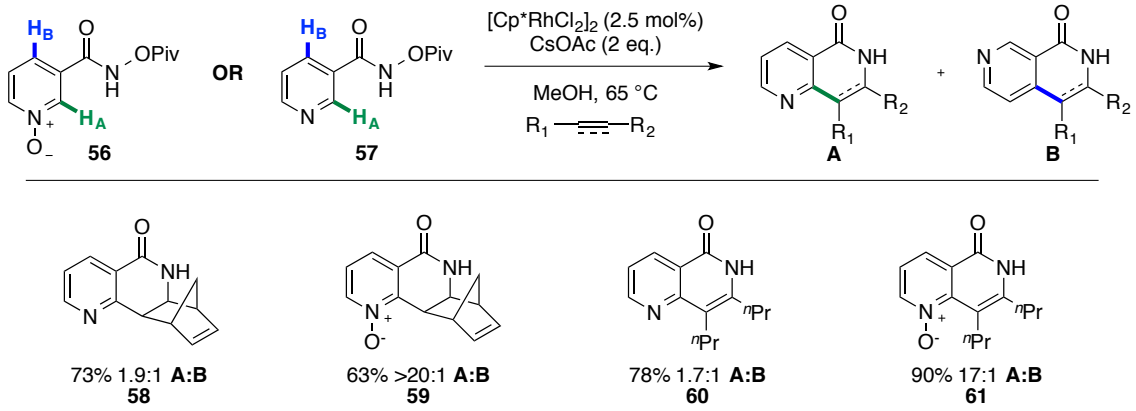

Scheme 1.24

1.10 Substrate scope

The internal oxidant strategy was employed by Park *et al.* in the synthesis of the indolizidine motif, a scaffold which is relevant to natural products and pharmaceuticals (Scheme 1.25).[53,54] To effectively control the regiochemistry of the annulation step, the alkyne substrate was tethered to the internal oxidant group of the hydroxamic ester **62**. The rhodium-catalysed intramolecular annulation furnished the pyridone **63** with a pendant hydroxyl group. This was subsequently used to assemble the indolizidine motif **64** *via* an intramolecular Mitsunobu reaction. Reduction of the pyridone **65**, followed by an oxidative coupling, furnished the pentacyclic scaffold **66**. Utilising this methodology, Park *et al*. reported the total synthesis of the phenanthroindolizidine alkaloids: (±)-septicine **65b**, (±)-antofine **66a** and (±)-tylophorine **66b**.

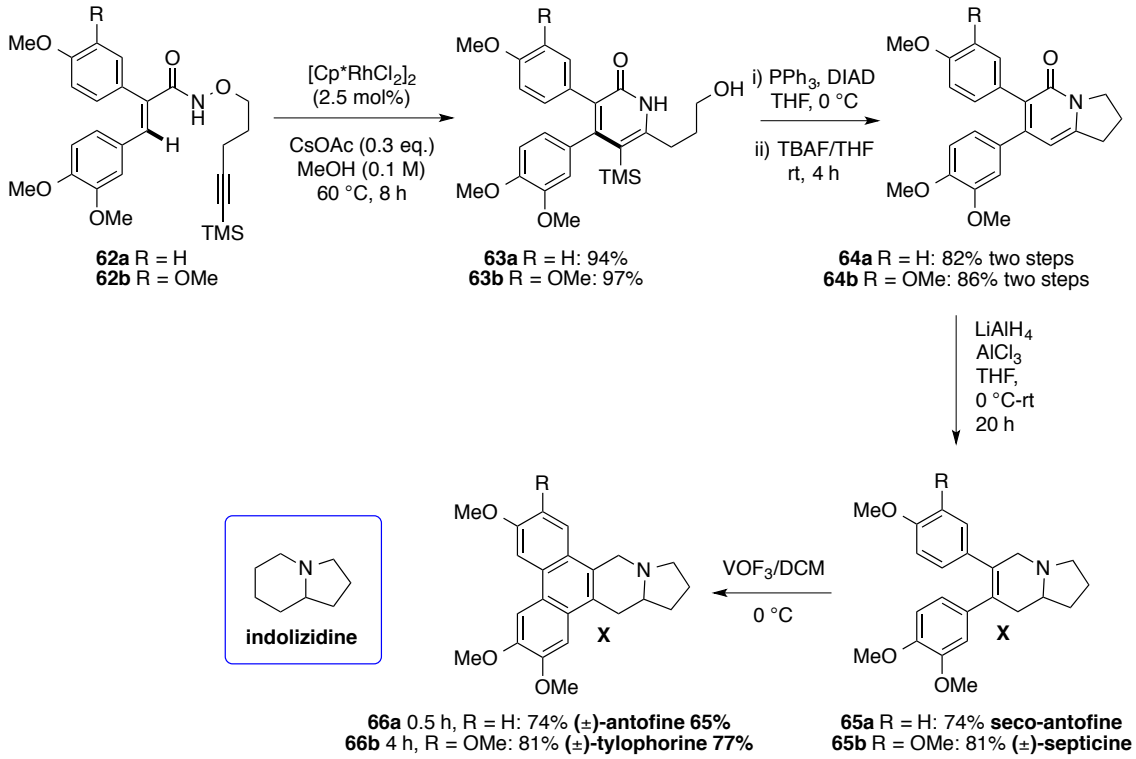

Scheme 1.25

Aside from alkenes and alkynes, numerous substrates have been reported as suitable coupling partners using this N-O based redox-neutral strategy. Glorius *et al.* exemplified the synthesis of isoquinolones from allenes **67** with cyclometallated intermediates generated from *N*-(pivaloxyloxy)benzamide derivatives **39** with $[Cp^*RhCl_2]_2$ (Scheme 1.26).[50] A range of 4-*Z*-alkyenylated dihydroisoquinolones **38** were prepared using a selection of monosubstituted allenes, with high regio- and stereoselectivity. Glorius *et al.* proposed the *Z*-selectivity arises from the rhodium approaching the least sterically encumbered face of the allene (**A**, Scheme 1.26). When sterically congested *N*-(pivaloxyloxy)benzamides or allenes were

employed, the resultant isoquinolones **70-72** formed, suggested steric interference outweighed electronic factors (**B**, Scheme 1.26).[50]

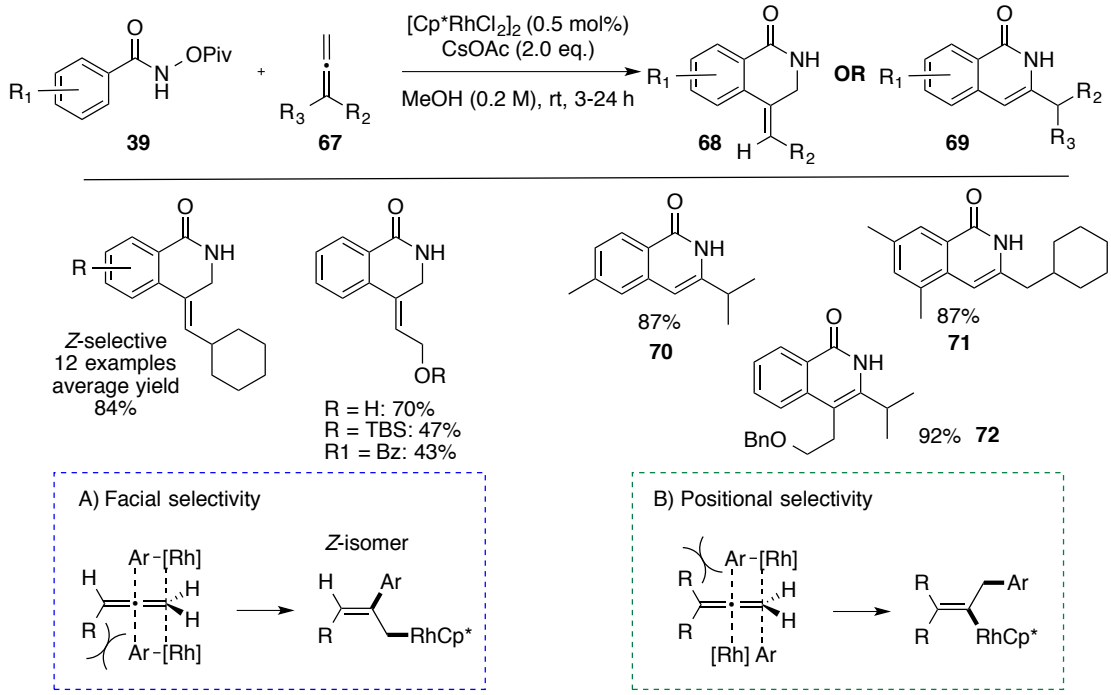

Scheme 1.26

Allenylation of *N*-methoxybenzamide derivatives **36**, using similar methodology, allowed Ma *et al.* to prepare poly-substituted allenyl-silyl-benzamides **74** using mild conditions, with excellent yields (Scheme 1.27).[55] These products could be diversified further to the corresponding isoquinolones, furans and alkynes.

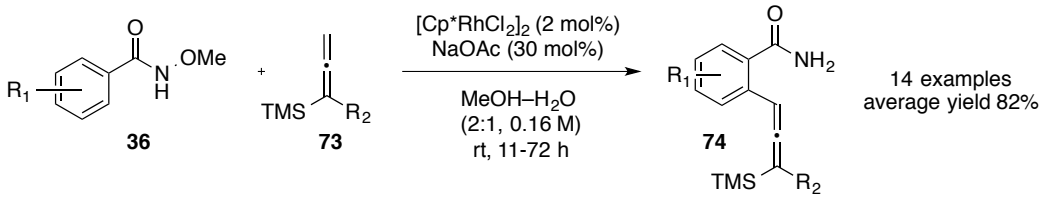

Scheme 1.27

C-H Activation can be used as a powerful tool for installing additional functional groups, which can offer a handle for versatile and divergent syntheses, which is particularly desirable for rapid library development. Glorius *et al.* realised the potential of combining C-H activation with *N*-methyliminodiacetic acid (MIDA) boronates to introduce a synthetic handle for Suzuki-Miyaura cross-coupling reactions (Scheme 1.28). MIDA boronates are bench and air stable (unlike many boronic acids), simply prepared and are compatible with a wide range of common synthetic reagents. They can be used directly in cross-coupling reactions, however they are less reactive than the corresponding boronic acid. Deprotection to reveal the corresponding reactive

boronic acid *in situ* can be achieved using mild, basic conditions. Based on the difference in reactivity, Burke *et al.* developed an iterative Suzuki-Miyaura cross-coupling reaction.[56] Treatment of alkynyl MIDA boronates **75** with *N*-(pivaloyloxy)benzamide derivatives **39** using $[Cp^*RhCl_2]_2$ furnished a range of 3-B-MIDA substituted isoquinolones **76**. Additional copper(II) acetate (0.4 equivalents) was required in order to achieve full conversion to the products. Only terminal alkynes were tolerated using these reaction conditions, highlighting a limitation of the substrate scope. The isoquinolone-boronates were subsequently coupled with a selection of aryl-bromides using standard Suzuki-Miyaura coupling conditions to afford 3-arylated isoquinolones **77** with excellent yields.

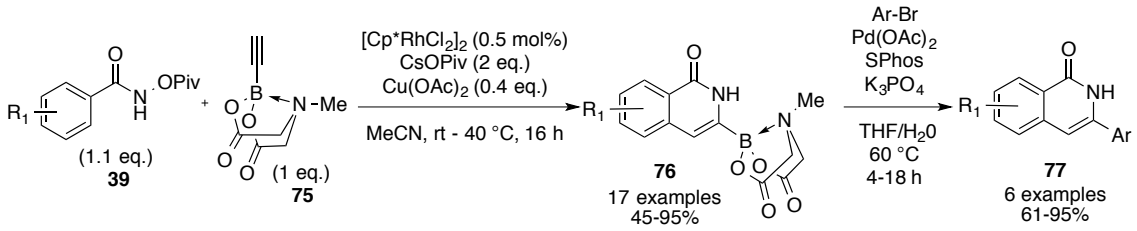

Scheme 1.28

In the same vein, Molander *et al.* found vinyltrifluoroborate **78** to be an efficient coupling partner with the hydroxamate ester **39** under these rhodium-catalysed conditions, this time observing selectivity for the 4-position (Scheme 1.29). The dihydroisoquinolones **79** were further diversified by oxidation to give the 4-hydroxydihydroisoquinolones, and protodebromination to afford 3,4-unsubtituted dihydroisoquinolones.[57] The latter example was used for the preparation of corydaldine **80**, a naturally occurring alkaloid used in Chinese and Indian traditional medicine.[58] Unsubstitued-dihydroisoquinolones had previously been prepared using *N*-(pivaloyloxy)benzamide and ethylene as a coupling partner.[34,36]

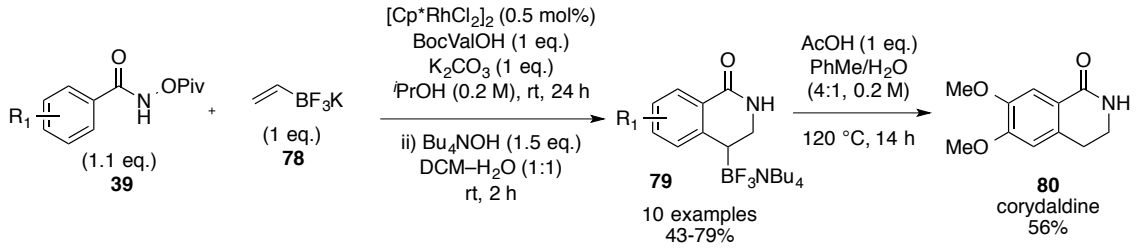

Scheme 1.29

Numerous methodologies have been developed using hydroxamic esters with various substrates to assemble diverse heterocyclic rings (Scheme 1.30). Using diazoesters, Rovis *et al.* exemplified the synthesis of isoindolinones **81** (**A**).[59] The groups of Glorius[60] and Cui[61] extended the substrate scope to include α,β-unsaturated aldehydes/ketones and vinyl diazoesters to prepare azepinones **82** and **83**, structural motifs commonly found in natural products (**B** and **C**). Fagnou *et al.* had previously prepared 3-substituted isoquinolones using terminal alkenes (*cf.* Table 1.1). An alternative synthesis, reported by Rovis *et al.,* used activated

cyclopropenes to prepare 4-substituted isoquinolones **84**.[62] Treatment of diynes with *N*-(pivaloxyloxy)benzamide **43** furnished 3-alkynlated isoquinolones **85**, which could be used as a functional handle for a range of diverse chemical transformations, including a sequential reaction with either another equivalent of *N*-(pivaloyloxy)benzamide **43** or with an unsaturated α-β-unsaturated oxime **87** to furnish fused *bis*-isoquinolones **86** or isoquinolone-pyridines **88**, respectively.[63]

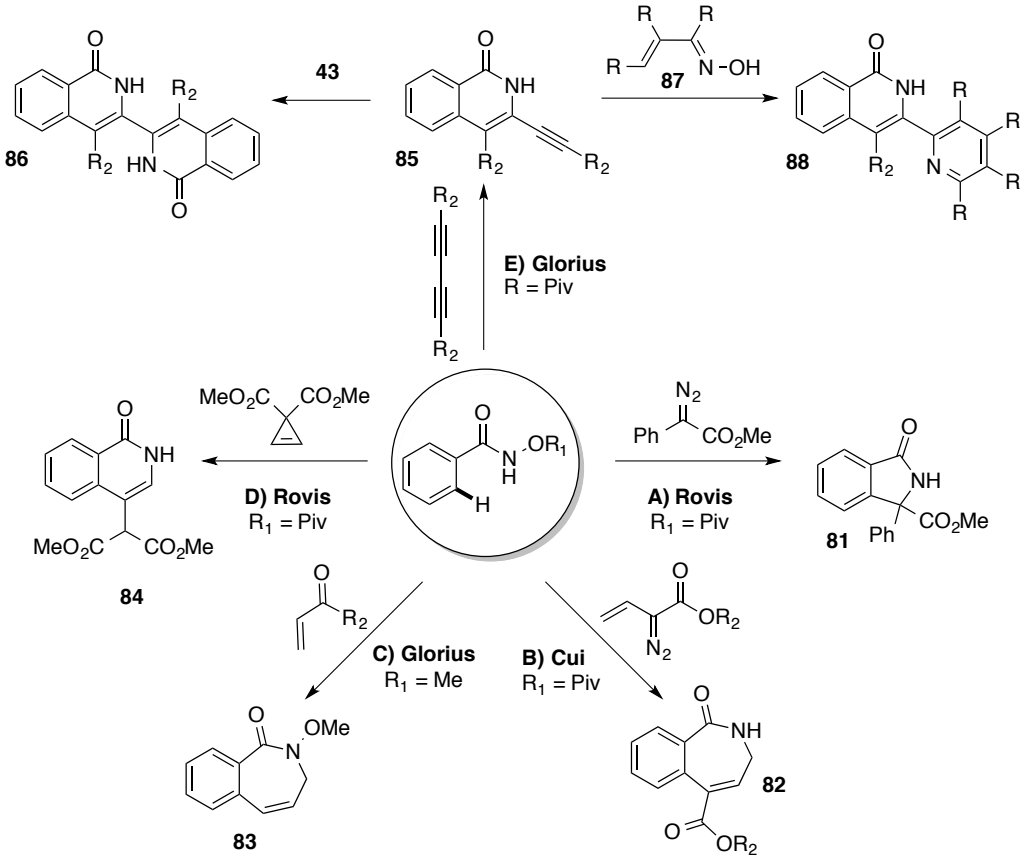

Scheme 1.30

The first example using internal oxidants with ketoximes was reported by Chiba *et al.* for the synthesis of isoquinolines from *O*-acetyl ketoximes **89** with alkynes (Scheme 1.31).[64] Nineteen isoquinolines **90**, bearing electron-donating or electron-withdrawing groups, were prepared with an excellent average yield of 82%, reflecting the high substrate tolerance of these reaction conditions. Unsymmetrical alkynes reacted with good regiocontrol in favour of the larger group adopting the 3-position; for example, treatment of *O*-acetyl acetophenone oxime with 1-phenyl-1-propyne furnished 1,4-dimethyl-3-phenylisoquinoline as a single regioisomer. Using the same strategy, Rovis *et al.* used α,β-unsaturated oximes **87** and ketoximes **91** to prepare a range of pyridines and isoquinolines (Scheme 1.31).[49]

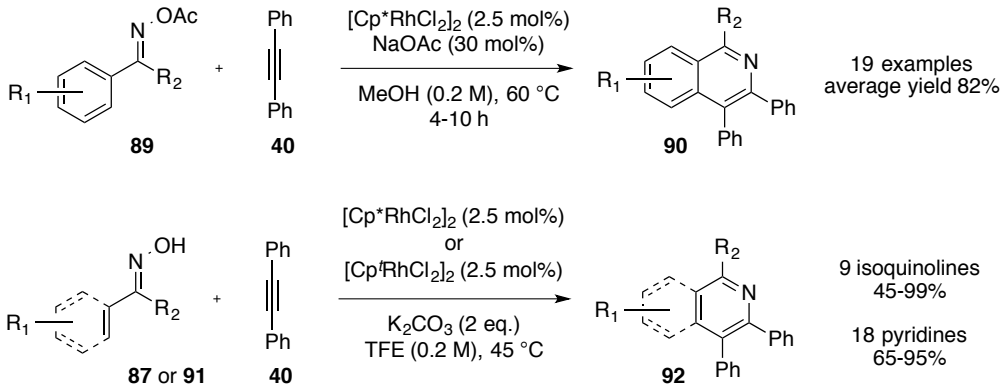

Scheme 1.31

Whilst investigating the mechanism of the reaction, Chiba *et al.* used the chalcone oxime isomers **93** and **95**, to determine the reactive isomer. The *E*-oxime **93** reacted with diphenylacetylene **40** to give the corresponding isoquinoline **94**, unlike the *Z*-oxime **95**, which deacetylated to give **96** under the reaction conditions (**A**, Scheme 1.32). This is presumably due to the availability of the lone pair of electrons on the nitrogen required to coordinate to the metal centre to facilitate C-H activation. The possibility of the reaction proceeding *via* a 6π-electrocyclisation was deemed to be implausible, based on an observation using the substrate **97** (**B**, Scheme 1.32). The oxime **97** was subjected to the standard reaction conditions, however only the deacetylated starting material **98** was observed. Addition of 4-octyne **41** to the reaction resulted in formation of the isoquinoline **99** and deacetylated starting material **98**.

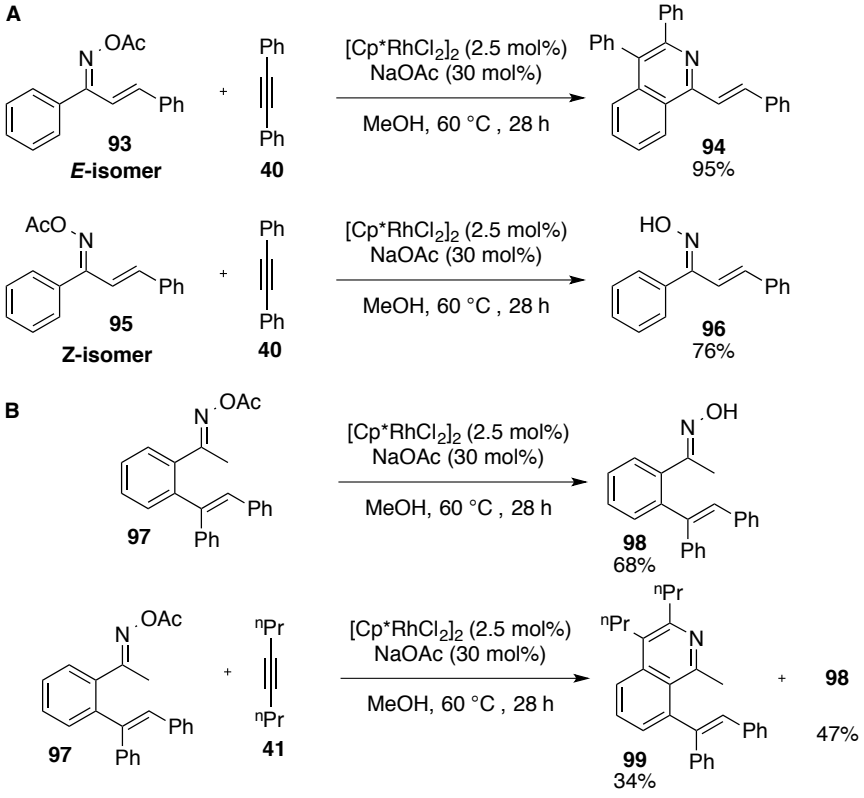

Scheme 1.32

1.11 Variants of the N-O strategy

The introduction of these rhodium-catalysed redox-netural systems has naturally evolved to encompass alternative substrates functionalised with cleavable N-O bonds. In the examples illustrated thus far the nitrogen from the N-O cleavage is incorporated into the final product, however, the oxygen-containing moiety is usually lost to the reaction medium. Lu *et al.* have developed a methodology to prepare *ortho*-hydroxyphenyl-substituted enamides **102** from *N*-phenoxy-acetamide **101** with alkynes, successfully incorporating both elements of the internal oxidant (16 examples, 32-83% yields, Scheme 1.33).[65] A side reaction in their synthesis, using ester-substituted alkynes, was identified as the formation of benzofuran **100**. By careful manipulation of the reaction additives and reaction solvent (addition of acetic acid in dichloromethane), fifteen exemplar benzofurans were prepared (Scheme 1.33). A solvent screen revealed the preferential formation of benzofurans when non-coordinating or bulky polar solvents, such as toluene, *tert*-butanol or dichloromethane, were used. In contrast, polar co-ordinating solvents resulted in formation of the *ortho*-hydroxyphenyl enamides **102**.

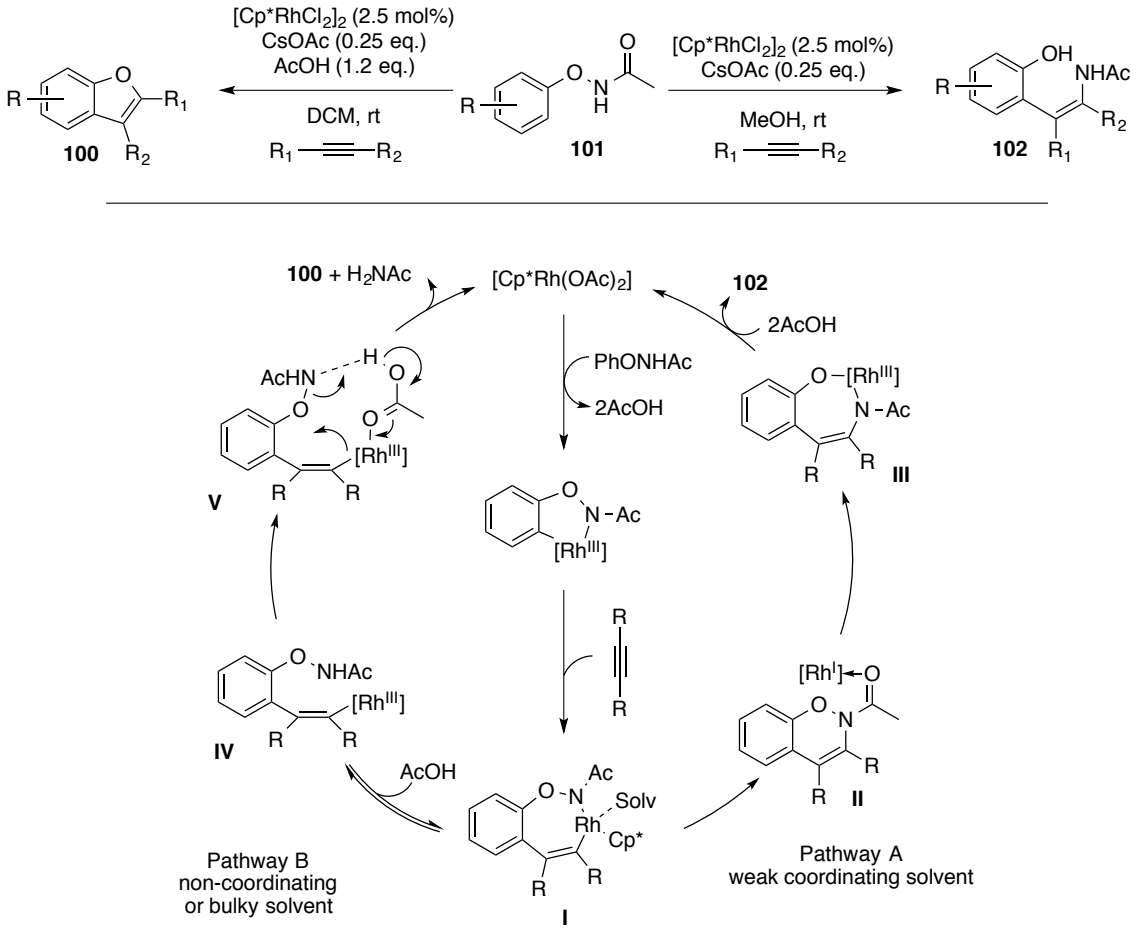

Scheme 1.33

A control experiment eliminated the intermediary enamide **102** in the formation of the benzofuran **100**, which suggested two separate mechanistic pathways. In weak coordinating

solvents, Lu *et al*. postulated the pathway A (Scheme 1.33). Coordination of a solvent molecule to the rhodium(III) centre **I** would create an 18 electron complex which would reductively eliminate to form the rhodium(I) intermediate **II**. Oxidative insertion **III**, followed by acid promoted dissociation from the product would furnish the enamide **102**. In contrast, in non-coordinating solvents, the nitrogen coordinated to the rhodium(III) centre in the 16 electron complex could be protonated to afford the intermediate **IV** (pathway B, Scheme 1.33). An intramolecular substitution **V**, mediated by acetic acid, would furnish the benzofuran **100**. Following this study, Lu *et al.* found that under similar conditions the reaction of alkenes with *N*-phenoxy-acetamide **101** generated the *ortho*-alkenylated phenols **103** (Scheme 1.34).[66]

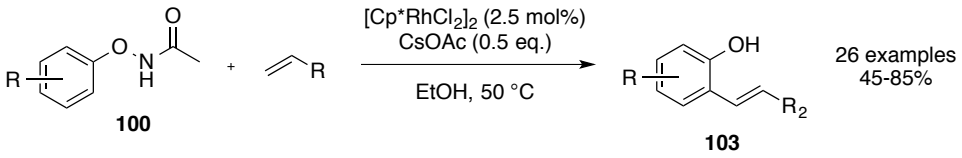

Scheme 1.34

Recognising the inherent difficulty of functionalising tertiary anilines at the *ortho*-position, due to their propensity to react at the *para*-position in classical S_EAr chemistry in order to avoid steric repulsion, You *et al*. developed a system whereby oxidised tertiary anilines would have a dual role as a traceless *ortho*-directing group (unlike acetanilides which would require an additional step to deprotect the aniline) and an internal oxidant for the reaction. Using their optimised conditions they were able to alkenylate twenty *N*-oxidised anilines **104** to give the corresponding unsaturated products **105** with *N*-substituents including *N,N*-dimethyl, a benzylated derivative and cyclic anilines (Scheme 1.35).[67] Only a trace of the product was observed with the *N,N*-diethyl derivative, suggesting that steric hindrance is still a limitation in these reactions.

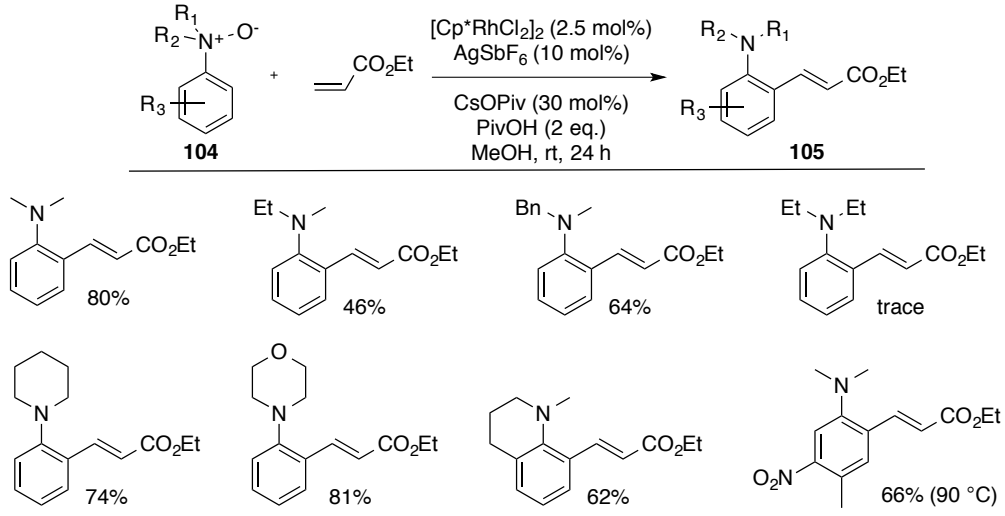

Scheme 1.35

1.12 Redox-neutral systems based on N-N cleavage

Based on the initial internal oxidant optimisation study by Fagnou *et al.* (Scheme 1.36),[34] functional groups with N-N bonds were deemed unreactive under the reaction conditions employed (*cf.* Figure 1.1). Further development has however identified hydrazines, hydrazones and nitroso-based directing groups to act as suitable internal oxidants for this C-H activation methodology.

Huang and Zhu have used *N*-nitroso-compounds **107** and alkynes to furnish *N*-substituted indoles **106** (Scheme 1.36). These were the first reported *N*-alkyl indole syntheses using a C-H activation protocol. Starting with the active catalyst, $[RhCp^*(OAc)_2]_2$, Huang *et al.* were able to utilise simple conditions in order to furnish the indoles **106**,[68] in comparison to Zhu's protocol,[69] although a super-heated solvent system was required in order to obtain good yields.

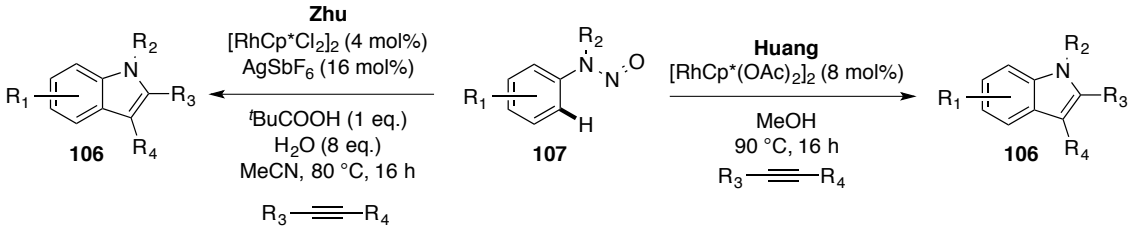

Scheme 1.36

An alternative approach to indole synthesis using an N-N bond cleavage was developed by Glorius *et al.*[70] using hydrazines **108** as their starting materials (Scheme 1.37). Under acidic conditions, in a sealed system, the hydrazines **108** reacted with a diverse range of alkynes to furnish substituted indoles. This approach offers an alternative substrate precursor compared with the traditional Fisher-indole synthesis that relies on the condensation of an aromatic hydrazine with an aldehyde/ketone. Unsymmetrical alkyl-aryl substituted alkynes reacted to preferentially install the aryl group in the 2-position of the indole.

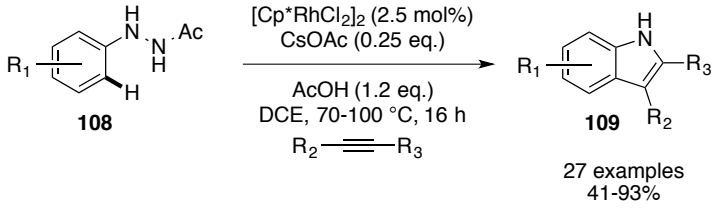

Scheme 1.37

The synthetic utility of this approach was further explored to include isoquinolines **111** prepared from hydrazones **110** (Scheme 1.38). Cheng *et al.* commented on the importance of the acetic

acid in the reaction medium, based on their postulated mechanism which would involve the protonation of the *N,N*-dimethyl group in order improve it as a leaving group.[71]

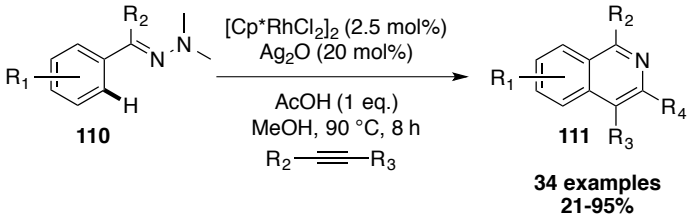

Scheme 1.38

1.13 Intermolecular N-O/N-N oxidants

A plethora of systems have been developed using a tethered internal oxidant and directing group, where they are combined in a single functional group (e.g. ketoximes, hydroxamate esters etc.). Glorius *et al*. reported an intermolecular example where the directing group has been separated from the N-O based oxidant for the *ortho*-C-H amination of 2-phenyl pyridines **112** and *N*-methoxybenzamides derivatives **36** (Scheme 1.39).[72] Using a specifically designed and optimised electron-deficient aryloxycarbamate **113** as an external oxidant, the aromatic substrates were aminated to afford Boc-protected anilines **114** and **115**, under mild conditions. Alternative protecting groups, including Cbz- and Fmoc-protected carbamates, were tolerated under the reaction conditions. *N*-Methoxybenzamide derivatives **36** were tolerated under the reaction conditions, where the N-O bond of the carbamate was selectively cleaved over the hydroxamic ether N-O bond. Further diversification of these substrates could be achieved using a subsequent internal-oxidant based C-H activation step, however this was not exemplified in their report.

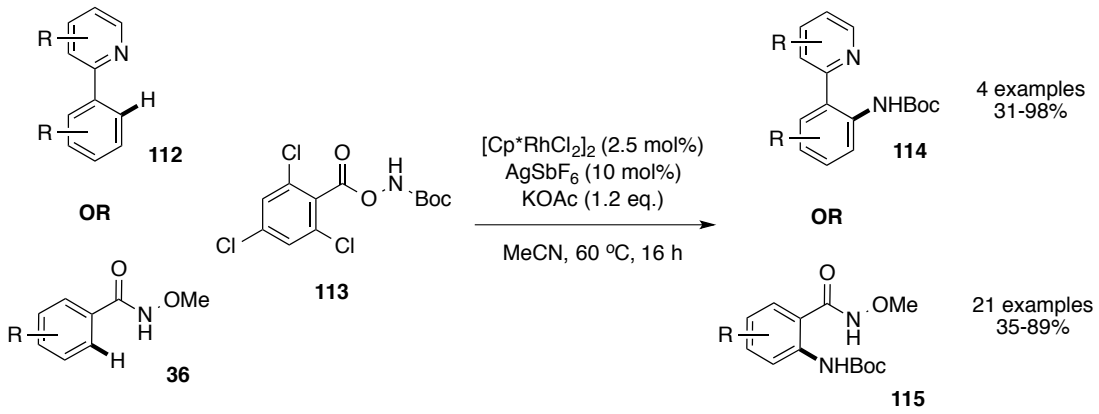

Scheme 1.39

Classic cross-coupling amination reactions typically generate stoichiometric waste from one of the coupling partners, either from the C-X or N-X bond. Alternative C-H activation strategies

require external oxidants that equally generate unwanted waste. Chang *et al.* used *p*-toluenesulfonyl azide **116** as a nitrogen source for the sulfoamidation of phenyl pyridines **112**, purines **118a,b**, a pyrazole **119** and ketoximes **120a-c** (Scheme 1.40).[73] The reaction was observed to tolerate electron-rich and electron-deficient aromatic systems, and the use of the azide **116** results in the generation of nitrogen as the stoichiometric waste. Although this synthetic approach could be challenging to perform on scale, due to the evolution of gas and the risks associated with azides, this methodology would prove to be synthetically useful to medicinal chemists for the preparation of libraries of compounds.

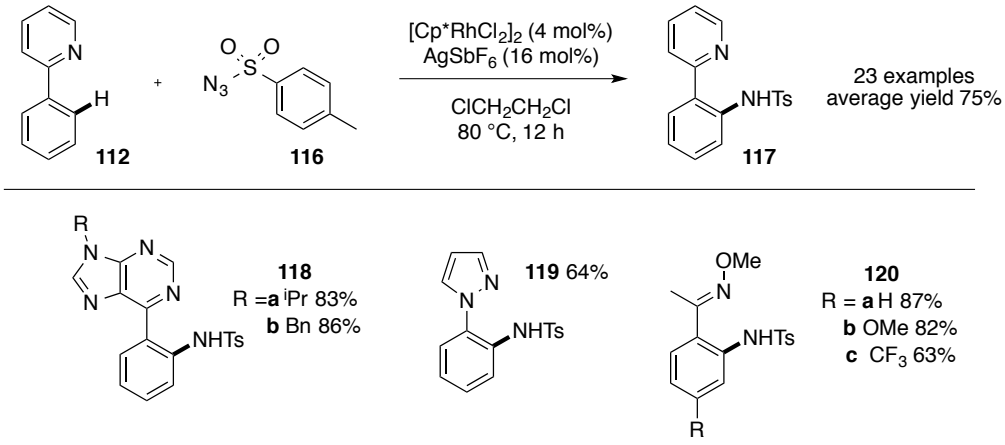

Scheme 1.40

1.14 Summary

The work outlined above illustrates the potential for succinct, atom-efficient processes to construct heterocyclic scaffolds using internal oxidants. The aforementioned systems employ mild conditions and negate the generation of excessive metal waste (typically copper and silver), highlighting the potential for large-scale synthesis using these catalytic systems. Excellent control over regioselectivity and stereoselectivity has been exemplified through ligand design and tailored reaction conditions. Strategies based on the cleavage of N-O or N-N bonds, either appended to the directing group or used as an external, milder oxidant, have led to the assembly of structures, such as indoles, isoquinolines and isoquinolones; scaffolds which are prevalent in natural products, agrochemicals and pharmaceuticals. Such powerful C-H activation methodologies will undoubtedly prove to be invaluable in future synthetic protocols.

1.15 Project Aims

A principle aim of the project is to develop a rhodium(III)-catalysed C-H activation protocol suitable for electron-rich alkenes — substrates that have not been as extensively explored in comparison to electron-deficient and electron-neutral alkenes and alkynes. Incorporation of an internal oxidant based system could provide a mild, expedient route to these compounds, compared with traditional syntheses. Currently, very little is understood about the regioisomeric preference of electron-rich alkenes, particularly in systems that employ internal oxidants. The initial aim of the project is to investigate the regioselectivity and reactivity of vinyl acetates and vinyl ethers as acyl anion or enolate equivalents under rhodium(III) C-H activation conditions, using an internal oxidant which favours a β-hydride elimination pathway (Scheme 1.41). Reaction *via* an enolate equivalent would provide a route to the α-aryl carbonyl motif, one that is difficult to achieve using traditional methodologies.

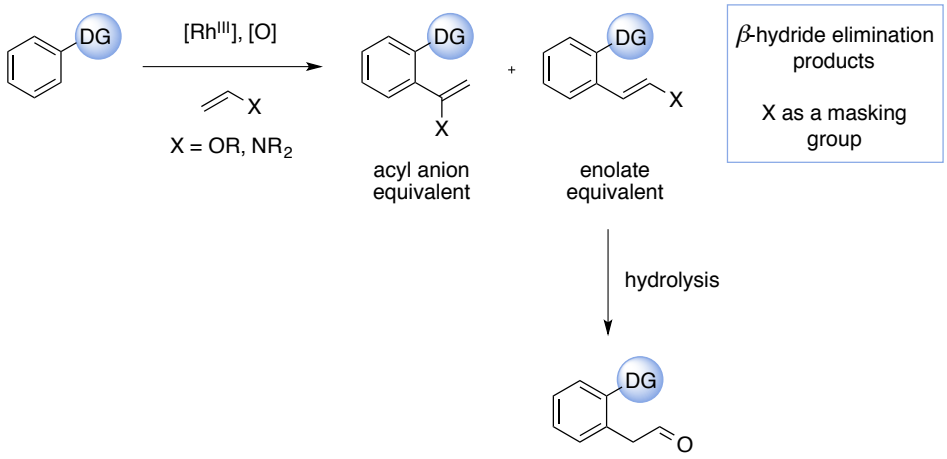

Scheme 1.41. Enamines and enol ethers/esters used as enolate equivalents using a directing group that favours β-hydride elimination.

Additionally, exploitation of the divergent pathways observed for various internal oxidants could be used with these electron-rich alkenes as a way of constructing heteroaromatic compounds with a functional handle for further diversification (Scheme 1.42).

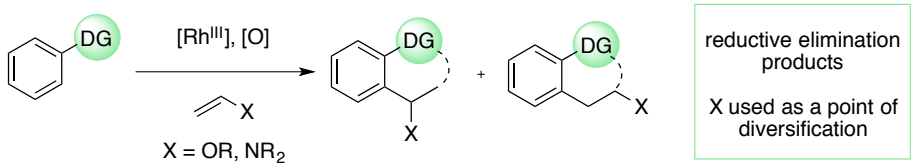

Scheme 1.42. Reductive elimination of enamines and enol ethers/esters to afford functionalised heterocycles.

Chapter 2

Rhodium-mediated C-H activation-annulation reactions with electron-rich alkenes

2.1 Introduction

In recent years, C-H activation methodologies using the rhodium catalyst, $[Cp^*RhCl_2]_2$, have been shown to tolerate a breadth of alkene and alkyne substrates with a variety of directing groups to furnish a myriad of heterocycles, generally with excellent yields. However, external oxidant-based systems, using $[Cp^*RhCl_2]_2$, rely on stoichiometric metal oxidants and precious metal additives, generally in sealed systems using super-heated solvents. As they stand, these systems are limited to small-scale synthesis and are not applicable for the large-scale manufacture of fine chemicals/pharmaceuticals. On the other hand, systems using internal oxidants allow for milder reaction conditions, lower catalyst loadings, and the reactions themselves produce organic-based waste products. The lower catalyst loadings and the inexpensive organic starting materials have great potential for process scale-up. Therefore continuous development of the existing systems is important if economically viable synthetic routes are to be used.

Reactions of this type have been thoroughly exemplified using electron-deficient and electron-neutral alkenes and alkynes. However, there is a paucity of examples using electron-rich alkenes (e.g. enamines and enols). To our knowledge, there was only a single example in the literature using an electron-rich alkene in a C-H coupling reaction of this type; Fagnou and co-workers used *N*-(pivaloyloxy)benzamide **43** in a reaction with 2,3-dihydrofuran **121**, an enol ether to give the dihydroisoquinolones **122** and **123** (>20:1 of **122:123**, Scheme 2.1).[34]

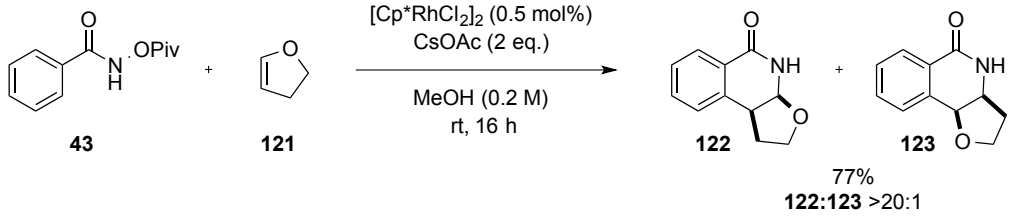

Scheme 2.1

This reaction allowed us to envisage a way to utilise this system for the coupling of electron-rich alkenes, with the potential to capture enol equivalents as a way of achieving the α-aryl carbonyl motif (Scheme 2.2).

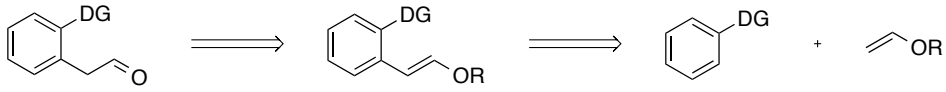

Scheme 2.2

Examples of natural products and medicinal remedies that display this *α*-aryl carbonyl bond include atropine **124**, gustastatin **125** and naproxen **126** (Figure 2.1). Atropine **124**, an alkaloid isolated from *Atropa Belladonna*, is used as an anticholinergic agent at muscarinic receptors;[74] gustastatin **125**, has potential capabilities as a human cancer cell growth inhibitor;[75] and naproxen **126** is a nonsteroidal anti-inflammatory drug.[76]

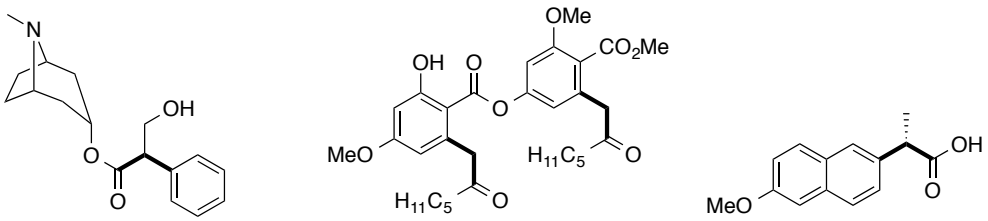

Figure 2.1

Despite its presence in numerous natural products and pharmaceutical agents, current methods of installing the *α*-aryl carbonyl motif suffer from multi-step sequences or installation of requisite disposable functionality, which is often expensive and environmentally unfriendly. The original aim of this investigation was to develop a C-H activation methodology for the coupling of enol/enolate equivalents with aromatic systems in order to introduce the *α*-aryl carbonyl motif.

2.2 Results and discussion

To commence our study, benzhydroxamic acid **127** and a range of hydroxamic esters **42, 43** and **128** were prepared according to literature procedures,[35,36] and subsequently treated with three illustrative enol/enamine equivalents (*n*-butyl vinyl ether, *N*-vinyl pyrrolidinone and vinyl acetate) using the conditions reported by the groups of Glorius and Fagnou; $[RhCp^*Cl_2]_2$ (1 mol%) with cesium acetate (30 mol%) in methanol at 60 °C.[34,36]

Reactions of benzhydroxamic acid **127** and *N*-(methoxy)benzamide **42** with *n*-butyl vinyl ether **129** were unsuccessful (entries 1 and 2, Table 2.1). In contrast, *N*-(acetoxy)- and *N*-(pivaloyloxy)benzamide, **128** and **43**, furnished the benzylic ether dihydroisoquinolone **130** as a single regioisomer, with a yield of 32% and 35% respectively (entries 3 and 4). The hemiaminal **131** was not observed in the ^{1}H NMR spectrum of the crude reactions. The regiochemistry of the isomer **130** was confirmed by ^{1}H NOESY NMR (Appendix 1.1).

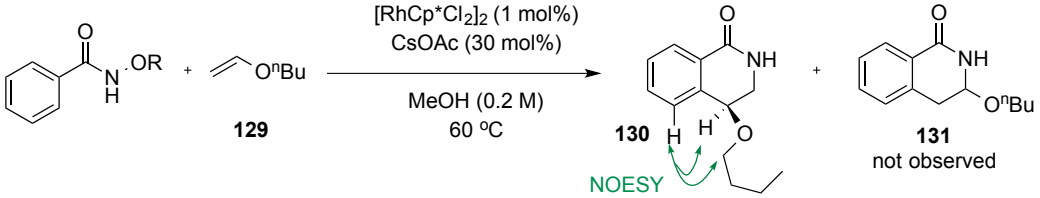

Entry	R	No.	Time (h)	Product (%) A	B
1	H	**127**	16	-	-
2	Me	**42**	16	-	-
3	Ac	**128**	48	32	-
4	Piv	**43**	48	35	-

Table 2.1. Yields of isolated products.

Reactions using *N*-vinyl pyrrolidinone **132** with the benzhydroxamic acid/esters **42**, **43**, **127** and **128**, were unsuccessful. Recovered *N*-vinyl pyrrolidinone and a single side product were isolated from the crude reaction using *N*-(acetoxy)- and *N*-(pivaloyloxy)benzamides, **128** and **43**. This isolated side product had also been observed in the crude ^{1}H NMR spectrum of the previous reactions with *n*-butyl vinyl ether **129**. Analysis of the product identified the compound as methyl phenyl carbamate **133**, presumably formed *via* a competing Lossen rearrangement (Scheme 2.3).[77–79]

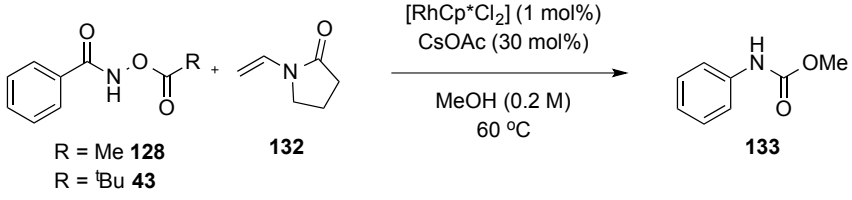

Scheme 2.3

2.3 The Lossen rearrangement

The base-mediated, thermal Lossen rearrangement typically requires benzhydroxamic acid derivatives as substrates.[77–79] Initial deprotonation of the hydroxamate ester **134** is followed by a rearrangement of a transient acyl nitrenoid **135** to give the intermediate isocyanate **136** (Scheme 2.4).

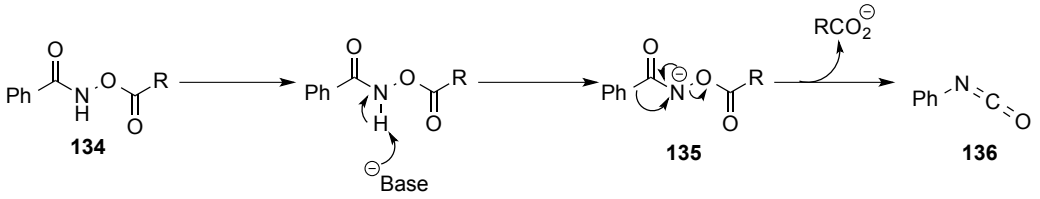

Scheme 2.4

Despite the toxicity associated with isocyanates, they are highly reactive, valuable intermediates that can be readily transformed *via* trapping of a nucleophile or, in the case of water as the nucleophile, degradation to the respective amine under aqueous conditions. Under our reaction conditions, solvent trapping with methanol furnished the methyl phenyl carbamate **133**.

In order to identify whether this reaction in our system was base or catalyst-induced, time-dependent ^{1}H NMR experiments were undertaken (Figure 2.2). The control reaction, using *N*-(pivaloyloxy)benzamide **43** and cesium acetate (30 mol%) in deuterated methanol-d_4, showed only unreacted starting material after four hours. Addition of the rhodium catalyst ($[RhCp^*Cl_2]_2$, 1 mol%) led to 100% conversion to the methyl phenyl carbamate-d_4 **133** within four hours at 60 °C, suggesting a metal-catalysed Lossen rearrangement.

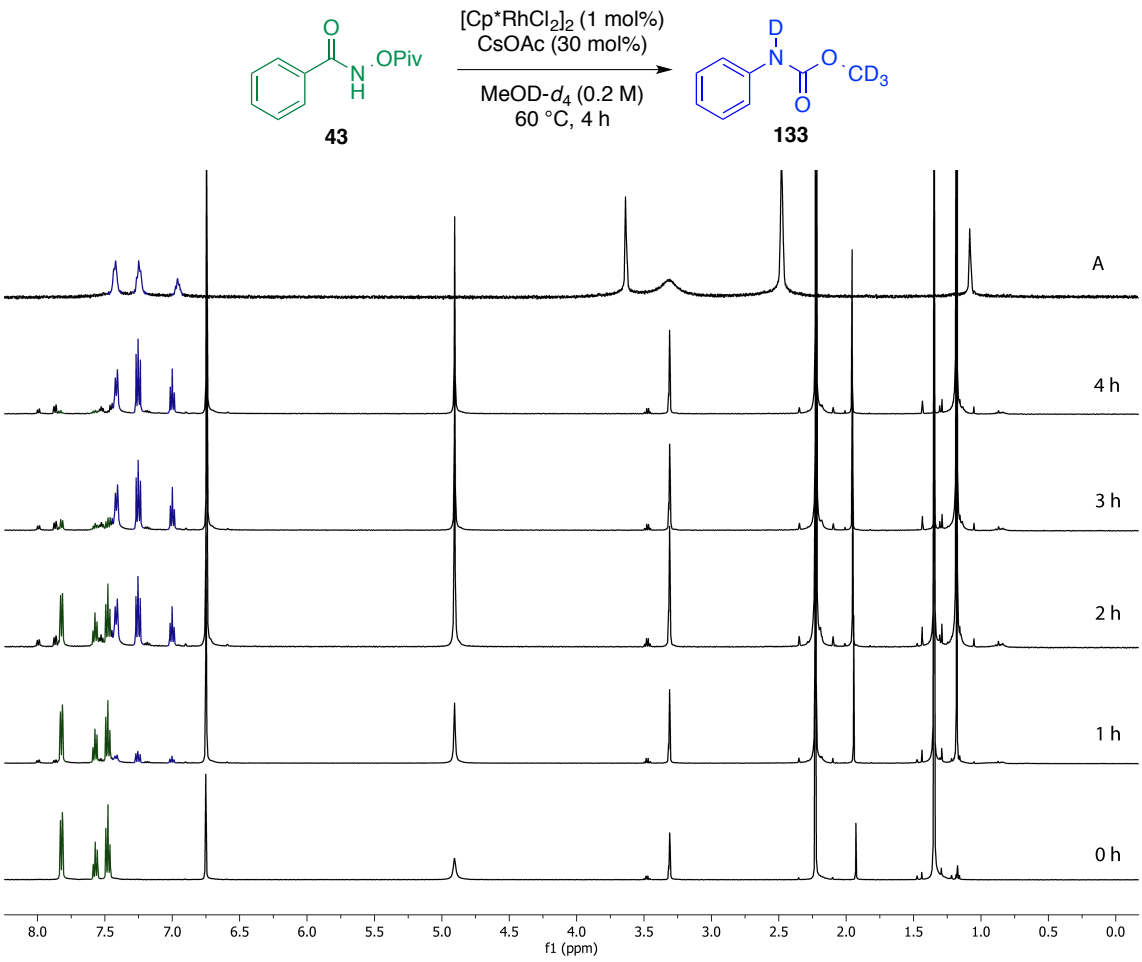

Figure 2.2. Time-dependent ^{1}H NMR study in MeOD-d_4 (500 MHz, 60 °C) Mesitylene singlets appear at δ 6.75 and 2.23 (internal standard). Spectrum A shows an authentic sample of methyl phenyl carbamate-d_4 in MeOD-d_4.

Complexation of the hydroxamate ester **43** with the rhodium catalyst would reduce the pK_a of the NH proton, allowing for deprotonation (by cesium acetate) and subsequent rearrangement to give the isocyanate **136** (Scheme 2.5). Hydroxamic acids are known to facilitate coordination to certain metal ions;[80] this interaction has been exploited in drug molecules whereby the hydroxamic acid is crucial for selectivity when there is a metal ion in an active site.[81,82] To lend further credibility to our theory, Roithová *et al*. reported a metal-assisted Lossen rearrangement, using basic salts of zinc and potassium, where the reaction proceeds *via* the metallated hydroxamate.[80,83]

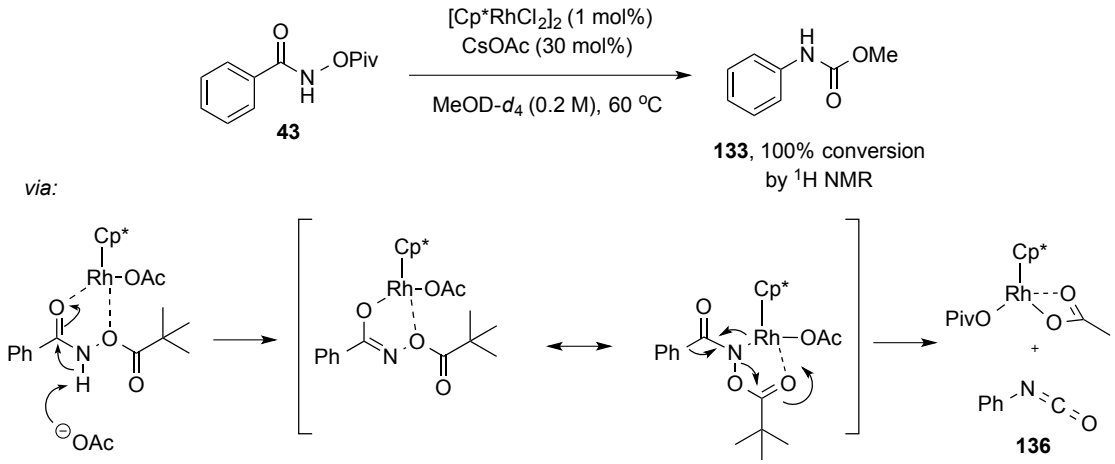
[Cp*RhCl2]2 (1 mol%)
CsOAc (30 mol%)
MeOD-d4 (0.2 M), 60 °C
OPiv
OMe
43
133, 100% conversion
by 1H NMR
via:
Cp*
Rh-OAc
Ph
OAc
PivO
136

Scheme 2.5

2.4 Optimisation study of enol ether substrates

An optimisation study was undertaken to simultaneously reduce the reaction time, increase the yield of the desired product and decrease the formation of the Lossen product. Temperature, substrate equivalents and reaction concentration were chosen as the three variables in an optimisation study. The upper and lower limits were selected as 30 °C and 50 °C, 1.5 and 5 equivalents of *n*-butyl vinyl ether **129** and reaction concentrations of 0.2 M and 1.0 M. For each of the experiments a ^{1}H NMR spectrum of the crude reaction mixture was taken after 16 hours to assess the conversion to methyl phenyl carbamate **133**, isoquinolone **137** and the ratio of regioisomers **130** and **131**. Each reaction was subsequently purified to obtain isolated yields of the dihydroisoquinolones. In order to monitor the reproducibility of the reactions, a mid-point experiment (40 °C, 0.6 M and 3.25 equivalents of *n*-butyl vinyl ether) was repeated to evaluate the continuity across the reaction series. Table 2.2 outlines the results collated from analysis of the ^{1}H NMR spectra of the crude reactions and the isolated yields of the regioisomers **130** and **131**. Significantly more carbamate **133** was observed at 50 °C (entry 5-8) compared with the reactions at 30 °C (entry 1-4). Additionally, the ^{1}H NMR data indicated that higher temperatures led to formation of the isoquinolone **137**, presumably from the thermal degradation of the benzylic ether **130** and/or the aminoacetal derivative **131**.

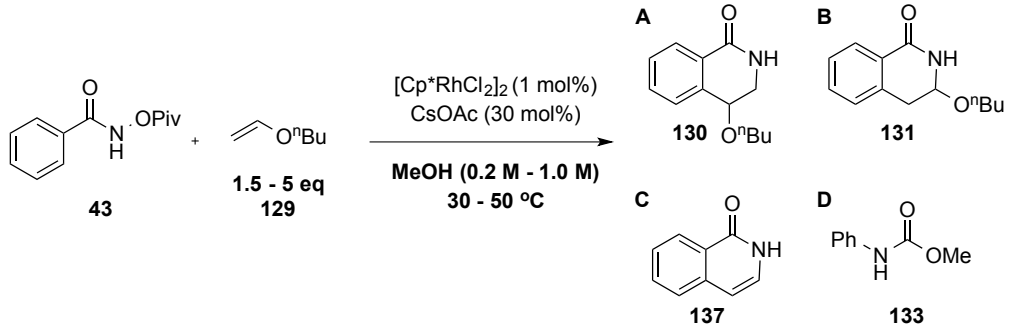

Entry	Variables: Temp (°C)	Variables: Conc (M)	Variables: Equiv 129	Ratio of products (by ^{1}H NMR): A	B	C	D	Ratio (A-C):D	Yield[a] % A+B
1	30	0.2	1.5	75	21	0	4	96:4	50
2	30	0.2	5	73	25	0	2	98:2	**76**
3	30	1	1.5	83	16	0	1	99:1	69
4	30	1	5	77	22	0	1	99:1	**74**
5	50	0.2	1.5	45	10	5	40	60:40	33
6	50	0.2	5	59	16	6	19	81:19	51
7	50	1	1.5	66	11	14	9	91:9	49
8	50	1	5	62	19	14	5	95:5	64
9	40	0.6	3.25	71	26	0	3	97:3	62
10	40	0.6	3.25	71	25	0	4	94:4	68

Table 2.2. [a]Yields of isolated products.

Following purification by flash column chromatography, traces of the isoquinolone **137** were observed in the ^{1}H NMR spectra of the benzylic ether **130** (the major regioisomer). Comparison of the R_F values revealed similarities between the isoquinolone **137** and the major regioisomer **130**. To unambiguously identify which regioisomer eliminated butanol to form the isoquinolone **137**, two pure samples (>95% purity by ^{1}H NMR) of regioisomers **130** and **131** were stirred with silica gel in $CDCl_3$ overnight (Scheme 2.6). The results indicated that the isoquinolone had formed from the aminoacetal **131**, not from elimination from the benzylic ether **130**.

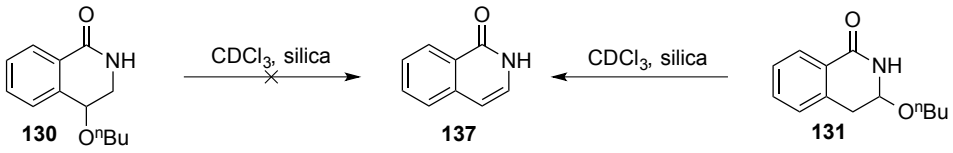

Scheme 2.6.

A reduction in temperature (30 °C) and use of excess *n*-butyl vinyl ether (5 eq.) produced the highest yield of 76% in 16 hours (*cf.* entry 2, Table 2.2) and 74% at a higher reaction concentration (1 M) (*cf.* entry 4, Table 2.2). Using the optimised conditions outlined in entry 4, the reaction was repeated with a ten-fold reduction in the rhodium precatalyst loading to 0.1 mol% (Scheme 2.7). Disappointingly, complete conversion was not achieved after 72 hours. Analysis of the ^{1}H NMR spectrum of the crude reaction mixture revealed 20% unreacted *N*-(pivaloyloxy)benzamide **43**, 64% conversion to the regioisomers **130** and **131** and 6% conversion to the methyl phenyl carbamate **133**. The material was purified to give 59% of the two regioisomers. Although full conversion was not achieved, a ten-fold reduction in catalyst loading produced 59% of the desired product with a turnover number (TON) of 590 compared with 74 from the reaction with 1 mol% of the catalyst (entry 4).

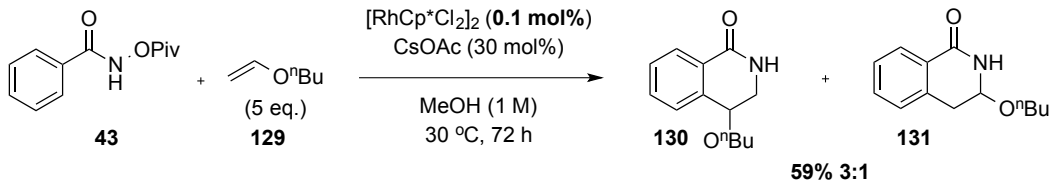

Scheme 2.7. Reduction in catalyst loading from 1 mol% to 0.1 mol%.

The conditions used in entry 2 (*cf.* Table 2.2) were applied to the reaction of ethyl vinyl ether **138** with *N*-(pivaloyloxy)benzamide **43**, resulting in an 87% yield of a 3:1 mixture of 4-ethoxy and 3-ethoxy-3,4-dihydroisoquinolin-1(*2H*)-ones **139** and **140** (Scheme 2.8).

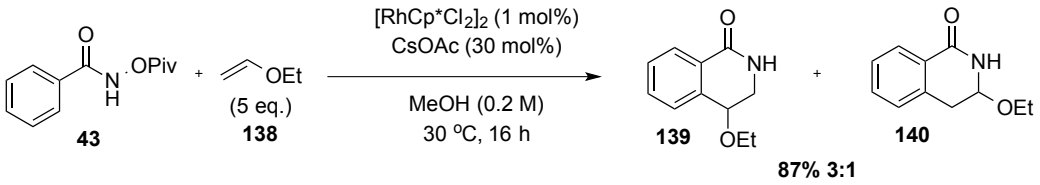

Scheme 2.8

2.5 Regiochemical considerations

Curiously, the regioselectivity observed throughout the experimental design study contrasted with the regioselectivity that Fagnou *et al.*[34] had reported with an analogous example (2,3-dihydrofuran **121**), wherein the aminoacetal regioisomer **122** was reported as the major product (Scheme 2.9). This difference in regioselectivity of the disubstituted versus the monosubstituted alkene would suggest a contrasting influence of steric effects *versus* electronic preference.

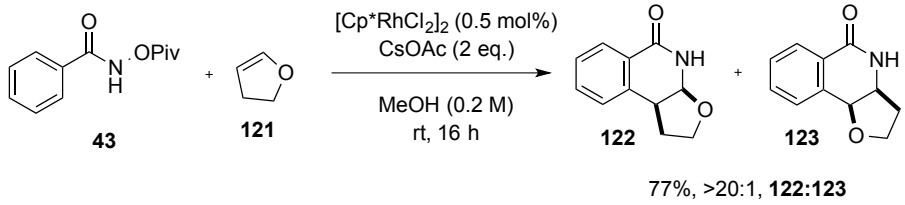

Scheme 2.9.[34] *Repeat of Fagnou's conditions to investigate the regioselectivity of 2,3-dihydrofuran **121**.*

In order to verify the regioselectivity observed in Fagnou's study,[34] the reported reaction conditions were repeated with 2,3-dihydrofuran **121** and *N*-(pivaloyloxy)benzamide **43** to meticulously investigate the structural assignment (Scheme 2.10). The spectral data reported in their study and the spectral data of the major regioisomer, isolated from our preparative experiment, matched accordingly. However, analysis of the ^{1}H NOESY NMR spectrum of the same material revealed inconsistencies with their assignment. The ^{1}H NOESY spectrum revealed two key interactions: a correlation between a doublet (δ 4.85 ppm H_d) with an aromatic proton and an overlapping ddd, resembling a broad triplet (δ 4.85 ppm H_c) with the NH proton, suggesting the regioisomer **123** (Scheme 2.10). Isolation and ^{1}H NOESY NMR analysis of the minor regioisomer revealed additional evidence for our assignment of the aminoacetal **122** as the minor regioisomer. The doublet H_a (δ 5.57 ppm) appeared downfield of the corresponding doublet H_d (δ 4.85 ppm) (Scheme 2.10). The downfield shift was expected considering its deshielded position at the junction of two electronegative heteroatoms. Additionally the ^{1}H NOESY NMR spectrum identified a correlation between the same doublet (H_A) with the NH proton (Appendix 1.1).

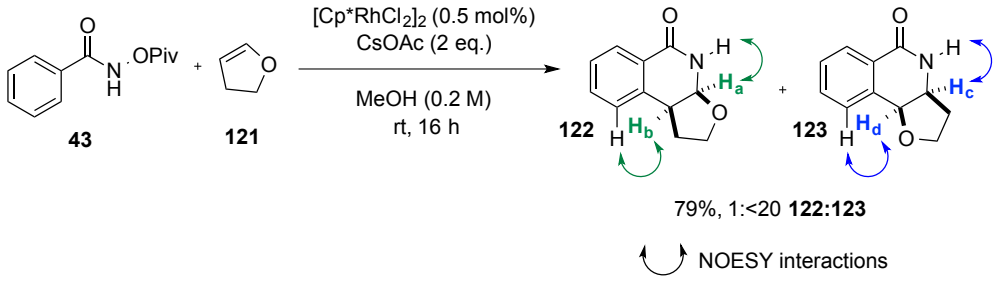

Scheme 2.10

Final confirmation of the structure was obtained *via* the collection of crystallographic data of the major regioisomer **123** (Figure 2.3, Appendix 1.1), validating our regiochemical assignment compared to the hemiaminal structure reported by Fagnou *et al.* (*cf.* Scheme 2.9).[34]

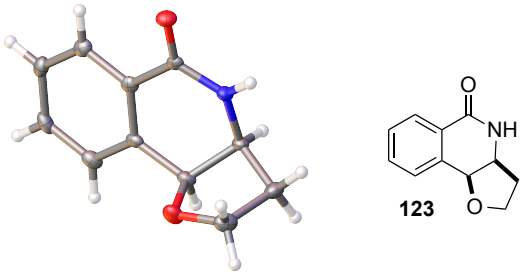

Figure 2.3

2.6 C-H activation/annulation with vinyl esters

Having optimised the annulation reaction using vinyl ethers, we were interested in exploring alternative electron-rich alkenes. Using the aforementioned screening conditions for vinyl ethers (see Table 2.1), the analogous *O*-acetylated compounds from vinyl acetate were expected to form (Table 2.3). However, the sole products from the reactions, using the benzhydroxamic acid and the *N-(*acetoxy/pivaloyloxy)benzamide, were isoquinolone **137** and the methyl phenyl carbamate **133** (entries, 1, 3 and 4). Decreasing the reaction temperature to 45 °C supressed the competing Lossen rearrangement to afford the isoquinolone **137** with a yield of 87% (entry 6). Conducting the reaction at room temperature produced the same yield, however the reaction required 72 hours to reach completion (entry 5). The isoquinolone product presumably arises from elimination of acetic acid from a dihydroisoquinolone intermediate **142** and is the synthetic equivalent of a direct hydroxamate/alkyne annulation reaction using acetylene as the alkyne. Gaseous ethylene has been used by the groups of Fagnou[35] and Glorius[36] to furnish 3,4-dihydroisoquinolones. However, to our knowledge, the use of gaseous alkynes in annulation reactions has not been investigated, and given the hazards and operational difficulties associated with such a process, the availability of a synthetic equivalent would be of great utility.

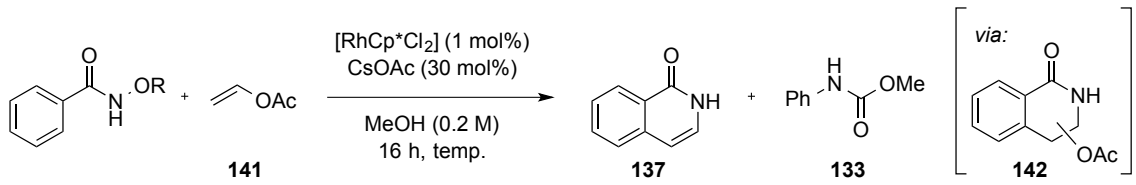

141 137 133 142

Entry	R	No	Temp. (°C)	Isolated Yield (%)	Conversion ^{1}H NMR 133 (%)
1	H	**127**	60	26	17
2	Me	**42**	60	-	0
3	Ac	**128**	60	79	15
4	Piv	**43**	60	69	11
5	Piv	**43**	rt	87[a]	0
6	Piv	**43**	45	87	0

Table 2.3. [a]72 hours.

Based on our previous observations and the reported ineffectiveness of the benzhydroxamic acid **127** as an internal oxidant,[34] the formation of the isoquinolone was surprising (entry 1, Table 2.3). In the presence of vinyl acetate and cesium acetate, we rationalised that the benzhydroxamic acid **127** could be acetylated during the reaction, thus forming the more

reactive substrate, *N*-(acetoxy)benzamide **128**. Analysis of the final crude reaction mixture by ^{1}H NMR indicated the presence of the Lossen product **133**, isoquinolone **137** and starting material **127**. Further investigation using a ^{1}H NMR time-course experiment identified that *N*-(acetoxy)benzamide **128** was formed *in situ*, before any signals corresponding to the isoquinolone **137** and methyl phenyl carbamate **133** were observed, supporting our proposition (Figure 2.4).

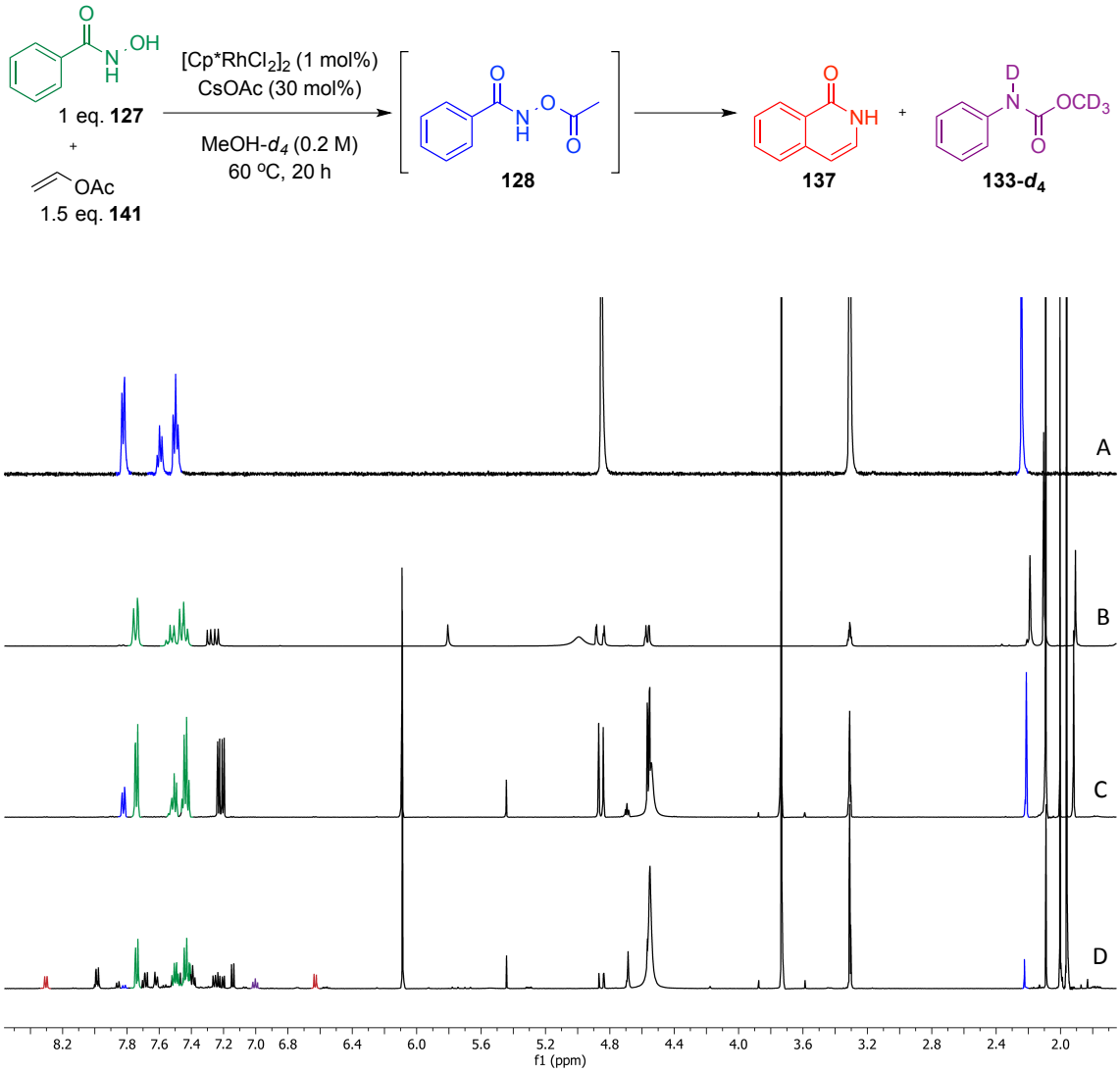

Figure 2.4. A) An authentic sample of *N*-(acetoxy)benzamide **128** in MeOD-d_4 B) 'Zero hour' ^{1}H NMR spectrum of the reaction. C) 'One hour' ^{1}H NMR spectrum. D) '16 hour' final ^{1}H NMR spectrum. Diagnostic peaks are highlighted in colour.

The various reaction components were monitored in a time course ^{1}H NMR study, over a period of 16 hours, using trimethoxybenzene as an internal standard (Figure 2.5). Within the first 15 minutes, depletion of the benzohydroxamic acid **127** (60%) coincided with formation of *N*-(acetoxy)benzamide **128** (31%), when the yield plateaued. Formation of the products (the Lossen-derived carbamate **133** and the isoquinolone **137**) were identified after 40 minutes as the concentration of *N*-(acetoxy)benzamide **128** began to decrease. After 16 hours the isoquinolone

137 and carbamate **133** were formed with yields of 17% and 10%, respectively. The delay in product formation, which coincided with a decrease in the transient hydroxamic ester, suggests that **128** is the true reactive species in the rhodium-catalysed annulation reactions.

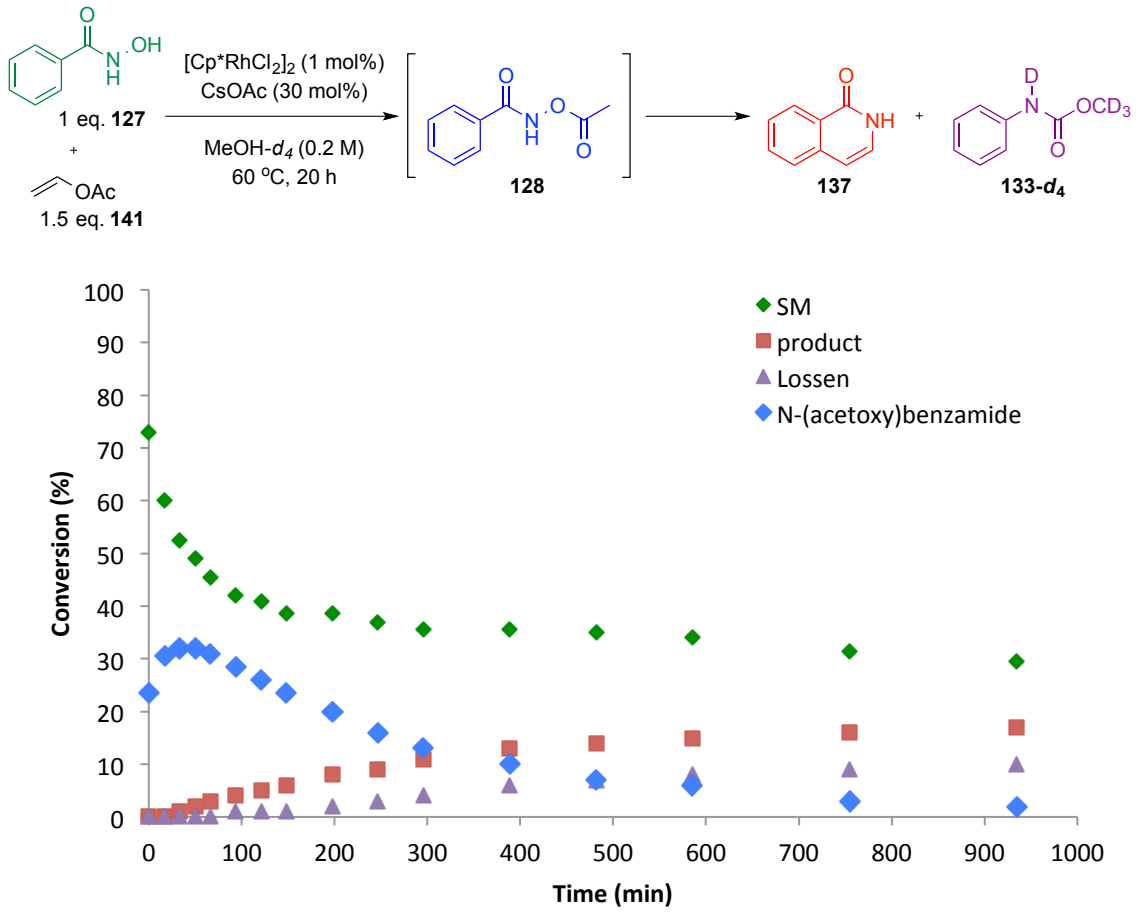

*Figure 2.5. ^{1}H NMR study of the formation and consumption of N-(acetoxy)benzamide **128** in situ. Legend: SM (**127**), product (**137**), Lossen (**133**) and N-(acetoxy)benzamide (**128**).*

2.7 A divergent mechanistic pathway

Based on our previous results with *N*-methoxybenzamide **42** in the internal oxidant screens, the isolation of unreacted starting material was expected; however a new product was identified, due to its strong blue fluorescence observed on examination of the TLC plate under a UV lamp (Scheme 2.11). Isolation of the tetracylic imide **143** returned a meagre 6% yield (the remaining crude reaction mixture contained unreacted starting material), however we were interested in optimising the synthesis due to the potential application of blue fluorescent compounds in organic light emitting diodes (oLEDs) and photovoltaic devices. Analysis of the compound identified the structure as isoindolo[2,1-*b*]isoquinoline-5,7-dione **143**, which had previously been reported *via* different synthetic routes (discussed in Chapter 5) without mention of its fluorescent properties.[84–88]

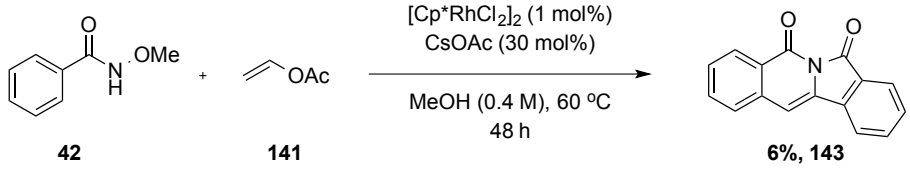

Scheme 2.11

The divergent mechanistic pathways of *O*-acylated hydroxamic acids (**128** and **43**) compared with *N*-methoxybenzamide **42** are well documented,[34,37,89,90] rationalising the formation of **143** as being a novel compound. Subsequent mechanistic studies, route optimisation and fluorometry data are discussed in Chapter 5.

2.8 Rate study: a comparison of reactivity

In order to compare the rate of the Lossen rearrangement to the C-H activation reaction, a time course ^{1}H NMR experiment at 333 K (60 °C) was undertaken (Figure 2.6). Using trimethoxybenzene as an internal standard, the reactions were monitored over 16 hours, (Figure 2.6). In less than four hours, the reaction of *n*-butyl vinyl ether **129** and *N*-(pivaloyloxy)benzamide **43** at 60 °C was complete (A, Figure 2.6). Within the first hour, 23% of the desired product **130** had formed and slowly increased to 26% over the next hour. In contrast, the formation of the methyl phenyl carbamate **133** rapidly increased to 40% over the first hour, continuing to rise to 58% by the end of the reaction. It should be noted that the reaction yield of **130** for the preparative experiment (1 mmol scale) was 35% (see Table 2.1). The difference in yield could be attributed to the scale of the reaction. To compare the reactivity of the alkene substrates, a reaction using vinyl acetate **141** and *N*-(pivaloyloxy)benzamide **43** was monitored (**B**, Figure 2.6).

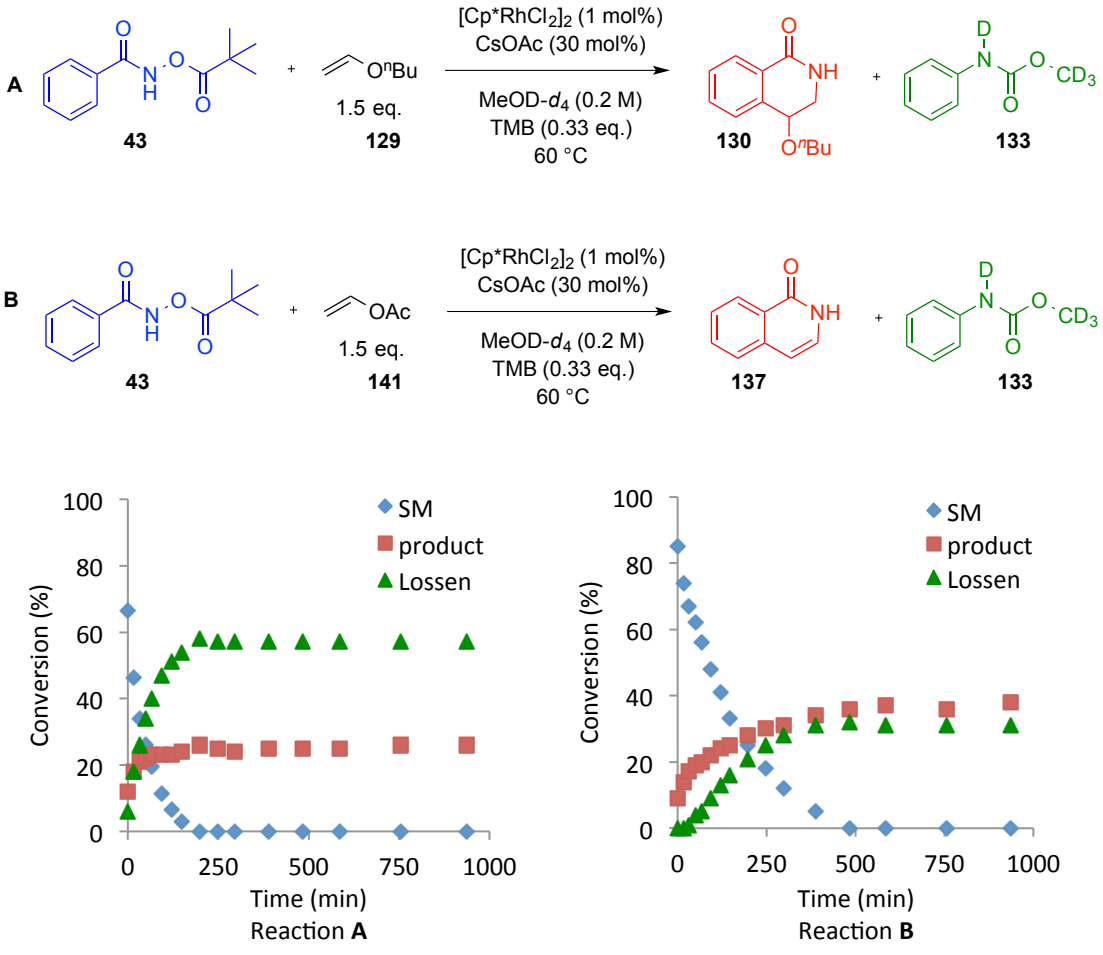

*Figure 2.6. ^{1}H NMR experiment (500 MHz, 333K, MeOD-d_4) to monitor the formation of methyl phenyl carbamate **133** compared to 4-butoxy-3,4-dihydroisoquinolin-1(2H)-one **130** (reaction A) or isoquinolone **137** (reaction B). Average values plotted for reaction B from two iterations.*

After eight hours, the starting material had been consumed to give the isoquinolone **137** (36%) and the Lossen carbamate **133** (32%). In the first hour, 20% of the isoquinolone had formed with only 5% of the carbamate **133** present.

The rate at which the Lossen product formed in the butyl vinyl ether reaction was significantly faster than the reaction with vinyl acetate. After one hour, 4% of the carbamate had formed in reaction B, compared to 40% in reaction A. It should be noted that the reaction yield of the isoquinolone **137** for the preparative experiment (1 mmol scale) was 69% (see Table 2.3) compared with this yield of 32%, which could be a result of the scale of the reaction. One could argue that the acetate group of vinyl acetate prevents electron donation into the vinylic portion of the molecule compared with *n*-butyl vinyl ether, which has increased electron density due to the inductive effect of the alkyl chain. Another possibility could be the accelerating effect of coordination of the acyl group of vinyl acetate to the rhodium centre (see Section 3.6.3 for further discussion). This difference in reactivity suggests electron-rich alkenes are not favourable substrates under these reaction conditions.

Interestingly, within the first ten minutes of both reactions, the desired annulated products were identified in the 'zero hour' ^{1}H NMR spectra with no trace of the methyl phenyl carbamate in the reaction with vinyl acetate and only 6% present in the reaction with butyl vinyl ether, indicating rapid reaction of the vinylic substrates. Based on this observation, the two preparative reactions were repeated at room temperature. Reaction of vinyl acetate with *N*-(pivaloyloxy)-benzamide **43** gave an encouraging yield of 87% (compared to a 76% yield at 30 °C, entry 2, Table 2.2), however the reaction took 72 hours to complete. Increasing the temperature to 45 °C reduced the reaction time to 16 hours, with yield of 87% (*cf.* Table 2.2). The reaction of *n*-butyl vinyl ether at room temperature furnished the dihydroisoquinolone products with a 77% yield of the two regioisomers (3:1, **130:131**) over 72 hours.

2.9 Conclusion

In summary, both reactions with vinyl esters and vinyl ethers were optimised to afford high yields, by selection of the internal oxidant and optimisation of the reaction conditions. The acyl hydroxamates, *N*-(acetoxy)- and *N*-(pivaloyloxy)benzamide, were identified as the most reactive substrates, however a competing reaction (Lossen rearrangement) was identified using these acylated hydroxamates. Based on the inactivity of the *N*-methoxybenzamide derivative, the reactivity of the benzhydroxamic acid was suprising. A ^{1}H NMR time-course study revealed *in situ* formation of *N*-(acetoxy)benzamide from the reaction of benzhydroxamic acid and vinyl acetate, suggesting the true reactive species.

The competing Lossen rearrangement was identified as a rhodium-catalysed process (using a ^{1}H NMR study), which was subsequently minimised by a reduction in the reaction temperature. Using experimental design, the annulation of butyl vinyl ether with *N*-(pivaloyloxy)benzamide was optimised from 35% to 76%. The annulation of vinyl acetate to give 3,4-unsubstituted isoquinolones was optimised from 69% to 86% by decreasing the reaction temperature to 45 °C.

Finally, the regiochemical preference of vinyl ethers to form the benzylic ether dihydroisoquinolones was confirmed with ^{1}H NMR NOESY studies and X-ray diffraction analysis on a single crystal of **123**, to disprove a previously reported assignment.[35] Comparison of the rates of reaction of the vinyl enol ethers *versus* the vinyl enol esters suggests that electron-rich substrates are less favourable under these reaction conditions.

Chapter 3

Rhodium(III)-catalysed synthesis of isoquinolones

3.1 Introduction

Isoquinolin-1(2*H*)ones are of significant interest due to their prevalence in alkaloidal natural products and synthetic therapeutic agents;[91–95] illustrative examples include anti-cancer agents **144**,[91] biological ligands **145**,[93] respiratory medicines **146**,[96] and hepatitis C intermediates **147**[97] (Figure 3.1).

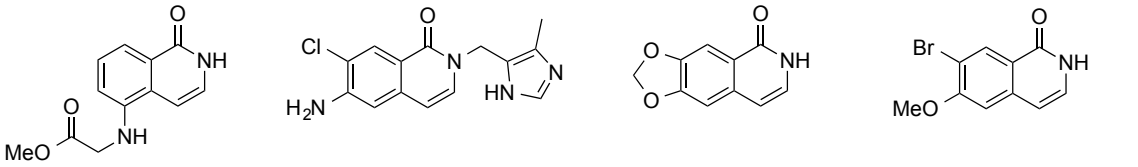

Figure 3.1

Traditional approaches to isoquinolones from *mono*functionalised arene starting materials include thermal rearrangement/electrocyclisations of cinnamoyl azides **148**,[98–100] intramolecular Friedel-Crafts reactions of benzamidoalkyl acetals **149**,[101] or multi-step approaches involving reaction of *ortho*-lithiated benzamide derivatives **150** with α-dicarbonyl compounds **151** (Scheme 3.1).[102]

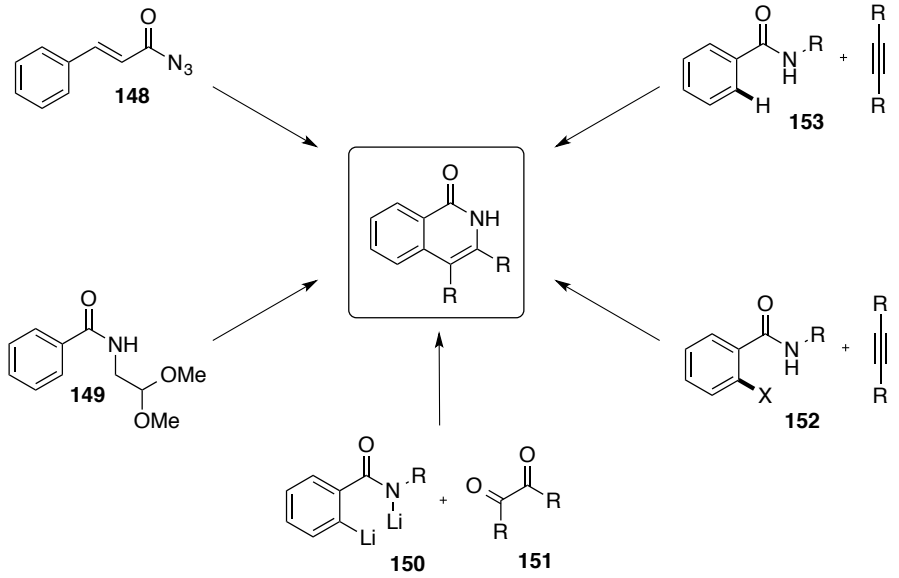

Scheme 3.1

Alternative routes require *ortho*-difunctionalised benzene precursors from which the heterocyclic ring can be further elaborated.[103] Systems using palladium,[104] nickel[105,106] and

copper[107] catalysts have been developed for cross-coupling reactions with 2-halobenzamides **152** with alkynes to afford substituted isoquinolones. These systems were rapidly surpassed by atom-efficient C-H activation protocols;[21,108,109] eliminating the requirement for bespoke halogenated starting materials e.g. **153**. Rhodium-catalysed C-H activation protocols typically require stoichiometric copper acetate as an oxidant to complete the catalytic cycle. Additionally, harsh conditions are required for C-H activation and large quantities of metal waste are generated. These systems have been superseded by the introduction of benzoyl hydroxamic ester derivatives as substrates by the groups of Fagnou[34,35] and Glorius,[36] allowing for mild conditions and organic based waste streams.

Although substituted isoquinolones have been thoroughly exemplified, 3,4-unsubstituted isoquinolones have not. To our knowledge, there are only two transition-metal catalysed examples, both of which rely on an annulation step with norbornadiene followed by a retro-Diels-Alder reaction to form the 3,4-unsubstituted isoquinolone (Scheme 3.2). Lautens *et al.*[104] used benzyl-protected 2-halobenzamides **154** in their palladium-catalysed annulation reaction at 130 °C, using norbornadiene as a co-solvent, to furnish seven isoquinolones **156** with an average yield of 42%. Fagnou *et al.*[35] reported a two-step synthesis to prepare the fused norbornene dihydroisoquinolone product **157** (91% yield) using an 'internal oxidant' based system, followed by a thermal retro-Diels-Alder reaction at 170 °C to give the corresponding isoquinolone **137**.

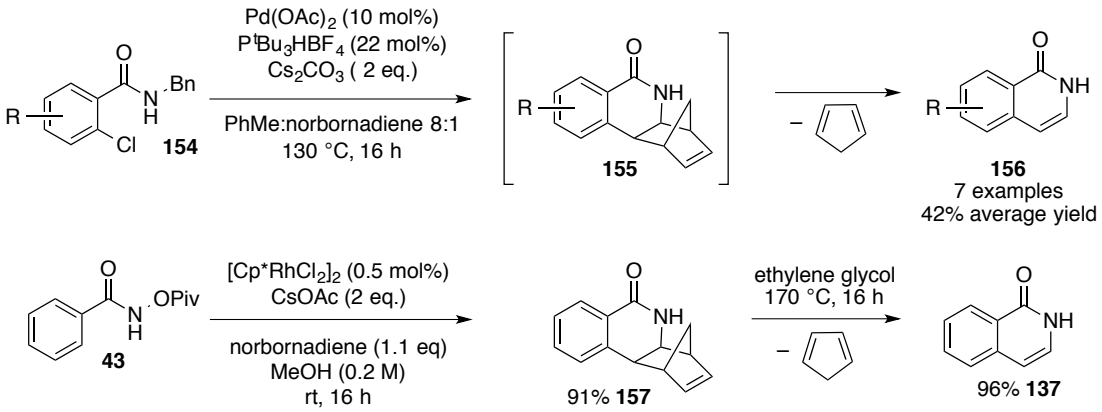

Scheme 3.2

Avoiding these high temperature rearrangements and incorporating a C-H activation protocol, using our rhodium-catalysed coupling of substituted *N*-(pivaloyloxy)benzamides with vinyl acetate, would offer a beneficial alternative. This reaction is the synthetic equivalent of a direct hydroxamate/alkyne annulation reaction using acetylene as the alkyne. To our knowledge, the use of gaseous alkynes in C-H activation/annulation reactions has not been investigated. Given the hazards and operational difficulties associated with such a process, the availability of a cheap and convenient synthetic equivalent such as vinyl acetate would be highly useful.[110]

3.2 Results and discussion: isoquinolone series 1

Having optimised the conditions for the synthesis of isoquinolones, we inferred that the methodology could be analogously applied to simple substituted aryl rings. A facile synthetic route was identified for the preparation of the pivalate substrates **160-167** from benzoic acids/acid chlorides, an ideal feedstock considering the low-cost and diverse substitution patterns commercially available (Table 3.1). Acid chlorides were either purchased or prepared from the equivalent acid using the Vilsmeier reagent,[111] generated from oxalyl chloride and catalytic *N,N'*-dimethylformamide. Subsequent reaction with *O*-(pivaloyloxy)ammonium chloride **158**[112] or *O*-(pivaloyloxy)ammonium triflate[35] (prepared by literature procedures), in either tetrahydrofuran with triethylamine or ethyl acetate−water (2:1) with potassium carbonate (Schotten-Baumann conditions), furnished the desired *N*-(pivaloyloxy)benzamide derivatives **160-167** (**A**, Scheme 3.3, 16-81% yield, Table 3.1).

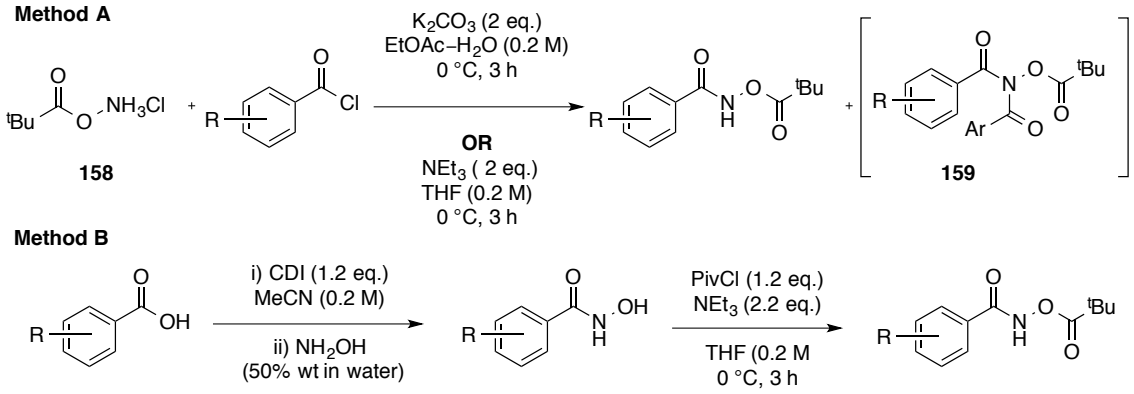

Scheme 3.3

Low yields of **161** and **162** were attributed to disubstitution of the amide **159** (**A**, Scheme 3.3). Despite increasing the equivalents of *O*-(pivaloyloxy)ammonium chloride **158** from 1 to 1.5 the side product was still identified in the reaction. It was subsequently found that replacing potassium carbonate with sodium hydrogen carbonate circumvented this disubstitution issue (see examples in Chapter 5). An alternative procedure, starting with the benzhydroxamic acid, furnished the product following acylation using pivaloyl chloride in tetrahydrofuran with triethylamine (**B**, Scheme 3.3). With a library of substrates in hand, the materials were reacted with vinyl acetate (1.5 equivalents) using the standard conditions: $[Cp^*RhCl_2]_2$ (1 mol%) and cesium acetate (30 mol%) in MeOH (0.2 M) at 45 °C for 16 hours (Table 3.1). To commence our study, *para*-substituted substrates were selected in order to avoid issues of regiocontrol (Table 3.1). Electron-deficient *p*-cyano- **161**, *p*-acetyl-, **162** and *p*-trifluoromethyl-*N*-(pivaloyloxy)-benzamides **163** reacted to give excellent 81%, 99% and 71% yields of **169**, **170** and **171**, respectively.

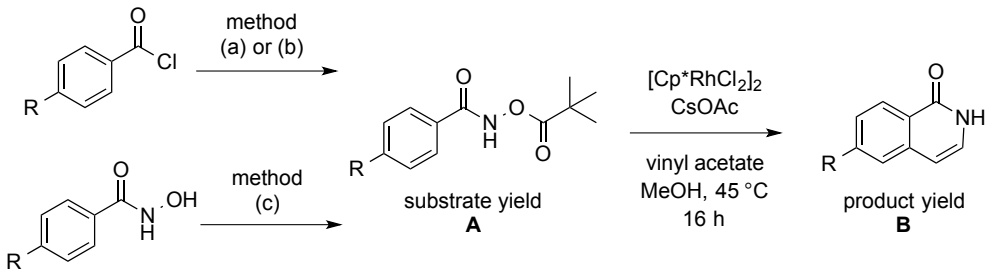

Entry	R	Yield A (%)	No.	Yield B (%)[d]	No.
1	H	88[c]	**160**	87	**168**
2	CN	16[b]	**161**	81	**169**
3	Ac	20[a]	**162**	99	**170**
4	CF_3	99[b]	**163**	71	**171**
5	OMe	81[b]	**164**	31, 63[e]	**172**
6	F	44[b]	**165**	68	**173**
7	Br	62[b]	**166**	70	**174**
8	I	47[b]	**167**	83	**175**

a) $PivONH_2$•HCl (1.1 eq.), K_2CO_3 (2 eq.), EtOAc–H_2O (2:1, 0.2 M), 0 °C, 3 h; b) $PivONH_2$•HCl (1.1 eq.), NEt_3 (2.0 eq.), THF (0.2 M), 0 °C, 3 h; c) Prepared according to a literature procedure from benzhydroxamic acid (1.0 eq.), pivaloyl chloride (1.0 eq), NEt_3 (1.2 eq.), THF, rt, 16 h.[36] d) Standard conditions for annulation: $[Cp^*RhCl_2]_2$ (1 mol%), CsOAc (30 mol%), MeOH (0.2 M), vinyl acetate (1.5 eq.), 45 °C, 16 h. d) 30 °C, 0.4 M.

*Table 3.1. Preparation of starting materials **160-167** and subsequent reaction with vinyl acetate to afford a library of isoquinolones **168-175** using the rhodium(III)-catalysed C-H activation/annulation protocol.*

Under the standard conditions, the electron-rich *p*-methoxy-*N*-(pivaloyloxy)-benzamide **164** furnished the isoquinolone **172** with a poor yield of 31% (entry 5, Table 3.1), with the remaining starting material rearranging to the Lossen carbamate. Electron-donating groups are reported to accelerate the Lossen rearrangement by increasing the electron density at the N-O bond, which consequently facilitates the release of the pivalate anion.[113,114] Additionally, Glorius *et al.* used a competition experiment to compare the reactivity of electron-deficient and electron-rich aromatic systems.[36] 4-Acetyl-*N*-methoxybenzamide **176** and 4-methoxy-*N*-methoxy-benzamide **177** were treated with styrene **4** under their standard reaction conditions (Scheme 3.4). After 7 minutes, the reactions were quenched and analysis of the ^{1}H NMR spectrum of the crude material revealed 28% conversion to the 4-acetyl-stilbene derivative **178** and only 9% of the 4-methoxy-stilbene product **179**, suggesting C-H insertion into electron-rich systems is less favourable.

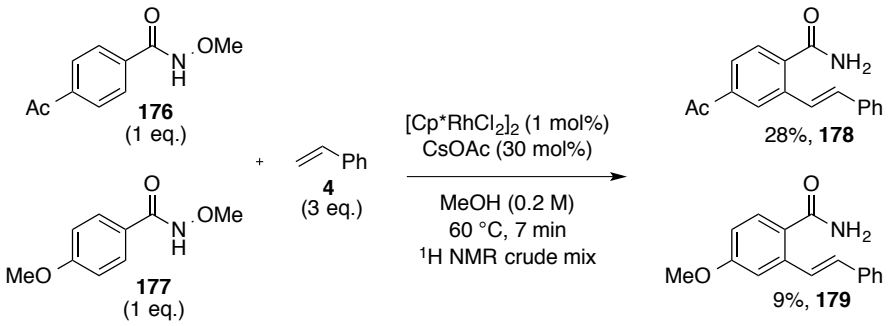

*Scheme 3.4. Glorius' competition experiment with electronically different substrates **176** and **177**.*[36]

To supress the competing reaction, the temperature was reduced to 30 °C and the concentration doubled to 0.4 M, which led to an improved yield of 63% of the isoquinolone **172** (entry 5). Halogenated substrates were tolerated under the reaction conditions (entries 6-8). Dehalogenated products were not observed in the crude reaction mixtures, rendering the products suitable for further cross-coupling reactions.

To investigate regiochemical effects in non-symmetrically substituted substrates, eight 3-substituted-*N*-(pivaloyloxy)benzamide derivatives were prepared **180-187** (Table 3.2). As predicted, in the reactions of substrates **180** and **181,** C-H activation occurred at the less-hindered position *para*- rather than *ortho*- to the phenyl/N-Boc substituent, giving **188** and **189** as single regioisomers (entries 1 and 2). The reactions of the *meta*-brominated **182** and *meta*-chlorinated **183** substrates gave predominantly the 7-bromoisoquinolone **190** and 7-chloroisoquinolone **191** by reaction at the less-hindered site (entries 3 and 4). In contrast, the *meta*-fluorinated substrate **184** produced an inseparable mixture of regioisomers in favour of the contiguously substituted product (71%, **192a**:**192b**, 2:1). The *ortho*-directing effect of strongly electronegative substituents on rhodium-mediated C-H activation has been previously reported.[38,115] Given the irreversibility of the C-H insertion step under these conditions, in this case it is almost certainly a kinetic preference.[35] This effect was also observed with the *meta*-methoxy derivative **185** which gave a 2:3 mixture of regioisomers **193a:193b**, while the protocatechuic acid derivatives **186** and **187** furnished the contiguously substituted isoquinolones **194b** and **195b** as single regioisomers (entries 7 and 8).

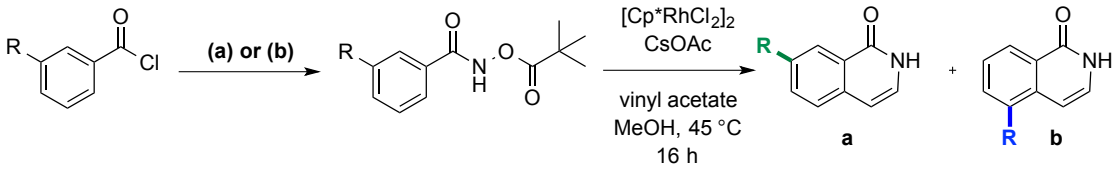

Entry	R	Yield SM %	No.	Product	Ratio[d] a: b	Yield[c] a+b	No
1	HNBoc	62[b]	**180**	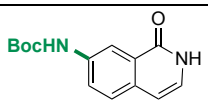	1:0	81	**188**
2	Ph	38[a]	**181**	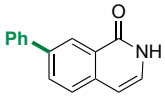	1:0	91	**189**
3	Br	57[a]	**182**	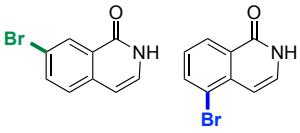	10:1	95	**190**
4	Cl	85[a]	**183**	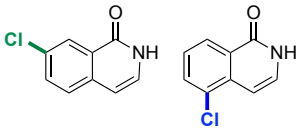	98:2	66	**191**
5	F	66[b]	**184**	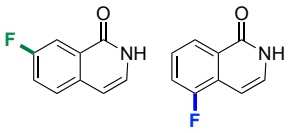	1:2	71	**192**
6	OMe	76[a]	**185**	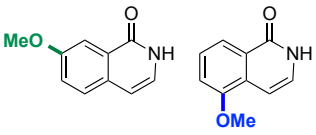	3:2	76	**193**
7	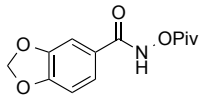	83[a]	**186**	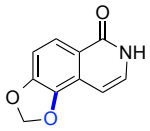	0:1	53	**194**
8	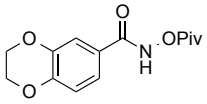	73[a]	**187**	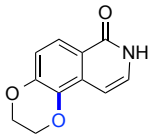	0:1	48	**195**

a) $PivONH_2$•HCl (1.1 eq.), K_2CO_3 (2 eq.), EtOAc–H_2O (2:1, 0.2 M), 0 °C, 3 h; b) $PivONH_2$•HCl (1.1 eq.), NEt_3 (2 eq.), THF (0.2 M), 0 °C, 3 h; c) Standard conditions for annulation: $[Cp^*RhCl_2]_2$ (1 mol%), CsOAc (30 mol%), MeOH (0.2 M), vinyl acetate (1.5 eq.), 45 °C, 16 h. d) Ratio of purified products.

Table 3.2

The protocatechuic acid derivatives **186**/**187** have reduced steric demands in comparison to the *meta*-methoxy derivative **185**, in which the methoxy group is free to rotate, leading to a mixture of isomers. In total, 16 isoquinolones were prepared using the standard conditions as outlined in Table 3.1 and 3.2.

3.3 Heterocyclic series 2

Having established a robust synthetic procedure for the preparation of isoquinolones, studies on heterocyclic analogues commenced. The starting materials **196-203** were prepared according to the procedures outlined in Section 3.1. The study began with thiophene derivatives, heterocycles electronically similar to the benzenoid substrates previously employed. Initial attempts using thiophene derivatives proved successful, albeit with lower yields compared with the benzenoid systems. The reactions of the thiophenyl substrate **196** and benzothiophenyl substrate **197** gave yields of 49% and 64%, respectively (entries 1 and 2, Table 3.3). To investigate the reactivity of the regioisomeric benzothiophene derivative, substrate **198** was prepared. Interestingly, no product was observed (entry 3). Analysis of the side products revealed a 70% conversion to the corresponding methyl carbamate (arising from methanol trapping the Lossen isocyanate formed in the reaction) and a further 15% of the free amide. Observation of the free amide was unexpected, as this would suggest an intermolecular N-O bond cleavage. The substrate scope was extended to include the benzofuran derivative **199**, however the reaction required 48 hours to achieve an average yield of 38% (entry 4). Additional products isolated from the reaction included the free amide and the carbamate.

Attempts to include *N*-heterocyclic compounds, using an *N*-methyl pyrrole derivative as the initial example, unfortunately, resulted in unreacted starting material. Similarly, the *N*-methyl indolyl derivative **200** furnished the product **207** in a low 16% yield. It became apparent that these relatively electron-rich systems were unsuitable for this rhodium-catalysed system. A recent study highlighted large rate differences in rhodium-mediated C-H activation reactions of various (hetero)aryl imines, the differing reactivity of substrates **196-200** appear in agreement with their finding.[116]

To broaden the substrate scope, a nicotinamide derivative **201** and the *N*-oxide derivative **202** (based on the reported enhanced reactivity of such substrates in C-H activation[52]) were added to the screening. After sixteen hours only unreacted starting material was identified in the crude reaction mixture of substrate **201** and **202**, with no carbamate observed, potentially suggesting detrimental coordination of the rhodium. To probe this coordination effect, further investigation using the quinoline-3-carboxylic acid **203** was conducted. Potential dative coordination of the lone pair of electrons on the nitrogen would be disfavoured by the steric interaction of the C_8 hydrogen of the quinoline-based substrate. Interestingly, the quinoline derivative **203** did indeed furnish the benzo[*b*][1,6]-naphthyridin-1(2*H*)-one **208** with a yield of 51%. In total, five heterocyclic pyridones were prepared using this methodology.

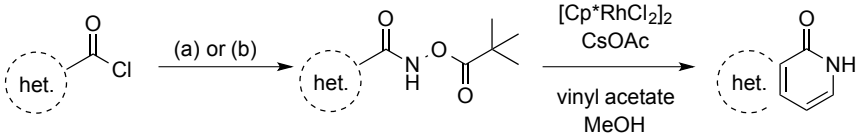

Entry	R	Yield SM (%)	No.	Product	Yield Product (%)[d]	No.
1	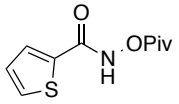	40[a]	**196**	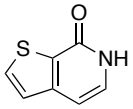	49	**204**
2	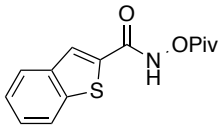	25[a]	**197**	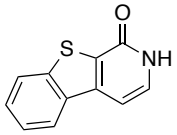	64	**205**
3	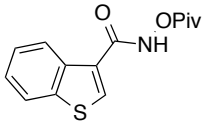	42[b]	**198**	-	-	-
4	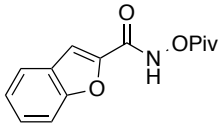	49[a]	**199**	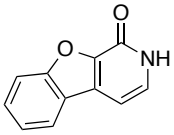	38[e]	**206**
5	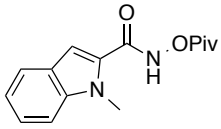	35[b]	**200**	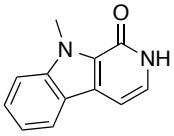	16	**207**
6	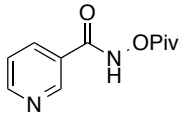	25[a]	**201**	-	-	-
7	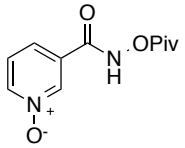	85[c]	**202**	-	-	-
8	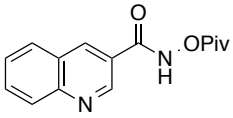	45[a]	**203**	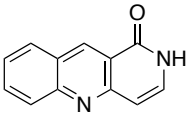	51	**208**

a) $PivONH_2$•HCl (1.1 eq.), K_2CO_3 (2 eq.), EtOAc–H_2O (2:1, 0.2 M), 0 °C, 3 h; b) $PivONH_2$•HCl (1.1 eq.), NEt_3 (2 eq.), THF (0.2 M), 0 °C, 3 h; c) Prepared according to the literature procedure;[52] d) Standard conditions for annulation: $[Cp^*RhCl_2]_2$ (1 mol%), CsOAc (30 mol%), MeOH (0.2 M), vinyl acetate (1.5 eq.), 45 °C, 16 h; e) 48 h.

Table 3.3. Formation of heterocyclic pyridones.

3.4 Substituted enol ester derivatives

Having exemplified the reaction with a variety of hydroxamate esters, natural progression to the investigation of vinylic acetate derivatives ensued. The main objective was to incorporate α- and β-substituents to furnish more highly substituted isoquinolones. Our initial attempt, using isopropenyl acetate **209**, produced 3-methylisoquinolin-1(*2H*)-one **215** in a disappointing 7% yield. The remainder of the starting material was converted to the methyl phenyl carbamate **133** (Table 3.4, entry 1). Attempts to reduce the reaction temperature to room temperature resulted in a mixture of only unreacted starting material and the carbamate. Before expanding the scope, attempted optimisation of the reaction conditions was investigated, using isopropenyl acetate as the model substrate.

The parameters selected for the optimisation study included: temperature (40-60 °C), reaction concentration (1-5 M) and substrate equivalents (1.5-5 eq.). The mid-point was repeated to verify continuity. The major product from each reaction was the carbamate **133**, with only traces (confirmed by ^{1}H NMR) of the desired product. In light of this observation, a number of alternative enol acetate derivatives **211-215** were tested. The corresponding aldehydes or ketones were used to prepare the derivatives shown in Table 3.4, using standard literature procedures.[117,118]

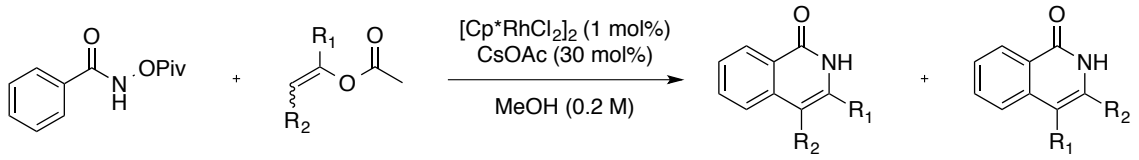

Entry	1	2	3	4	5	6
SM		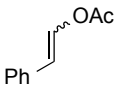	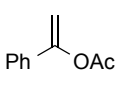	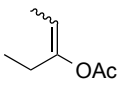	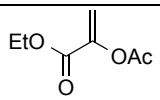	
No.	**209**	**211**	**212**	**213**	**214**	**215**
Product	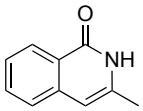	-	-	-	-	-
No.	**210**					
Yield (%)	7	-	-	-	-	-

Table 3.4

Reactions of these alkenyl substrates (Table 3.4), at various temperatures, resulted in mixtures of unreacted starting material **43** and the methyl phenyl carbamate **133**. Any attempt to increase the temperature above 45 °C led to full conversion to the carbamate **133**. The reaction of α-acetoxy styrene **211** led to degradation to the starting phenylacetaldehyde, as well as benzamide and carbamate **133** (entry 2). Concerned that steric hindrance may have prevented

coordination to the metal centre, a cyclic alkene, vinylene carbonate **216**, was selected as a model substrate (Scheme 3.5). The tethered *cis*-arrangement would give some indication as to whether steric factors were playing a part in the substrate selectivity. Interestingly vinylene carbonate furnished 4-hydroxyisoquinolone **217** with a 78% yield as a single regioisomer (confirmed by the ^{1}H NOESY NMR spectrum and literature data[119]).

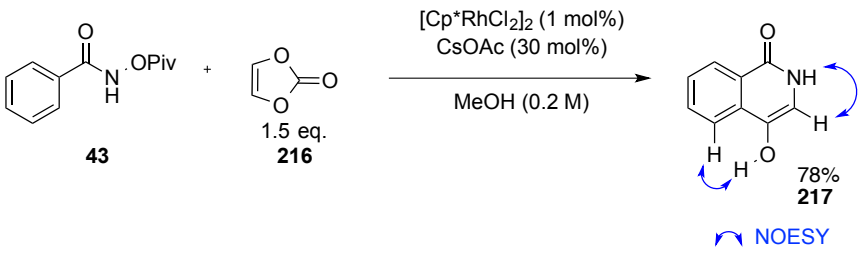

Scheme 3.5

The substrate screen suggested 1,1-disubstituted and *trans*-1,2-disubstituted enol acetates were not accommodated in the reaction compared with monosubstituted and *cis*-1,2-cyclic alkenes. This was perhaps unsurprising, as Glorius[36] and Fagnou[34] reported only monosubstituted or 1,2-*cis*-alkenes (e.g. 2,3,-dihydrofuran, norbornadiene and 1,3-cyclohexadiene) in their pioneering studies of intermolecular C-H activation/annulation protocols with *N*-(pivaloyloxy)benzamide.

In summary, the oxidative rhodium-catalysed coupling of vinyl acetate to a variety of electron-rich/deficient, aromatic and heteroaromatic, pivaloyl hydroxamates was successfully achieved**.** This synthesis presents a streamlined route for the preparation of 3,4-unsubstituted isoquinolones using an internal oxidant and mild reaction conditions. This method provides an attractive alternative to systems requiring external oxidants, which typically require superheated solvents with an excess of copper(II) acetate and silver(I) salts. Furthermore, the use of vinyl acetate, as a replacement for acetylene, offers a safe and cheap alternative and could find important application in the synthesis of isoquinolone-based compounds.

3.5 Methodology application: intermediates for Hepatitis C virus protease inhibitors

3.5.1 Merck's MK-1220 virus inhibitor

Hepatitis C is a chronic viral infection that affects an estimated 170-200 million people worldwide[120] and over time a significant portion of patients develop chronic liver disease. Current limitations with pharmaceutical therapeutics are their limited efficacy and often serious side effects. As a result very few patients complete their treatment. Merck recently identified MK-1220 **218** as a potent and efficacious hepatitis C virus protease inhibitor with a potentially superior therapeutic profile (Figure 3.2).[97]

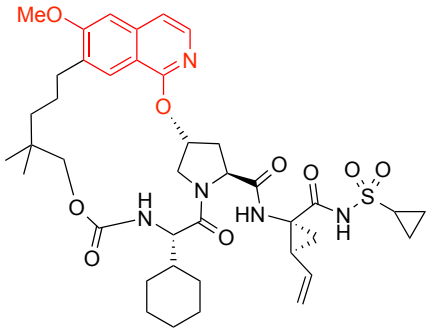

218
MK-1220 Merck
Hepatitis C virus protease inhibitor

Figure 3.2

Despite the obvious challenges of preparing the macrocyclic ring, the methods for preparing individual fragments were additionally cumbersome. The heterocyclic fragment embedded in the macrocyclic structure is an ether-linked 6-methoxyisoquinoline, prepared from the 7-bromo-6-methoxyisoquinolone **147** (Scheme 3.6). The key step in the reported three-step medicinal chemistry route required a thermal rearrangement (250 °C) of a cinnamoyl azide **219**, resulting in an overall yield of 35% (A, Scheme 3.6).[97] Based on the low yield of the cyclisation step (65%) and the high temperature required for the rearrangement, an alternative strategy was sought for the process route.[121] Their survey of the literature identified the challenge of preparing this isoquinolone, particularly in achieving high regioselectivity for the cyclization step.[121] These challenges were confirmed by the results of their exploration of potential routes, including an attempted bromination of **221**, which resulted in the undesired regioisomer **222**, and an attempted Friedel-Crafts cyclisation of **223** formed **224** instead of **147**. Their final optimised 5-step synthesis, from the unsaturated tetrasubstituted intermediate **220**, was achieved in 55% overall yield (B, Scheme 3.6).

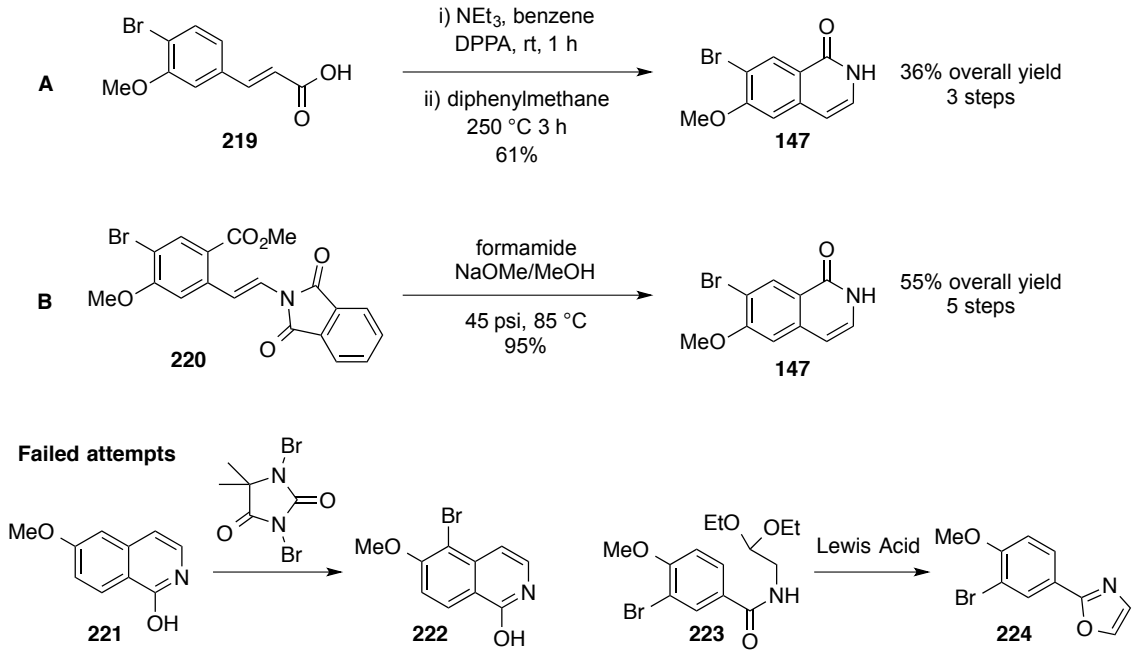

Scheme 3.6 Key cyclisation steps from the discovery chemistry (A)[97] *and the optimised process route (B).*[121]

To investigate the application of this methodology to the synthesis of the intermediate **147**, the corresponding 3-bromo-4-methoxy-*N*-(pivaloyloxy)benzamide **226** was prepared quantitatively from the cheap, commercially available benzoic acid **225** (Table 3.5). Using our standard conditions, the desired regioisomer **147** was observed and isolated with a yield of 46% (entry 1). The remaining starting material had rearranged to form the corresponding carbamate as a consequence of the competing Lossen rearrangement. By reducing the temperature of the reaction to 30 °C (entry 2) and increasing the concentration to 0.4 M (entry 3), the yield was improved from 46% to 85%. Additionally, the product was isolated as a single regioisomer. Our approach reduced the number of synthetic steps from five (for the process route) to three, resulting in a higher overall yield of 85%.

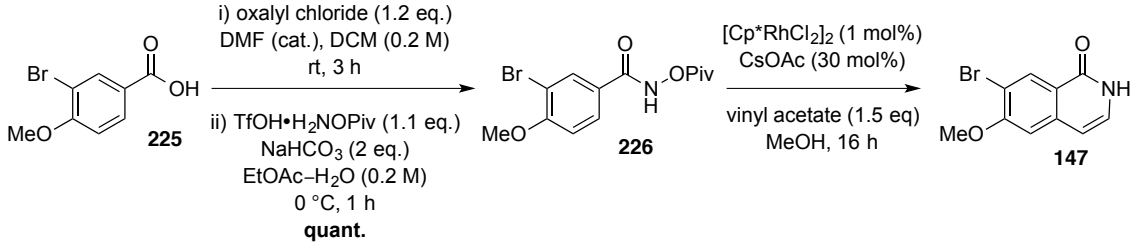

Entry	Conc. (M)	Temp. (°C)	Time (h)	Yield (%)
1	0.2	45	16	46
2	0.2	30	48	72
3	0.4	30	16	85

Table 3.5

3.5.2 Bristol-Myers-Squibbs asunaprevir and analogues

Asunaprevir **227**, a Bristol-Myers-Squibb drug currently in phase III clinical trials for the treatment of hepatitis C virus infection, and its analogues rely on a 4-methoxy-7-chloroisoquinoline fragment for improved activity relating to cardiovascular events.[122] Preparation of asunaprevir and its analogue **228** originate from three key fragments, one of which is 1,7-dichloro-4-methoxyisoquinoline **229** which is tethered to the core molecule *via* an S_NAr reaction with *N*-Boc-hydroxyproline (Figure 3.3).[122]

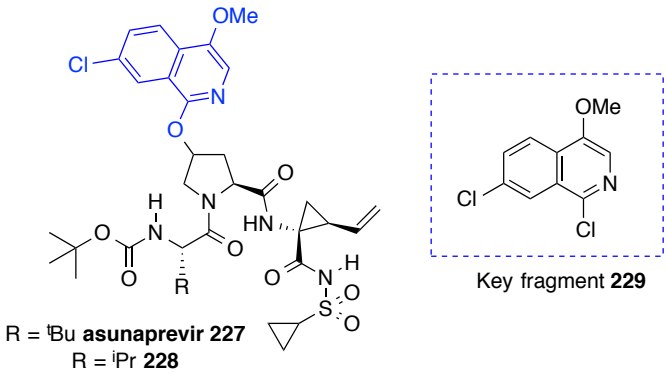

Figure 3.3.

Scola *et al.*[123] reported the synthesis of 4-hydroxy-7-chloroisoquinolone **235**, the precursor to the key fragment **229**, in five-steps with an overall yield of 41% (Scheme 3.7). Using a Heck reaction with butyl vinyl ether, followed by hydrolysis, the acetophenone derivative **232** was subsequently brominated to afford the *α*-halo carbonyl **233**. Displacement of the bromine *via* a S_N2 reaction with sodium diformylamide furnished the cyclisation precursor **234**, which was immediately treated with methanol and acetic acid to afford the 4-hydroxy-7-chloroisoquinolone **235** (78% yield over two steps).

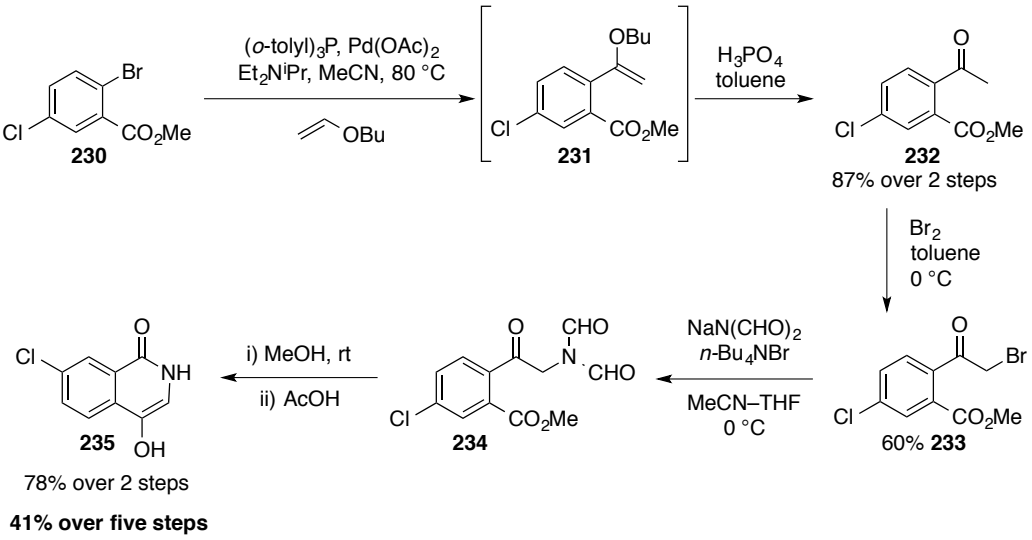

Scheme 3.7

Having previously shown that our C-H activation/annulation chemistry would furnish the 7-chloroisoquinolone **191a** (66% yield, see Table 3.2) in two steps from the commercially available 3-chlorobenzoyl chloride **236**, it was evident that using the same 3-chloro-*N*-(pivaloyloxy)benzamide **183** with vinylene carbonate **216**, instead of vinyl acetate, would furnish the 4-hydroxy-7-chloroisoquinolone **235** in a more succinct synthesis than that developed by Scola *et al*.[124] Pleasingly, 4-hydroxy-7-chloroisoquinolone **235** was isolated as a single regioisomer (65%) using our standard C-H activation conditions (Scheme 3.8). Using our optimised methodology the number of steps required to prepare the isoquinolone **235** was reduced from the original six-step route (with an overall yield of 41%) to a two-step route with an overall yield of 55%.

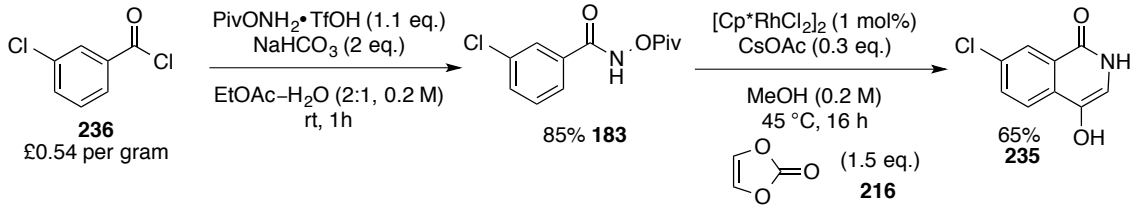

Scheme 3.8

3.6 Mechanistic considerations

3.6.1 Deuterated vinyl esters

Following our optimisation and exemplification of the isoquinolone synthesis (*cf.* Section 3.1) we were interested in the determining the mechanism of the reaction and specifically in probing the regiochemistry of the reaction with vinyl esters. In order to gain a better insight into the electronic preferences of the rhodium catalyst, further examination of the regiochemical outcome, with respect to the acetate portion, was undertaken (Scheme 3.9).

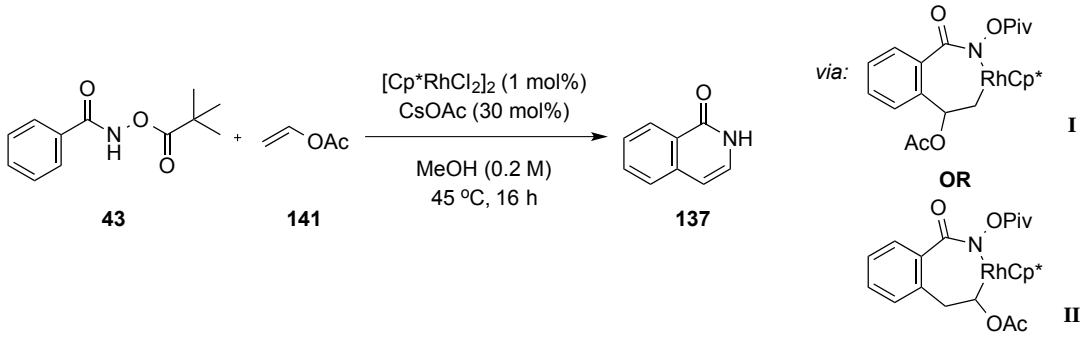

Scheme 3.9

Preparation of regiospecifically isotopically-labelled vinyl acetate **141** would provide further information about the regiochemical preference (Scheme 3.10). To acquire this information either the α-monodeuterated **238** or β-bisdeuterated **237** vinyl acetate would have to be prepared.

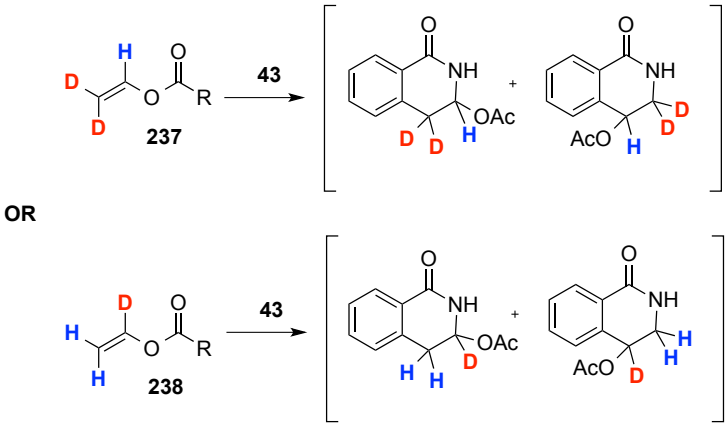

Scheme 3.10

Vinyl acetate is typically prepared on an industrial scale by oxidative condensation of ethylene and acetic acid using oxygen in the presence of a palladium catalyst.[125,126] This approach would be unsuitable for our labelling study, as we would need to be able to differentiate between the two carbon atoms in the alkene (Scheme 3.10). Surprisingly, the synthesis of regiospecifically labelled vinyl acetate was unknown. Three different approaches were identified; acylation of

deuterated acetaldehyde (**A**, Scheme 3.11), acylation of heptenoic acid followed by ring closing metathesis to give vinyl acetate (**B**) and finally, alkenylation of a formyl anhydride (**C**).

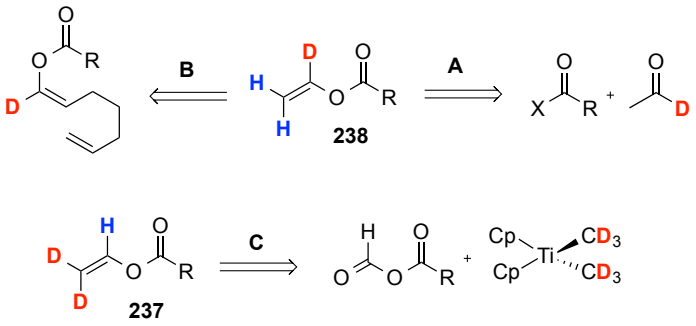

Scheme 3.11

An initial literature search for the acylation of acetaldehyde **239** indicated a lack of examples, presumably owing to the propensity of the acetaldehyde enolate towards polymerisation. However, a report published by Sladkov and Petrov identified a viable strategy.[127] Predicting a difficult separation of the desired vinyl ester product from the reaction medium, due to its low boiling point, lauryl chloride **240** was used instead of acetyl chloride to provide a stable, non-volatile substrate to separate. Firstly vinyl laurate was used instead of vinyl acetate in our standard C-H activation/annulation conditions. The isoquinolone was obtained with a yield of 86%, indicating no detrimental effect with the substitution. Addition of lauryl chloride to a solution of formaldehyde and pyridine at 0 °C, with subsequent heating, unfortunately, did not yield the desired vinyl laurate **241** (Scheme 3.12). Instead a complex mixture of products was obtained.

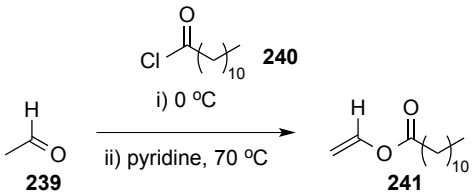

Scheme 3.12

Based on the failed reaction (Scheme 3.12) and the paucity of similar preparative techniques using these substrate types, route B was investigated (Scheme 3.13). A route was envisaged starting from the reduction of 6-heptenoic acid to the deuterated aldehyde **244**. Acylation of the corresponding enolate **243** followed by a ring closing metathesis would provide the desired deuterated vinyl ester **237** with elimination of cyclopentene **242**. Significant literature precedent exists for the ring-closing metathesis of enol esters with terminal alkenes. These have been shown to work effectively for the formation of cyclic enol ethers using molybdenum[128,129] and ruthenium[130–133] based catalysts.

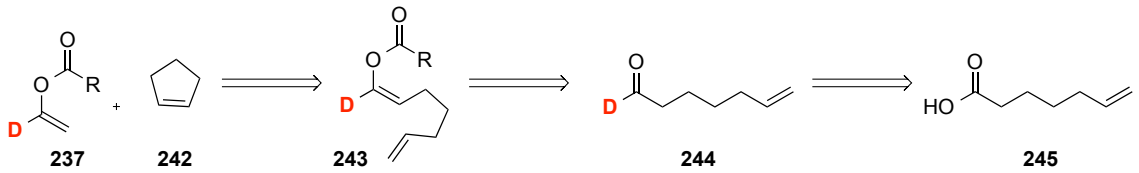

Scheme 3.13

Following the successful reduction of the unsaturated acid **245** to the *bis*-deuterated alcohol **246** (100% D, by ^{1}H NMR), using lithium aluminium deuteride, attempts were made to oxidise the unsaturated compound to the aldehyde **244** (Scheme 3.14). Both Dess-Martin periodinane[134] and Swern[135] oxidation led to the formation of several side products. The oxidation mediated by pyridinium chlorochromate (PCC) gave a 65% yield of the aldehyde **244**, which was not sufficient for the multi-step synthesis. Tetrapropylammonium perruthenate (TPAP) successfully furnished the aldehyde **244** on a smaller scale (65%); however scale up resulted in the formation of multiple side products. Based on the assumption that sufficient material would be required to screen several conditions for the metathesis step, an alternative approach was considered.

Preparation of the Weinreb amide **247** from the acid chloride (prepared using 6-heptenoic acid **245** and the Vilsmeier reagent[111]) produced several by-products (Scheme 3.14). Fortunately, formation of the desired product **247** was realised *via* the mixed anhydride generated from isobutyl chloroformate, obtained with a yield of 96%. Reduction of the Weinreb amide **247** using lithium aluminium deuteride gave the deuterated aldehyde with a yield of 85% (100% D by ^{1}H NMR). Acylation of the aldehyde using potassium *bis*(trimethylsilyl)amide (KHMDS) and hexanoyl chloride furnished the enol ester **248** with a modest yield of 32% (*E:Z* 1.8:1).

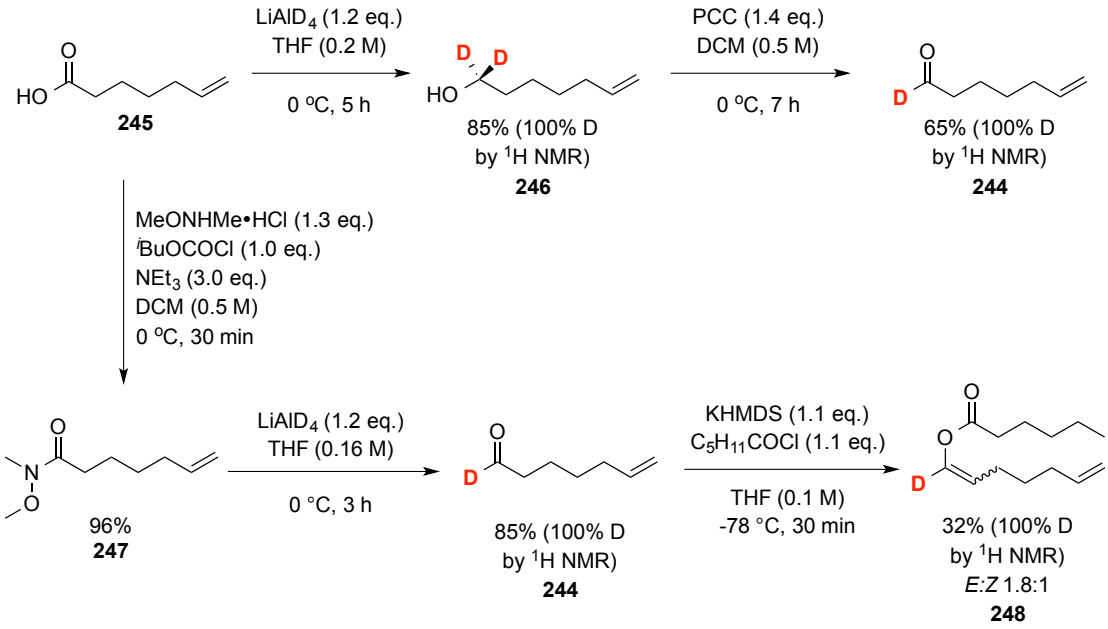

Scheme 3.14

At this stage four catalysts were screened in deuterated toluene-d_8 (Grubbs and Hoveyda-

Grubbs 1st and 2nd generation catalysts **G2-G4** Table 3.6). The reactions were monitored by ^{1}H NMR over two hours. Unreacted starting material was observed using both **G1** and **G3** (entries 1 and 3). Promisingly, the product **249** and cyclopentadiene **242** were observed in the reactions using the catalysts **G2** and **G4** (entries 2 and 4). In both reactions, the product conversion ceased after the first hour, suggesting catalyst poisoning. The reaction in deuterated dichloromethane-d_2 at a lower temperature resulted in only 5% conversion to product (entry 5).

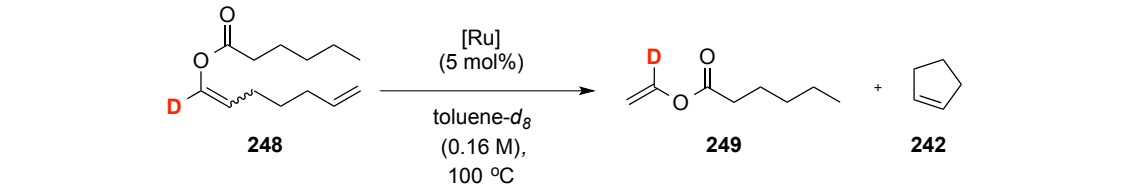

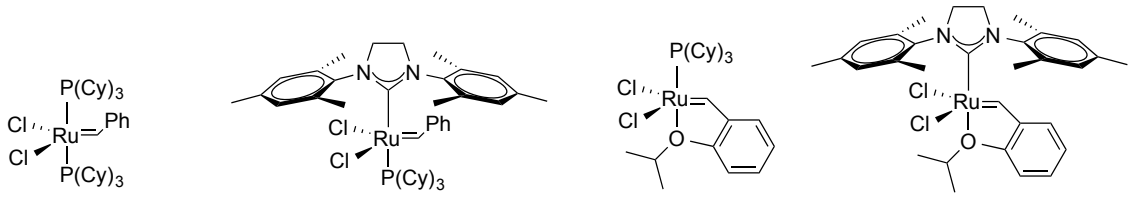

1st Generation Grubbs catalyst **G1**

2nd Generation Grubbs catalyst **G2**

1st Generation Hoveyda-Grubbs catalyst **G3**

2nd Generation Hoveyda-Grubbs catalyst **G4**

Entry	Catalyst	^{1}H NMR ratio **248:249**
1	G1	100:0
2	G2	84:16
3	G3	100:0
4	G4	87:13
5	G2	95:5[a]
6	G2	89:11[b]

*^{1}H NMR ratio of **248:249** from the crude reaction mixture.*

[a]DCM-d_2 (0.16 M), 45 °C. [b]Ethylene bubbled through the reaction.

Table 3.6

Enol ethers are used to terminate ring-opening metathesis polymerisation reactions (ROMP) by formation of the ruthenium Fisher carbene complex **251**.[133,136] The Fisher carbene is more stable than the intermediate alkylidene (or methylidene) **250** that is formed during the alkene metathesis i.e. the equilibrium should favour the formation of species **251** (Scheme 3.15). Concerned that the product **249** was inhibiting catalytic activity, the reaction was repeated with ethylene gas bubbling through the solvent,[137,138] however the yield was not improved (entry 6, Table 3.6)

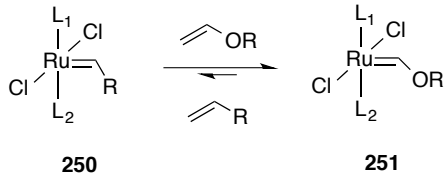

250 **251**

Scheme 3.15

Following the unsuccessful attempts using the metathesis strategy, we decided to move on to our third approach. Petasis *et al.*[139] reported a methylenation of the cyclic anhydride **252** to produce the vinyl lactone **253** (and the *bis*-vinyl cyclic ether **254**) using dimethyl titanocene (**A**, Scheme 3.16). Using this method we reasoned that treatment of a formyl anhydride **255** with deuterated dimethyl titanocene-d_6 could provide the required vinyl ester **237** (**B**, Scheme 3.16).

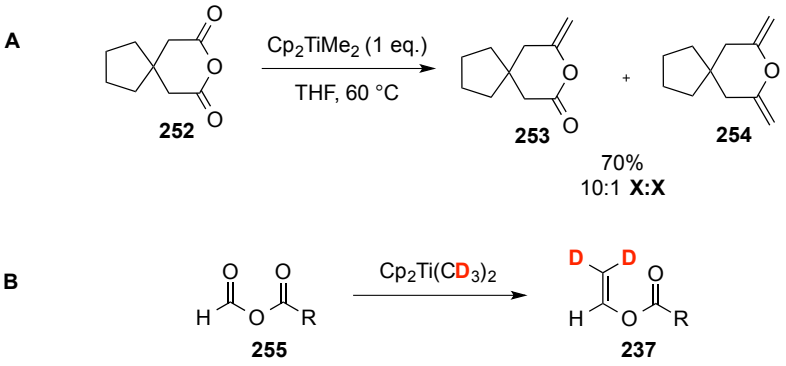

Scheme 3.16

Following a procedure by Naef *et al.*,[140] the formyl anhydride **258** was prepared from formic acid **256** and hexanoyl chloride **257** in dimethylaniline (57%, Scheme 3.17). The alkylating reagent, dimethyl titanocene-d_6 **260**, was synthesised from titanocene dichloride **259** and deuterated methyllithium to give the product in a solution of toluene (the concentration was determined by ^{1}H NMR).[141] Isolation of the compound was avoided due to the reported instability of the complex when exposed to moisture and light.[139] The dimethyl titanocene solution **260** was added immediately to succinic anhydride, as a trial reaction, to identify whether the complex was active. Analysis of the crude ^{1}H NMR spectra indicated traces of the desired allylic product **261**, however the majority of the material remained unreacted. Benzaldehyde was used as an alternative substrate to test the dimethyl titanocene solution **260**; consumption of the aldehyde was observed by ^{1}H NMR, however no vinylic peaks corresponding to the deuterated styrene **262** were observed, suggesting an issue with the dimethyl titanocene reagent **260**.

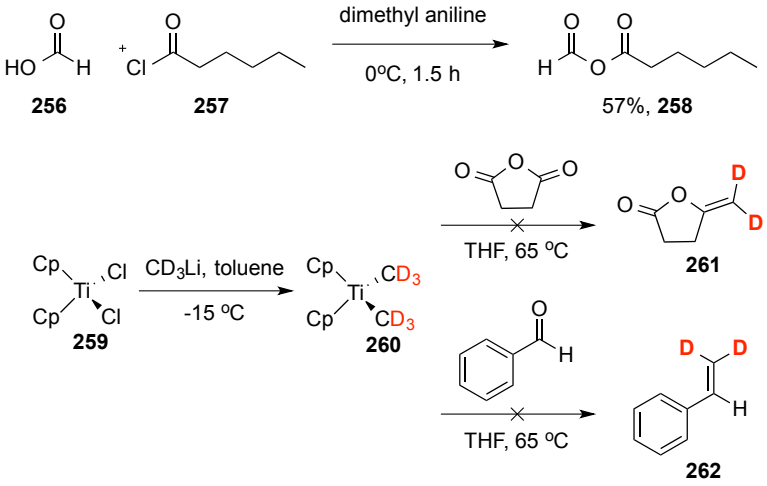
dimethyl aniline
0ºC, 1.5 h
256
257
57%, 258
CD3Li, toluene
-15 ºC
259
260
THF, 65 ºC
261
THF, 65 ºC
262

Scheme 3.17

3.6.2 A vinyl ester surrogate

Following our failed attempts to prepare deuterated vinyl acetate, we decided to focus on a deuterated substrate that would be easier to synthesise than vinyl acetate. *O*-Vinyl-*N,N'*-diisopropylcarbamate **265** was selected as an analogous reactant (Scheme 3.18). The material was simply prepared following a procedure by Clayden *et al.*[142] *via* a lithium-mediated decomposition of tetrahydrofuran **263** to give the lithium acetaldehyde enolate **264**, which was subsequently acylated using *N,N'*-diisopropyl carbamoyl chloride to afford the desired product **265** (83%). Selective incorporation of a deuteron at the α-position was achieved by directed lithiation using *sec*-BuLi, followed by a quench using deuterium chloride in deuterium oxide to afford **265-d_1** (87% D by ^{1}H NMR).

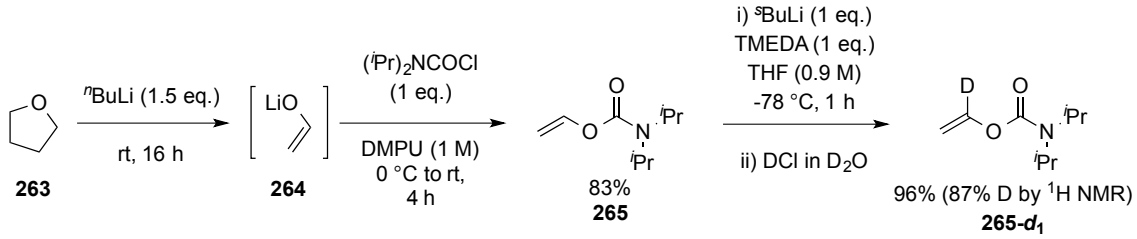

Scheme 3.18

To assess whether the vinyl carbamate was a suitable alternative for vinyl acetate, the non-deuterated carbamate **265** was used under the standard reaction conditions (Scheme 3.19). The reaction produced the isoquinolone **137** as the sole product with a reasonable yield of 50% (compared to 87% with vinyl acetate). Unfortunately, attempts with the deuterated variant **265-d_1** produced the isoquinolone **137-d_1** with a yield of 5%. Several iterations of the reaction with different batches of the starting material resulted in the same yield, suggesting catalyst poisoning. Despite the poor yield, the isoquinolone **137-d_1** was isolated and the regioselective incorporation of the deuteron in the 3-position was confirmed by ^{1}H NMR (85% D by ^{1}H NMR).

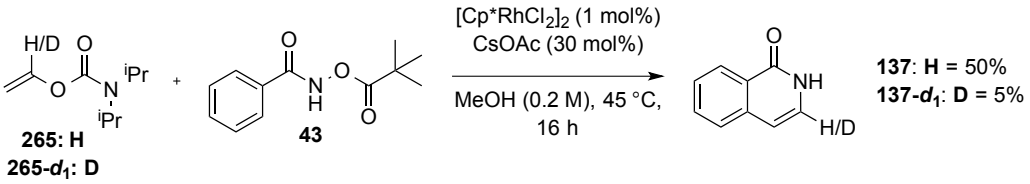

Scheme 3.19

Assuming the regioselectivity of *O*-vinyl-*N,N'*-diisopropylcarbamate **265** is comparable to that of vinyl acetate, the isolated product suggests the reaction proceeds through an aminoacetal intermediate. This result contrasts with the regioselectivity observed using vinyl ethers which furnished the benzylic ethers as the major regioisomer (Figure 3.4).

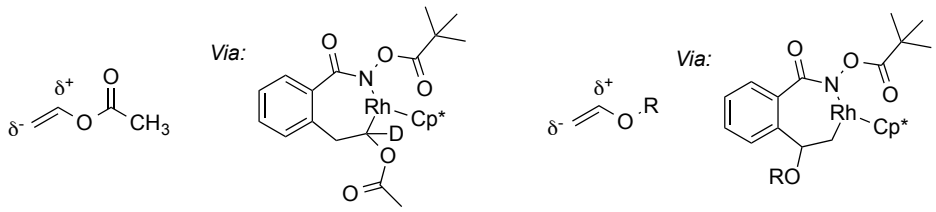

Figure 3.4

3.6.3 Factors influencing regiochemical preference of alkenyl substrates

Once the regiochemical preference for the enol ether substrates and vinyl acetate had been established (*cf.* Section 2.4 and 3.6.2), we were interested to find out whether the carbonyl moiety has a role in the regioselectivity of the reaction. *N*-Boc-dihydropyrrole **266** was selected as a model substrate for the study. Using the standard conditions, *N*-Boc-dihydropyrrole **266** and *N*-(pivaloyloxy)benzamide **43** furnished the aminal **267**, with a yield of 45% (Scheme 3.20). The regioisomer was confirmed by a ^{1}H NMR NOESY spectrum and an X-ray structure of a single crystal of **267** (Scheme 3.20 and Appendix 2.2).

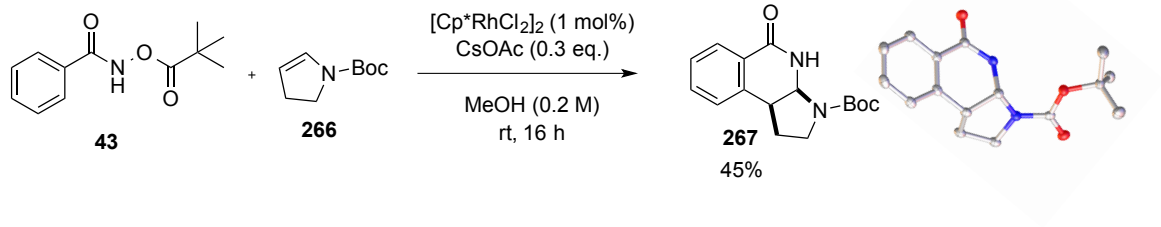

*Scheme 3.20 Regioisomer **267** confirmed with an X-ray crystal structure.*

Having observed a similar selectively with the *O*-vinyl-*N,N*-diisopropyl carbamate **265-*d*$_1$**, as our vinyl acetate surrogate (see Scheme 3.19), we considered potential interactions between the carbonyl group and the rhodium catalyst. Xia *et al.* reported the carbonyl-stabilised key intermediate **I**, by computational calculations using DFT methods, with ethylene as a model substrate (Figure 3.5).[37] Based on the rhodacycle **II**, it is possible to imagine an alternative stabilisation occurring *via* the carboxyl group of the pyrrole **III** or vinyl acetate **IV**, through a five-membered intermediate.

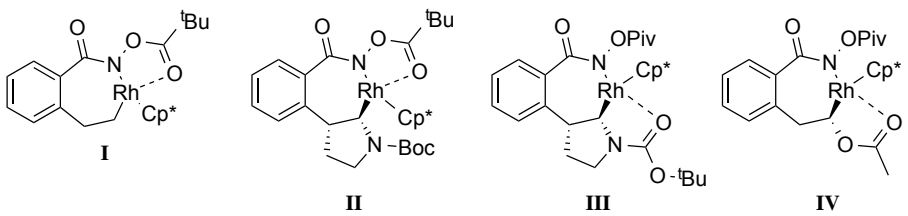

Figure 3.5

3.7 Conclusion

In summary, a robust, efficient C-H activation protocol for the synthesis of isoquinolones from simple hydroxamate/oxime esters using vinyl acetate as an acetylene equivalent has been established. This protocol avoids the necessity for gaseous acetylene in order to achieve the desired 3,4-unsubstituted isoquinolones and provides an effective and facile synthetic route compared with existing procedures.

In total, sixteen exemplar 3,4-unsubstituted isoquinolones, bearing electron-donating/withdrawing groups, were prepared with an average yield of 75%. Oxygen and sulfur-based heterocycles were also tolerated, however nitrogen-containing aromatics proved to be less reactive. Despite this observed trend, five heterocyclic examples were successfully prepared.

The limitations of the reaction conditions were brought to light when our attempts to react various substituted vinylic acetate derivatives with *N*-(pivaloyloxy)benzamide under rhodium catalysis proved unsuccessful (only cyclic alkenes were tolerated under the existing reaction conditions). Comparison of vinyl ethers to vinyl acetate indicated a significant difference in reactivity, which we believe is a result of either the increased electron density in the vinylic portion of the molecule or the coordination of the acyl group to the rhodium centre. Generally, electron-rich substrates (with regards to the aromatic or vinylic reactant) had a detrimental effect on the activity of the catalyst.

Having failed to prepare selectively-deuterated vinyl acetate, we were able to use a deuterated surrogate (*O*-vinyl-N,*N'*-diisopropylcarbamate) in order to assess the regiochemical preference. The results contrasted with those found using *n*-butyl vinyl ether, suggesting an additional interaction between the carbonyl of the vinyl acetate and the metal centre (also observed using *N*-Boc-dihydropyrrole).

Finally, the utility of this methodology was exemplified with the succinct synthesis of two intermediates for hepatitis C virus protease inhibitors, MK-1220 and asunaprevir. Excellent regioselectivity meant that the desired intermediates were simply prepared using our optimised methodology.

Chapter 4

Rhodium(III)-catalysed synthesis of isoquinolines

4.1 Introduction

Isoquinolines are prevalent scaffolds in pharmaceutical agents, natural products and other fine chemicals;[143–149] there are over 400 members in the isoquinoline alkaloid family alone.[148] Traditional syntheses of isoquinolines from *mono*-substituted arene precursors include the well-established Bischler-Napieralski,[150] Pictet-Spengler,[151] Pictet-Gams,[152] and Pomeranz-Fritsch reactions (Scheme 4.1).[153,154] In each case the key cyclisation step proceeds *via* an S_EAr mechanism, which inherently limits the substrate scope to electron-rich aromatic systems. To address this limitation, alternative approaches using *ortho*-disubstituted aromatic precursors as templates for annulation of the heterocyclic component have been developed. The primary approach is to install alkenes/alkynes *ortho*- to an imine or imine precursor, (typically using cross-coupling methodologies with *ortho*-halogenated substrates) which can undergo an electrophilic-induced intramolecular cyclisation to afford isoquinolines.[155–161] Larock *et al.* utilised cross-coupling methodology of 2-iodobenzaldeyde imines with internal alkynes to give a range of isoquinolines.[162,163] Other methods include reactions using benzyne with vinyl amines and 2-azidoacrylates[164] with α-diazocarbonyl compounds.[165] Despite broadening the variety of substrates available, atom economy is still a drawback in the design of these new systems.

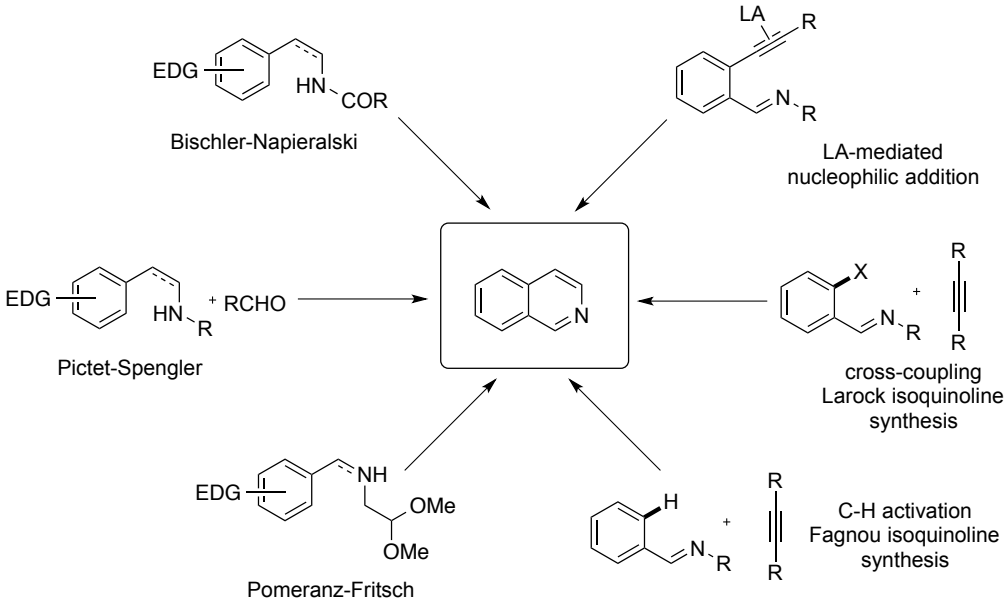

Scheme 4.1

In recent years, numerous C-H activation/annulation approaches to isoquinolines have been developed using various rhodium, ruthenium and palladium catalysts.[24,25,166–168] This chemistry

combines the synthetic flexibility of using mono-substituted arene precursors while obviating the requirement for electronic activation towards S_EAr chemistry inherent in the classical approaches named above. The process involves conversion of a C-H bond to a C-C bond and hence to facilitate catalytic turnover an oxidant is required, which, in the case of rhodium, is typically stoichiometric copper acetate. Alternative protocols based on 'internal' oxidants have been developed by the groups of Fagnou[34] and Chiba.[64] Using ketoximes as superior directing groups allows for milder conditions, while cleavage of the N-O bond maintains the active rhodium(III) catalyst without generating metal-based waste streams.[39,49,64,160,169–171] Recent work by Cheng *et al.* identified hydrazones (cleaving N-N bonds) as a new oxidizing direction groups for the synthesis of isoquinolines.[71]

Having established a novel and robust synthetic procedure for the preparation of 3,4-unsubstituted isoquinolones (Section 3.1), application of this methodology was extended to the synthesis of isoquinolines. Chiba *et al.*[64] have demonstrated a similar protocol, reacting internal alkynes with acetylated oximes to afford isoquinolines. However acetylene has not been used in this type of reaction, which encouraged us to proceed with our investigation using vinyl acetate as an acetylene equivalent.

4.2 Results and discussion

To commence the investigation, ketoximes **268-271** were examined using the previously developed reaction conditions (entries 1-4, Table 4.1).[110] Disappointingly, the ketoxime reacted to give <5% of the corresponding isoquinoline **272**. Competing deacylation of ketoximes esters **270** and **271** resulted in the formation of ketoxime **268** (entries 3 and 4). Increasing the reaction temperature to 60 °C improved the yield of the reactions with *O*-acetylated oxime **271** from 3% to 24% (entry 8).

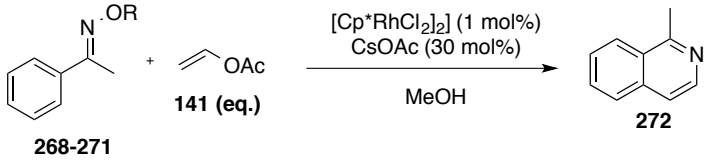

Entry	Reactant	R	**141** (eq.)	Conc. (M)	Temp. (°C)	^{1}H NMR yield (%)[a]
1	**268**	H	1.5	0.2	45	5
2	**269**	Me	1.5	0.2	45	0
3	**270**	Piv	1.5	0.2	45	5
4	**271**	Ac	1.5	0.2	45	3
5	**268**	H	1.5	0.2	60	4
6	**269**	Me	1.5	0.2	60	0
7	**270**	Piv	1.5	0.2	60	4
8	**271**	Ac	1.5	0.2	60	24
9	**271**	Ac	1.5	0.2	60	10
10	**271**	Ac	1.5	0.2	60	2[b]
11	**271**	Ac	1.5	0.2	60	0[c]
12	**271**	Ac	1.5	2	60	19
13	**271**	Ac	5	2	60	48
14	**271**	Ac	10	2	60	75
15	**271**	Ac	20	2	60	30
16	**271**	Ac	neat	2	60	0
17	**271**	Ac	10	2	60	**79**
18	**271**	Ac	10	1	60	56

[a][Cp*RhCl$_2$]$_2$ (1 mol%), CsOAc (0.3 eq.), MeOH, 60 °C, 48 h; [b]1 eq. of CsOAc instead of 0.3 eq; [c]K_2CO_3 (1 eq.) was used instead of CsOAc. Trimethoxybenzene was used as an internal standard.

Table 4.1

Proceeding with *O*-acetylated ketoxime **271**, the number of equivalents of cesium acetate was increased from 0.3 to 1 equivalent, however this had a detrimental effect on the yield, where the oxime **268** was again observed in the ^{1}H NMR of the crude reaction (entries 9 and 10). Fagnou *et al.*[35] observed an improved yield when cesium acetate was replaced with potassium carbonate when using the *O*-pivaloyl ketoxime **270** with diphenyl acetylene, however under these conditions again only the deacylated oxime **268** was observed. To avoid increasing the catalyst

loading, the concentration of the reaction was increased ten-fold to 2 M, and the number of equivalents of vinyl acetate were investigated (entries 12-16). This screening revealed that 10 equivalents of vinyl acetate were necessary to obtain an optimal yield of 75% (entry 14 and 17). Given the low cost and volatility of vinyl acetate (ensuring simple purification), we considered the excessive addition of the substrate to be acceptable. Reducing the concentration to 1 M reduced the yield from 79% to 56% of the isoquinoline (entries 17 and 18). With our optimized conditions in hand, the scope of the reaction utilizing a broad range of substrates was investigated, the results of which are summarized in Table 4.2 and 4.3.

Substrates **273-282** were prepared from the corresponding acetophenones by formation of the *(E)*-oxime using hydroxylamine in refluxing ethanol–pyridine.[64] Subsequent acetylation of the crude oxime, using acetic anhydride and catalytic 4-dimethylaminopyridine (DMAP) in pyridine, furnished the desired products with overall yields for the two steps ranging from 44 to 95% (Table 4.2).[64] To commence the substrate scoping, *ortho*- and *para*-derivatives were considered to avoid issues of regiocontrol. Electron-deficient *p*-nitro- and *p*-trifluoromethyl-*O*-acetylated oximes reacted to afford the corresponding isoquinolines, **283** and **284**, in good yield, however introduction of a methyl group reduced the yield of **285** to 44%. Halogens were well tolerated, with 8-fluoro- **286** and 6-chloro-, bromo-, and iodoisoquinolines (**287**-**289**) being formed in reasonable to good yields (41-72%, Table 4.2). Using the mixture of *E*- and Z-naphthylisoquinoline ketoxime isomers **280** (3:1, *E*-:*Z*-), we were expecting a maximum yield of 75%, based on the study reported by Chiba *et al.*[64] (*cf.* Scheme 1.32). The naphthylisoquinoline **280** reacted to give the tricylic isoquinoline **290** with a yield of 24%. The LCMS of the crude reaction identified peaks corresponding to unreacted starting material (the *E*- and *Z*-isomers), two separate peaks for the *E*- and *Z*-deacylated starting materials and the product peak (entry 9, Table 4.2). The relative signals were difficult to quantify from the ^{1}H NMR spectrum of the crude reaction. Electron-rich groups had a detrimental effect on the yield, with the *ortho*- and *para*-methoxy derivatives reacting to give 14% and 9% of the corresponding isoquinolines **291** and **292**, respectively (entries 10 and 11). The poor yields observed from reactions using electron-rich substrates paralleled the trend observed with the synthesis of isoquinolones (Section 3.1).

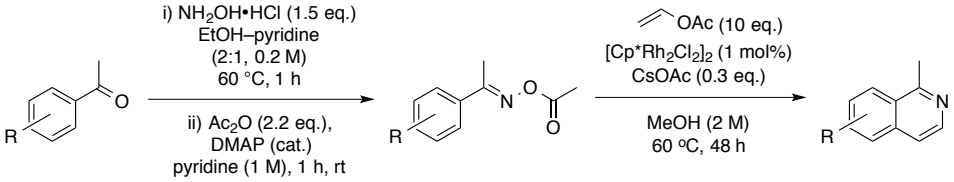

Entry	SM	Yield SM %	No.	Product	Yield (%)	No.
1	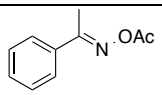	80	**271**	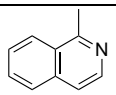	57	**272**
2	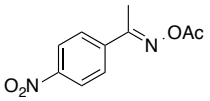	95	**273**	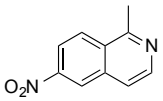	83	**283**
3	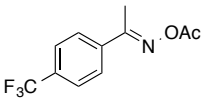	80	**274**	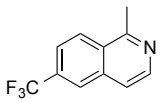	82	**284**
4	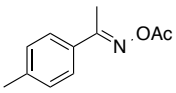	82	**275**	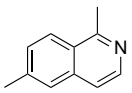	44	**285**
5	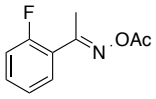	44	**276**	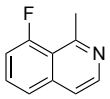	41	**286**
6	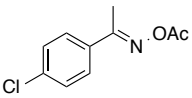	74	**277**	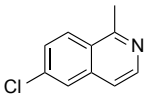	60	**287**
7	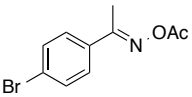	78	**278**	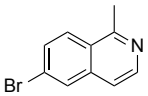	72	**288**
8	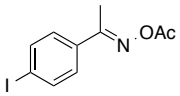	81	**279**	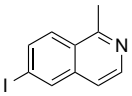	64	**289**
9	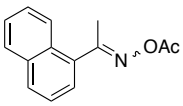	87 (*E:Z, 3:1)*	**280**	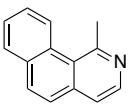	24	**290**
10	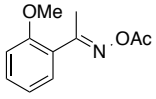	82	**281**	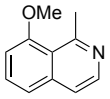	14	**291**
11	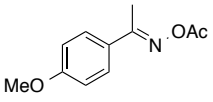	94	**282**	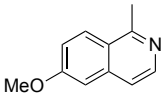	9	**292**

Table 4.2

O-Acetylated *meta*-substituted oximes were investigated to probe regiochemical effects in non-symmetrically substituted substrates (Table 4.3). The 3-bromo **293** and 3-fluoroketoximes **294** reacted to give regioisomeric mixtures of the 7- to 5-substituted isoquinolines (2.7:1 **298a:298b** (50%) and 1:5 **299a:299b** (47%), respectively). As predicted, the *meta*-methylated derivative

295 gave a regioisomeric ratio significantly in favour of C-H activation at the less-hindered position (10:1 **300a:300b**, 52%). In contrast to the methyl example, the *meta*-methoxy derivative was isolated as a 1:1.4 regioisomeric ratio of **301a:301b** in favour of reaction at the sterically congested *ortho*-position. The *ortho*-directing effect of electronegative substituents in rhodium-catalysed C-H activation has been previously noted.[35] To illustrate this effect, the (3,4-methylenedioxy)acetophenone ketoxime **297** was prepared (to remove steric bias from the C-H selectivity), which pleasingly, furnished solely the contiguously substituted isoquinoline **302**.

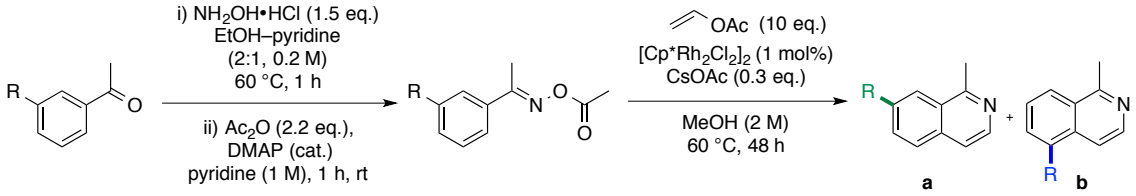

Entry	R	Yield SM %	No.	Product	Ratio[a] a:b	Yield a+b	No.
1	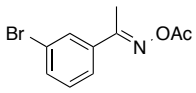	97	**293**	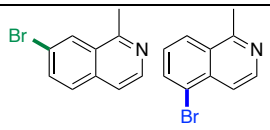	2.7:1	50	**298**
2	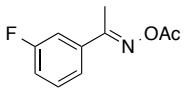	73	**294**	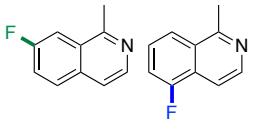	1:5	47	**299**
3	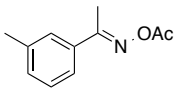	90	**295**	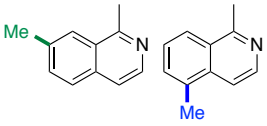	10:1	52	**300**
4	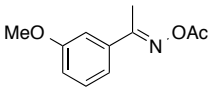	94	**296**	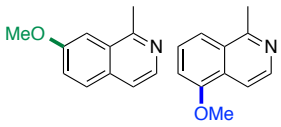	1:1.4	58	**301**
5	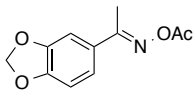	77	**297**	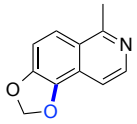	-	36	**302**

Table 4.3 [a]Ratio of purified products.

Substrates **303-306** were prepared in order to assess the tolerance of varied substituents at the α-position, in addition to an example of C-H activation of a heterocyclic example **307**. Replacing the α-methyl substituent with various functional groups proved mostly unsuccessful (entries 1-3, Table 4.4), with the exception of the tetralone derivative **306** which furnished the tetracyclic isoquinoline **308** with a yield of 11%, indicating potential for optimisation (entry 4).

Unfortunately only a trace of the fused thienopyridine **309** was identified from the reaction mixture by ^{1}H NMR analysis (entry 5).

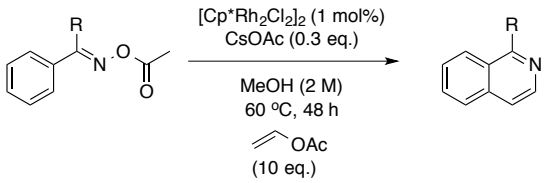

Entry	SM	No.	Product	Yield (%)	No.
1	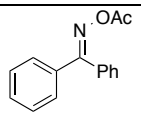	**303**	-	0	-
2	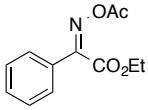	**304**	-	0	-
3	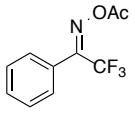	**305**	-	0	-
4	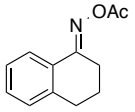	**306**	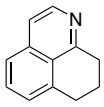	11	**308**
5	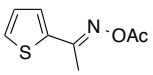	**307**	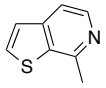	trace	**309**

Table 4.4

In summary, the rhodium(III)-catalysed synthesis of 3,4-unsubstituted isoquinolines was optimised and exemplified with seventeen representative compounds. To ensure the catalyst loading was maintained at 1 mol%, the equivalents of vinyl acetate were increased to ten-fold in order to maximise the yield. Considering the wide availability of methyl ketones as precursors, coupled with the low cost of vinyl acetate, this methodology presents a significant alternative to the current methods available for preparing 3,4-unsubstituted isoquinolines.

4.3 Methodology application: decumbenine B

Having observed a single regioisomer in the reaction of 3,4-(methylenedioxy)acetophenone ketoxime derivative **297**, we were interested in applying our methodology to the corresponding aldoxime **312** in the hope of preparing the isoquinoline intermediate **310** used in Orito's synthesis of decumbenine B. This naturally occurring alkaloid was isolated from the plant tubers of *Corydalis decumbens* and has been used for the treatment of hypertension, rheumatoid arthritis and sciatic neuraligia.[96] The first total synthesis of decumbenine B, reported by Zhu *et al.,* required 18 steps from piperonal.[172] The route was succeeded by a ten-step linear synthesis by Orito[173] and then by an improved seven-step convergent procedure by Larock.[162,163] The intermediate isoquinoline **310,** prepared by Orito *et al.,*[173] relies on a key Pictet-Gams cyclisation, resulting in a yield of 22% over five steps (Scheme 4.2).

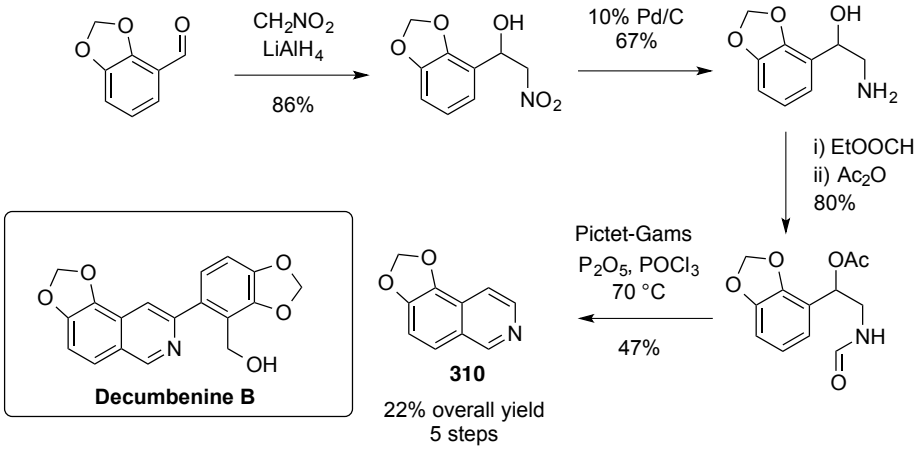

Scheme 4.2 Orito et al., synthesis of decumbenine B.[173]

By application of the previously developed methodology, the aldoxime **312** was converted to the intermediate isoquinoline **310** as a single regioisomer with a yield of 26% (21% over three steps from piperonal, Scheme 4.3). The remaining starting material had rearranged to give the corresponding nitrile **313**. Attempts to optimize the conditions by increasing the catalyst and base loading proved unsuccessful. Exchange of the *O*-acetyl ketoxime for the *O*-pivaloyl ketoxime group resulted in 100% conversion to the corresponding nitrile **313**. This result was perhaps unsurprising as aldoximes are susceptible to elimination to nitriles; examples include reactions catalyzed by ruthenium,[174,175] palladium,[176–178] copper,[179] among others.[180–183] Although disappointing for the intended purpose, the potential for a rhodium-catalysed rearrangement of ketoximes has been identified and is currently under investigation, as nitriles are valuable intermediates in chemical synthesis.

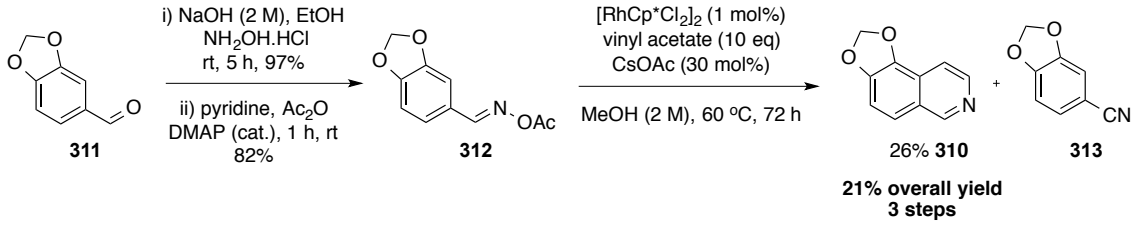

Scheme 4.3

4.4 Conclusion

In conclusion, a C-H activation protocol has been optimised and developed for the synthesis of seventeen 3,4-unsubstituted isoquinolines. Electron-deficient ketoximes were particularly effective substrates under these conditions, however, electron-rich derivatives were less reactive, leading to competing deacetylation of the starting materials. The synthetic utility of vinylic esters as acetylene synthons has broad application in the synthesis of heterocycles. To demonstrate the application of this methodology, a three-step synthesis of the decumbenine B intermediate **310** was achieved. Additionally, a rhodium-catalyzed rearrangement of aldoximes to nitriles was identified.

4.5 Future work

The isoquinoline alkaloids have been identified as potent therapeutic agents for a host of anticancer, antimalarial and antiviral applications, to name but a few.[149,184] The most prevalent scaffolds within this class of compounds are based on natural berberine and palmatine, and the synthetic coralyne, of whose analogues have been extensively studied (Figure 4.1).[149] A common motif embedded in these structures is a 3-arylisoquinoline.

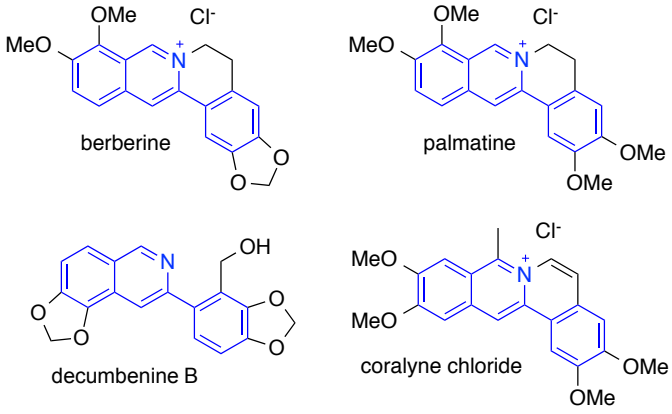

Figure 4.1

Larock *et al.*[162,163] reported a succinct synthesis of decumbenine B using a key palladium-catalysed coupling of terminal acetylenes **315** with 2-iodobenzalimines **314** to furnish 3-arylisoquinolines (Scheme 4.4), significantly improving access to these scaffolds. The drawback of this system is the requirement for a halogenated starting material to undergo the cross-coupling reaction.

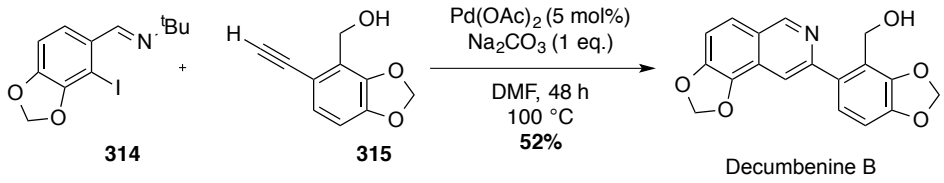

Scheme 4.4

Using a similar disconnection, a C-H activation annulation would offer an alternative, succinct pathway for the synthesis of these alkaloidal scaffolds and their analogues (Scheme 4.5). This methodology will be investigated in due course.

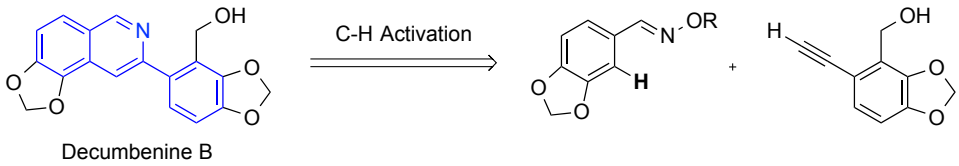

Scheme 4.5

Chapter 5

Synthesis of tetracylic fluorescent imides

5.1 Introduction

5.1.1 A divergent mechanistic pathway revisited

Whilst screening the reactions of hydroxamic esters (see Section 2.6), an unexpected product was isolated from the rhodium(III)-catalysed reaction of *N*-methoxybenzamide **42** with vinyl acetate **141** (Figure 5.1). The isoindolo[2,1-*b*]isoquinoline-5,7-dione **143** was isolated with a low yield of 6%, along with unreacted starting material.[85] Investigation of the spectrochemical properties of the molecule identified a strong blue fluorescence (λ_{abs} 375 nm, λ_{emis} 413 nm, dichloromethane). The ability to simply tailor the fluorescence of a key scaffold for a particular purpose is highly attractive. Based on the structure of the tetracyclic imide **143**, one could envisage tuning the fluorescent and physical properties (in terms of solubility and/or crystallinity) by modification of the aromatic rings using various substituents.

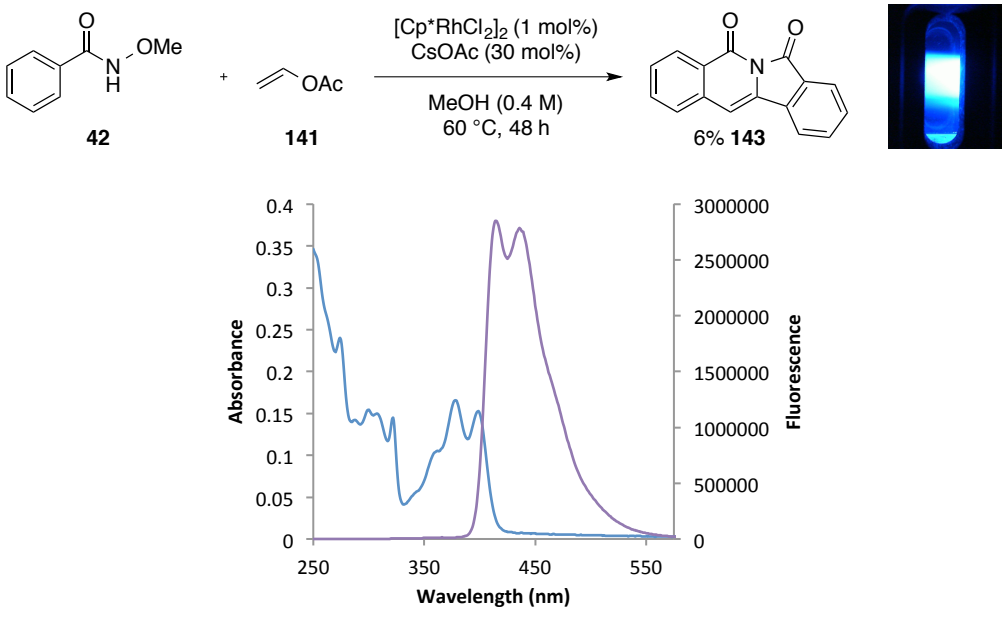

*Figure 5.1. Absorbance and emission spectra for imide **143** in dichloromethane.*

5.1.2 Application of aromatic fluorescent molecules

In recent years the development of luminescent and π-functionalised materials, for application in organic semi-conductors[185,186] and electroluminescent organic materials,[187–193] has driven the demand for succinct, efficient syntheses of polycyclic and heterocyclic compounds. This class of polycyclic aromatic compounds are of particular interest due to their stability, their fluorescent properties in the solid state and their ability to transport charge.[194] The basic requirements for organic electroluminescent materials are the capability to undergo charge transfer to an electrode, the ability to transport charge and to fluoresce efficiently.[187]

Fluorescent compounds are particularly attractive for use in organic light-emitting diodes (oLEDs). Many green and red-light emitting diodes have been developed, however highly efficient and stable blue-light emitters are still rare.[195] Fluorene-based polymers are commonly used in blue-light emitting materials, due to their good thermal stability and solubility and their photoluminescent quantum yield.[196–198] For example, Chen and Kieffer *et al.* developed fluorene based polymers **323**-**325** for oLED applications (Scheme 5.1).[195] The carbazole derivative **318** was prepared *via* an Ullman coupling of carbazole **316** and 4-iodoaniline **317**. The oligomeric strands **320**-**322** were prepared by a Buchwald-Hartwig coupling of the aniline **318** with the dibromofluorene **319** to afford the intermediates **320**-**322** with yields of 53-68%. A subsequent Suzuki coupling furnished the final oligomers, which displayed high photoluminescent quantum yields (ranging from 59-64% in chloroform) with λ_{max} emission values of 493 nm for **323** and **324** and 446 nm for **325**.

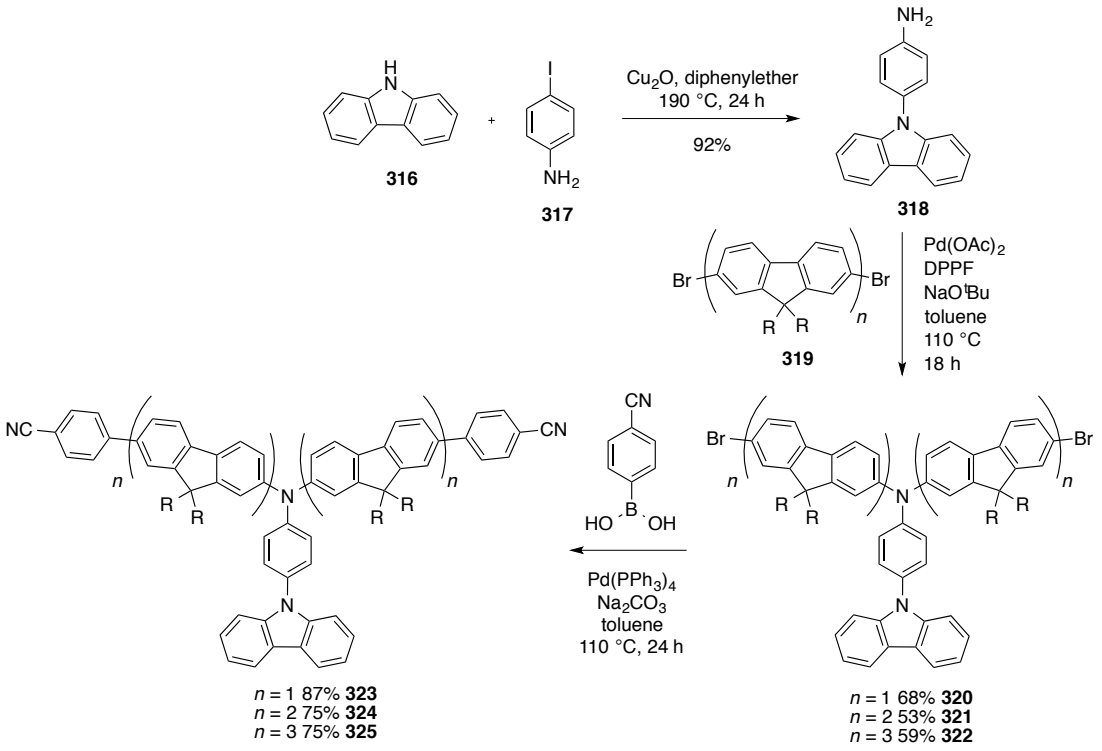

Scheme 5.1

In recent years, white polymer light-emitting diodes (WPLEDs) have received attention due to their potential application in backlight and full-colour displays with colour filters.[199] Wang *et al.* incorporated three primary colour emitters (blue (λ_{max} 445 nm), green (λ_{max} 515 nm) and red (λ_{max} 624 nm)) in a single polymer **330** to cover the whole visible range spectrum from 400 to 700 nm (Scheme 5.2). Generally in a macromolecule, the energy from the shorter wavelength fluorophore will transfer to the longer wavelength emitter, causing emission only from the latter to be observed. To circumvent this issue, Wang *et al.* decreased the green and red emissive components, with respect to the blue fluorene to ensure this transfer of energy was compensated for, ensuring separate blue, green and red emission. The polymer was assembled *via* a Suzuki polymerisation coupling of the brominated monomers **326**, **328** and **329** with the fluorene boronic acid **327**.

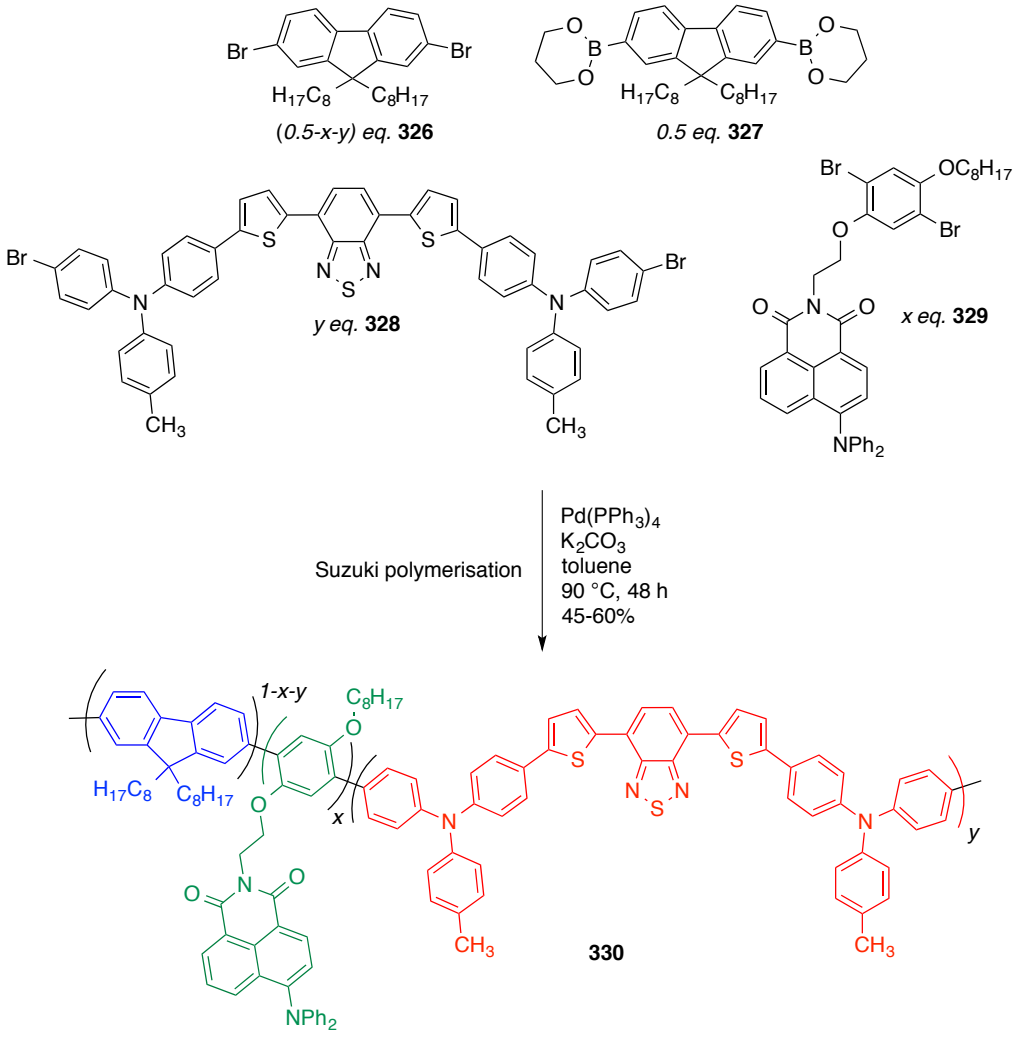

Scheme 5.2

In biological systems, fluorescence microscopy is one of the most widely used approaches for high-resolution, non-invasive imaging of live organisms.[200] Exogenous organic fluorophores are the most commonly used tags for fluorescence-based imaging. Shorter-wavelength fluorophores are infrequently used as longer wavelength dyes are widely available and are less likely to cause

photodamage to labelled biomolecules.[201] Many cells autofluoresce when exposed to UV light and therefore eliminate the requirement for UV sensitive exogenous fluorophores. Despite these considerations, blue-fluorescent probes can provide a contrasting colour that can be easily distinguished from the longer wavelength probes (that are typically green, yellow, orange and red). Multicolour assays are often used for immunofluorescence, *in situ* hybridization and neuronal tracing, and nucleic acid/protein microarrays.[201] Aside from Cascade blue® **331**, most blue fluophores for biological imaging are based on the coumarin scaffold, for example Alexa Fluor® 350 **332**, 4-amino-4-methyl-coumarin (AMCA-X) **333** and Pacific Blue™ **334** (Figure 5.2).

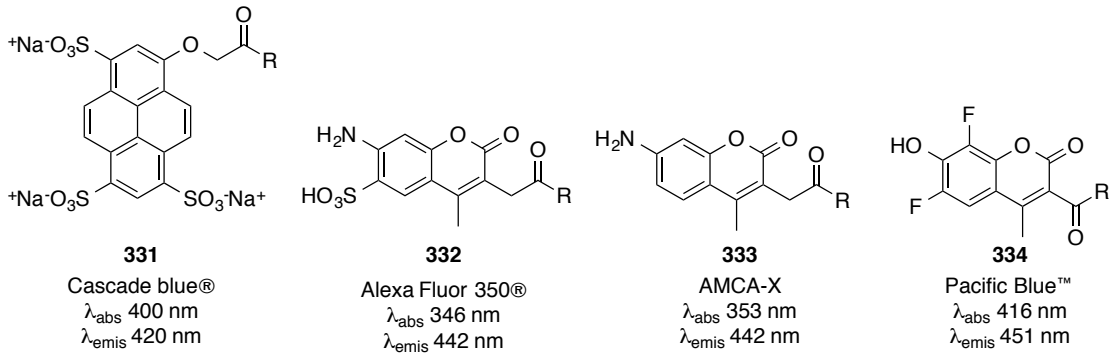

331
Cascade blue®
λ_{abs} 400 nm
λ_{emis} 420 nm

332
Alexa Fluor 350®
λ_{abs} 346 nm
λ_{emis} 442 nm

333
AMCA-X
λ_{abs} 353 nm
λ_{emis} 442 nm

334
Pacific Blue™
λ_{abs} 416 nm
λ_{emis} 451 nm

Figure 5.2

5.1.3 Assembly of polyaromatic scaffolds *via* rhodium(III)-catalysed C-H activation

In the past decade, numerous reports of polyaromatic or heteroaromatic scaffolds have been explored, due to the demand for novel conducting materials. C-H activation methodology has proved highly useful in the synthesis of these scaffolds. Numerous examples of rhodium(III)-catalysed cleavage of C-H/N-H or C-H/O-H bonds with subsequent annulation reactions with alkynes have been reported for the synthesis of polycyclic compounds.[109,202–207] For example, Cheng *et al*. reported the synthesis of highly substituted naphthyridine-based polyheteroaromatic compounds **336** from *N*-hydroxbenzamidines **335** with diphenyl acetylene **40** (Scheme 5.3).[202] Using copper(II) acetate and the oxime (N-O) bond as a source of an internal and external oxidant, they were able to achieve three C-H bond insertions to form the pentacyclic fused core. Derivatives of the polyaromatic compound **336** displayed absorbance maxima from 380-450 nm and fluorescence maxima from 500-530 nm.

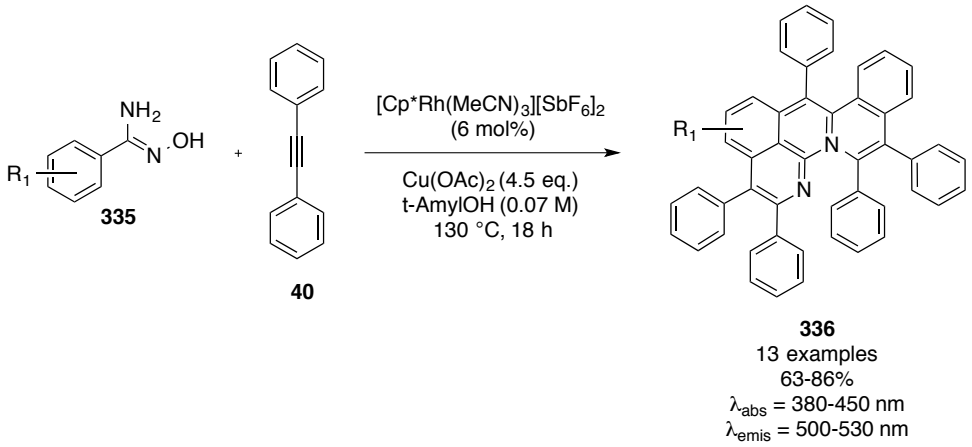

Scheme 5.3

Using a combination of an internal and external oxidant, Shi *et al.* utilised the oxidative rhodium(III)-catalysed annulation of aryl ketoximes **337** with three units of phenyl acetylene **40** to form sterically congested 1-methyl-4-phenyl-3-tetraphenylnaphthyl isoquinolines **338**, with an average yield of 72% across 12 examples (Scheme 5.4).[170]

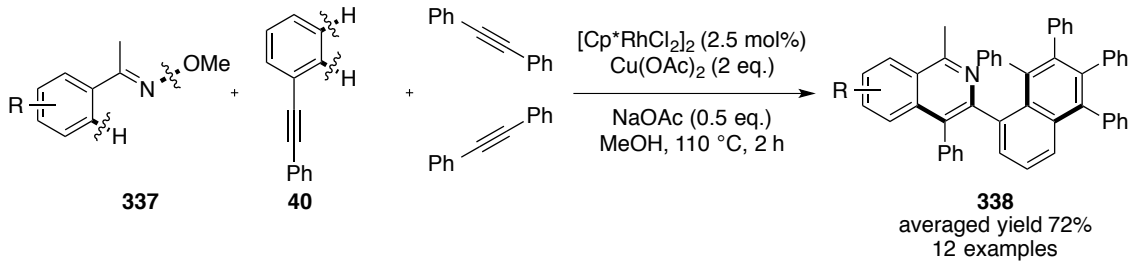

Scheme 5.4

The groups of Song[206] and Miura[109] reported the synthesis of fused isoquinolone scaffolds **339** from the rhodium(III)-catalysed annulation of benzamides **15** with diphenylacetylene **40** (Scheme 5.5) using silver carbonate and copper acetate as oxidants, respectively.

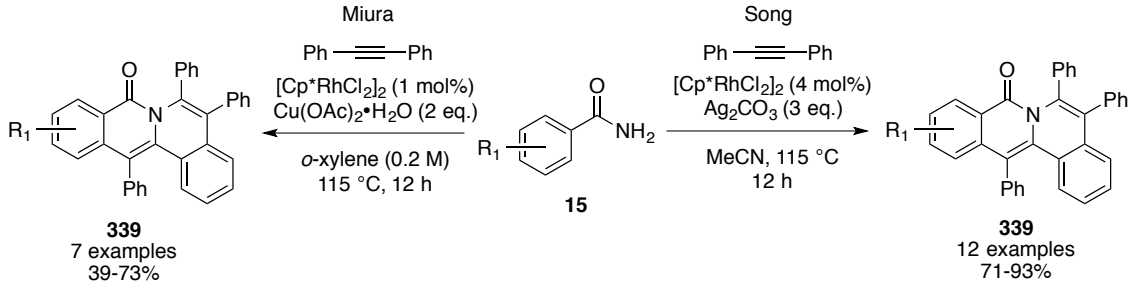

Scheme 5.5

Under Miura's copper(II)-rhodium(III) conditions, annulation of the phenyl-substituted benzamide derivatives **340** with diphenyl acetylene substrates **341** furnished a range of isoquinoline-1-(*2H*)ones **342**. These structures displayed fluorescence in the solid state within a range of 370-420 nm,[109] however, the tetracyclic compounds **339** (Scheme 5.6) did not fluoresce.

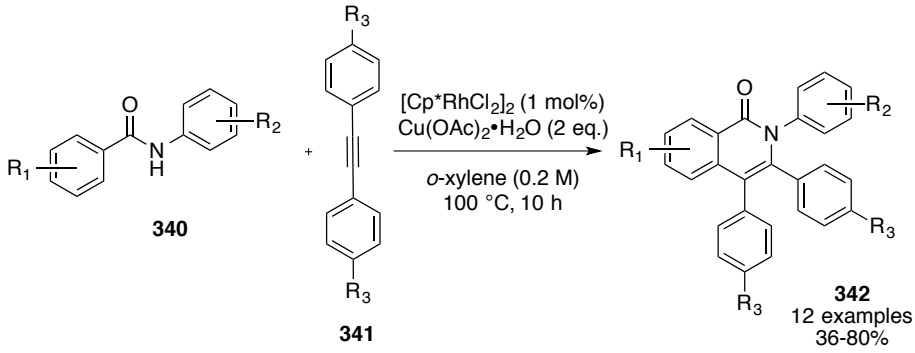

Scheme 5.6

Based on a similar isoquinolone framework, Zhang *et al.*[208] used the internal oxidant strategy, using the *N*-(acetoxy)benzamide derivative **343** with diphenylacetylene **40** to construct the pyrido[3,4-*g*]-isoquinoline framework **344**. To improve the solubility, the isoquinolone **344** was alkylated with bromohexane to afford a mixture of the *N*- and *O*- alkylated products, **345-347**. The compounds fluoresced in a similar region to one another (at approximately 470 nm) and were found to have quantum yields ranging from 0.092-0.25 in solution (using quinine in 1N H_2SO_4 as a standard), with lower values observed in the solid state (0.033-0.22) (Table 5.1). Interestingly, the fluorescent yield diminished with the gradual transformation of the pyridine ring to the cyclic amide (**345** to **346** to **347**).

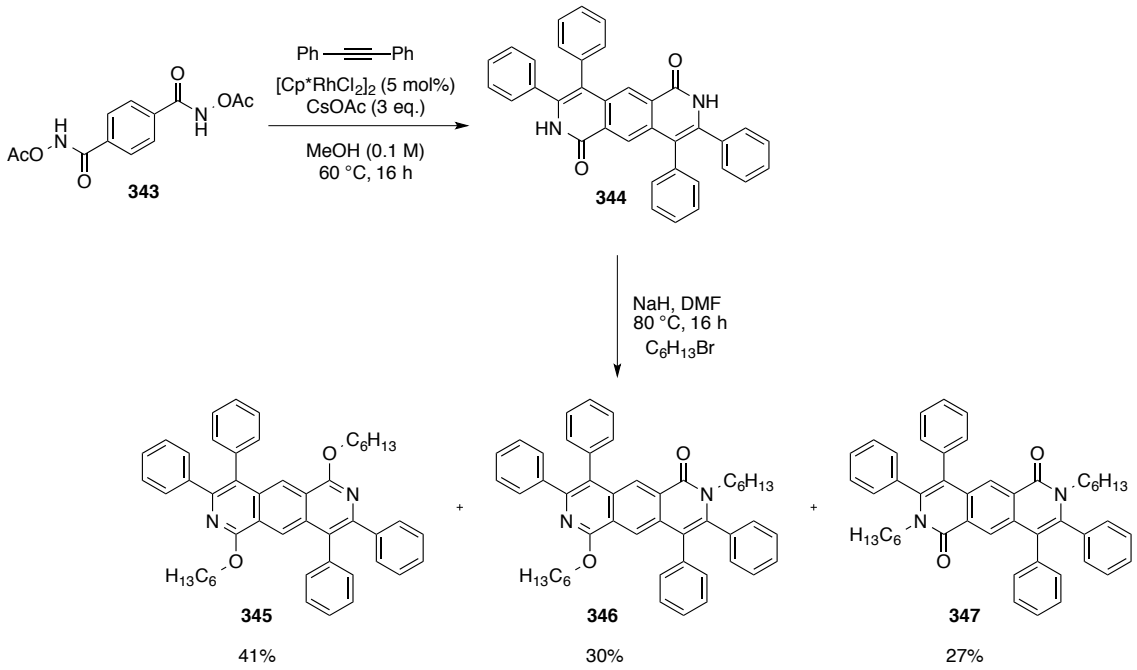

Entry	Compounds	Absorption λ_{max} (nm)	Fluorescence λ_{max} (nm)	$\Phi_{solution}$	Φ_{solid}
1	**345**	278, 362	447, 470	0.25	0.22
2	**346**	266, 356	472, 470	0.098	0.07
3	**347**	258, 354	469, 469	0.092	0.033

Table 5.1

Considering the vast application of fluorescent molecules, both in the field of material chemistry and in biological application, the ability to tune the fluorescent and physical properties of a fluorescent scaffold would be a highly desirable attribute.

5.2 Mechanistic studies

The tetracyclic imide **143** had been previously reported, however the compound was never fully characterized.[84–88,90] Additionally, there is no reference to its fluorescent properties. The existing synthetic routes require harsh conditions with step-wise procedures. Godfrey *et al.* reported the synthesis of the imide **143** *via* a thermal cyclisation at 240 °C of the diammonium salt of 2,2'-dicarboxy-desoxybenzoin **348** in diphenylamine (Scheme 5.7).[90]

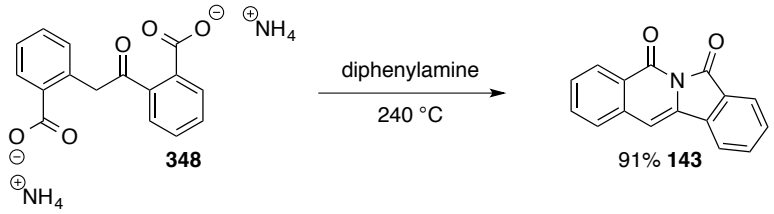

Scheme 5.7[90]

The pursuit of this route for the synthesis of the tetracyclic imide scaffold would be of interest, as the scope for tailoring the fluorescent properties towards a variety of applications would be of interest. In order to optimise the yield using this methodology, further understanding of the mechanism was required. Based on the structure of the imide **143**, it was apparent that two units of the *N*-methoxybenzamide derivative **42** had reacted with one unit of vinyl acetate, however the mechanism of the reaction was not evident. A route *via* activation of the isoquinolone **137** was rejected based on the full recovery of the starting material **137** upon resubjection to the reaction conditions with both the *N*-methoxybenzamide derivative **42** and the more reactive *N*-(pivaloyloxy)benzamide **43** (Scheme 5.8). The latter substrate resulted in a rearrangement to the corresponding methyl phenyl carbamate *via* the Lossen rearrangement.

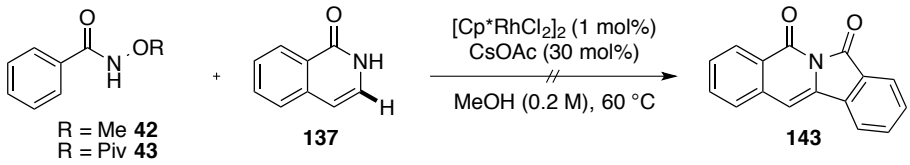

Scheme 5.8

In a separate study within the Marsden group, a C-H activation reaction using vinyl ethers/esters with acetophenone **349**, catalysed by $[Cp^*RhCl_2]_2$ with copper(II) acetate as a stoichiometric oxidant, was in development (Scheme 5.9). A trace of 2-vinylacetophenone **350** was observed when vinyl laurate **241** was treated with acetophenone **349**, presumably *via* elimination of lauric acid from the rhodacycle **I**.

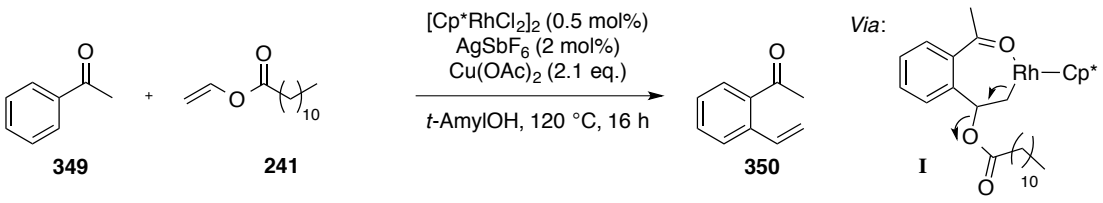

Scheme 5.9

Despite the fact that the directing group and oxidant system was different to the system using *N*-methoxybenzamide **42** and vinyl acetate **141**, the formation of 2-vinyl-*N*-methoxy-benzamide **351** and 2-vinyl-benzamide **352** were investigated as putative intermediates (Scheme 5.10). The following mechanistic studies were carried out by Michael Watt within the Marsden group. To commence this study, vinyl acetate **141** was replaced with 2-vinylbenzamide **351** and 2-vinyl-*N*-methoxybenzamide **352** (Scheme 5.10). Interestingly, the formation of imide **143** was not observed in the reaction using 2-vinyl benzamide **351**, however, the reaction of 2-vinyl-*N*-methoxy benzamide **352** with *N*-methoxybenzamide **42** gave the imide **143** and the stilbene-derivative **353** with yields of 25% and 30%, respectively.

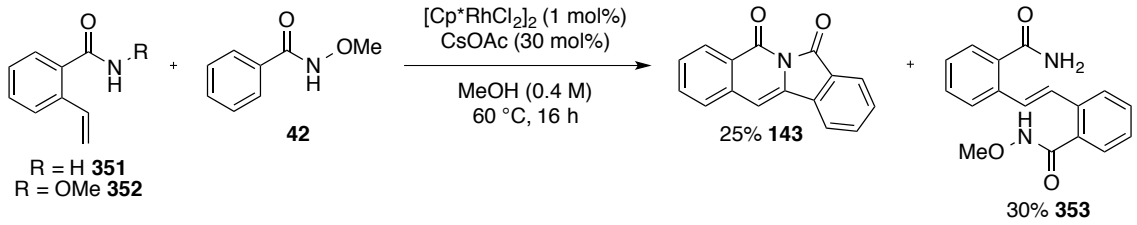

Scheme 5.10

The stillbene derivative **353** was found to be highly insoluble in methanol, and only sparingly soluble in DMF and DMSO. The intermediate **353** was isolated and re-subjected to the reaction conditions above, however more aggressive heating under microwave conditions (80 °C) were used to aid solubility (Scheme 5.11). The imide was isolated with a yield of 18%, suggesting the stilbene derivative **353** as a possible reaction intermediate. In order to generate significant quantities of the stilbene **353**, the cyclisation precursor to the imide **143**, the addition/elimination reaction of *N*-methoxybenzamide **42** with vinyl acetate **141** to generate 2-vinyl-*N*-methoxybenzamide **352** would have to be high yielding. The 6% yield of the isolated imide **143** from the initial reaction of *N*-methoxybenzamide **42** with vinyl acetate **141** would suggest that this was not the case.

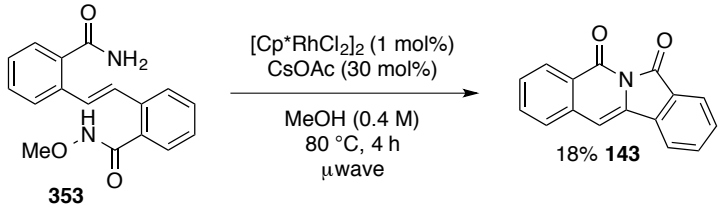

Scheme 5.11

Based on these putative intermediates, a catalytic cycle for the formation of the tetracyclic imide was proposed. Initial formation of *N*-methoxy-2-vinylbenzamide **352** could proceed *via* elimination of acetic acid from the rhodacycle **II** (Scheme 5.12)

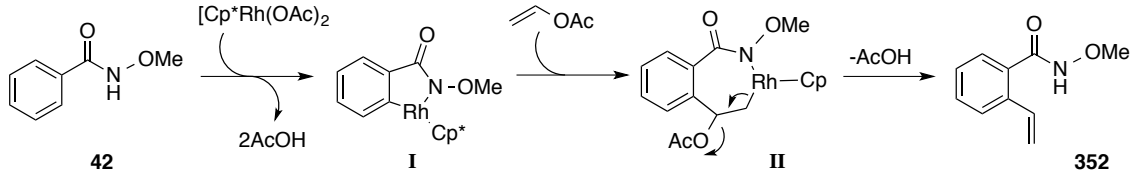

Scheme 5.12

Coordination of the rhodium(III) active catalyst, [Cp*Rh(OAc)$_2$] to *N*-methoxybenzamide **42**, followed by coordination of the vinylic substrate **352** would result in the formation of the seven-membered rhodacycle **III** (Scheme 5.13). Subsequent *β*-hydride elimination from the six-membered **IV** rhodacycle (*via* a ligand exchange), followed by N-OMe bond cleavage could furnish the stilbene **353** intermediate. These initial steps follow the classic rhodium(III)-catalysed oxidative Heck mechanism.

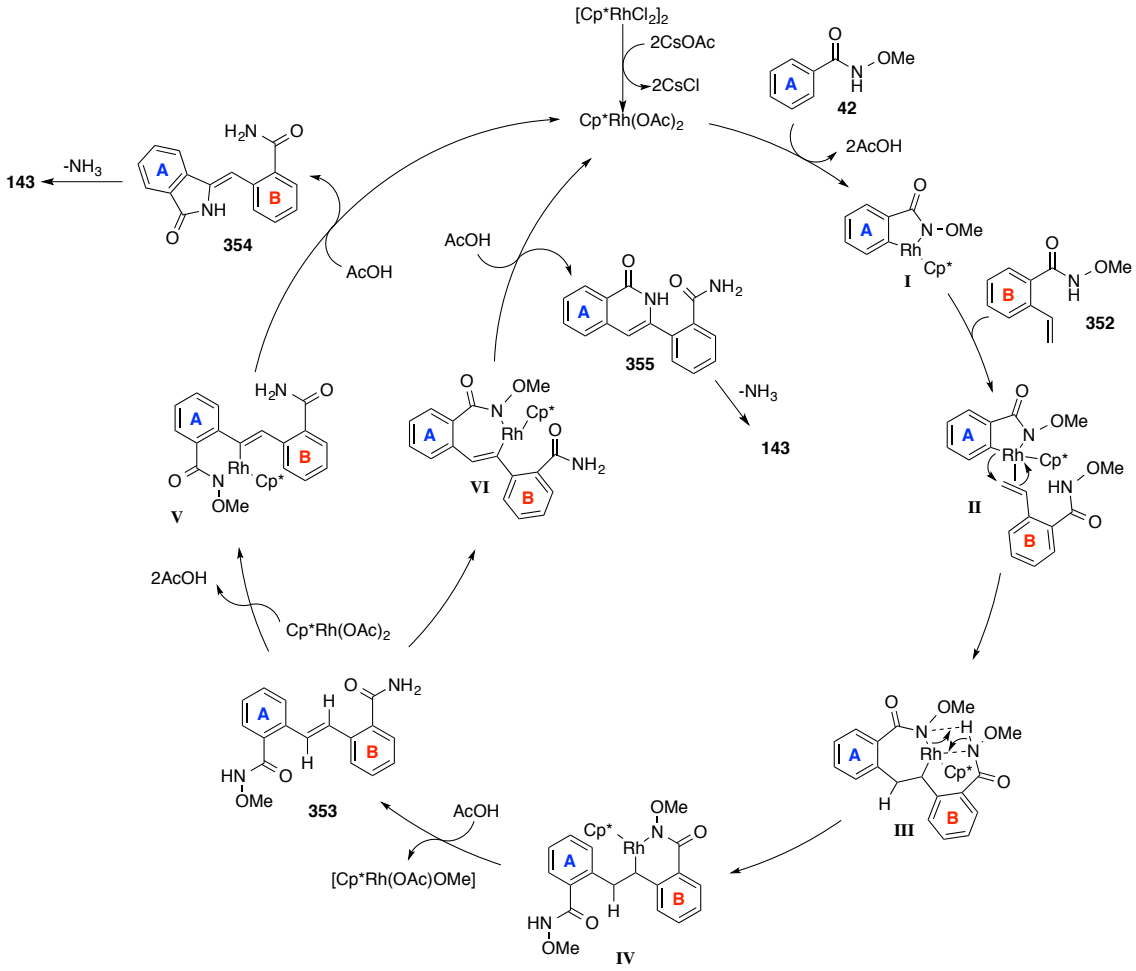

Scheme 5.13

Insertion of the catalyst into the alkenyl C-H bond could proceed *via* two pathways, either through formation of the six-membered rhodacycle **V** or by insertion into the adjacent C-H bond, to form the seven-membered rhodacycle **VI**. In order to distinguish the aromatic rings, a fluorine atom was introduced into the *N*-(pivaloyloxy)benzamide substrate in a study carried out by a co-worker (Scheme 5.14). Had the fluorine been incorporated into the isoquinolone portion of the imide, it would have suggested a seven-membered rhodacycle **VI**, and *vice versa* for the six-membered rhodacycle **V** (Scheme 5.13). The reaction of 4-fluoro-*N*-(methoxy)benzamide **356** and 2-vinyl-*N*-methoxy benzamide **352** furnished the imide **360**, suggesting the formation of a six-membered rhodacycle **358** followed by reductive elimination to form **360**. Subsequent release of ammonia from cyclisation of the *exo*-cyclised lactam **359** would give the imide **360**.

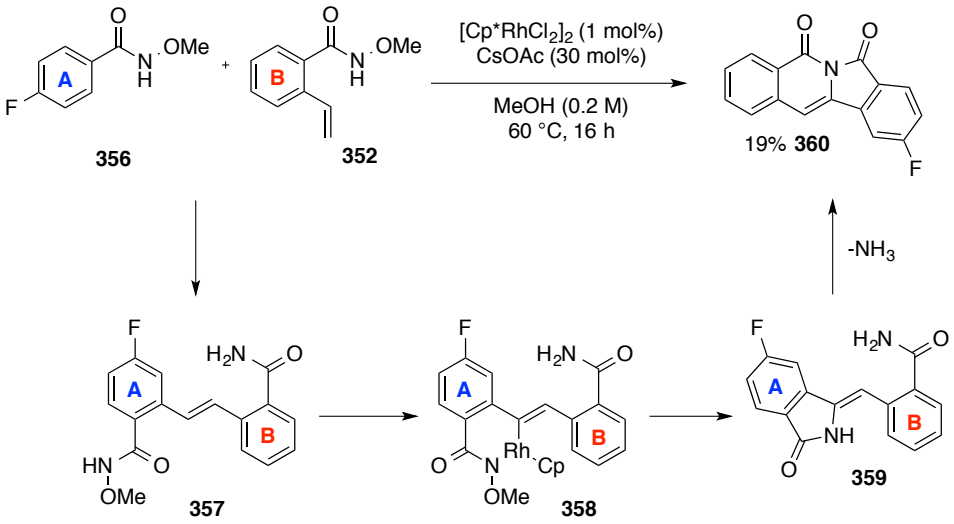

Scheme 5.14

Additional literature evidence would suggest this pathway was favoured. A report by Glorius *et al.* identified the intramolecular cyclisation reaction of the *ortho*-benzamide stilbene **361** to give the *exo*-cyclised lactam **362** (*via* **363**) under rhodium(III)-catalysed system using copper(II) acetate as an oxidant (Scheme 5.15).[20]

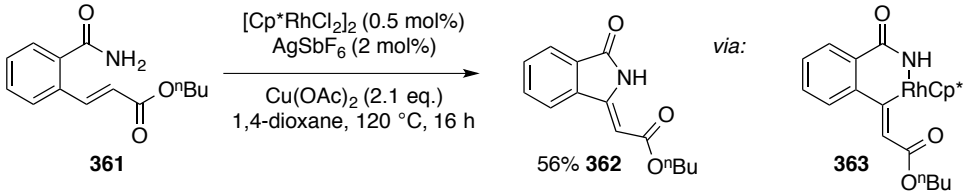

Scheme 5.15

Subsequent C-N bond formation *via* a reductive elimination (which would cleave the N-OMe bond to regenerate the rhodium(III) catalyst) would lead to the formation of lactam **354**, which could undergo cyclisation, with loss of ammonia, to afford the imide **143**.

This short study revealed potential intermediates in the catalytic system. Attempted optimisation of the original reaction conditions however proved futile based at least in part on the poor solubility of these compounds (see Scheme 5.10). The alternative reaction, starting from the *N*-methoxy-2-vinyl benzamide derivative **352**, improved the yield of the imide from 6% to 25%, however there were recurrent issues with the solubility of the product and intermediate stilbene derivatives.

We envisaged an alternative approach, exploiting the well-established rhodium(III)-catalysed C-H activation/annulation of hydroxamate esters **366** with unsymmetrical alkyl-aryl internal alkynes **367** to prepare substituted isoquinonolones **365**, bearing an *ortho*-carboxylate on the pendent phenyl ring (Scheme 5.16). Subsequent cyclisation of the intermediate isoquinolone **365**, could provide the target imide **364** in two steps from the starting materials.

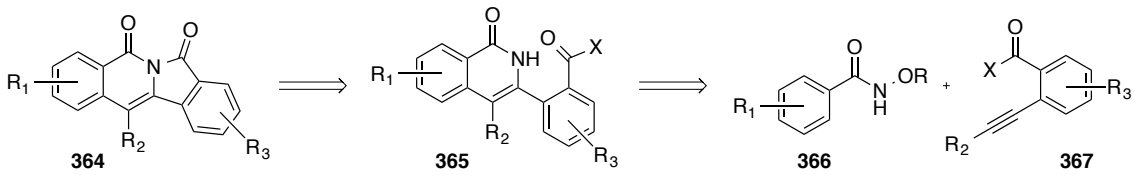

Scheme 5.16

Fagnou[35] *et al.* observed excellent regioselectivity in the annulation reactions *N*-(pivaloyloxy)-benzamide **43** with alkyl-aryl internal alkynes **368**, whereby the aromatic group was consistently installed at the 3-position of the isoquinolone **369a-c** (Scheme 5.17). However, to our knowledge, no examples of *ortho*-substituted phenyl groups on the internal alkyne had been used in these annulation protocols.

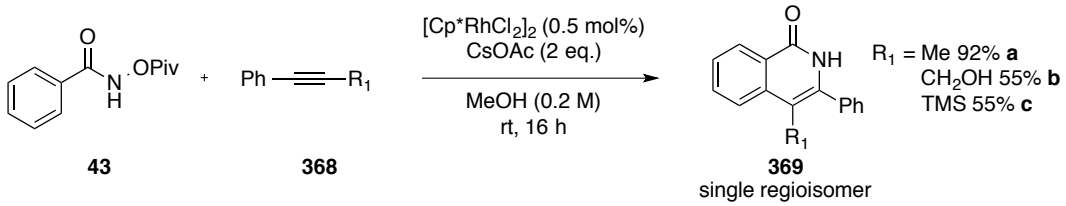

Scheme 5.17[34]

If a similar regiochemical outcome could be achieved from the coupling of a 2-alkynyl-benzoate derivative **367** with a *N*-(pivaloyloxy)benzamide substrate **366**, subsequent cyclisation of the isoquinolone intermediate **365** would provide the imide **364** *via* a succinct, efficient route (Scheme 5.16). Additionally, the *N*-(pivaloyloxy)benzamide substrates **366** are prepared from the corresponding benzoic acids, of which derivatives are widely available. Facile synthesis of the bespoke alkynes **367** could be achieved *via* the well-established Sonogashira reaction, with a

variety of aliphatic terminal alkynes to choose from. Additionally, introduction of an aliphatic group at the C_4 position could address the solubility issues, previously observed with the former routes. We were confident that introduction of a group at this position would not impact the planar π-system responsible for the fluorescent properties of the molecule. Careful design of the substrates could be used to tailor the fluorescent properties of the molecule, resulting in a diverse library of imides.

5.3 Optimisation and synthesis of novel imides

With a new synthetic approach in hand, a range of *ortho*-carboxyl-substituted phenylalkyne substrates were prepared. Methyl 2-(oct-1-yn-1-yl)benzoate **370** was prepared *via* a Sonogashira reaction of methyl 2-iodobenzoate with 1-octyne (Scheme 5.18).[209] Pleasingly, the subsequent reaction of the alkyne **370** and *N*-(pivaloyloxy)benzamide **43**, using the rhodium catalyst, $[Cp^*RhCl_2]_2$, employed by Fagnou *et al.*[35] gave a mixture of the desired imide **372** and the uncyclised isoquinolone **371** as a 1:1 mixture with a yield of 87% (^{1}H NMR yield using mesitylene as an internal standard). Gratifyingly, the undesired regioisomer was not observed in the ^{1}H NMR spectrum of the crude reaction mixture.

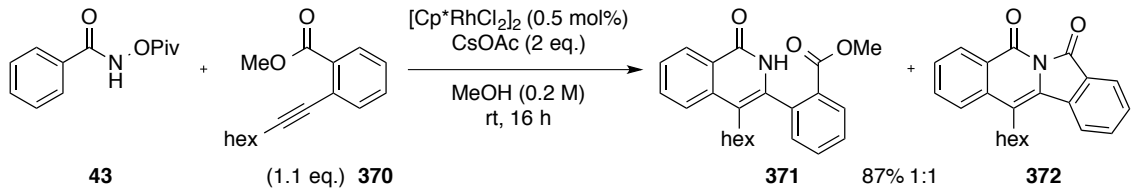

43 (1.1 eq.) **370** **371** 87% 1:1 **372**

Scheme 5.18

Interestingly, observation of the *ortho*-carboxyl-substituted isoquinolone **371** in deuterated chloroform over 24 hours revealed a slow conversion to the cyclised imide **372**, presumably aided by residual acid in the chloroform (Figure 5.3). Full conversion to the product was achieved after one week in chloroform.

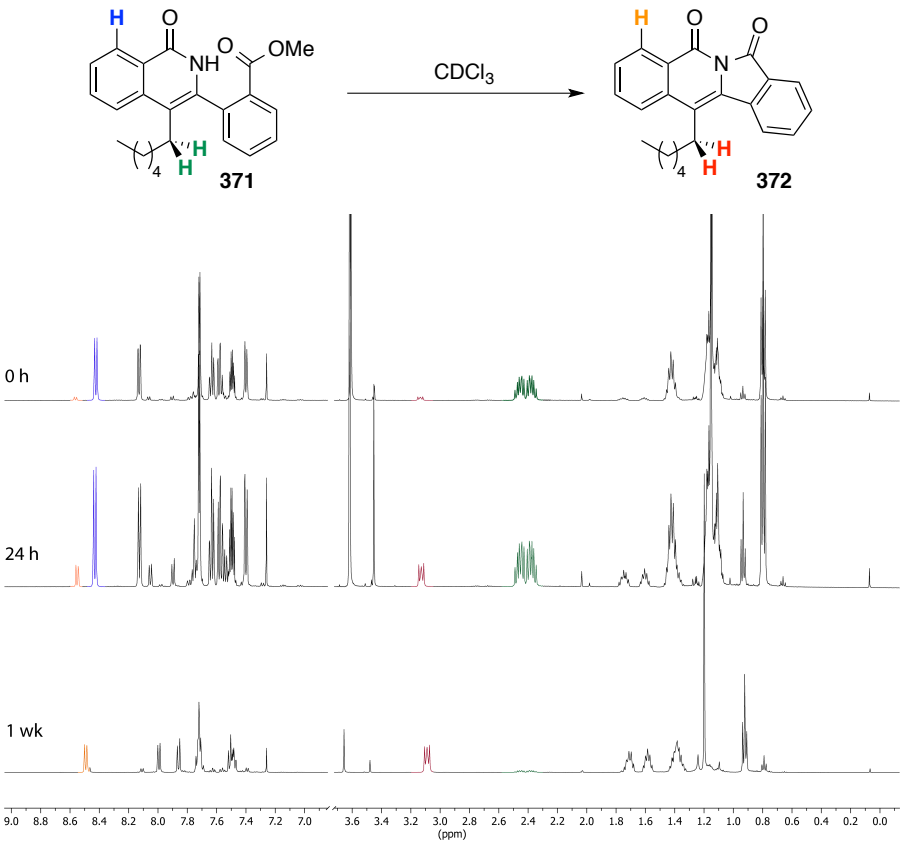

Figure 5.3

Based on this observation, the methanol from the crude reaction mixture was removed *in vacuo* and the residue redissolved in acetonitrile with *p*-toluenesulfonic acid and heated to 80 °C to achieve full conversion to the imide **372** (Scheme 5.19). An attempt to purify the crude reaction mixture by column chromatography resulted in poor recovery of the imide, with most of the product hydrolysing to form the corresponding acid **373** on the column.

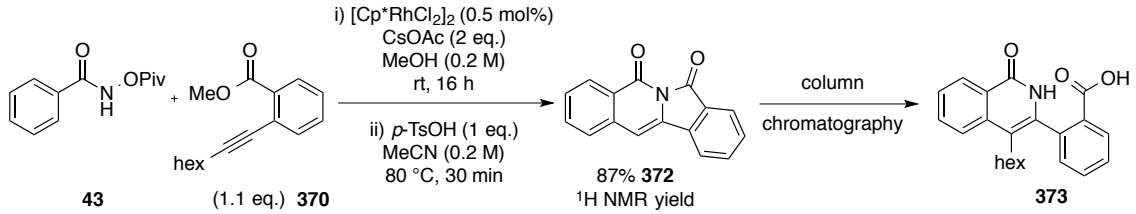

Scheme 5.19

The instability of the imide in nucleophilic solvents became apparent from a ^{1}H NMR study in deuterated methanol (Figure 5.4). On dissolution in deuterated methanol-d_4, the ^{1}H NMR spectrum indicated a 3:1 ratio of the imide **372** and the uncyclised isoquinolone **371**. The alcoholysis of the imide in deuterated MeOD-d_4 was monitored over six hours at 23 °C and 50 °C at 30 minute intervals (Figure 5.4). Within the time taken to heat the sample to 50 °C within the ^{1}H NMR machine, the imide had undergone 100% conversion to the ring-opened

isoquinolone **371**. The reaction monitored at room temperature indicated an initial 25% conversion to the corresponding isoquinolone, rising to 84% over six hours. The stability of the imide in nucleophilic solvents is of fundamental importance if these scaffolds are to have application as a fluorescent unit in aqueous environments.

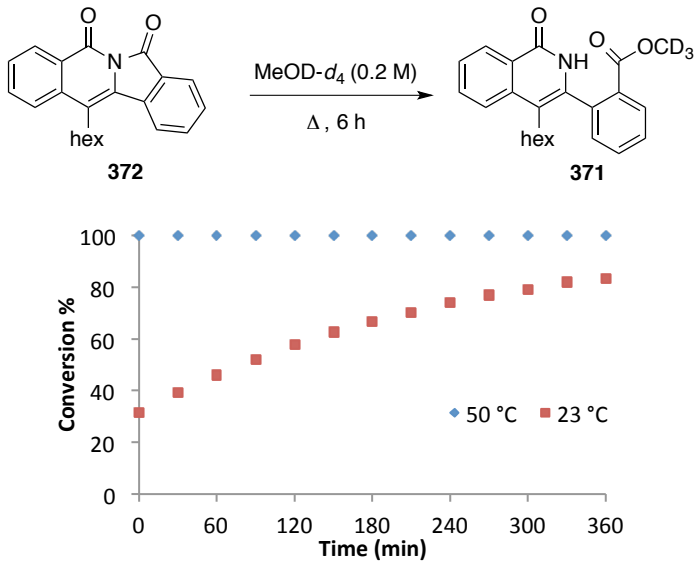

Figure 5.4

Polar aprotic solvents were screened as alternative reaction solvents, in the hope of isolating the imide as the sole product from the reaction. The conditions screened in Table 5.2 resulted in a lower yield of the mixture of products, **371** and **372**, compared to the reaction in methanol (Table 5.2, entry 1). Reactions in tetrahydrofuran and 1,4-dioxane were unsuccessful (entries 2 and 3). The reaction in acetonitrile gave an improved yield of 50% (entry 4), however the most promising result was achieved using a solvent blend of acetonitrile and methanol (9:1) which gave a 1:0.3 ratio of the imide **372** to the methyl ester derivative **371** with a combined yield of 75% (entry 7). The yield was however still lower than the methanolic system (entry 1), which re-focussed effort towards optimising the purification step.

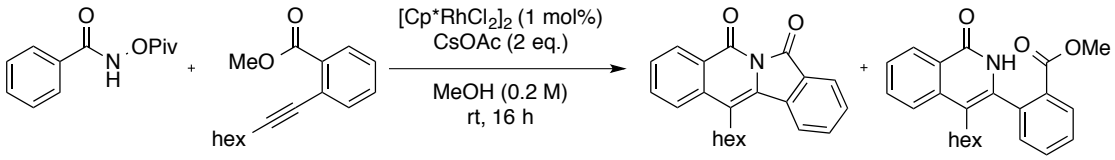

43 **370** **372** **371**

Entry	Solvent	^{1}H NMR yield % **371** and **372**	Ratio **372**:**371**
1	MeOH	87	1:1.3
2	THF	6	1:0
3	Dioxane	0	-
4	MeCN	50	1:0
5	MeCN:MeOH (3:1)	64	1:1.3
6	MeCN:MeOH (9:1)	75	1:0.3

Table 5.2

Chromatography, including HPLC and standard flash silica chromatography proved unsuccessful, with poor recovery of the imide **372** and uncyclised product **371**, with additional hydrolysed acid **373** observed. Treatment of the crude reaction mixture from the initial rhodium-catalysed annulation reaction (using conditions in entry 1, Table 5.2) with 2M HCl in ether led to precipitation of the imide **372**, which could be isolated from the reaction mixture and subsequently recrystallized from ethyl acetate to afford the pure product **372**, albeit with a lower yield of 53%. The solubility of the imide **372** in a variety of organic solvents, including tetrahydrofuran, dichloromethane, and acetonitrile, was significantly improved compared with the original imide **143** lacking the hexyl chain.

5.4 Improving the imide stability

Aware that the instability of the imide might complicate or compromise any potential application as a fluorophore, we were interested to see if the scaffold could be modified to circumvent this issue. Introduction of an electron-donating group *ortho*- to the carboxyl group could reduce its electrophilicity, making it less susceptible to nucleophilic attack (Scheme 5.21). The difficulty with the design of suitable alkyne substrates was that three contiguously substituted functional groups were required to achieve our target molecule, in the following order: a (pseudo)halide for the Sonogashira coupling; an ester to complete the cyclisation; and an electron-donating group to potentially decrease the electrophilicity of the adjacent carboxyl group.

In order to test the hypothesis, the synthesis of the *ortho*-propoxy alkyne **386** was undertaken (Scheme 5.21). Alkylation of methyl salicylate **381** with bromopropane catalysed by lithium iodide, followed by hydrolysis of the ester gave the 2-propoxybenzoic acid **382** (83% over two steps).[210] To install an *ortho*-iodide for the subsequent Sonogashira coupling, we envisaged a route using *ortho*-lithiation of **382**, followed by addition of an electrophilic iodine source. Benzoic acids are commonly used as strong *ortho*-directing groups in lithiation chemistry.[211] However, Mortier *et al.* observed competing reaction pathways for the *ortho*-lithiation of 2-methoxybenzoic acid **374**, whereby *sec*-BuLi could either attack the lithiated benzoic acid functionality (CO_2Li), to form the corresponding *sec*-butyl ketone **378** on work up, or displace the alkoxy group *via* an addition-elimination sequence to form the 2-*sec*-butylbenzoic acid (neither of which were quantified in the report, Scheme 5.20).[212] Addition of *N,N,N',N'*-tetramethylethylenediamine (TMEDA) (one equivalent) successfully suppressed the addition-elimination reaction, resulting in yields of 71% with methyl iodide and 46% using iodine. Similar examples with various electrophiles using *ortho*-lithiated-2-alkoxybenzoic acids have been reported in the literature with similar yields.[211,213]

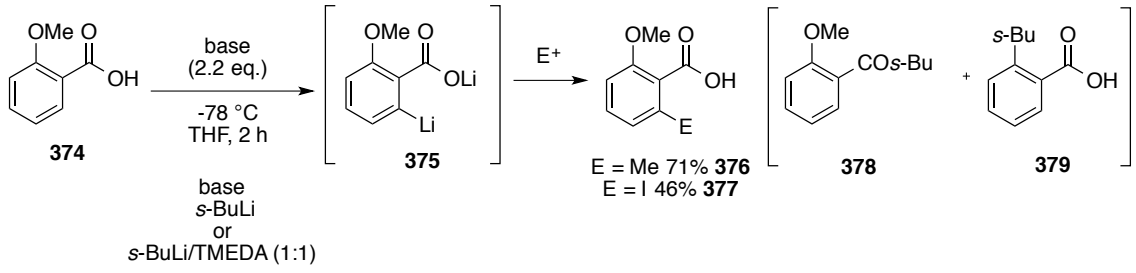

Scheme 5.20

Ortho-lithiation with a *sec*-BuLi-TMEDA complex, followed by iodination produced a mixture of the desired product **384** and the *sec*-butyl ketone **383** (identified as 1.75:1 mixture of **384**:**383**, observed in the ^{1}H NMR spectrum of the crude reaction mixture). The mixture was taken through to the next step, as attempted purification of the acid resulted in a low recovery (Scheme 5.21).[212,214] Esterification provided methyl 2-iodo-6-propoxy benzoate **385** with a yield of 32% over 2 steps. A subsequent Sonogashira coupling,[209] using $PdCl_2(PPh_3)_2$ (2 mol%) with copper(I) iodide (5 mol%), gave the target alkyne **386** with a yield of 90%. Application of the rhodium-catalysed annulation conditions furnished the model imide **387**. The ^{1}H NMR spectrum of the crude reaction mixture indicated 100% conversion to the products, with a 4:1 ratio of the imide **387** to the methyl ester isoquinolone derivative, unlike the 1:1 ratio observed from the crude reaction without the propoxy group (*cf.* Scheme 5.18). The poor recovery of the imide **387** (28%) from the precipitation method may have been a result of the solubilising propyl group.

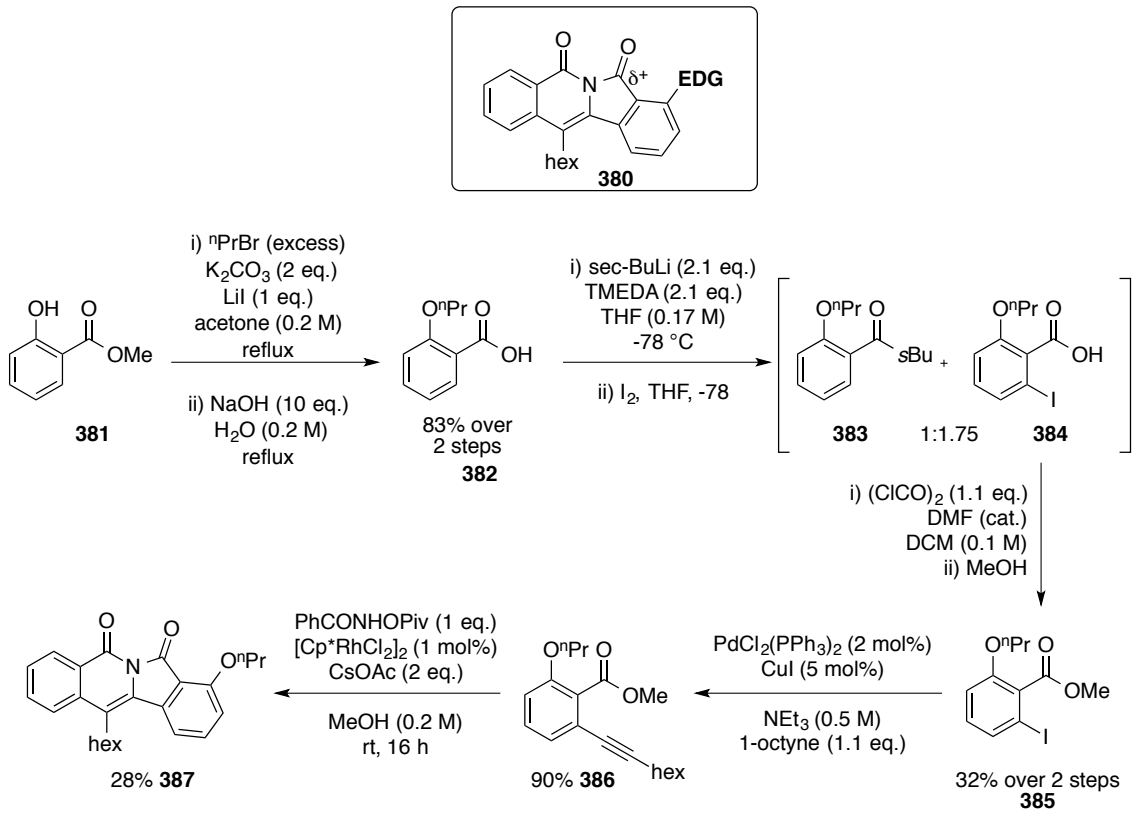

Scheme 5.21

The analogue bearing the free hydroxyl group **393** was subsequently developed as a more readily accessible alternative (Scheme 5.22). 2,6-Dihydroxybenzoic acid **388** was protected as the isopropylidene acetal **389** before treatment with triflic anhydride to afford the Sonogashira precursor **390**. Application of the previous cross-coupling conditions in triethylamine were unsuccessful, owing to the insolubility of the starting material. Switching the solvent from triethylamine to acetonitrile at 80 °C, with diethylamine as a base, gave the desired product **391** with a yield of 62%.[215] Using the standard C-H activation conditions, the annulation with *N*-(pivaloyloxy)benzamide **43** furnished the corresponding isoquinoline **392** with an excellent yield of 96%. A benefit of this strategy over the previous was the facile purification of the cyclisation precursor **392**, which could be isolated with high purity by column chromatography, ensuring simple purification after the final cyclisation step. Treatment of the isoquinolone **392** with sodium hydride furnished the imide **393** with a yield of 63%. The phenolic handle offers an additional point of diversification, however, this was not investigated in this study.

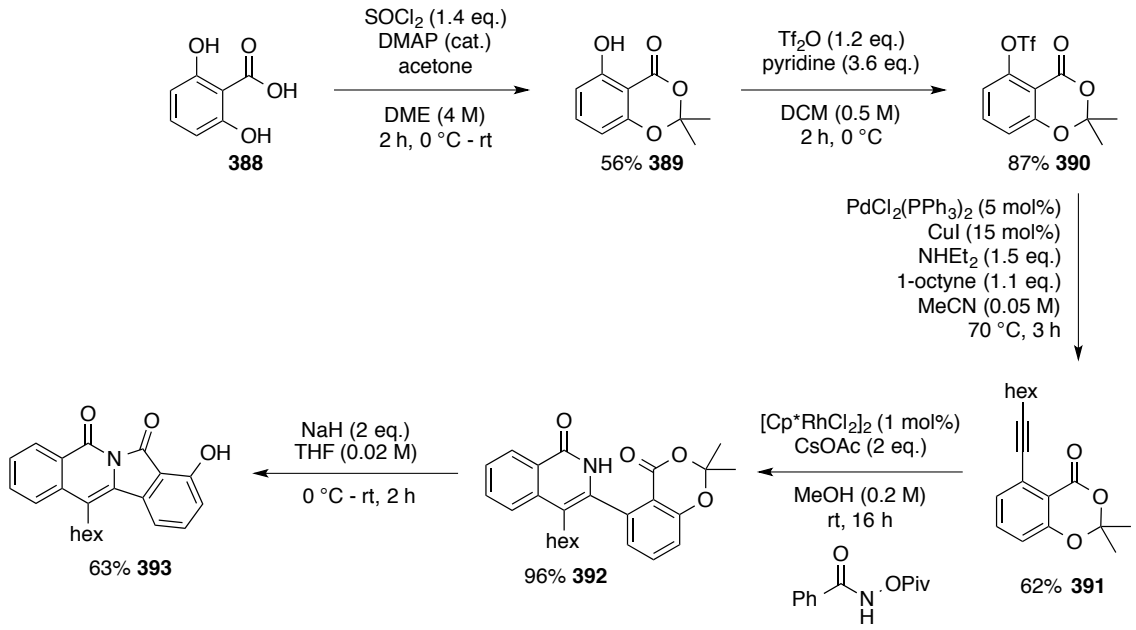

Scheme 5.22

Comparison of the rate of ring-opening of the imide of the *ortho*-propoxy derivative **387** with the parent imide **372** at different temperatures was qualitatively investigated (Figure 5.5). The imides were heated in deuterated methanol-d_4 for 30 minutes at various temperatures. The *ortho*-propoxy imide **387** had not undergone ring opening at room temperature (compared to the parent imide **372** with 35%) and only 30% at 60 °C (at 100% for **372**). The rate of alcoholysis of the parent imide was significantly faster than the propoxy derivative. Although alcoholysis had not been prevented entirely, the stability of the imide had significantly improved in comparison to the parent imide.

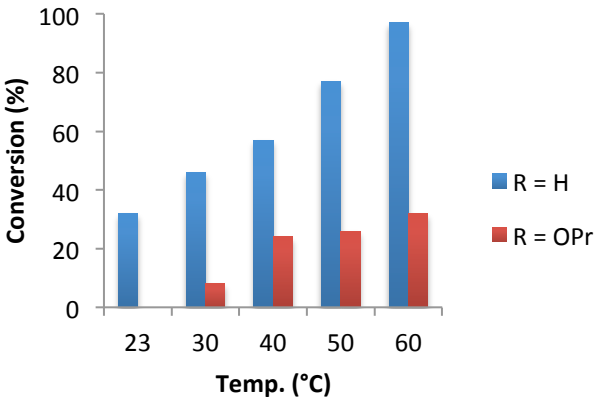

Figure 5.5

5.5 Extension of the conjugated π-system

The ability to tune the fluorescent properties on a particular scaffold, using various functional groups, is highly advantageous in the design of bespoke materials. For example, photovoltaic devices absorb in the visible light to IR region to maximise absorbance from sunlight,[194] whereas organic light emitting diodes can be tailored to a specific wavelength to emit particular colours. Biological sensors range from blue/green emitters (450-550 nm) to near-infrared (600-700 nm), based on the requirements of the biological system under investigation, or indeed the laser source used for excitation.[201]

The fluorescent properties of an aromatic system can be altered significantly by substitution. Both the nature and position of a substituent can alter the photochemical properties. Extension of the conjugated π-system is a well-established method to induce a bathochromic shift in fluorescence and absorbance. Additionally, a larger degree of conjugation generally increases the fluorescence quantum yield.[216] Functional groups bearing non-bonding electrons can increase the molar absorption coefficient and bathochromatically shift (red shift) the absorption and fluorescence spectra to longer wavelengths. These groups are known as auxochromes, and there are two main categories; acidic (-COOH, -OH, $-SO_3H$) and basic ($-NH_2$, $-NR_2$). Auxochromes extend the conjugated π-system and therefore raise the energy of the HOMO and lower the energy of the LUMO, so that less energy is required for an electronic transition, therefore a bathochromic shift is observed.

Investigation into substitution effects on the photochemical properties began, by introducing substituents that would effectively extend the aromatic π-system and incorporate auxochromes (-OH and $-NR_2$). To commence the investigation of imides with extended π-systems, the naphthyl derivative **397** was prepared from the reaction of *N*-(pivaloyloxy)-2-naphthamide **396** with the bicyclic alkyne **391** (Scheme 5.23). Rhodium(III)-catalysed C-H activation/annulation furnished a mixture of regioisomers (crude ratio of 70:11:19 of **397**:**398**:**399**) which were separated to give a yield of 51% of **397**, mixed fractions of **397**:**398** (5:2, 27%) and 1% of **399**. The undesired regioisomers were not fully characterised, however diagnostic peaks of the H_{10} proton were observed in the ^{1}H NMR spectrum. The major regioisomer **397** was subsequently treated with sodium hydride in tetrahydrofuran to afford the naphthylimide **400** with a yield of 69%.

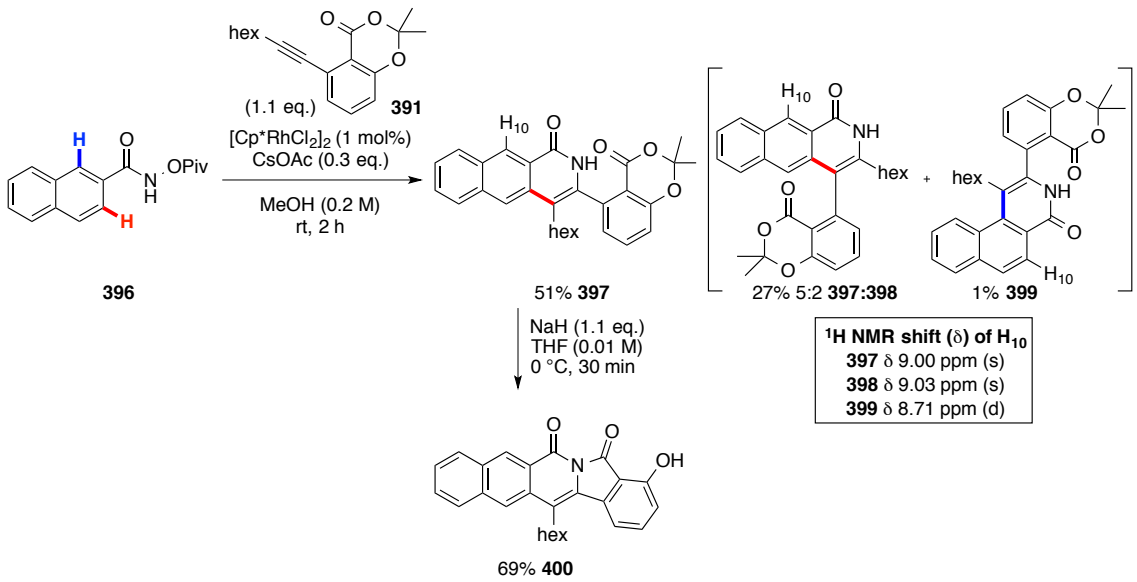

Scheme 5.23

To investigate the effect of electron-donating groups, two examples with auxochrome groups (-OH and NR_2) were prepared. The *N*-(pivaloyloxy)-biphenylamino derivative **405** was prepared in three steps *via* a key Suzuki coupling of 4-(dimethylamino)phenylboronic acid **401** with ethyl 4-bromobenzoate **402** to furnish the biphenyl intermediate **403** with a yield of 79% (Scheme 5.24).[217] Following hydrolysis of the ester **403**, the acid **404** was converted to the acid chloride for the reaction with *N*-(pivaloyl)ammonium triflic acid under Schotten-Baumann[218,219] conditions to furnish the substrate **405** with a yield of 45%.

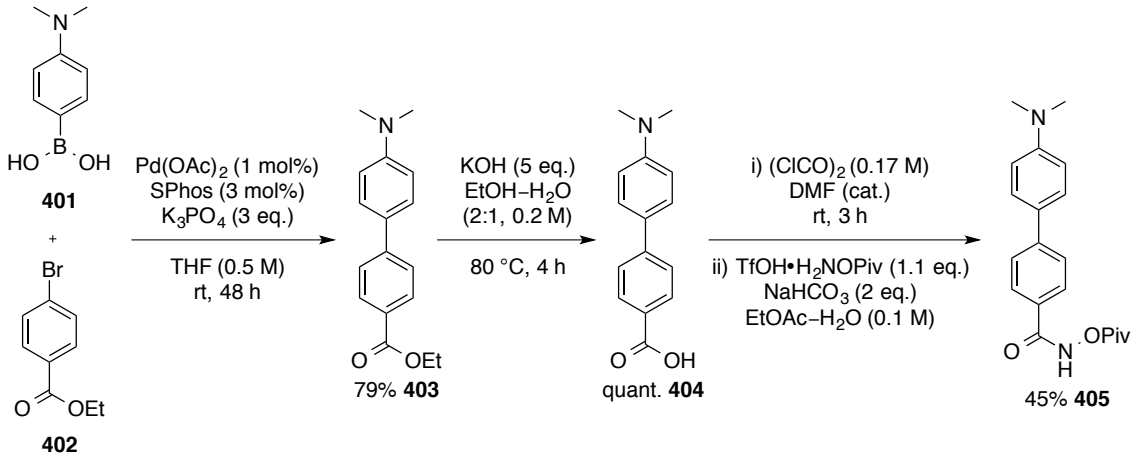

Scheme 5.24

With the substrate **405** in hand, the imide precursor **406** was prepared, *via* the standard reaction conditions, as a 4:1 mixture of regioisomers of the desired isoquinolone **406** to the regioisomer **407**, which were separated by column chromatography and fully characterised (Scheme 5.25). Treatment of the imide precursor **406** with sodium hydride furnished the desired imide **408** with a yield of 50%.

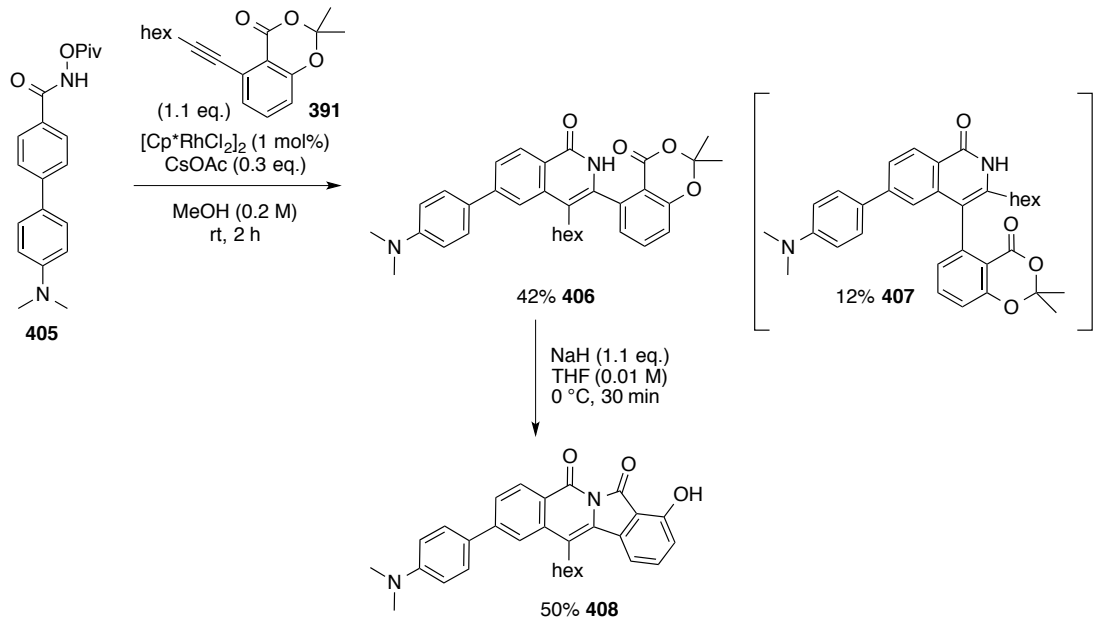

Scheme 5.25

The *para*-hydroxy derivative **416** was subsequently prepared for a comparison to the *ortho*-phenolic imide **393** previously prepared (see Scheme 5.26). The alkyne **414** was prepared *via ortho*-lithiation of 4-methoxybenzoic acid **409**, with subsequent iodination to afford the 2-iodo-4-methoxybenzoic acid derivative **410**. Demethylation of the methoxy group was achieved using boron tribromide to afford 2-iodo-4-hydroxybenzoic acid **411**, which was used without further purification. Acid-catalysed esterification furnished the methyl ester **412** with a yield of 76% over two steps. The phenol **412** was subsequently protected as the methoxymethyl ether **413** prior to the Sonogashira coupling reaction, which gave the alkyne **414** with a yield 67%.

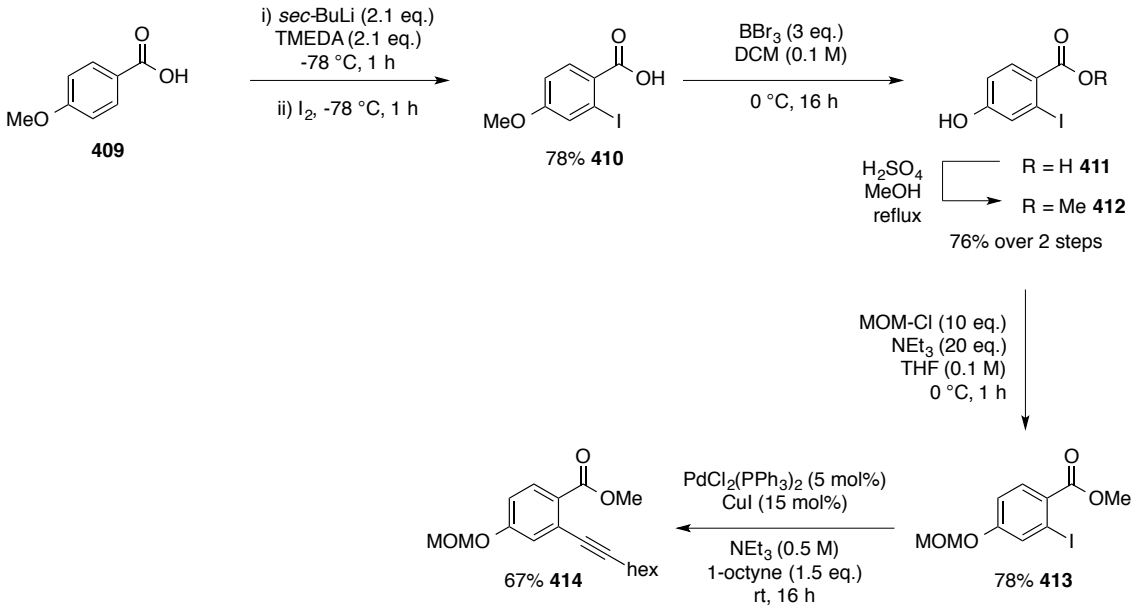

Scheme 5.26

The alkyne **414** was treated with *N*-(pivaloyloxy)benzamide **43** using the standard rhodium(III)-catalysed annulation procedure to afford the MOM-protected imide **415** with a yield of 35%. Deprotection of the phenol was achieved under acidic conditions to give the *para*-phenolate derivative **416** with a yield of 62%.

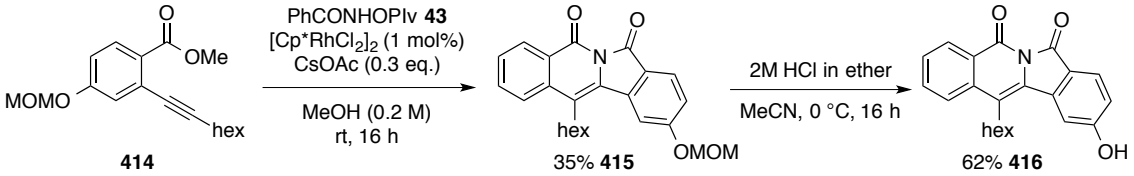

Scheme 5.27

Fluorescent compounds can be incorporated into polymeric semi-conducting materials for light harvesting in photovoltaic cells and printed organic thin-film transistors.[220–222] Polythiophene structures are very common motifs in semi-conductors as they have high photostability and conduct charge efficiently.[223] They are of particular interest due to ideal solution phase processing and good film-forming properties.[194] In the interest of extending the π-system, two model compounds **423** and **424** substituted with a thiophene ring, were prepared by a co-worker in the Marsden group *via* the rhodium-catalysed annulation methodology (Scheme 5.28). A Suzuki coupling of 2,5-dibromothiophene **418** with methyl 4-boronic benzoate **417** gave the *para*-substituted bromothiophene derivative **419**. Hydrolysis of the ester **419** to the acid **420**, followed by acid chloride formation and reaction with the *O*-pivaloylhydroxylamine triflic acid salt gave the *N*-(pivaloyloxy)-substrate **421**, with a yield of 51% over three steps. Using two methyl 2-alkynyl benzoate substrates **370** and **386**, the thiophene substituted imides **423** and **424** were prepared with yields of 32% and 28%, respectively.

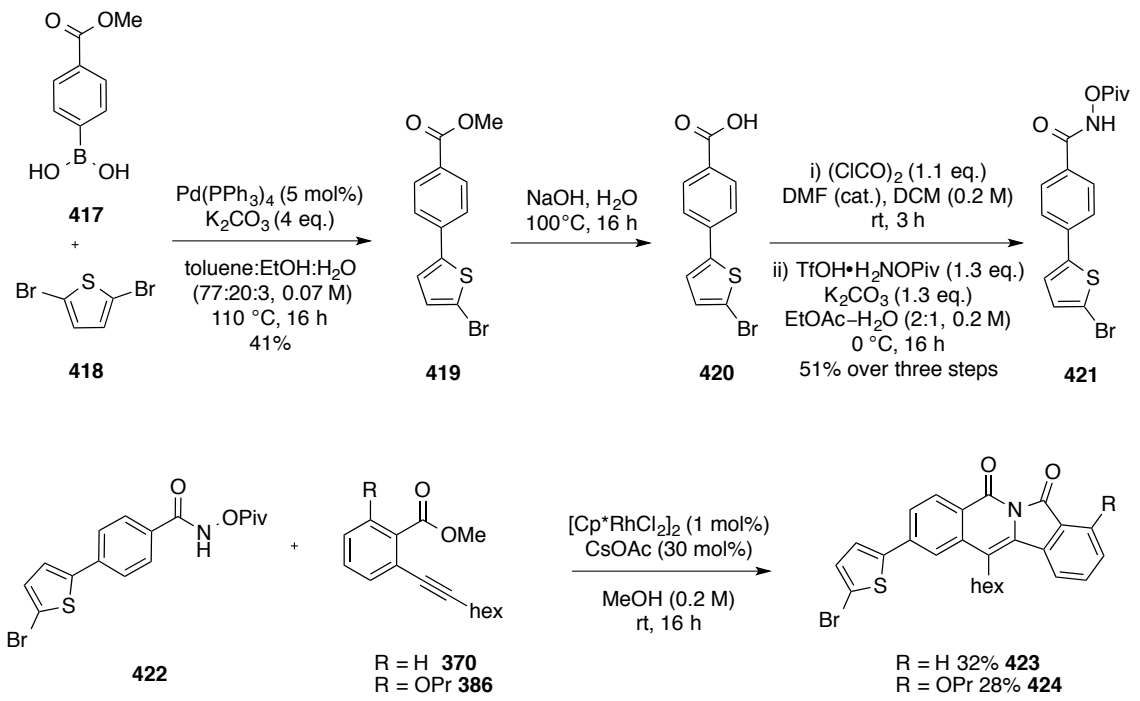

Scheme 5.28

The synthesis of aromatic based semi-conductors is typically achieved using transition-metal catalysed polymerisation.[224,225] The palladium-catalysed Suzuki coupling is the most common method as the polymerisation step is high yielding, largely unaffected by the presence of water and generally requires low catalyst loadings.[226–229] A disadvantage of the system is that reaction times normally exceed 48 hours for high molecular weight polymers. Additionally two halides and two boronic acid equivalents are extruded from the reaction, generating excess waste.

A polymerisation strategy utilising C-H activation could provide an atom-efficient method for the polymerisation of aromatic monomers. For example, Marks *et al.* reported the synthesis of 5,5'-*bis*(4-*n*-hexylphenyl)-2,2'-bithiophene (dH-PTTP) **428** for phenylene-thiophene-based organic field-effect transistors *via* a key Stille coupling of the organostannane **426** with 1-bromo-4-*n*-hexylbenzene **427** (Scheme 5.29).[230] Fagnou *et al.* illustrated the effectiveness of palladium catalysed C-H activation for the formation of the thiophene dimer **428** *via* a single step direct arylation of the dithiophene **425** using 1-bromo-4-*n*-hexylbenzene **427**, avoiding the requirement to prefunctionalise the starting material **425** with an improvement in yield of 87%, compared with 60% over two steps.[231]

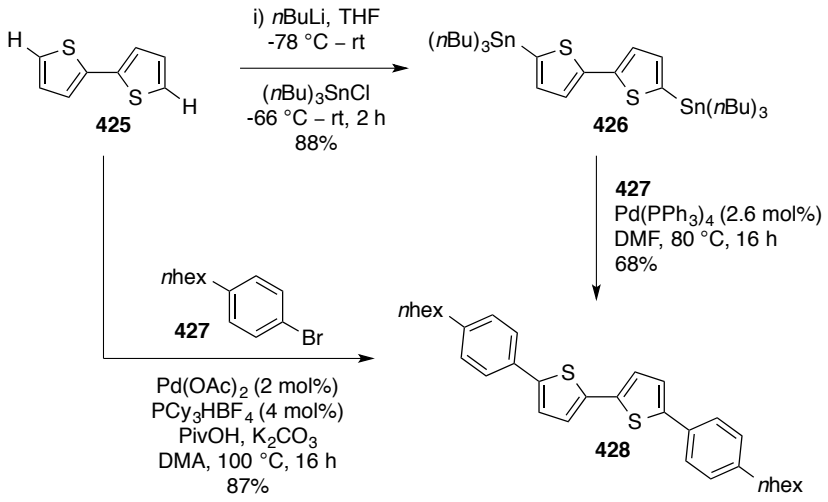

Scheme 5.29[231]

To our knowledge, there are no existing methodologies using rhodium(III)-catalysed C-H activation/annulation reactions using internal or external oxidants to mediate a polymerisation reaction. Using our methodology, we were interested in investigating a strategy using block co-polymerisation (-(A-B-B-A)$_n$-), *via* an A2B2 strategy, using a dimeric unit of the *N*-(pivaloyloxy)benzamide derivative **429** with a *bis*-alkynyl acetonide substrate **430** (Scheme 5.30). A system of this kind would only generate by-products such as pivalic and acetic acid from the C-H activation step, and hydrogen and acetone in the subsequent cyclisation to prepare **432**.

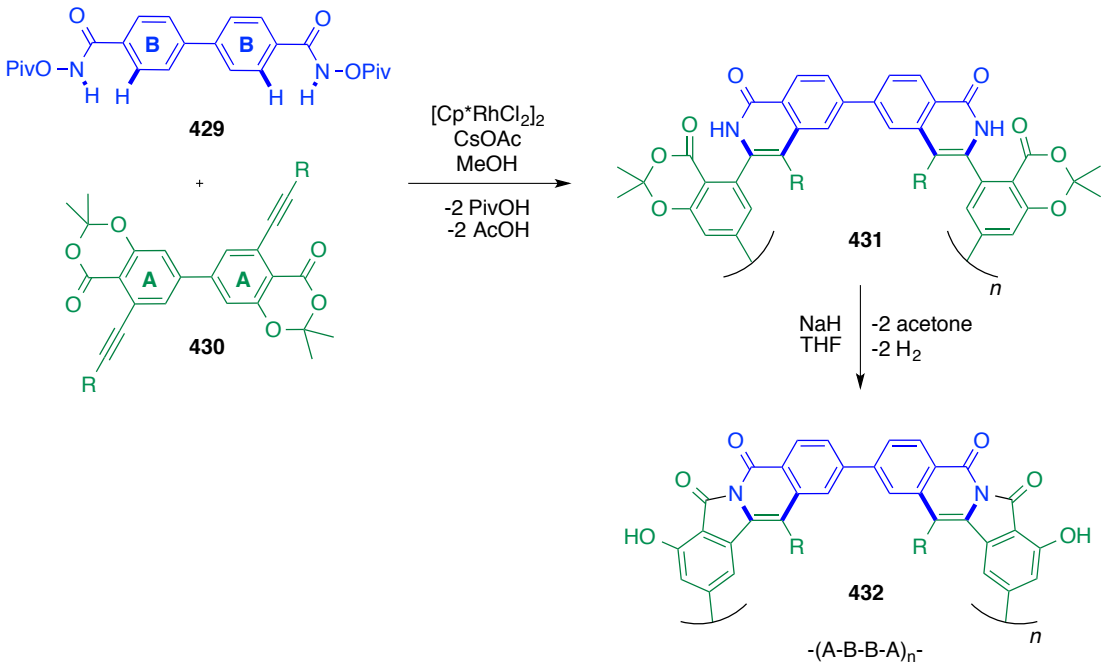

Scheme 5.30

To commence the investigation, the dimeric imide **435** was proposed as a model for the polymerisation reaction (Scheme 5.31). To prepare the substrate for the rhodium-catalysed C-H activation/annulation reaction the biphenyl-4,4'-dicarboxylic acid **433** was converted to the biphenyl-*N*-(pivaloyloxy)-derivative **429** with a yield of 91%. Under the C-H activation/annulation conditions, the fused *bis*-isoquinolone precursor **434** was prepared with a yield of 69%, although a higher catalyst loading and reaction temperature (to solubilise the intermediate **434**) were required to achieve full conversion to the product. Disappointingly, the attempted cyclisation of the substrate **434** was unsuccessful. Reaction monitoring revealed formation of the mono-cyclised product, with no further conversion on addition of excess sodium hydride. The termination of the reaction at this point may have been a result of the insolubility of the intermediate product in the reaction medium, observed as a suspension in solution. By switching the solvent from tetrahydrofuran to *N,N'*-dimethylformamide, in the hope of solubilising the intermediate monocyclised product (identified by LCMS), it was hoped that the issue would be circumvented. However, this was unsuccessful and the same outcome was observed. In future, these issues could be circumvented by addition of aliphatic groups on the aromatic ring systems to aid solubility.

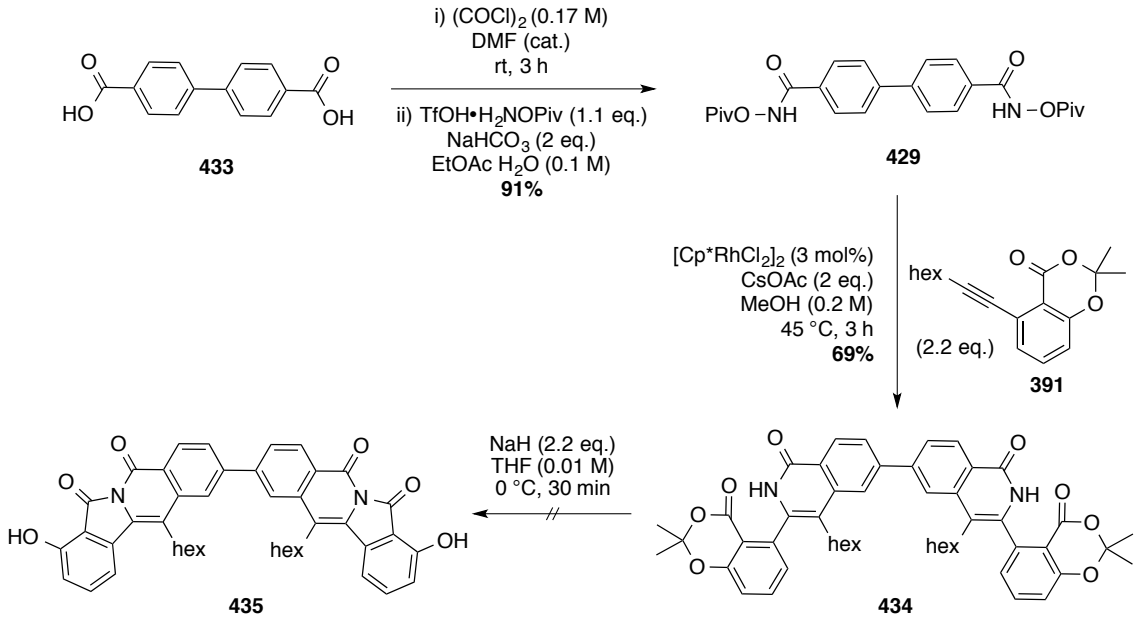

Scheme 5.31

In summary, nine imides were prepared using the rhodium(III)-catalysed C-H activation/-annulation route *via* the *ortho*-methyl ester isoquinolone **438** or the acetonide isoquinolone **436**, followed by cyclisation using sodium hydride (Scheme 5.32). Introduction of the electron-donating phenol group or ethers significantly improved the stability of the imide to ring-opening in nucleophilic solvents and was achieved using the acetonide derivatives **436**. To extend the π-system, with the intention of modifiying the spectrochemical properties, various *N*-(pivaloyloxy)benzamide derivatives were prepared to incorporate a naphthyl, thiophene and phenyl aniline moiety into the imide. The spectrochemical and electrochemical data are reported herein.

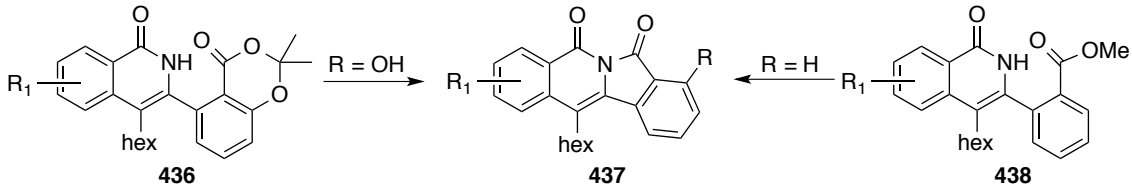

Scheme 5.32

5.6 Fluorescence and absorbance properties

With a variety of imides in hand, we were interested in investigating the effect of the substituents on the photochemical properties. To commence the study, the absolute quantum yield (Φ_F) of the parent imide was measured in dichloromethane. The fluorescence quantum yield is a measure of fluorescence efficiency i.e. the ratio of photos absorbed to photons emitted through fluorescence. The value is an indication of the probability of deactivation of the excited state *via* a non-radiative mechanism. Fluorescence quantum yields are typically measured against a well-studied standard, which has a known and high quantum yield. The ratio of the integrated fluorescence of the sample *versus* the standard can very simply provide the quantum yield of the sample compound.

Fluorescence measurements are normally collected at very low concentration solutions (10^{-5} or 10^{-6} M) in order to minimise re-absorption effects, and multiple readings are taken at different concentrations to ensure linearity. At higher concentrations, aggregation of the compound in solution can lead to self-quenching, where the fluorescence of one molecule is absorbed by another and is therefore not detected, causing non-linear effects.[232]

Whilst working with these low concentrations the compounds and solvent must be of high purity and glassware must be scrupulously clean to ensure no contaminants effect the fluorescent readings. The standard is generally selected so as to have a similar absorbance and emission wavelength of the sample of interest. Based on the wavelength (λ_{max}) of the absorbance and fluorescence maxima of the imide **372** (λ_{abs} 384 nm, λ_{emis} 420 nm), 9,10-diphenyl-anthracene (λ_{abs} 375 nm, λ_{emis} 410 nm) was selected as a standard, as its reported quantum yield is close to unity (0.95 in cyclohexane, which was later corrected to 0.97 in dichloromethane for our study, see Experimental 6.11).[233] The quantum yield of imide **372** was calculated as Φ_F 0.44, using equation (1), with the values of the gradient obtained from a plot of the integrated fluorescence *versus* absorbance (Figure 5.6). The molar absorption coefficient (ε) for the imide **372** was calculated as 2.34 x 10^4 $M^{-1}cm^{-1}$ at λ_{abs} 383 nm (see Experimental 6.11).

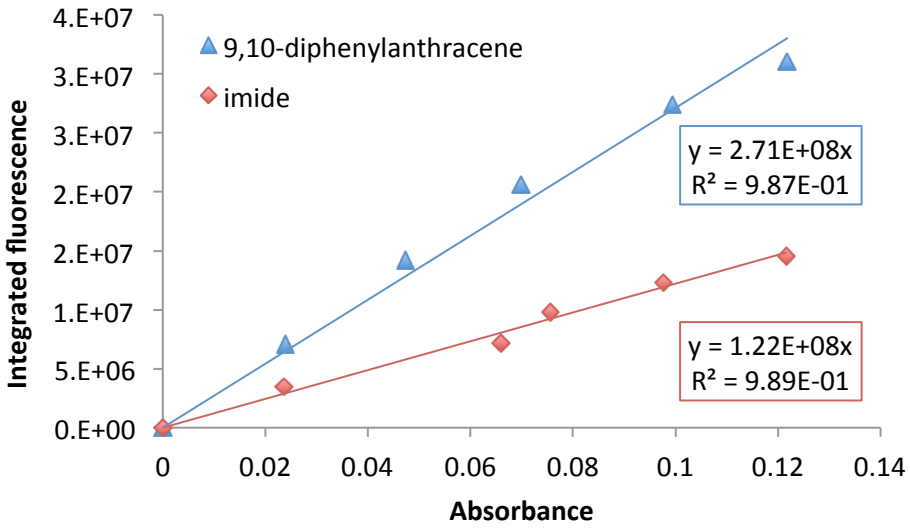

$$\phi_X = \phi_{St}\left(\frac{Gradient_X}{Gradient_{St}}\right) \qquad (1)$$

$$\phi_X = 0.97\left(\frac{1.22\times10^8}{2.71\times10^8}\right)$$

$$\phi_X = 0.44$$

*Figure 5.6. Quantum yield calculation for imide **372***

The photochemical properties of the imides were subsequently measured in order to compare the effect of various substituents on the parent imide scaffold. The absorbance spectrum features multiple peaks, which can be assigned to various Franck-Condon vibronic transitions. When there is little difference to the nuclear configuration of the molecules in its excited state (ν') compared to the ground state (ν''), the operation of the Franck-Condon principle will mean that the 0-0 transition is the most intense, although ν'=1, 2, 3 etc. will still exist (Figure 5.7).[234] In solution, any vibrational excitation is rapidly lost through collisions with solvent molecules and emission therefore occurs from the ν'=0 level of the excited electronic state. Therefore the 0-0 transition was used to compare the imides (Table 5.3 and Figure 5.8).

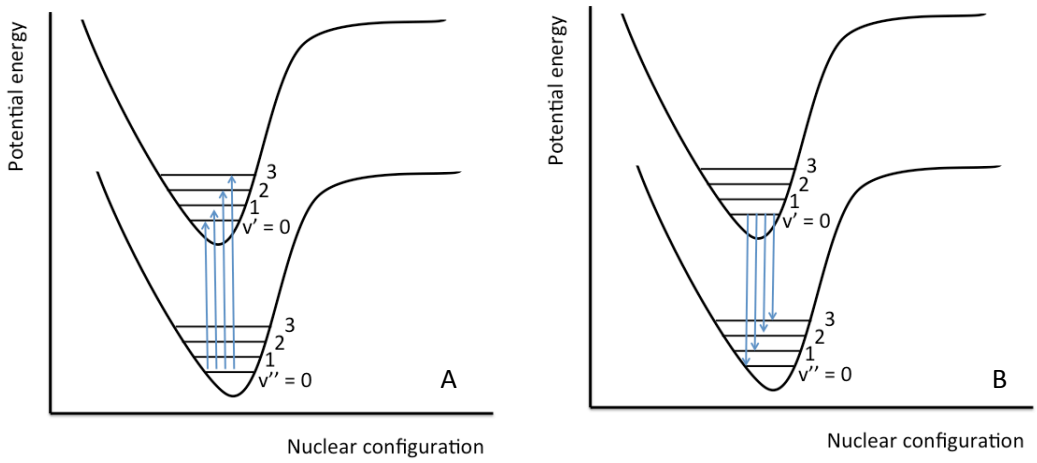

Figure 5.7. Potential energy curves highlighting the individual vibrational energy levels and their involvement in absorption (A) from the ν' = 0 level of the ground electronic state and the emission (B) from the ν' = 0 level of the electronically excited state.[234]

A bathochromic shift was observed with all of the substituted imides except for the *para*-hydroxy imide derivatives **415** and **416**, which were slightly shifted into the blue region (~7 nm, G and H, Table 5.3 and Figure 5.8). The largest bathochromic shift of 24 nm was observed for the naphthyl derivative **400** (F). The 0-0 transitions were smaller than the original imide **372** (A), however not by a significant factor (1-4 nm). Generally, small Stokes shifts are detrimental to fluorescence, as photons are reabsorbed before the radiative pathway can occur, which is known as fluorescent quenching.[201] In biological dyes Stokes shifts of >100 nm are highly desirable to reduce interference in order to observe a strong fluorescent signal.[235] Characteristic absorption peaks were observed for the thiophene ring of imides **423** and **424** at 320 and 331 nm (C and D, Figure 5.8), respectively. 2-Phenylthiophene and 2-(α-naphthyl)-thiophene absorb at 283 nm (cyclohexane) and 296 nm (ethanol),[236] indicating a significant bathochromic shift due to the increased conjugation of the imide ring. Three characteristic absorbances were measured for the naphthyl unit of imide **400** (F), at 375, 357 and 340 nm, which are significantly red shifted compared to the absorbance peaks of naphthalene, which absorbs at 220, 275 and 310 nm.[237] Molar absorptivity values and relative quantum yields (Φ_{rel}) were calculated from single values to give a relative comparison to the parent imide **372**. No significant differences were observed in the quantum yield of imides **387**, **393** and **400**, however the thiophene derivatives, **423** and **424**, and the *para*-hydroxy imides **415** and **416** indicated a much lower yield (Φ_{rel} ~0.15). This result was surprising, as conjugation of the π-system typically increases the quantum yield. This could be a result of the thiophene twisting out of the plane of the conjugated π-system, which could be investigated using other thiophene-substituted derivatives.

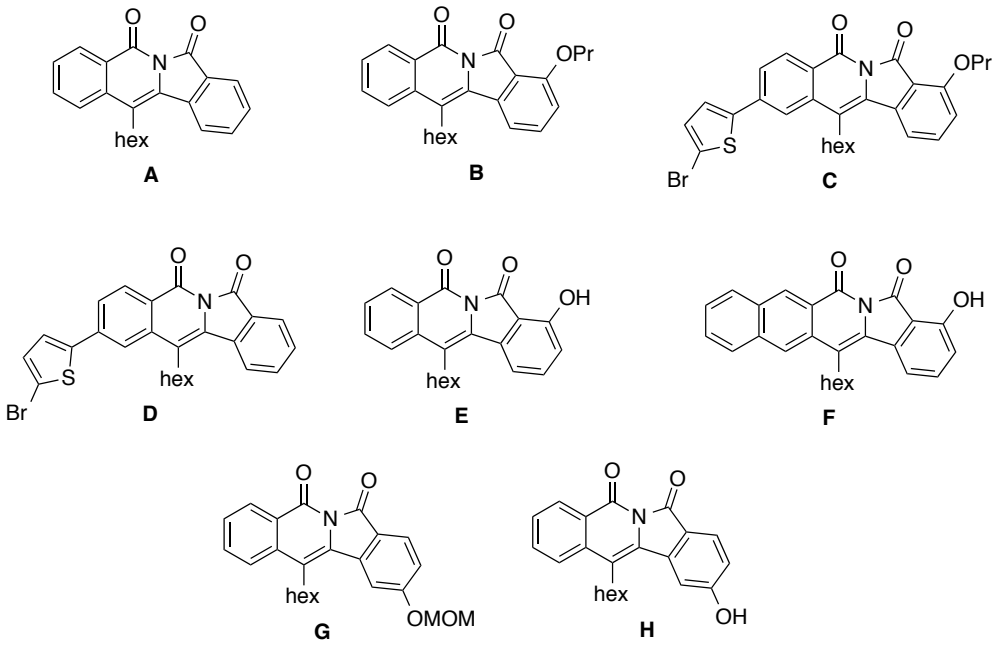

Imide	Entry	Absorbance (nm) ν''→ ν'		Fluorescence (nm) ν'→ ν''		ν'→ ν'' 0→0 (nm)	ε =A/cl (10^4 $M^{-1}cm^{-1}$)	Φ_{rel}
		0→1	0→0	0→0	0→1			
372	A	383*	403	418	439	15	2.34	0.44
387	B	392	413*	427	442	14	2.81	0.32
424	C	395	416*	428	452	12	3.28	0.15
423	D	390*	408	422	446	14	2.07	0.15
393	E	394	416*	427	449	11	2.68	0.45
400	F	408	429*	441	466	12	3.14	0.44
415	G	377*	398	409	433	11	2.51	0.17
416	H	375*	396	407	431	11	2.01	0.15

Table 5.3. Data for the 0→1 and 0→0 absorption and emission peaks, including the v' (0→0) to v'' (0→0) shift in dichloromethane. Molar absorptivity (ε) is given from a single measurement at the λ_{max} (abs), indicated by the asterix. The Φ_{rel} is given in relation to the quantum yield measured for imide **A**.*

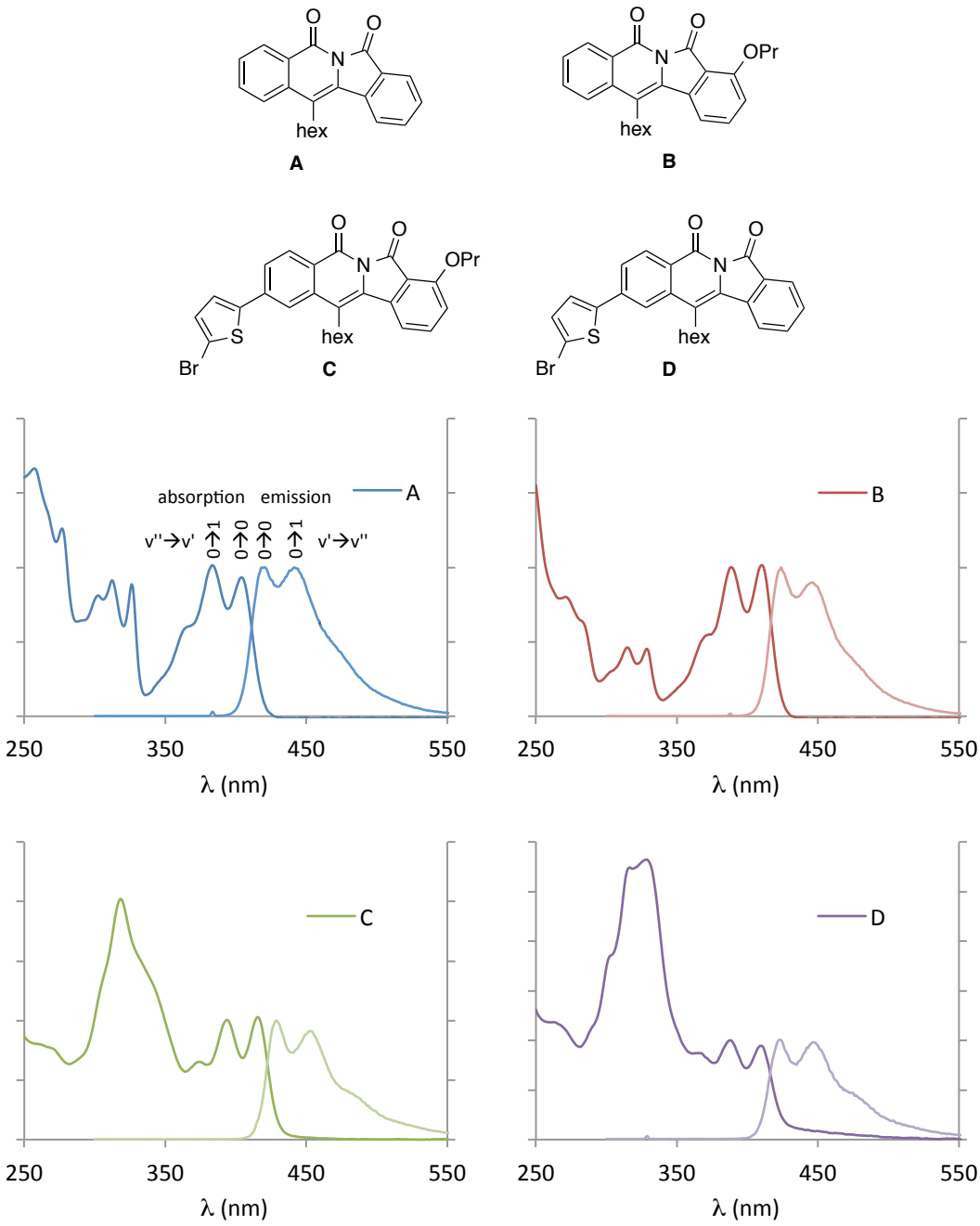

*Figure 5.8. Normalised absorption and emission spectra for compounds **A-D** in dichloromethane. Spectra A is labelled with the vibration transitions of 0-0 and 0-1 of the groud state (v') and the excited electronic state (v'')*

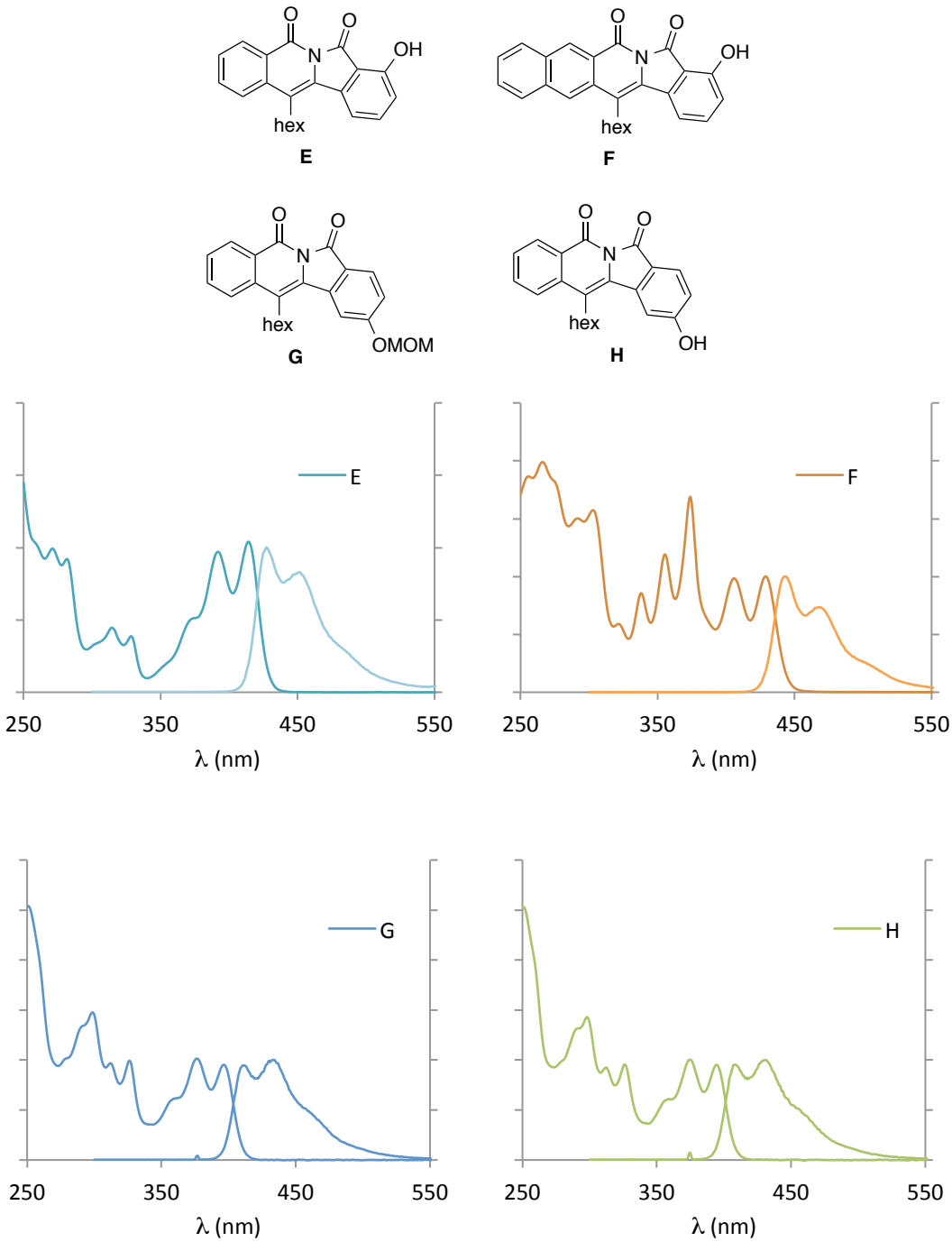

*Figure 5.8 cont. Normalised absorption and emission spectra for compounds **E-H** in dichloromethane.*

5.7 Cyclic voltammetry

Cyclic voltammetry is commonly used to characterise the electrochemical properties of conducting polymers. In order to conduct efficiently, without degradation of the polymer, the redox system must be reversible. This analytic technique can be used to: i) identify the formal redox potentials of a species; ii) determine whether the process is reversible; iii) determine the electron stoichiometry of a system.[238,239] A voltammogram is obtained by measuring the current at the working electrode during the cyclical potential scan rate (*versus* a reference electrode e.g. the saturated calomel electrode (SCE)). Unlike linear sweep voltammetry (E_0 to E_1, A, Figure 5.9), cyclic voltammetry continues with a reverse scan (from E_1 to E_2), to complete the cycle. During the scan the current is recorded and as potential and current are both functions on time, they can be interrelated. In the forward scan, as the potential approaches that of the anodic oxidation potential the current begins to rise and a peak (i_{pA}) is observed (B, Figure 5.9). On the reverse cycle (E_1 to E_2), the respective reduction reaction begins and the peak cathodic current (i_{pC}) and the associated peak potential (E_{pC}) can be obtained.

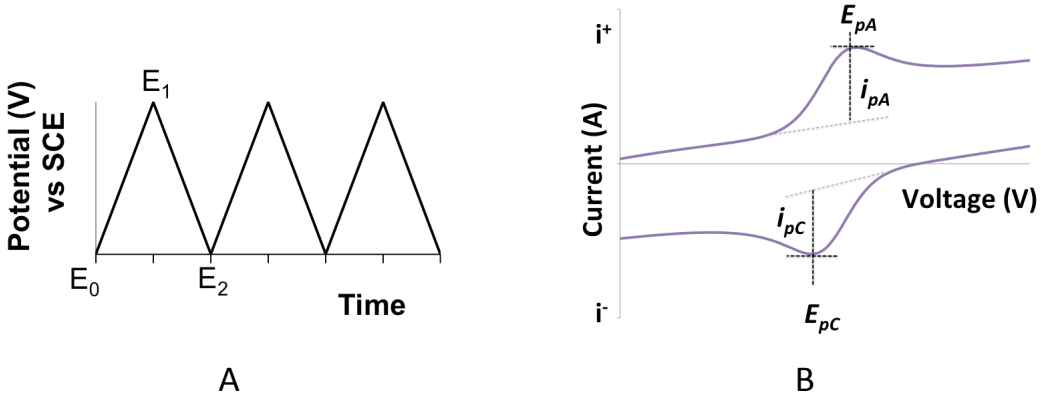

Figure 5.9

The formal reduction potential ($E^{0'}$) for a reversible couple is centred between E_{pA} and E_{pC}. The peak separation can provide important information about the electrochemical reversibility of a redox system. The Nernst equation (equation 2) can be used to determine the electron stoichiometry of a system. The number of electrons transferred in the electrode reaction (n) for a reversible couple can be determined from the separation between the peak potentials (equation 4). Therefore a one-electron process will exhibit a ΔE_p value of 0.059 V.

$$E = E^{0'} - \frac{RT}{nF}\ln(Q) \qquad (2)$$

$$E = E^{0'} - 2.303 \times \frac{RT}{nF}\log\left(\frac{[R]}{[O]}\right) \qquad (3)^{1}$$

$$E = \frac{E_{pA}+E_{pC}}{2} = \frac{0.059}{n}\log\left(\frac{[R]}{[O]}\right) \qquad (4)$$

[1] The Nernst equation is more commonly written in base-10 log form, therefore a conversion factor of 2.303 is applied.

The cyclic voltammograms of the imide **372**, **387**, **423** and **424** were measured to determine whether the imides would undergo reversible reduction, and therefore give some indication as to whether these scaffolds would be suitable in a conducting polymer. The voltammograms were collected at different scan rates to ensure consistency of the two reduction peaks. All potentials quoted were referenced to an internal ferrocene/ferrocenium standard and were obtained at varying scan rates (v) of 20-1000 mVs^{-1} (Figure 5.10). For example, the ferrocene/ferrocenium couple under these conditions was observed at $+0.45 \leq E_{1/2} \leq 0.46$ V *versus* Ag/AgCl, providing two observed reduction potentials of the imide **372** at – 1.33 V and – 1.79 V (*vs* Fc/Fc^{+}) (taken at the midpoint).

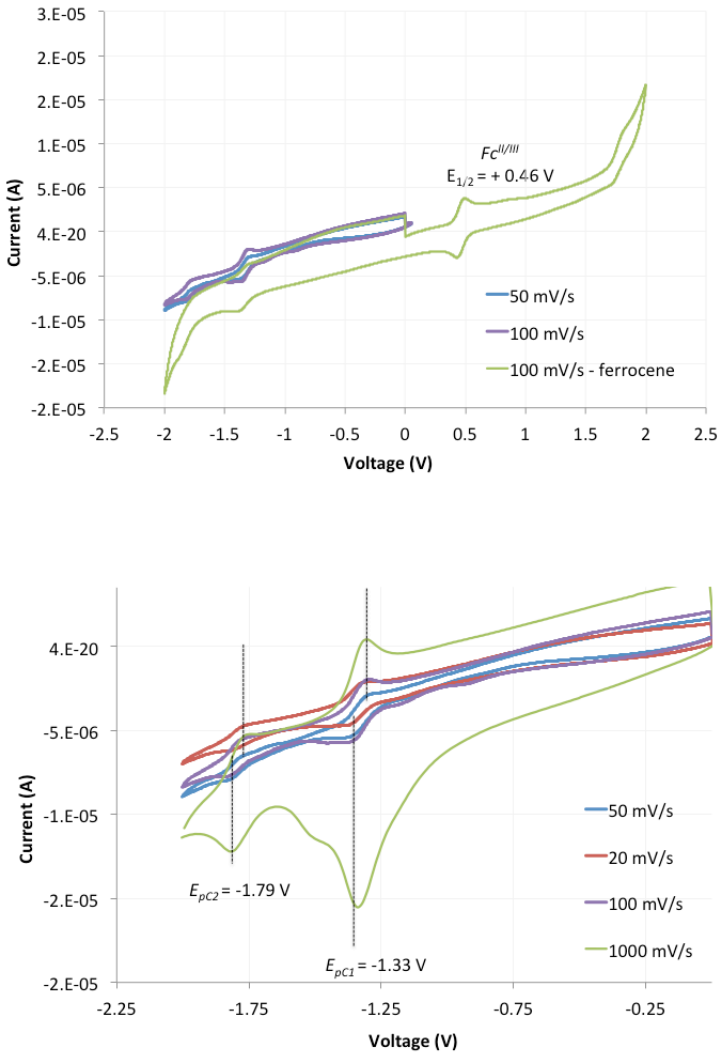

*Figure 5.10. Cyclic voltammograms of the parent imide **372** (1.0 mM) in non-aqueous media ($CH_3CN/[^nBu_4N]BF_4$ 0.10 M), v = 20-1000 mVs^{-1}, T = 298 K, [Fc] = 1.0 mM; E_{pC1} and E_{pC2} ascribed to the imide reduction.*

Each imide was measured to assess the first (E_{pC1}) and second cathodic reduction peak (E_{pC2}) in order to evaluate the reversibility of the reduction process and compare the formal reduction potential ($E^{0'}$) (Table 5.4, for voltammograms see Experimental 6.12). Unsuprisingly, the

electron-rich propoxy substituted imides **387** and **424** (entries 2 and 4) were harder to reduce than their counterparts **372** and **423** (entries 1 and 3). Extension of the π-system by addition of the thiophene substituent reduced the E_{pC2} values by approximately 0.06 V (both in the case of the **387** and **424**).

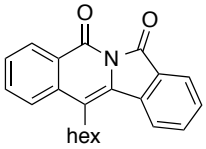

372

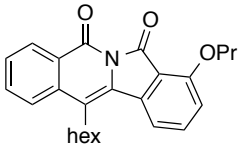

387

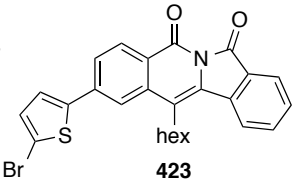

423

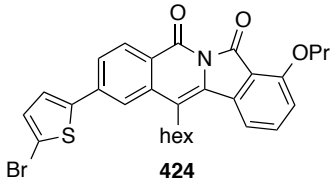

424

Entry	Entry	E_{pC1} (V)	ΔE_{pC1} (V)	E_{pC2} (V)	ΔE_{pC2} (V)
1	**372**	-1.33	0.066	-1.79	0.048
2	**387**	-1.38	0.053	-1.80	0.058
3	**423**	-1.33	0.031	-1.73	0.031
4	**424**	-1.37	0.014	-1.74	0.014

Table 5.4

In all cases, the ΔE_{pC1} values were <0.06 V (bar the ΔE_{pC1} value of imide **372**, entry 1), suggesting two reversible reduction processes. Although the reduction potentials are significantly lower, i.e. harder to reduce, than those used in photovoltaic materials (for example the perylene bis(imides) reported by Lemmetyinen *et al.*[240] range from ΔE_{pC1} values of -0.90 V to -1.15 V, and ΔE_{pC2} values of -1.35 V to -1.18 V), there is still potential to reduce the value by further π-conjugation.

5.8 Metal complexes

In biological systems, metal ions are responsible for normal cell functioning. Perturbations in ion concentration or localizations have been shown to contribute to ageing and disease.[241] The advent of confocal light microscopy, used in cell imaging, has spurred efforts towards identification of small fluorescent molecules that can be used *in situ* to monitor cellular events. Synthetic fluorophores can be used to visualize the presence of specific metal ions, both within the cell organelles and in the extracellular medium. Further understanding of their role in cellular processes will undoubtedly contribute towards the discovery of new treatments for a variety of human disorders.[241] Effective fluorescent probes must fulfil certain criteria in order to be of effective use: the sensor must be selective for a particular ion over those in much higher cellular concentration (e.g. Na^+, K^+, Mg^{2+} and Ca^{2+}); dyes with absorption and emission spectra within the visible light region are desirable, in order to minimize sample damage and reduce autofluorescence; high quantum yields, water solubility and low toxicity are mandatory; and 'turn on' emission increase or shift in the absorption and emission are preferable over 'turn-off' emission quenching to maximise spatial resolution.[241]

With this application in mind, we were interested in exploring the possibility of the tetracyclic imide **372** acting as a ligand for a host of metals. Encouragingly, the mass spectrum revealed the formation of a species with two ligands centred around a sodium ion (Figure 5.11). Based on the rigid conformation of the tetracyclic aromatic **372**, and the availability of the oxygen lone pairs, it was possible to imagine the imide acting as a bidentate ligand to the sodium metal to give the metal complex **439**. Based on this observation, we were encouraged to screen alternative metal complexes.

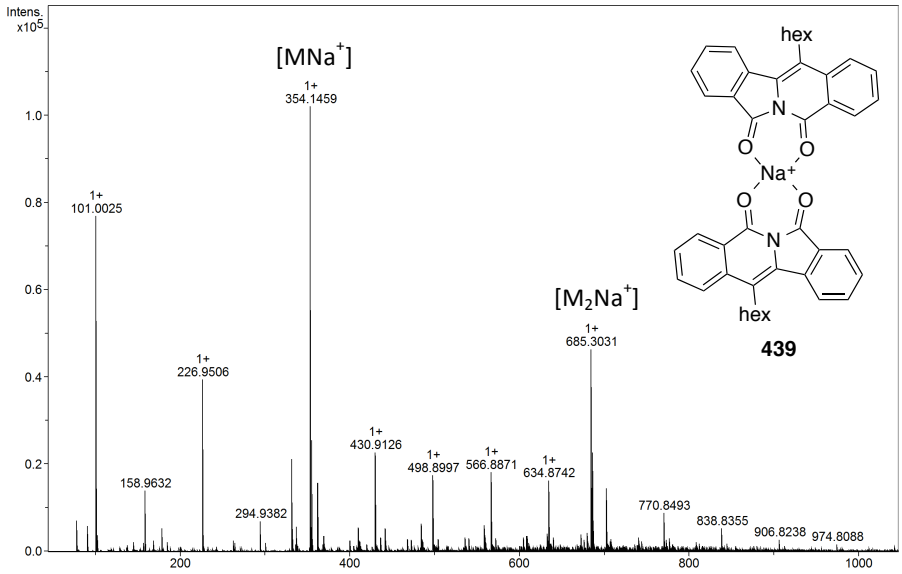

*Figure 5.11. High-resolution mass spectrum of imide **372** (ESI^+).*

A selection of metal salts were chosen, based on their characteristic colour changes when coordinated to various ligands and their solubility in ethyl acetate. The intention of the qualitative screen was to identify colour changes on addition of the colourless solution of the imide **372** (sample **A**, Figure 5.12). A colour change would signify coordination of the imide to the metal. Copper tetrafluoroborate, cobalt tetrafluoroborate, zinc triflate and europium triflate were tested in the screening. The solution of copper tetrafluoroborate displayed a colour change from blue (sample **B**) to bright green (sample **C**) on addition of the imide **372**. Colour changes were also observed with cobalt tetrafluoroborate solution (from pink (sample **D**) to orange (sample **E**)) and europium triflate (colourless (sample **G)** to yellow (sample **H**)) on addition of the imide **372** (sample **A**). The colourless solution of zinc triflate in ethyl acetate changed to a light blue (sample **F**) on addition of the imide solution. Having identified coordination of the imide to the metals, the samples were exposed to UV light to observe the effect on fluorescence. All of the samples were exposed to a standard UV lamp (λ = 254/365 nm), however only a single sample (**F**) diplayed fluorescence.

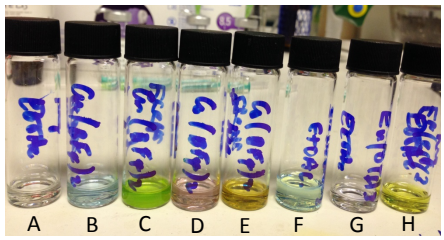

Figure 5.12. All solutions in ethyl acetate:
*A) **372**; B) $Cu(BF_4)_2$; C) **372** and $Cu(BF_4)_2$; D) $Co(BF_4)_2$; E) **372** and $Co(BF_4)_2$;*
*F) **372** and $Zn(OTf)_2$; G) $Eu(OTf)_3$; H) **372** and $Eu(OTf)_3$.*

To investigate the fluorescent properties of the zinc complex, UV/Vis and fluorimetry data were collected upon titrating zinc triflate into the solution of imide. Unfortunately, at low concentrations (10^{-5} and 10^{-6} M), only the absorbance and fluorescence of the imide **372** were observed, suggesting dissociation of the complex. At lower concentrations the complex is not present at appreciable levels which is indicative of a small association constant (Figure 5.13).

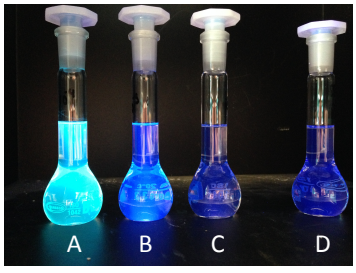

*Figure 5.13. Solutions A-C contain imide: $Zn(OTf)_2$ (2:1) at A) 10^{-4}; B) 10^{-5} M; C)10^{-6} M; D) Solution of imide **372** at 10^{-6} M under a UV lamp (λ 365 nm).*

To qualitatively assess the shift in fluorescence, a titration at a higher concentration of 10^{-4} M was executed (Figure 5.14). A bathochromic shift of the fluorescence maxima (λ_{max}) from 440 nm to 462 nm was observed. Suprisingly, the fluorescence continued to shift until 2.14 equivalents of zinc triflate had been added. The fluorescence spectra indicates the lack of a clear isosbestic point, suggesting a non-linear relationship between zinc(II) triflate and the imide **372** at varying concentrations.

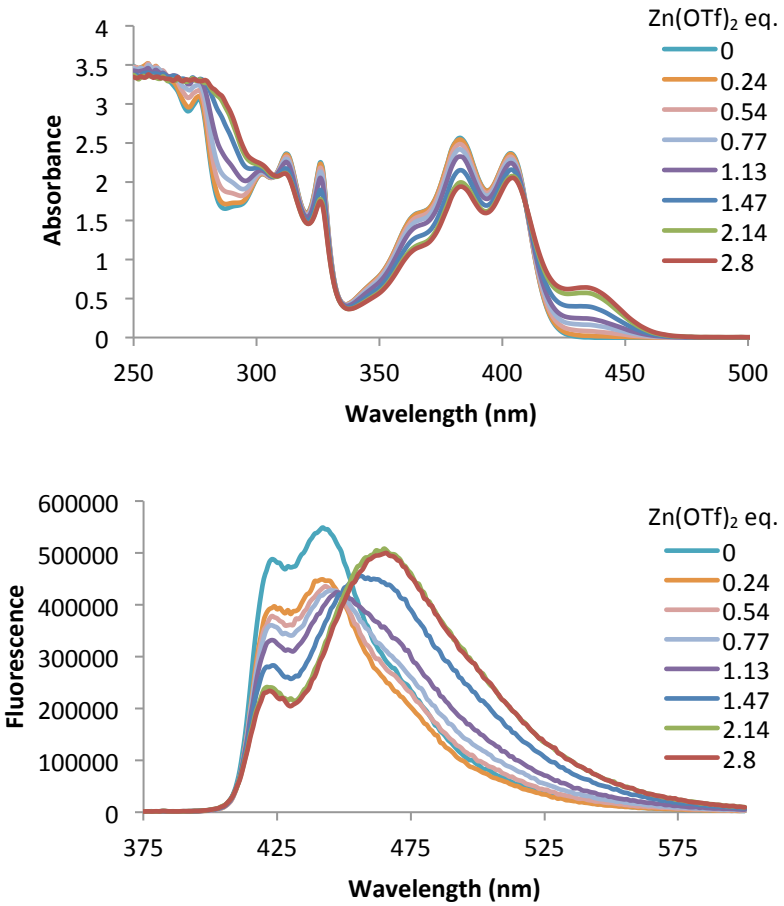

*Figure 5.14. A titration study in spectrophotometric grade DCM. A mixed solution of the imide **372** with $Zn(OTf)_2$ was titrated into the solution of the imide **372** (2×10^{-4} M). Emission measured at an excitation wavelength of λ=383 nm. Legend indicates the equivalents of $Zn(OTf)_2$ added.*

In a separate study, multiple crystallisation trials were prepared in various solvents, using a 2:1 ratio of the imide **372** to zinc triflate (based on the stoichiometry of the sodium dimer [M_2Na^+] observed in the mass spectrum). The zinc complex **440** was isolated from slow evaporation of a solution of acetone, from which the crystal structure of the zinc complex was confirmed (Figure 5.15). Peak shifts in the ^{1}H NMR and IR spectrum were observed however the complex, unsurprisingly, could not be identified by high-resolution mass spectrometry (HRMS).

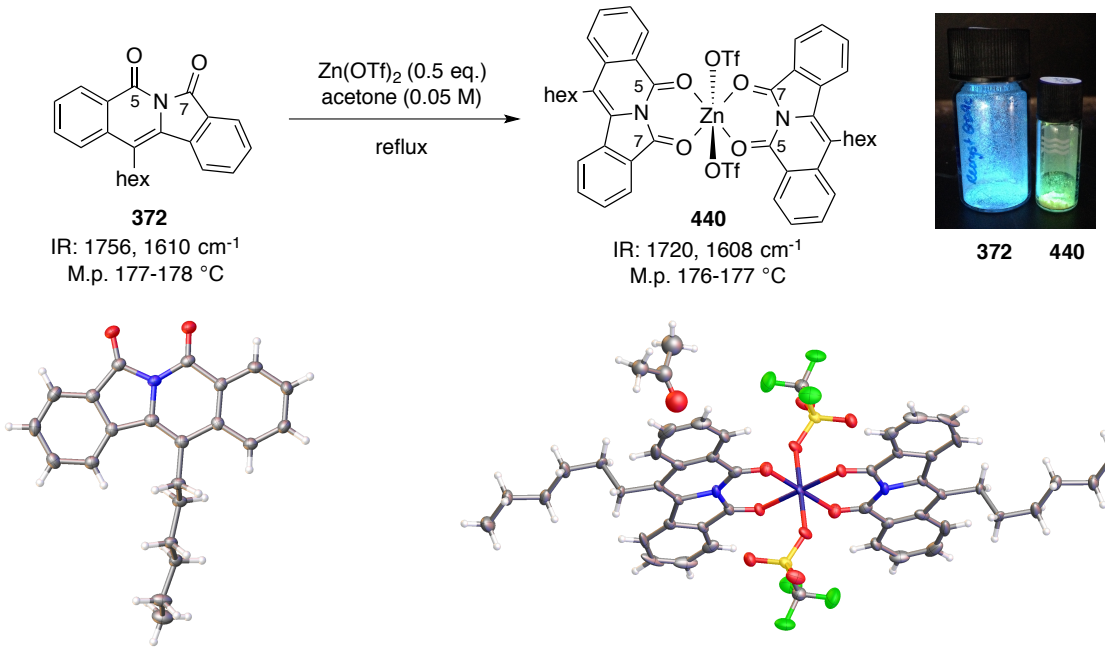

Bond	**372** Bond length (Å)	**440** Bond length (Å)
C_5-O	1.221	1.219
C_5-N	1.399	1.398
C_7-O	1.206	1.233
C_7-N	1.424	1.407

*Figure 5.15. X-ray crystal structure of the imide **372** and the zinc complex **440**. Image of the samples fluorescing in the solid state.*

Comparison of the X-ray crystal structures of the free imide **372** with the complexed imide **440** revealed key differences in the bond lengths of the C_7-O and C_7-N bond. The C_7-N bond is shortened from 1.424 Å (in **372**) to 1.407 Å (in **440**), as the C_7-O bond is lengthened from 1.206 Å to 1.233 Å, suggesting delocalisation of electrons from the nitrogen into the carboxyl group in the complexed imide. The isoquinolone portion of the imide is mainly unaffected in the complex. The bite angle (O-Zn-O) of the zinc in the complex was 86.15° (see Appendix for X-ray crystal structures).

Considering the weak binding of the neutral imide ligand **372** to the zinc(II) centre, our attention turned to neutral zinc complexes, whereby the ligand could covalently bind to the metal. Deprotonation of the *para*- and *ortho*-hydroxy imides, **416** and **393**, in the presence of a zinc(II) source could lead to the formation of neutral zinc complexes **441** and **442** (Scheme 5.33).

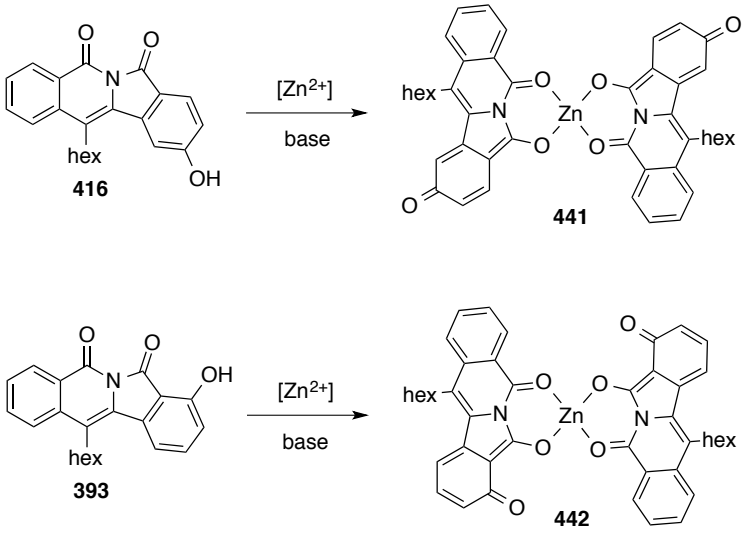

Scheme 5.33

With the phenolic imides in hand, investigation into the formation of neutral zinc complexes commenced (Scheme 5.34). Treatment of the *ortho*-hydroxy imide **393** with half an equivalent of $Zn(OTf)_2$ in DCM containing triethylamine produced a colour change from bright yellow to orange, which was encouraging based on a previous observation: the intermediate sodium phenolate imide **443**, formed *via* deprotonation of the acetonide isoquinolone **392**, was observed as an orange solution. On addition of acid (to reprotonate the phenolate anion), the solution changed colour from orange to bright yellow to give the imide **393** in its protonated form. Despite this observation, no discernable products were observed either from reaction sampling or from the final crude reaction. The identical reaction with the *para*-hydroxy imide **416** was equally unsuccessful.

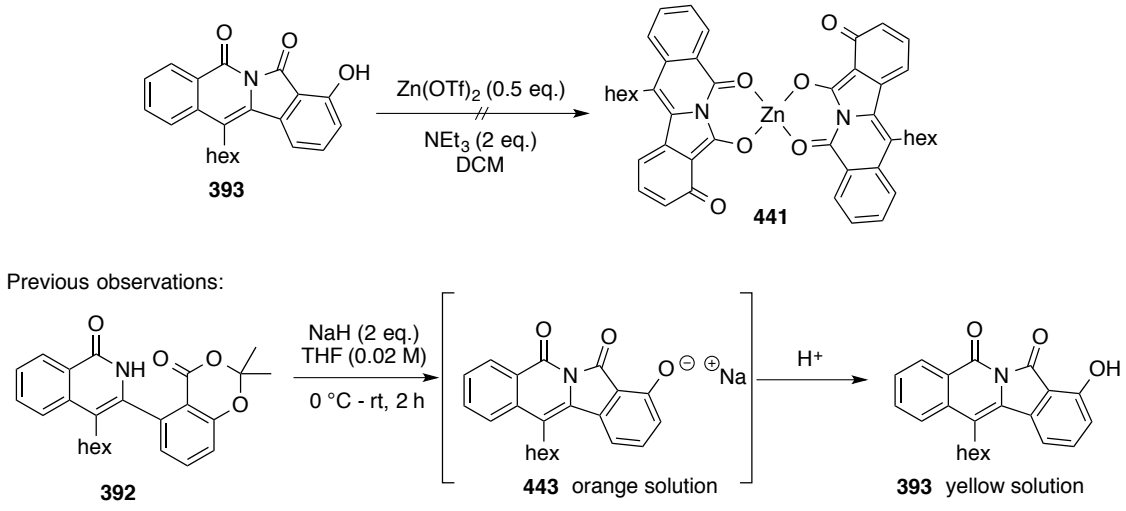

Scheme 5.34

Alternative combinations of bases and solvents were examined with both imides, however despite observing the colour change, any reaction monitoring of the reaction mixture and the crude reaction (by LCMS (ESI^+), TLC or HRMS (ESI^+ and ESI^-) revealed only the unreacted

imide. To simplify the reaction conditions, diethylzinc was employed to simultaneously act as a base and a source of zinc(II).[242,243] Evolution of ethane gas as the only by-product would ensure that purification of a resulting complex would be simplified. On addition of the diethylzinc (0.5 equivalents added as a 1 M solution in hexanes), to the homogeneous solution of the imide **393** in tetrahydrofuran (THF) a colourless precipitate formed, which was subsequently filtered from the reaction. The solid proved to be insoluble in all solvents, including DMSO, suggesting it was either inorganic material or potentially polymeric organic material.

Petrus and Sobota reported a crystal structure of the tetrameric cluster complex from the reaction of diethylzinc with methyl salicylate in their study of catalyst preparation for polymerisation reactions (Scheme 5.35).[243] Treatment of the cluster **444** with pyridine led to the formation of the monomeric zinc species **445**. Coordination of the ligand **381** to the metal centre, *via* the lone pair of electrons on the carbonyl atom and a covalent phenolic bond, would be equivalent to the mode in which the imide **393** could potentially bind to the zinc. Unfortunately, treatment of the insoluble precipitate from the previous reaction using the imide **393** with pyridine made little difference to the solubility of the material even on heating.

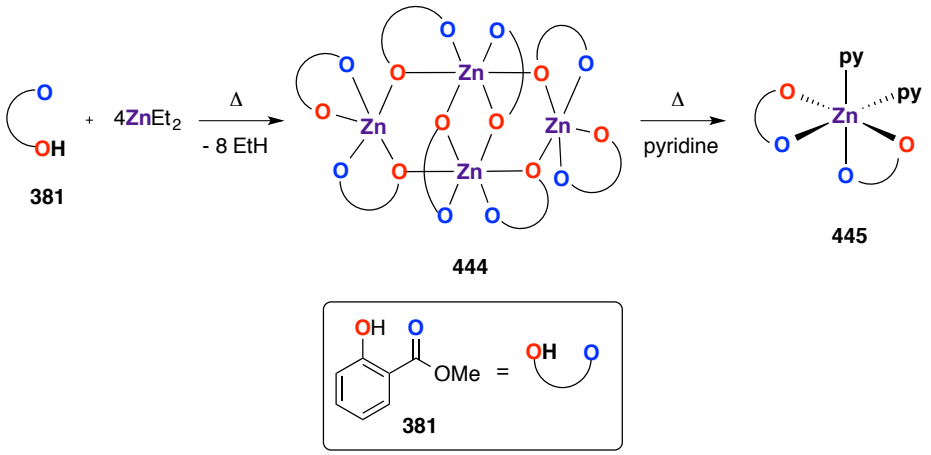

Figure 5.35[243]

In summary, coordination of the parent imide **372** with various metal salts was confirmed by qualitative colour changes, however fluorescence was only observed with zinc(II) triflate. Attempts to characterise the complex in solution were unsuccessful due to weak binding, however at higher concentrations crystals were grown to confirm the structure by X-ray crystallography. The crystal structure confirmed the 2:1 ratio of ligand **440** to zinc, which was previously proposed based on the sodium dimer in the mass spectrum. Attempted formation of neutral-zinc complexes were unsuccessful.

5.9 Conclusion

In summary, a fluorescent tetracyclic imide was identified and isolated from the rhodium(III)-catalysed annulation of *N*-(methoxy)benzamide with vinyl acetate. Subsequent mechanistic investigations identified putative intermediates, giving an indication as to the formation of the imide in the reaction. Based on the structure of the highly fluorescent molecule, the potential for tailoring the spectrochemical properties of the system, by addition of susbstituents, seemed promising. However, the initial synthetic routes suffered from issues with solubility and optimisation of yields proved futile.

An alternative approach, using the rhodium(III)-catalysed annulation of *N*-(pivaloyloxy)-benzamide derivatives with 2-alkynyl benzoate esters was identified a succinct route to the same scaffold. Using this approach the solubility and substrate scope was simultaneously addressed using bespoke starting materials. The starting materials were simply prepared from benzoic acid derivatives, and the alkynes assembled *via* a Sonogashira coupling.

Rhodium(III)-catalysed annulation of the 2-alkynyl benzoate esters resulted in formation of the desired isoquinolone and imide. Issues with the imide stability in nucleophilic solvents were addressed by incorporation of an *ortho*-electron-donating group to reduce the electrophilicity of the adjacent carboxyl group.

In total, nine imides were prepared using this methodology, including examples with auxochromic groups (-OH and $-NR_2$) and conjugated π-systems (naphthyl and thiophene derivatives). Their spectrochemical properties were subsequently investigated. A study of the quantum yield (Φ) of the parent imide **372** gave a value of Φ_{rel} 0.44 (in dichloromethane). Substitution on the parent imide using hydroxyl and π-conjugated systems led to bathochromic shifts in the absorbance and emission values. The electrochemical properties of four representative imides were analysed and found to have two reversible reduction peaks, which was promising for future tailoring towards semi-conductor applications.

Finally, a zinc-imide complex was prepared from a 2:1 mixture of the parent imide and zinc(II) triflate, however isolation proved cumbersome due to the weak binding. Attempts to prepare neutral zinc complexes from the *ortho*- and *para*-hydroxy imides were unsuccessful.

5.10 Future work

The application scope for this imide scaffold is plentiful, based on these preliminary findings. Using our methodology, the scaffold offers three points for diversification, which could be exploited to serve a particular application (Figure 5.16). Further modifications could be made to the aromatic core to tune the fluorescent and physical properties of the scaffold towards semi-conductor or biological applications. The modification of the side chain has not been fully explored, but could be used to tether additional components to the fluorophore. The interconversion of the fluorescent imides to the non-fluorescent isoquinolones could be exploited as a pH sensitive fluorescent switch. Studies into the rate of interconversion at different pH levels and the behaviour in various solvents would provide additional information for this potential application.

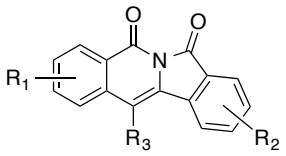

Figure 5.16

The initial foray into a C-H activation polymerisation methodology, using the biphenyl-*N*-(pivaloyloxy)-derivative **429** (see Scheme 5.31) proved unsuccessful, based on the solubility of the intermediate mono-cyclised imide. However, introduction of additional lipohilic groups to the precursors could potentially circumvent this issue to allow the formation of a polymeric material with the fluorescent imide embedded in the chain (see Scheme 5.30).

The observed fluorescence of the imide with zinc highlighted the potential for alternative fluorescent metal-imide complexes. Studies are currently underway collaboratively with the group of Dr Patrick McGowan to investigate the synthesis of titanium-imide complexes for use in cell line imaging for anti-cancer agents.

Chapter 6

Experimental

6.1 General methods

All experiments were conducted in oven-dried glassware, under a dry nitrogen atmosphere with anhydrous solvents, unless otherwise stated. Hygroscopic cesium acetate (CsOAc) was stored in a desiccator. Anhydrous solvents were obtained from the solvent purification system (SPS). Anhydrous methanol was stored on 3Å molecular sieves. All other solvents and reagents were obtained from commercial sources and used without further purification. *O*-(Pivaloyl)-hydroxylammonium chloride[112] and *O-(*pivaloyl)-hydroxylamine triflic acid[34] were prepared according to literature procedures.

Flash silica chromatography was performed using Fischer Matrix silica gel (35-70 μm particles) and thin layer chromatography was carried out using pre-coated silica plates (Merck silica Kieselgel $60F_{254}$). Spots were visualised using UV fluorescence (λ_{max} = 254 nm) or chemical staining with potassium permanganate. All chromatography eluents were HPLC grade and used without purification. Petrol refers to petroleum ether (b.p. 40-60°C).

Proton (^{1}H) and carbon ($^{13}C\{^{1}H\}$) nuclear magnetic resonance spectra were recorded using a Bruker DPX 300, a Bruker DRX 500 or a Bruker Avance 500 spectrometer using an internal deuterium lock. ^{1}H NMR chemical shifts (δ) are quoted in ppm downfield of tetramethylsilane or residual solvent peaks and coupling constants (*J*) are quoted in Hz. $^{13}C\{^{1}H\}$ NMR spectra were recorded with broadband proton decoupling at 75 MHz and 125 MHz. NMR spectra were processed using MestreNova software. Assignments were made on the basis of chemical shift and coupling data, using COSY and DEPT where necessary. Infra-red spectra were recorded on a Perkin Elmer Spectrum One FT-IR spectrometer, with absorption reported in wavenumbers (cm^{-1}). High-resolution electrospray mass spectra (ESI-MS) were measured on a Bruker MicroTOF-Q or Bruker MaXis Impact spectrometer in positive mode. Melting points were determined using a Griffin D5 variable temperature apparatus and are uncorrected.

6.2 ^{1}H NMR studies

^{1}H NMR study of the Lossen rearrangement

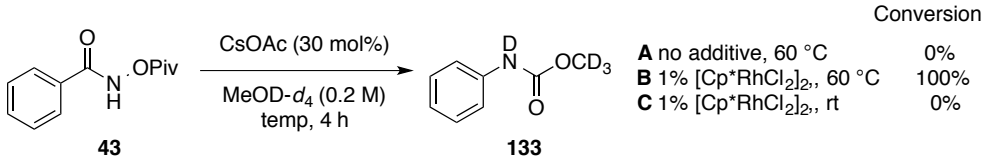

43 **133**

N-(Pivaloyloxy)benzamide (22 mg, 0.10 mmol), CsOAc (6 mg, 0.3 mmol) and [Cp*RhCl$_2$]$_2$ (0.6 mg, 1 μmol) for **B** and **C**) were weighed into a NMR tube fitted with a Young's tap under an N_2 atmosphere. To each NMR tube was added mesitylene (14 μL, 0.10 mmol), followed by MeOD (0.5 mL, 0.2 M). The tubes were sealed and shaken and reactions **A** and **B** were heated to 60 °C. ^{1}H NMR analysis was taken at the following time points: 0, 1, 2, 3 and 4 hours. After this time the reactions **A** and **C** contained unreacted starting material and reaction **B** showed >95% conversion to the methyl phenyl carbamate.

^{1}H NMR study of the annulation reactions of vinyl acetate and butyl vinyl ether

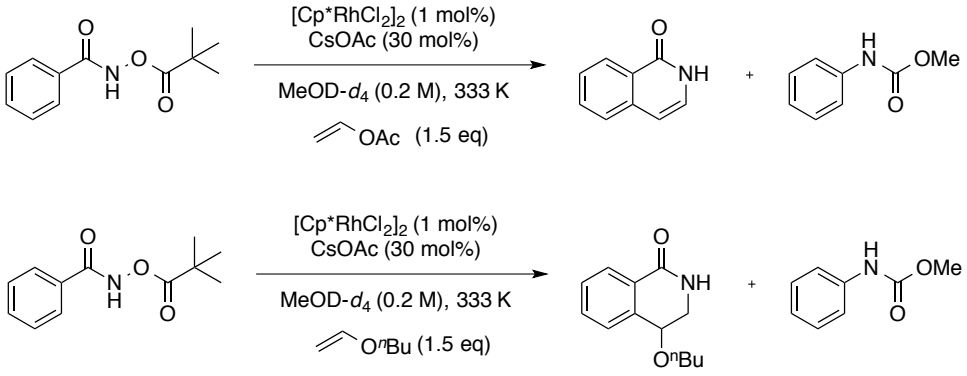

N-(Pivaloyloxy)benzamide (22 mg, 0.10 mmol), CsOAc (6 mg, 0.3 mmol), trimethoxybenzene (5.6 mg, 0.03 mmol) and vinyl acetate (14 μL, 0.15 mmol) or butyl vinyl ether (20 μL, 0.15 mmol) were dissolved in MeOD-d_4 (0.5 mL, 0.2 M) in a septum-topped vial under an N_2 atmosphere. To each NMR tube (fitted with a Young's tap), [Cp*RhCl$_2$]$_2$ (0.6 mg, 1 μmol) was added followed by the solution containing the remaining reactant. The tubes were sealed, shaken and the reactions were heated to 60 °C (333 K) in the ^{1}H NMR machine. ^{1}H NMR spectra were acquired at regular time intervals to compare the rate of product formation (isoquinolone or 4-butoxy,3,4-dihydroisoquinolones) *versus* the Lossen rearrangement.

^{1}H NMR study of *in situ* formation of *N*-(acetoxy)benzamide

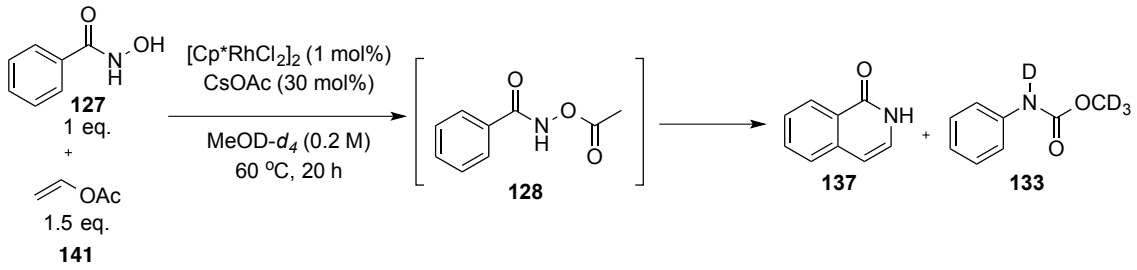

Benzhydroxamic acid (14 mg, 0.10 mmol), CsOAc (6 mg, 0.3 mmol), trimethoxybenzene (5.6 mg, 0.033 mmol) and vinyl acetate (14 μL, 0.15 mmol) were dissolved in MeOD-d_4 (0.5 mL, 0.2 M) in a septum-topped vial under an N_2 atmosphere. To each NMR tube (fitted with a Young's tap), $[Cp^*RhCl_2]_2$ (0.6 mg, 1 μmol) was added followed by the reaction solution containing the remaining reactant. The tube was sealed, shaken and the reaction was heated to 60 °C (333 K) in the ^{1}H NMR machine. ^{1}H NMR spectra were acquired at regular time intervals to identify the formation of *N*-(acetoxy)benzamide *in situ.*

6.3 Alkenyl substrate scope

Optimisation study for vinyl ethers

N-(Pivaloyloxy)benzamide (221 mg, 1.00 mmol), *n*-butyl vinyl ether (194 µL, 1.50 mmol or 647 µL, 5.00 mmol), $[Cp^*RhCl_2]_2$ (6 mg, 1 mol%) and CsOAc (58 mg, 30 mol%) were dissolved in MeOH (5.0 mL, 0.2 M or 1.0 mL, 1.0 M) under N_2 in a sealed vessel. After 16 hours the reaction solution was concentrated *in vacuo* (^{1}H NMR spectra were taken from the crude samples) and purified by flash silica chromatography using 50% EtOAc in hexane with 5% NEt_3. The desired fractions were concentrated and analysed.

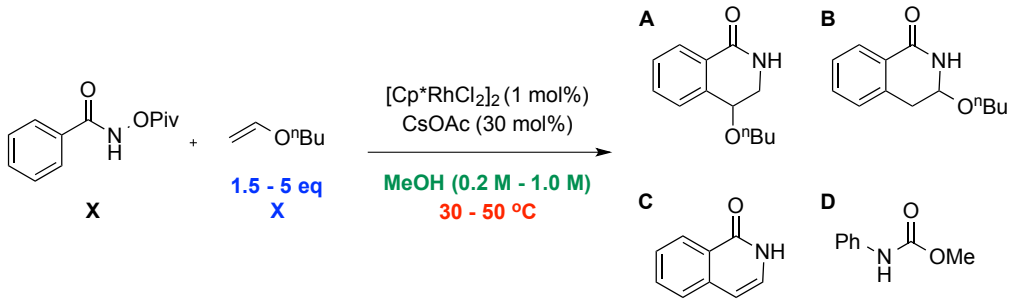

Entry	Variables			Yield % (by ^{1}H NMR)				Ratio	Isolated Yield %
	Temp (°C)	Conc (M)	X (Eq.)	A	B	C	D	(A+B+C):D	A+ B
1	30	0.2	1.5	75	21	0	4	24 :1	50
2	30	0.2	5	73	25	0	2	49:1	**76**
3	30	1	1.5	83	16	0	1	99:1	69
4	30	1	5	77	22	0	1	99:1	**74**
5	50	0.2	1.5	45	10	5	40	3:2	33
6	50	0.2	5	59	16	6	19	81:9	51
7	50	1	1.5	66	11	14	9	91:9	49
8	50	1	5	62	19	14	5	19:1	64
9	40	0.6	3.25	71	26	0	3	97:3	62
10	40	0.6	3.25	71	25	0	4	24:1	68

Table 2.2

4-Butoxy-3,4-dihydroisoquinolin-1(*2H*)-one 130

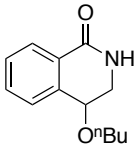

Isolated as a brown oil. Yields from the optimisation study are outlined in Table 2.2. δ_H (300 MHz, $CDCl_3$) 8.09 (1H, dd, *J* 7.6, 1.2, H_8), 7.54 (1H, td, *J* 7.5, 1.4, H_6), 7.47-7.43 (2H, m, H_5 and H_7), 7.13 (1H, br s, NH), 4.50-4.48 (1H, m, H_4), 3.70 (1H, ddd, *J* 12.8, 4.1, 2.6, H_3), 3.62 (1H, ddd, *J* 12.8, 5.8, 3.4, H_3), 3.56 (1H, dt, *J* 9.0, 6.5, OCH_2), 3.45 (1H, dt, *J* 9.0, 6.6, OCH_2), 1.60-1.52 (2H, m, OCH_2CH_2), 1.31-1.40 (2H, m, $O(CH_2)_2CH_2$), 0.88 (3H, t, *J* 7.4, $O(CH_2)_3CH_3$); δ_C (75 MHz, $CDCl_3$) 165.9 (C_qO), 138.7

(C_q), 132.1 (C_6), 128.7 (C_7), 128.3 (C_q), 128.0 (C_8), 126.7 (C_5), 72.4 (C_4), 68.9 (C_3), 44.7 (O*C*H$_2$), 31.7 (OCH$_2$*C*H$_2$), 19.3 (O(CH$_2$)$_2$*C*H$_2$), 13.9 (O(CH$_2$)$_3$*C*H$_3$); HRMS (ESI$^+$): *m/z* calculated for formula $C_{13}H_{17}NNaO_2$ [MNa$^+$]: 242.1151; found 242.1158; IR (ν_{max}, film, cm^{-1}): 3255, 3064, 2870, 1944, 1668, 1473, 1090.

3-Butoxy-3,4-dihydroisoquinolin-1(*2H*)-one 131

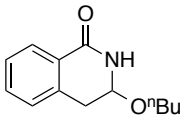

Isolated as an orange oil. Yields from the optimisation study are outlined in Table 2.2. δ_H (500 MHz, $CDCl_3$) 8.49 (1H, br s, NH), 8.08 (1H, dd, *J* 7.7, 1.2, H_8), 7.47 (1H td, *J* 7.5, 1.4, H_6), 7.35 (1H, td, *J* 7.5, 1.0, H_7), 7.24 (1H, dd, *J* 7.5, 1.0, H_5), 4.88 (1H, td, *J* 4.5, 2.5, H_3), 3.58 (1H, dt, *J* 9.2, 6.7, OC*H*$_2$), 3.38 (1H, dt, *J* 9.0, 6.5, OC*H*$_2$), 3.29 (1H, dd, *J* 16.4, 4.5, H_4), 3.10 (1H, dd, *J* 16.4, 4.5, H_4), 1.51-1.45 (2H, m, OCH$_2$C*H*$_2$), 1.31-1.23 (2H, m, O(CH$_2$)$_2$C*H*$_2$), 0.85 (3H, t, *J* 7.5, O(CH$_2$)$_3$C*H*$_3$); δ_C (75 MHz, $CDCl_3$) 167.0 (C_qO), 136.5 (C_q), 132.7 (C_6), 128.1 (C_7), 127.8 (C_5), 127.5 (C_q), 126.9 (C_8), 80.3 (C_3), 67.1 (C_4), 33.8 (OCH$_2$), 31.5 (OCH$_2$*C*H$_2$), 19.2 (O(CH$_2$)$_2$*C*H$_2$), 13.7 (O(CH$_2$)$_3$*C*H$_3$); HRMS (ESI$^+$): *m/z* calculated for formula $C_{13}H_{17}NNaO_2$ [MNa$^+$]: 242.1151; found 242.1142; IR (ν_{max}, film, cm^{-1}): 2956, 2889, 1652, 1475, 1343, 1228.

4-Ethoxy- and 3-ethoxy-3,4-dihydroisoquinolin-1(*2H*)-one.

Ethyl vinyl ether (481 μL, 5.00 mmol) was added to a solution of *N*-(pivaloyloxy)benzamide (221 mg, 1.00 mmol), CsOAc (57.0 mg, 0.30 mmol) and $[Cp^*RhCl_2]_2$ (6 mg, 1 mol%) in MeOH (5.00 mL, 0.20 M) that was left stirring overnight at 30 °C for 16 hours. The crude reaction mixture was concentrated *in vacuo* and purified by flash silica chromatography using 10% hexane in EtOAc with 5% NEt_3 to give two regioisomers **139** (134 mg, 65%) and **140** (45.6 mg, 22%) as orange amorphous solids. Samples of the solids were cystallised from hexane–EtOAc.

4-Ethoxy-3,4-dihydroisoquinolin-1(2*H*)-one 139

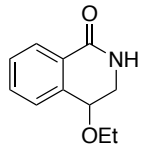

Major regioisomer. M.p. 130-132 °C (hexane–EtOAc); δ_H (300 MHz, $CDCl_3$) 8.11 (1H, dd, *J* 7.4, 1.4, H_8), 7.55 (1H, td, *J* 7.4, 1.4, H_6), 7.47 (1H, td, *J* 7.6, 1.4, H_7), 7.42 (1H, d, *J* 7.3, 1.4, H_5), 6.10 (1H, br s, NH), 4.50 (1H, t, *J* 4.6, H_4), 3.76-3.45 (4H, m, OCH_2 and H_3), 1.22 (3H, t, *J* 7.0, CH_3); δ_C (75 MHz, $CDCl_3$) 165.5 (C_qO), 138.1 (C_q), 132.1 (C_6), 128.8 (C_7), 128.4 (C_q), 128.2 (C_8), 126.9 (C_5), 72.3 (C_4), 64.5 (C_3), 44.9 (O*C*H$_2$), 15.4 (OCH$_2$*C*H$_3$); HRMS (ESI$^+$): *m/z* calculated for formula: $C_{11}H_{14}NO_2$ [MH^+] 192.1023; found 192.1023; IR (ν_{max}, solid, cm^{-1}): 3302, 2890, 1605, 1439, 1113.

3-Ethoxy-3,4-dihydroisoquinolin-1(*2H*)-one 140

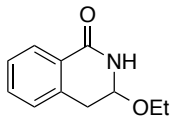

Minor regioisomer. M.p. 130-132 °C (hexane–EtOAc); δ_H (300 MHz, $CDCl_3$) 8.09 (1H, d, *J* 8.0, H_8), 7.48 (1H, td, *J* 7.5, 3.7, H_6), 7.36 (1H, t, *J* 7.5, H_7), 7.25 (1H, d, *J* 7.1, H_5), 6.61 (1H, br s, NH), 4.89 (1H, td, *J* 4.4, 2.3, H_3), 3.65 (1H, dq, *J* 9.1, 7.0, OCH_2CH_3), 3.43 (1H, dq, *J* 9.1, 7.0, OCH_2CH_3), 3.32 (1H, dd, *J* 15.9, 4.5, H_4), 3.11 (1H, d, *J* 16.4, H_4), 1.15 (3H, t, *J* 7.0, OCH_2CH_3); δ_C (75 MHz, $CDCl_3$) 160.1 (C_qO), 136.4 (C_q), 132.6 (C_6), 128.6 (C_7), 127.9 (C_q), 127.7 (C_5), 127.0 (C_8), 80.3 (C_3), 62.6 (O*C*H$_2$), 34.0 (C_4), 15.1 (*C*H$_3$); HRMS (ESI$^+$): *m/z* calculated for formula: $C_{11}H_{13}NNaO_2$ [MNa^+] 214.0838; found 214.0833; IR (ν_{max}, solid, cm^{-1}): 3282, 2925, 1650, 1490, 1033.

Verification of regiochemistry: repeat of Fagnou experiment.[34]

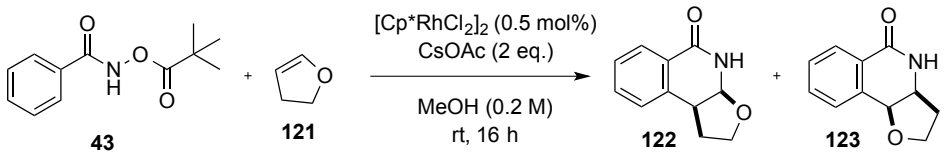

Dihydrofuran (83 μL, 1.1 mmol) was added to a solution of *N*-(pivaloyloxy)benzamide (221 mg, 1.00 mmol), CsOAc (384 mg, 2.00 mmol) and $[Cp^*RhCl_2]_2$ (3 mg, 0.5 mol%) in MeOH (5 mL, 0.2 M). The solution was left to stir at room temperature for 24 hours. The material was concentrated and purified using flash silica chromatography with 8% isopropanol in toluene to separate a mixture of regioisomers (145 mg, 77%, **123**) and (5 mg, 3%, **122**).

2,3,3a,4-Tetrahydrofuro[3,2-*c*]isoquinolin-5(*9bH*)-one 123

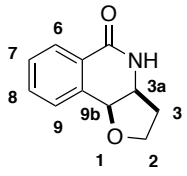

Isolated as a cream solid (145 mg, 77%). R_F 0.08 (8% isopropanol in toluene). δ_H (300 MHz, $CDCl_3$) 8.16 (1H, dd, *J* 7.3, 1.2, H_6), 7.61-7.45 (3H, m H_7, H_8, H_9), 6.00 (1H, br s, NH), 4.85 (1H, d, *J* 4.6, H_{9b}), 4.36-4.34 (1H, m, H_{3a}), 4.13-3.99 (2H, m, H_2), 2.52-2.39 (1H, m, H_3), 2.19-2.09 (1H, m, H_3); δ_C (75 MHz, $CDCl_3$) 164.8 (C_5), 135.3 (C_q), 132.7 (C_8), 129.4 (C_7), 129.1 (C_9), 128.0 (C_6), 127.4 (C_q), 72.2 (C_{9b}), 66.7 (C_2), 54.3 (C_{3a}), 34.9 (C_3); HRMS (ESI^+): *m/z* calculated for formula: $C_{11}H_{11}NNaO_2$ $[MNa^+]$ 212.0682; found 212.0680; IR (ν_{max}, solid, cm^{-1}): 3196, 2957, 1668, 1456, 1335, 1040.

1,3a,4,9b-Tetrahydrofuro[2,3-*c*]isoquinolin-5(*2H*)-one 122

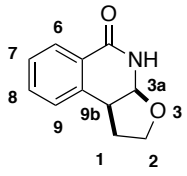

Isolated as an orange oil (5 mg, 3%). R_F 0.15 (8% isopropanol in toluene), δ_H (300 MHz, $CDCl_3$) 8.07 (1H, dd, *J* 7.8, 1.3, H_6), 7.45 (1H, td, *J* 7.5, 1.4, H_8), 7.31 (1H, td, *J* 7.6, 1.1, H_7), 7.23 (1H, dd, *J* 7.6, 0.5, H_9), 6.76 (1H, br s, NH), 5.51 (1H, dd, *J* 6.0, 1.6 H_{3a}), 3.98-3.99 (2H, m, H_2), 3.48 (1H, ddd, *J* 14.4, 8.3, 6.2, H_{9b}), 2.50-2.38 (1H, m, H_1), 2.12-2.00 (1H, m, H_1). Insufficient material to obtain a good quality ^{13}C spectrum. HRMS (ESI^+): *m/z* calculated for formula $C_{11}H_{11}NNaO_2$ $[MNa^+]$ 212.0682; found 212.0689; IR (ν_{max}, solid, cm^{-1}): 3254, 2935, 1695, 1471, 1190, 1042.

6.4 Preparation of hydroxamate esters

N-Methoxybenzamide 42[34]

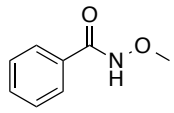

A solution of *O*-methylhydroxylamine hydrochloride (1.50 g, 18.0 mmol) and potassium carbonate (4.18 g, 30.0 mmol) in EtOAc–water (2:1, 270 mL) was cooled to 0 °C in an ice bath. Benzoyl chloride (1.7 mL, 15 mmol) was added dropwise into the reaction, ensuring the temperature was maintained at 0 °C. Following the addition, the solution was warmed to room temperature and left stirring overnight. After 16 hours, the reaction solution was diluted with EtOAc (100 mL) and washed with water (100 mL) and brine (100 mL). The organic layer was dried with $MgSO_4$, filtered and concentrated *in vacuo* to give *N*-methoxybenzamide as a colourless solid (1.43g, 69%). R_F 0.45 (9:1 EtOAc–petrol); δ_H (500 MHz, $CDCl_3$) 8.72 (1H, br s, NH), 7.74 (2H, d, *J* 7.2, ArH), 7.54 (1H, t, *J* 7.7, ArH), 7.45 (2H, t, *J* 7.7, ArH), 3.90 (3H, s, MeO); δ_C (75 MHz, $CDCl_3$) 166.6 (C_qO), 132.1 (C_4), 131.9 (C_q), 128.7 (C_3 and C_5), 127.1 (C_2 and C_6), 64.6 (MeO); HRMS (ESI^+): *m/z* calculated for formula $C_8H_{10}NO_2$ [MH^+]: 152.0706; found 152.0708. Spectral data consistent with the literature.[34]

N-Acetoxybenzamide 128[34]

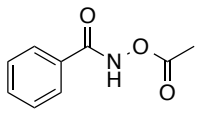

A solution of benzhydroxamic acid (0.7 g, 5 mmol), 2 M NaOH (2.30 mL), and acetic anhydride (0.60 mL, 5.5 mmol) in DCM (15 mL) was stirred at room temperature for 16 hours. After this time the reaction mixture was diluted with EtOAc (20 mL) and the organic layer was sequentially washed with 1 N HCl (20 mL), water (2 × 20 mL) and brine (20 mL). The organic layer was dried over $MgSO_4$, filtered and concentrated *in vacuo* to give *N*-acetoxybenzamide, which was recrystallised from Et_2O–pentane to give colourless crystals (0.75 g, 83%). R_F 0.44 (50% hexane–EtOAc); δ_H (500 MHz, $CDCl_3$) 9.45 (1H, br s, NH), 7.82 (2H, d, *J* 7.2, ArH), 7.58 (1H, t, *J* 7.6, ArH), 7.48 (2H, t, *J* 7.9, ArH), 2.31 (3H, s, Me); δ_C (75 MHz, $CDCl_3$) 169.2 (C_qO), 166.4 (C_qO), 132.8 (C_4), 130.7 (C_q), 128.8 (C_3 and C_5), 127.5 (C_2 and C_6), 18.4 (Me); HRMS (ESI^+): *m/z* calculated for formula $C_9H_9NNaO_3$ [MNa^+]: 202.0475; found 202.0469. IR (ν_{max}, solid, cm^{-1}): 3143, 2957, 1792, 1651, 1313, 1198, 1021, 895, 693. Spectral data consistent with the literature.[34]

N-(Pivaloyloxy)benzamide 43[244]

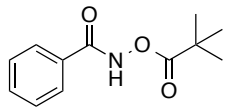

A solution of benzhydroxamic acid (1.47 g, 10.7 mmol), NEt_3 (1.30 mL, 11.0 mmol) and pivaloyl chloride (1.30 mL, 11.0 mmol) in THF (60 mL, 0.18 M) was stirred at room temperature for 16 hours. The reaction mixture was diluted with EtOAc (50 mL) and washed with 1 N HCl (50 mL), water (2 x 50 mL)

and brine (50 mL). The organic layer was dried over $MgSO_4$ and concentrated *in vacuo* to give an amorphous cream solid. The material was crystallised from Et_2O–pentane to give a colourless microcrystalline powder, *N*-(pivaloyloxy)benzamide (2.08 g, 88%). M.p. 170-172 °C (Et_2O–pentane, [lit. M.p. 169-170 °C][244]); R_F 0.80 (50% EtOAc in hexane); δ_H (500 MHz, $CDCl_3$) 9.30 (1H, br s, NH), 7.83 (2H, d, *J* 7.9, H_2 and H_6), 7.58 (1H, t, *J* 7.9, H_4), 7.48 (2H, t, *J* 7.9, H_3 and H_5), 1.38 (9H, s, $(CH_3)_3$); δ_C (75 MHz, $CDCl_3$) 177.0 (*C*$OC(CH_3)_3$), 166.8 (*C*ONH), 132.7 (C_4), 131.0 (C_1), 128.8 (C_3 and C_5), 127.5 (C_2 and C_6), 38.5 (CO*C*$(CH_3)_3$), 27.1 ($COC(CH_3)_3$); HRMS (ESI^+): *m/z* calculated for formula $C_{12}H_{15}NNaO_3$ [MNa^+]: 244.0944; found 244.0939. IR (ν_{max}, solid, cm^{-1}): 3240, 2975, 1781, 1650, 1516, 1482, 1369, 1267, 1068, 1025. Spectral data consistent with the literature.[244]

General Procedure (A) for the synthesis of hydroxamic esters

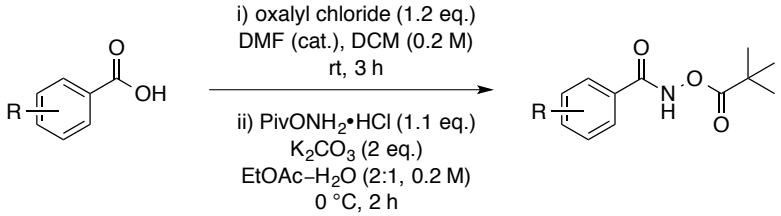

Oxalyl chloride (1.2 eq.) was added to a solution of the benzoic acid derivative (1 eq.) in anhydrous DCM (0.2 M) with DMF (2 drops). The solution was stirred at room temperature for 3 hours, after which time the solvent was removed *in vacuo* to afford the crude acid chloride. The intermediate was diluted in EtOAc (5 mL) and transferred to a flask containing *O*-(pivaloyl)hydroxylammonium chloride (1.1 eq.) and K_2CO_3 (2 eq.) dissolved in a 2:1 mixture of EtOAc–H_2O (0.2 M) at 0 °C. After 2 hours, the reaction was quenched with sat. $NaHCO_3$ (50 mL) and extracted with EtOAc (50 mL). The two phases were separated and the organic layer was washed with brine (50 mL). The organic layer was dried over $MgSO_4$, filtered and concentrated *in vacuo*. The final compound was purified by crystallisation or flash silica chromatography.

General Procedure (B) for the synthesis of hydroxamic esters

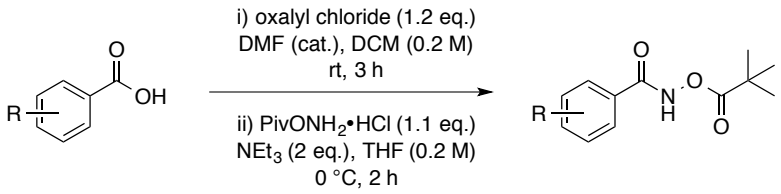

Oxalyl chloride (1.2 eq.) was added to a solution of the benzoic acid derivative (1 eq.) in anhydrous DCM (0.2 M) with DMF (2 drops). The mixture was stirred at room temperature for 3 hours, after which time the solvent was removed *in vacuo* to afford the crude acid chloride. The intermediate was diluted in THF (5 mL) and transferred to a flask containing *O*-(pivaloyl)hydroxylammonium chloride (1.1 eq.) and NEt_3 (2 eq.) in THF (0.2 M) at 0 °C. After 2 hours, the reaction was concentrated *in vacuo* and the residue was re-diluted with sat. $NaHCO_3$ (50 mL) and EtOAc (50 mL). The two phases were separated and the organic layer was washed with brine (50 mL). The organic layer was dried over $MgSO_4$, filtered and concentrated *in vacuo*. The final compound was purified by crystallisation or flash silica chromatography.

4-Cyano-*N*-(pivaloyloxy)benzamide 161

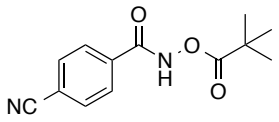

The final compound was isolated as a colourless solid (459 mg, 37%), by flash column chromatography using 10-20% EtOAc in hexane, from 4-cyanobenzoic acid (736 mg, 5.00 mmol) following general procedure B. A sample was taken and crystallised from $CDCl_3$. R_F 0.33 (9:1 hexane–EtOAc); m.p. 103.4-105.5 °C ($CDCl_3$); δ_H (500 MHz, $CDCl_3$) 9.30 (1H, br s, NH), 7.92 (2H, d, *J* 8.5, H_2 and H_6), 7.78 (2H, d, *J* 8.6, H_3 and H_5), 1.37 (9H, s, $(CH_3)_3$); δ_C (75 MHz, $CDCl_3$) 176.8 (*C*OC$(CH_3)_3$), 165.0 (*C*ONH), 134.8 (C_1), 132.6 (C_3 and C_5), 128.2 (C_2 and C_6), 117.7 (*C*N), 116.2 (C_4), 38.5 (CO*C*$(CH_3)_3$), 27.0 (COC(*C*$H_3)_3$); HRMS (ESI^+): *m/z* calculated for formula $C_{13}H_{14}N_2NaO_3$ [MNa^+] 269.0897; found 269.0895; IR (ν_{max}, solid, cm^{-1}): 3223, 2982, 2234, 1781, 1648, 1519, 1480, 1398, 1366, 1308, 1281, 1064.

4-Acetyl-*N*-(pivaloyloxy)benzamide 162

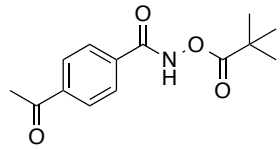

The final compound was isolated as a colourless solid (105 mg, 10%), by flash column chromatography using 30% EtOAc in hexane, from 4-acetylbenzoic acid (329 mg, 2.00 mmol) following general procedure A. δ_H (300 MHz, $CDCl_3$) 9.72 (1H, s, NH), 7.98 (2H, d, *J* 8.4, H_2 and H_6), 7.87 (2H, d, *J* 8.4, H_3 and H_5), 2.61 (3H, s, $COCH_3$), 1.34 (9H, s, $(CH_3)_3$); δ_C (75 MHz, $CDCl_3$) 197.5 (*C*OCH_3), 176.9 (*C*OC$(CH_3)_3$), 165.6 (*C*ONH), 140.0 (C_4), 134.8 (C_1), 128.6 (C_3 and C_5), 127.8 (C_2 and C_6), 38.5 (CO*C*$(CH_3)_3$), 27.0 (COC(*C*$H_3)_3$), 26.9 (CO*C*H_3); HRMS (ESI^+): *m/z* calculated for formula $C_{14}H_{17}NNaO_4$ [MNa^+] 286.1050; found 286.1048; IR (ν_{max}, solid, cm^{-1}): 3209, 2975, 1779, 1682, 1514, 1070.

4-(Trifluoromethyl)-*N*-(pivaloyloxy)benzamide 163

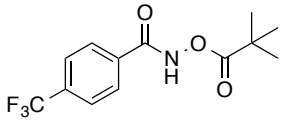

The final compound was isolated as a colourless crystalline solid (813 mg, 60%), by crystallisation from Et_2O–pentane, from 4-(trifluoromethyl)benzoic acid (1.36 g, 4.69 mmol) following general procedure B. M.p. 121-124 °C (Et_2O–pentane); δ_H (300 MHz, $CDCl_3$) 9.53 (1H, br s, NH), 7.91 (2H, d, *J* 8.1, H_2 and H_6), 7.71(2H, d, *J* 8.2, H_3 and H_5), 1.36 (9H, s, $(CH_3)_3$); δ_C (75MHz, $CDCl_3$) 177.1 (*C*OC$(CH_3)_3$), 165.5 (*C*ONH), 134.5 (q, *J* 32.9, *C*$_4$), 134.3 (C_1), 128.1 (C_2 and C_6), 126.0 (q, *J* 3.7, C_3 and C_5), 123.6 (q, *J* 272.8, *C*F_3), 38.6 (CO*C*$(CH_3)_3$), 27.1 (COC(*C*$H_3)_3$); HRMS (ESI^+): *m/z* calculated for formula $C_{13}H_{15}F_3NO_3$ [MH^+] 290.0999; found 290.0997; IR (ν_{max}, solid, cm^{-1}): 2978, 1780, 1663, 1582, 1323, 1128, 1065, 1016.

4-Methoxy-*N*-(pivaloyloxy)benzamide 164

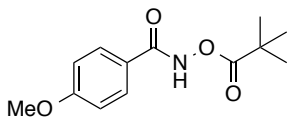

The desired compound was isolated as a colourless crystalline solid (613 mg, 81%), by crystallisation from $CHCl_3$, from 4-methoxybenzoyl chloride (510 mg, 3.00 mmol) following general procedure B. M.p. 149-150 °C ($CHCl_3$); δ_H (300 MHz, $CDCl_3$) 9.27 (1H, br s, NH), 7.81 (2H, d, *J* 9.0, H_2 and H_6), 6.96 (2H, d, *J* 9.0, H_3 and H_5), 3.88 (3H, s, OMe), 1.38 (9H, s, $(CH_3)_3$); δ_C (75 MHz, $CDCl_3$) 177.3 (*C*OC$(CH_3)_3$), 166.7 (*C*ONH), 163.2 (C_4), 129.5 (C_2 and C_6), 123.0 (C_1), 114.1 (C_3 and C_5), 55.5 (OMe), 38.5 (CO*C*$(CH_3)_3$), 27.1 (COC(*C*$H_3)_3$); HRMS (ESI^+): *m/z* calculated for formula $C_{13}H_{17}NNaO_4$ [MNa^+] 274.1050; found 274.1045; IR (ν_{max}, solid, cm^{-1}): 3259, 2974, 1774, 1605, 1494, 1318, 1260, 1073, 1028. Spectral data consistent with the literature.[34]

4-Fluoro-*N*-(pivaloyloxy)benzamide 165

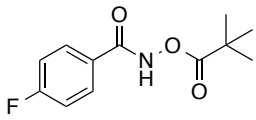

The final compound was isolated as a colourless microcrystalline powder colourless microcrystalline powder (317 mg, 44%), by flash column chromatography using 20% EtOAc in hexane, from 4-fluorobenzoic acid (420 mg, 3.00 mmol) following general procedure B. δ_H (300 MHz, $CDCl_3$) 9.26 (1H, br s, NH), 7.86 (2H, dd, *J* 8.7, 5.3, H_2 and H_6), 7.17 (2H, t, *J* 8.6, H_3 and H_5), 1.38 (9H, s, $(CH_3)_3$); δ_C (75 MHz, $CDCl_3$) 177.1 (*C*OC$(CH_3)_3$), 165.9 (*C*ONH), 165.4 (d, *J* 252.8, C_4), 130.0 (d, *J* 9.2, C_2 and C_6), 127.0 (d, *J* 3.3, C_1), 116.1 (d, *J* 22.1, C_3 and C_5), 38.5 (CO*C*$(CH_3)_3$), 27.2 (COC(*C*$H_3)_3$); HRMS (ESI^+): *m/z* calculated for formula $C_{12}H_{14}FNNaO_3$ [MNa^+] 262.0850; found 262.0847; IR (ν_{max}, solid, cm^{-1}): 3194, 2976, 1784, 1652, 1602, 1493, 1237, 1075.

4-Bromo-*N*-(pivaloyloxy)benzamide 166

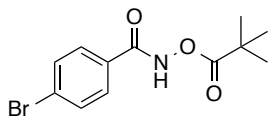

The final compound was isolated as a colourless microcrystalline powder (924 mg, 62%), by flash column chromatography using 10-50% EtOAc in hexane, followed by a crystallisation using EtOAc–hexane, from 4-bromobenzoic acid (1.01 g, 5.00 mmol) following general procedure B. R_F 0.28 (20% EtOAc in hexane); M.p. 141-142 °C (EtOAc–hexane); δ_H (500 MHz, $CDCl_3$) 9.24 (1H, br s, NH), 7.69 (2H, d, *J* 8.7, H_2 and H_6), 7.62 (2H, d, *J* 8.7, H_3 and H_5), 1.37 (9H, s, $(CH_3)_3$); δ_C (75 MHz, $CDCl_3$) 177.0 (*C*OC$(CH_3)_3$), 165.8 (*C*ONH), 132.1 (C_3 and C_5), 129.7 (C_1), 129.0 (C_2 and C_6), 127.6 (C_4), 38.5 (CO*C*$(CH_3)_3$), 27.0 (COC(*C*$H_3)_3$); HRMS (ESI^+): calculated for formula $C_{12}H_{14}{}^{79}BrNNaO_3$ [MNa^+] 322.0049; found 322.0050; IR (ν_{max}, solid, cm^{-1}): 3165, 2980, 1779, 1644, 1480, 1069. Spectral data consistent with the literature.[245]

4-Iodo-*N*-(pivaloyloxy)benzamide 167

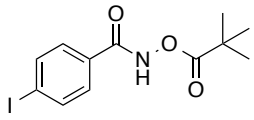

The final compound was isolated as a colourless crystalline solid (489 mg, 47%), by crystallisation from EtOAc–hexane, from 4-iodobenzoyl chloride (799 mg, 3.00 mmol) following general procedure B. M.p. 152-153 °C (EtOAc–hexane); δ_H (300 MHz, MeOD-d_4) NH peak missing, 7.78 (2H, d, *J* 8.6, H_2 and H_6), 7.46 (2H, d, *J* 8.6, H_3 and H_5), 1.24 (9H, s, $(CH_3)_3$); δ_C (75 MHz, MeOD-d_4) 177.5 ($COC(CH_3)_3$), 167.2 ($CONH$), 139.2 (C_3 and C_5), 132.3 (C_q), 130.1 (C_2 and C_6), 100.2 (C_4), 39.4 ($COC(CH_3)_3$), 27.5 ($COC(CH_3)_3$); HRMS (ESI^+): *m/z* calculated for formula $C_{12}H_{14}INNaO_3$ [MNa^+] 369.9911; found 369.9903; IR (ν_{max}, solid, cm^{-1}): 3140, 2971, 1781, 1648, 1584, 1475, 1007, 1004. Spectral data consistent with the literature.[36]

***tert*-Butyl (3-((pivaloyloxy)carbamoyl)phenyl) carbamate 180**

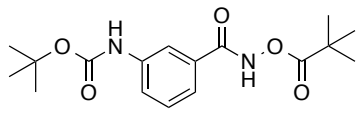

The desired compound was isolated as a colourless amorphous solid (628 mg, 62%), by flash column chromatography using 20% EtOAc in hexane, from 3-((*tert*-butoxycarbonyl)-amino)benzoic acid (1.01 g, 3.00 mmol) following general procedure B. δ_H (300 MHz, $CDCl_3$) 9.39 (1H, br s, NH), 7.85 (1H, s, H_2), 7.55 (1H, d, *J* 7.6, H_4), 7.48 (1H, d, *J* 7.6, H_6), 7.38 (1H, t, *J* 7.8, H_5), 6.58 (1H, s, NH), 1.52 (9H, s, $OC(CH_3)_3$), 1.36 (9H, s, $(CH_3)_3$); δ_C (75 MHz, $CDCl_3$) 177.1 ($CO_2{}^tBu$), 166.4 ($COC(CH_3)_3$), 152.9 ($CONH$), 139.0 (C_3), 131.7 (C_1), 129.5 (C_5), 122.6 (C_4), 122.0 (C_6), 117.4 (C_2), 81.1 ($OC(CH_3)_3$), 38.5 ($C(CH_3)_3$), 28.4 ($OC(CH_3)_3$), 27.1 ($C(CH_3)_3$); HRMS (ESI^+): *m/z* calculated for formula $C_{17}H_{24}N_2NaO_5$ [MNa^+] 359.1577; found 359.1571; IR (ν_{max}, solid, cm^{-1}): 3288, 2978, 1781, 1727, 1672, 1591, 1543, 1480, 1236, 1159, 1078.

***N*-(Pivaloyloxy)-[1,1'-biphenyl]-3-carboxamide 181**

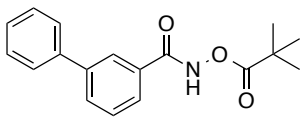

The desired compound was isolated as a colourless amorphous solid (223 mg, 38%), by flash column chromatography using 20% EtOAc in petrol, from 3-biphenylcarboxylic acid (490 mg, 2.00 mmol) following general procedure A. R_F 0.33 (20% EtOAc in petrol); δ_H (300 MHz, $CDCl_3$) 9.33 (1H, s, NH), 8.05 (1H, t, *J* 1.6, ArH), 7.82-7.76 (2H, m, ArH), 7.63-7.58 (2H, m, ArH), 7.55-7.35 (4H, m, ArH), 1.38 (9H, s, $(CH_3)_3$); δ_C (75 MHz, $CDCl_3$) 177.1 ($COC(CH_3)_3$), 166.8 ($CONH$), 142.0 (C_3), 139.8 (C_q), 131.5 (C_1), 131.4, 129.3, 129.0, 128.0, 127.2, 126.3, 126.1, 38.5 ($COC(CH_3)_3$), 27.1 ($COC(CH_3)_3$); HRMS (ESI^+): *m/z* calculated for formula: $C_{18}H_{20}NO_3$ [MH^+] 298.1438; found 298.1436; IR (ν_{max}, solid, cm^{-1}): 3038, 2975, 1786, 1652, 1514, 1077.

3-Bromo-*N*-(pivaloyloxy)benzamide 182

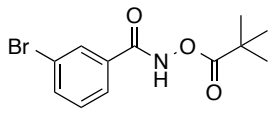

The desired compound was isolated as a colourless amorphous solid (850 mg, 57%) by flash column chromatography using 20% EtOAc in hexane, from 3-bromocarboxylic acid (1.01 g, 5.00 mmol) following general procedure A. R_F 0.13 (20% EtOAc in hexane); δ_H (300 MHz, $CDCl_3$) 9.27 (1H, s, NH), 7.96 (1H, t, *J* 1.6, H_2), 7.80-7.63 (2H, m, H_4 and H_6), 7.35 (1H, t, *J* 7.9, H_5), 1.36 (9H, s, $(CH_3)_3$); δ_C (75 MHz, $CDCl_3$) 176.7 (*C*OC$(CH_3)_3$), 165.1 (*C*ONH), 135.5 (C_4), 132.6 (C_1), 130.7 (C_5), 130.3 (C_2), 126.0 (C_6), 122.8 (C_3), 38.5 (CO*C*$(CH_3)_3$), 27.2 (COC(*C*$H_3)_3$); HRMS (ESI^+): *m/z* calculated for formula $C_{12}H_{14}{}^{79}BrNNaO_3$ [MNa^+] 322.0049; found 322.0053; IR (ν_{max}, solid, cm^1): 3251, 2816, 1784, 1660, 1301, 1068.

3-Chloro-*N*-(pivaloyloxy)benzamide 183

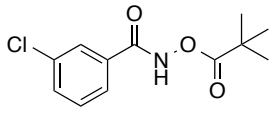

The desired compound was isolated as a colourless crystalline solid (1.09 g, 85%), by crystallisation from EtOAc–pentane, from 3-chlorobenzoyl chloride (640 μL, 5.00 mmol) following general procedure A. In this reaction *O*-pivaloylhydroxyamine triflic acid[35] (1.47 g, 5.50 mmol) was used instead of *O*-pivaloylhydroxyamine hydrochloric acid. R_F 0.6 (10% EtOAc in hexane); M.p. 89-92 °C (EtOAc–pentane); δ_H (300 MHz, $CDCl_3$) 9.73 (1H, s, NH), 7.75 (1H, t, *J* 1.7, H_2), 7.64 (1H, d, *J* 7.7, H_6), 7.48 (1H, ddd, *J* 8.0, 2.0, 1.0, H_4), 7.34 (1H, t, *J* 7.9, H_5), 1.32 (9H, s, $(CH_3)_3$); δ_C (75 MHz, $CDCl_3$) 177.0 (*C*OC$(CH_3)_3$), 165.4 (*C*ONH), 135.0 (C_1), 132.7 (C_3 and C_4), 130.2 (C_5), 127.9 (C_2), 125.6 (C_6), 38.6 (CO*C*$(CH_3)_3$), 27.1 (COC(*C*$H_3)_3$); HRMS (ESI^+): *m/z* calculated for formula $C_{12}H_{14}{}^{35}ClNNaO_3$ [MNa^+] 278.0554; found 278.0548; IR (ν_{max}, solid, cm^{-1}): 3190, 2971, 1782, 1660, 1569, 1516, 1476, 1465, 1302, 1270, 1229, 1154, 1068, 1027.

3-Fluoro-*N*-(pivaloyloxy)benzamide 184

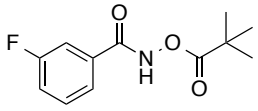

The desired compound was isolated as a colourless amorphous solid (474 mg, 66%) by flash column chromatography using 20% EtOAc in hexane, from 3-fluorobenzoic acid (420 mg, 3.00 mmol) following general procedure B. δ_H (300 MHz, $CDCl_3$) 9.30 (1H, s, NH), 7.61-7.56 (1H, m, H_6), 7.55-7.50 (1H, m, H_2), 7.47 (1H, td, *J* 8.0, 5.4, H_5), 7.31-7.29 (1H, m, H_4), 1.39 (9H, s, $(CH_3)_3$); δ_C (75 MHz, $CDCl_3$) 177.1 (*C*OC$(CH_3)_3$), 165.5 (*C*ONH), 162.8 (d, *J* 248.7, C_3), 133.1 (d, *J* 7.0, C_1), 130.7 (d, *J* 7.9, C_5), 123.1 (d, *J* 3.2, C_6), 119.9 (d, *J* 21.2, C_4), 115.0 (d, *J* 23.3, C_2), 38.6 (CO*C*$(CH_3)_3$), 27.3 (COC(*C*$H_3)_3$); HRMS (ESI^+): *m/z* calculated for formula $C_{12}H_{14}FNNaO_3$

[MNa^+] 262.0850; found 262.0847; IR (ν_{max}, solid, cm^{-1}): 3194, 2976, 1784, 1652, 1602, 1493, 1237, 1075.

3-Methoxy-N-(pivaloyloxy)benzamide 185

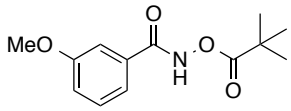

The desired compound was isolated as an amorphous solid (984 mg, 76%), by flash column chromatography using 20% EtOAc in hexane, from 3-methoxybenzoic acid (760 mg, 5.00 mmol) following general procedure A. δ_H (300 MHz, $CDCl_3$) 9.41 (1H, s, NH), 7.25 (3H, m, H_2, H_5 and H_6), 6.98 (1H, dt, *J* 9.8, 3.4, H_4), 3.74 (3H, s, OMe), 1.37 (9H, s, $(CH_3)_3$); δ_C (75 MHz, $CDCl_3$) 177.0 (*C*OC$(CH_3)_3$), 166.6 (*C*ONH), 159.8 (C_3), 132.1 (C_1), 129.8 (C_5), 119.3 (C_4 or C_6), 119.2 (C_4 or C_6), 112.3 (C_2), 55.5 (OMe), 38.5 (CO*C*$(CH_3)_3$), 27.0 (*C*OC$(CH_3)_3$); HRMS (ESI^+): *m/z* calculated for formula $C_{13}H_{17}NNaO_4$ [MNa^+] 274.1050; found 274.1055; IR (ν_{max}, solid, cm^{-1}): 3550, 3212, 2970, 1783, 1667, 1067.

***N*-(Pivaloyloxy)benzo[*d*][1,3]dioxole-5-carboxamide 186**

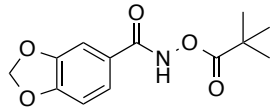

The desired compound was isolated as a colourless crystalline solid (663 mg, 83%), by crystallisation using EtOAc, from piperonylic acid (498 mg, 3.00 mmol) following general procedure A. M.p. 141-142 °C (EtOAc); δ_H (300 MHz, $CDCl_3$) 9.17 (1H, s, NH), 7.39 (1H, dd, *J* 8.1, 1.7, H_6), 7.29 (1H, d, *J* 1.7, H_4), 6.86 (1H, d, *J* 8.1, H_7), 6.05 (2H, s, OCH_2O), 1.36 (9H, s, $(CH_3)_3$); δ_C (75 MHz, $CDCl_3$) 177.2 (*C*OC$(CH_3)_3$), 166.4 (*C*ONH), 151.4 (OC_q), 148.1 (OC_q), 124.8 (C_1), 122.6 (C_6), 108.3 (C_4), 107.9 (C_7), 101.9 (OCH_2O), 38.5 (CO*C*$(CH_3)_3$), 27.0 (COC(*C*$H_3)_3$); HRMS (ESI^+): *m/z* calculated for formula $C_{13}H_{15}NNaO_5$ [MNa^+] 288.0842; found 288.0848; IR (ν_{max}, solid, cm^{-1}): 3215, 2971, 1771, 1645, 1479, 1263, 1094.

***N*-(Pivaloyloxy)-2,3-dihydrobenzo[*b*][1,4]dioxine-6-carboxamide 187**

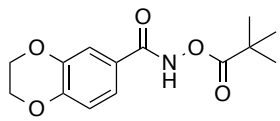

The desired compound was isolated as a colourless microcrystalline solid (565 mg, 73%) by flash column chromatography using 33% EtOAc in hexane, followed by crystallisation from hexane–EtOAc, from 2,3-dihydrobenzo[*b*][1,4]dioxine-6-carboxylic acid (500 mg, 2.77 mmol) following general procedure A. M.p. 126-129 °C (hexane–EtOAc); δ_H (300 MHz, $CDCl_3$) 9.29 (1H, br s, NH), 7.37-7.29 (2H, m, H_5 and H_7), 6.89 (1H, d, *J* 8.4, H_8), 4.34-4.21 (4H, m, $O(CH_2)_2O$), 1.35 (9H, s, $(CH_3)_3$); δ_C (75 MHz, $CDCl_3$) 177.2 (*C*OC$(CH_3)_3$), 166.3 (*C*ONH), 147.6 (OC_q), 143.6 (OC_q), 123.9 (C_1), 121.1 (C_7), 117.6 (C_5), 117.0 (C_8), 64.6 (O(*C*$H_2)_2$O), 64.1 (O(*C*$H_2)_2$O), 38.5 (CO*C*$(CH_3)_3$), 27.0 (COC(*C*$H_3)_3$); HRMS (ESI^+): *m/z* calculated for formula $C_{14}H_{17}NNaO_5$

[MNa^+] 302.0999; found 302.0998; IR (ν_{max}, solid, cm^{-1}): 3208, 2976, 1777, 1645, 1488, 1288, 1062.

Heterocyclic pivalate esters

***N*-(Pivaloyloxy)thiophene-2-carboxamide 196**

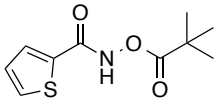

The desired compound was isolated as a colourless amorphous solid (455 mg, 40%) by flash column chromatography using 10% EtOAc in hexane, from 2-thiophene carboxylic acid (641 mg, 5.00 mmol) following general procedure A. R_F 0.22 (10% EtOAc in hexane); δ_H (300 MHz, $CDCl_3$) 9.18 (1H, s, NH), 7.67 (1H, dd, *J* 3.8, 1.2, H_3), 7.59 (1H, dd, *J* 5.0, 1.2, H_5); 7.13 (1H, dd, *J* 5.0, 3.8, H_4), 1.38 (9H, s, $(CH_3)_3$); δ_C (75 MHz, $CDCl_3$) 177.1 ($COC(CH_3)_3$), 161.9 ($CONH$), 133.6 (C_2), 131.7 (C_3), 130.5 (C_5), 127.9 (C_4), 38.5 ($COC(CH_3)_3$), 27.0 ($COC(CH_3)_3$); HRMS (ESI^+): *m/z* calculated for formula: $C_{10}H_{13}NNaO_3S$ [MNa^+] 250.0508; found 250.0502; IR (ν_{max}, solid, cm^{-1}): 3208, 2938, 1784, 1625, 1478, 1245, 1070.

***N*-(Pivaloyloxy)benzo[*b*]thiophene-2-carboxamide 197**

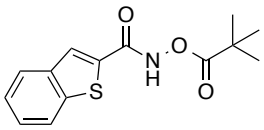

The desired compound was isolated as a colourless amorphous solid (356 mg, 25%) by flash column chromatography using 30-50% EtOAc in hexane, from benzothiophene-2-carboxylic acid (891 mg, 5.00 mmol) following general procedure A. R_F 0.41 (50% EtOAc in hexane); δ_H (300 MHz, $CDCl_3$) 9.33 (1H, br s, NH), 7.93 (1H, s, H_3), 7.90-7.87 (2H, m, H_4 and H_7), 7.51-7.40 (2H, m, H_5 and H_6), 1.38 (9H, s, $(CH_3)_3$); δ_C (75 MHz, $CDCl_3$) 177.0 ($COC(CH_3)_3$), 162.0 ($CONH$), 138.6 (C_qS), 133.2 (C_qS), 127.6 (C_6), 127.0 (C_5), 125.5 (C_4), 125.1 (C_7), 122.7 (C_3), 38.5 ($COC(CH_3)_3$), 27.0 ($COC(CH_3)_3$), one quaternary peak missing; HRMS (ESI^+): *m/z* calculated for formula $C_{14}H_{15}NNaO_3S$ [MNa^+] 300.0665; found 300.0654; IR (ν_{max}, solid, cm^{-1}): 3170, 2970, 1781, 1632, 1528, 1064.

***N*-(Pivaloyloxy)benzofuran-2-carboxamide 199**

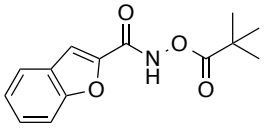

The desired compound was isolated as a colourless crystalline solid (258 mg, 49%) by crystallisation from EtOAc, from benzo[*b*]furan-2-carboxylic acid (416 mg, 2.00 mmol) following general procedure A. M.p. 111-115 °C (EtOAc); δ_H (300 MHz, $CDCl_3$) missing NH peak, 7.70 (1H, d, *J* 7.8, H_4), 7.59 (1H, s, H_3), 7.53 (1H, d, *J* 8.2, H_7), 7.50-7.43 (1H, m, H_6), 7.32 (1H, t, *J* 7.4, H_5), 1.38 (9H, s, $(CH_3)_3$); δ_C (75 MHz, $CDCl_3$) 176.6 ($COC(CH_3)_3$), 157.2 ($CONH$), 155.2 (C_qO), 146.2 (C_qO), 127.8 (C_6), 127.1 (C_q), 124.2 (C_5), 123.0 (C_4), 112.8 (C_7), 112.1 (C_3), 38.6 ($COC(CH_3)_3$), 27.2

($COC(CH_3)_3$); HRMS (ESI^+): *m/z* calculated for formula: $C_{14}H_{15}NNaO_4$ [MNa^+] 284.0893; found 284.0889; IR (ν_{max}, solid, cm^{-1}): 3128, 2971, 1787, 1653, 1072.

1-Methyl-*N*-(pivaloyloxy)-*1H*-indole-2-carboxamide 200

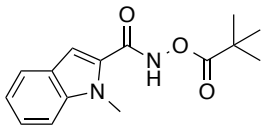

The desired compound was isolated as a colourless amorphous solid (392 mg, 35%) by flash column chromatography using 0-5% EtOAc in hexane, from 1-methyl-*1H*-indole-2-carboxylic acid (718 mg, 4.10 mmol) following general procedure B. R_F 0.28 (20% EtOAc in hexane); δ_H (300 MHz, $CDCl_3$) 9.27 (1H, s, NH), 7.67 (1H, d, *J* 8.0, H_4), 7.44-7.36 (2H, m, H_5 and H_7), 7.18 (1H, ddd, *J* 7.9, 6.3, 1.5, H_6), 7.08 (1H, s, H_3), 4.04 (3H, s, NMe), 1.39 (9H, s, $(CH_3)_3$); δ_C (75 MHz, $CDCl_3$) 177.2 ($COC(CH_3)_3$), 162.0 (*C*ONH), 139.4 (C_1), 127.2 (C_q), 125.9 (C_q), 125.0 (C_6), 122.3 (C_4), 120.8 (C_5), 110.2 (C_3), 106.1 (C_7), 38.5 ($COC(CH_3)_3$), 31.4 (NMe), 27.1 ($COC(CH_3)_3$); HRMS (ESI^+): *m/z* calculated for formula $C_{15}H_{18}N_2NaO_3$ [MNa^+] 297.1210; found 297.1211; IR (ν_{max}, solid, cm^{-1}): 3179, 2973, 1783, 1660, 1520, 1464, 1267, 1114, 1073, 1028.

***N*-(Pivaloyloxy)isoquinoline-3-carboxamide 203**

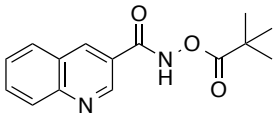

The desired compound was isolated as a colourless crystalline solid (365 mg, 45%), by crystallisation from DCM, from quinoline-3-carboxylic acid (520 mg, 3.00 mmol) following general procedure B. M.p. 154-156 °C (DCM); δ_H (300 MHz, $CDCl_3$) 10.24 (1H, br s, NH), 9.24 (1H, d, *J* 2.0, H_2), 8.62 (1H, d, *J* 1.8, H_4), 8.09 (1H, d, *J* 8.5, H_5), 7.82 (1H, t, *J* 7.1, H_7), 7.78 (1H, d, *J* 7.1, H_8), 7.59 (1H, app t, *J* 7.3, H_6), 1.36 (9H, s, $(CH_3)_3$); δ_C (75 MHz, $CDCl_3$) 176.9 ($COC(CH_3)_3$), 164.9 (*C*ONH), 149.4 (NC_q), 147.8 (C_2), 136.8 (C_4), 131.9 (C_7), 129.2 (C_5), 128.9 (C_8), 127.8 (C_6), 126.7 (C_q), 124.0 (C_q), 38.5 ($COC(CH_3)_3$), 27.0 ($COC(CH_3)_3$); HRMS (ESI^+): *m/z* calculated for formula $C_{15}H_{16}N_2O_3$ [MH^+] 273.1234; found 273.1230; IR (ν_{max}, solid, cm^{-1}): 3096, 1765, 1695, 1523, 1291, 1079.

6.5 Preparation of isoquinolone derivatives

General Procedure (C) for the synthesis of isoquinolones

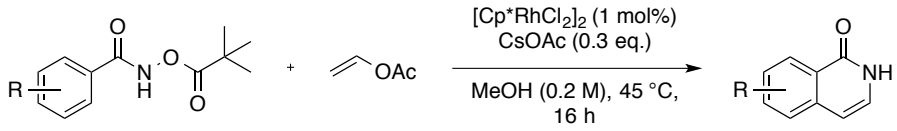

Vinyl acetate (138 μL, 1.50 mmol) was added to a solution of $[Cp^*RhCl_2]_2$ (0.01 eq.), CsOAc (0.3 eq) and the *N*-(pivaloyloxy)benzamide derivative (1 eq.) in MeOH (0.2 M) in a vial under a nitrogen atmosphere. The reaction was heated to 45 °C for 16 hours, after which time the solvent was removed *in vacuo* and the crude material was purified by recrystallisation or flash silica chromatography.

Isoquinolin-1*(2H)*-one 168

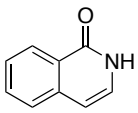

The product was triturated with a 2:1 mixture of Et_2O–MeOH (5 mL) and crystallised from MeOH. The desired compound was isolated as a colourless solid (126 mg, 87%) from *N*-(pivaloyloxy)benzamide (221 mg, 1.00 mmol) following general procedure C. δ_H (500 MHz, DMSO-d_6) 11.25 (1H, br s, NH), 8.19 (1H, d, *J* 9.0, H_8), 7.69-7.66 (2H, m, H_6 and H_5), 7.65-7.47 (1H, m, H_7), 7.19 (1H, d, *J* 9.0, H_3), 6.54 (1H, d, *J* 9.0, H_4); δ_C (75 MHz, DMSO-d_6) 161.8 (C_1), 137.8 (C_q), 132.3 (C_6), 128.9 (C_3), 126.6 (C_8), 126.3 (C_5 or C_7), 126.2 (C_5 or C_7), 126.0 (C_q), 104.6 (C_4); HRMS (ESI^+): *m/z* calculated for formula C_9H_8NO [MH^+]: 146.0600; found 146.0606; IR (ν_{max}, solid, cm^{-1}): 3286, 3158, 2852, 1633, 1548, 1475, 1343, 1228. Spectral data consistent with the literature.[35]

6-Cyanoisoquinolin-1(*2H*)-one 169

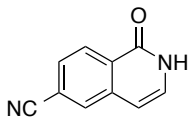

The product was triturated with a 2:1 mixture of Et_2O–MeOH (5 mL) and crystallised from MeOH. The desired compound was isolated as a pale yellow solid (68 mg, 81%) from 4-cyano-*N*-(pivaloyloxy)benzamide (120 mg, 0.49 mmol) following general procedure C. M.p. 307-312 °C (MeOH); δ_H (300 MHz, DMSO-d_6) 11.62 (1H, s, NH), 8.28 (1H, d, *J* 8.4, H_8), 8.25 (1H, s, H_5), 7.81 (1H, dd, *J* 8.3, 1.4, H_7), 7.35-7.29 (1H, m, H_3), 6.62 (1H, d, *J* 7.1, H_4); δ_C (75 MHz, DMSO-d_6) 160.9 (C_1), 137.9 (C_q), 131.3 (C_3), 131.0 (C_5), 128.4 (C_q), 128.0 (C_7), 127.9 (C_8), 118.3 (CN), 114.6 (C_6), 103.6 (C_4); HRMS (ESI^+): *m/z* calculated for formula $C_{10}H_7N_2O$ [MH^+] 171.0553; found 171.0575; IR (ν_{max}, solid, cm^{-1}): 3307, 2227, 1652, 1539, 1498, 1460, 1337, 1235.

6-Acetylisoquinolin-1(*2H*)-one 170

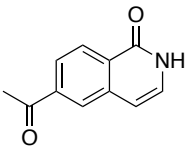

The product was filtered from the crude reaction mixture and washed with MeOH–Et_2O (1:4) (5 mL). The desired compound was isolated as a tan amorphous solid (48 mg, 99%) from 4-acetyl-*N*-(pivaloyloxy)-benzamide (68 mg, 0.25 mmol) following general procedure C. δ_H (300 MHz, DMSO-d_6) 11.79 (1H, s, NH), 8.28 (1H, d, *J* 1.2, H_5), 8.26 (1H, d, *J* 8.3, H_8), 7.93 (1H, dd, *J* 8.3, 1.2, H_7), 7.29 (1H, d, *J* 7.1, H_3), 6.68 (1H, d, *J* 7.1, H_4), 2.67 (3H, s, $COCH_3$); δ_C (75 MHz, DMSO-d_6) 198.0 ($COCH_3$), 161.4 (C_1), 139.3 (C_q), 138.0 (C_q), 130.1 (C_3), 128.6 (C_q), 127.2 (C_7), 127.1 (C_5), 124.5 (C_8), 104.8 (C_4), 27.0 ($COCH_3$); HRMS (ESI^+): *m/z* calculated for formula $C_{11}H_{10}NO_2$ [MH^+] 188.0706; found 188.0699; IR (ν_{max}, solid, cm^{-1}): 3299, 2911, 1751, 1692, 1542, 1461, 1347, 1267, 1186.

6-(Trifluoromethyl)isoquinolin-1(*2H*)-one 171

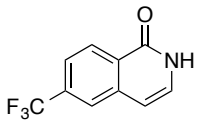

The product was triturated with a 2:1 mixture of Et_2O–MeOH (5 mL) and crystallised from $CHCl_3$. The desired compound was isolated as a pale yellow crystalline solid (151 mg, 71%) from 4-trifluoromethyl-*N*-(pivaloyloxy)benzamide (289 mg, 1.00 mmol) following general procedure C. R_F 0.2 (50% EtOAc in hexane); M.p. 176-181 °C ($CHCl_3$); δ_H (300 MHz, $CDCl_3$) 11.6 (1H, br s, NH), 8.53 (1H, d, *J* 8.4, H_8), 7.86 (1H, s, H_5), 7.71 (1H, dd, *J* 8.4, 1.4, H_7), 7.29 (1H, d, *J* 7.1, H_3), 6.65 (1H, d, *J* 7.1, H_4); δ_C (75 MHz, $CDCl_3$) 163.7 (C_1), 138.2 (C_q), 134.5 (q, *J* 32.4, C_6), 129.3 (C_3), 128.6 (C_8), 128.3 (C_q) 123.8 (q, *J* 272.9, CF_3), 123.8 (q, *J* 3.9, C_5), 123.0 (q, *J* 3.2, C_7), 106.6 (C_4); HRMS (ESI^+): *m/z* calculated for formula $C_{10}H_7F_3NO$ [MH^+] 214.0474; found 214.0475; IR (ν_{max}, solid, cm^{-1}): 3299, 2911, 1751, 1692, 1542, 1461, 1347, 1267, 1186.

6-Methoxyisoquinolin-1(*2H*)-one 172

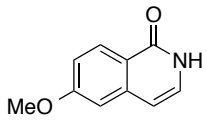

Vinyl acetate (138 μL, 1.50 mmol) was added to a solution of $[Cp^*RhCl_2]_2$ (6 mg, 0.01 mmol), CsOAc (58 mg, 0.3 mmol) and 4-methoxy-*N*-(pivaloyloxy)benzamide (251 mg, 1.00 mmol) in MeOH (2.5 mL, **0.4 M**) in a vial under a nitrogen atmosphere. The reaction was heated to **30 °C** for 16 hours, after which time the solvent was removed *in vacuo*. The product was isolated by flash column chromatography using a solvent gradient of 50% EtOAc in hexane followed by a solvent swap to 5% MeOH in DCM. The product was crystallised from EtOAc to afford colourless crystalline needles (110 mg, 63%). M.p. 179-181 °C (EtOAc); δ_H (300 MHz, $CDCl_3$) 11.12 (1H, br s, NH), 8.33 (1H, d, *J* 8.9, H_8), 7.15 (1H, d, *J* 7.1, H_3), 7.08 (1H, dd, *J* 8.9, 2.5, H_7), 6.91 (1H, d, *J* 2.5, H_5), 6.48 (1H, d, *J* 7.2, H_4), 3.92 (3H, s, OMe); δ_C (75 MHz, $CDCl_3$) 163.9 (C_qO),

163.0 (C_qO), 140.3 (C_q), 129.3 (C_8), 128.3 (C_3), 116.5 (C_7), 107.0 (C_5), 106.4 (C_4), 55.5 (OMe), missing a quaternary carbon; HRMS (ESI$^+$): *m/z* calculated for formula $C_{10}H_9NNaO_2$ [MNa$^+$] 198.0525; found 198.0529; IR (ν_{max}, solid, cm^{-1}): 3162, 1605, 1468, 1231.

6-Fluoroisoquinolin-1(*2H*)-one 173

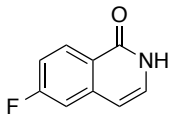

The product was triturated with a 4:1 mixture of Et_2O–MeOH (5 mL) and crystallised from acetone. The desired compound was isolated as pale yellow crystalline needles (40 mg, 71%) from 4-fluoro-*N*-(pivaloyloxy)-benzamide (239 mg, 1.00 mmol) following general procedure C. M.p. 207-210 °C (acetone); δ_H (300 MHz, DMSO-*d*$_6$) 11.34 (1H, br s, NH), 8.22 (1H, dd, *J* 8.8, 6.1, H_8), 7.49 (1H, dd, *J* 10.1, 2.5, H_5), 7.32-7.27 (1H, m, H_7), 7.23 (1H, d, *J* 7.1, H_3), 6.54 (1H, d, *J* 7.2, H_4); δ_C (75 MHz, DMSO-*d*$_6$) 164.3 (d, *J* 249.2, C_6), 161.2 (C_1), 140.3 (d, *J* 10.8, C_q), 130.5 (C_3), 130.1 (d, *J* 10.3, C_8), 122.9 (d, *J* 1.5, C_q), 114.7 (d, *J* 23.7, H_7), 110.9 (d, *J* 21.9, H_5), 104.1 (d, *J* 3.1, H_4); HRMS (ESI$^+$): *m/z* calculated for formula C_9H_6FNNaO [MNa$^+$] 186.0326; found 186.0323; IR (ν_{max}, solid, cm^{-1}): 3392, 2968, 1669, 1551, 1408, 1015. Spectral data consistent with the literature.[99]

6-Bromoisoquinolin-1*(2H)*-one 174

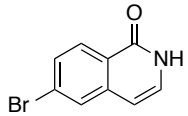

The product was isolated by flash column chromatography using 50% EtOAc in hexane. The desired compound was isolated as a colourless solid (186 mg, 70%) from 4-bromo-*N*-(pivaloyloxy) benzamide (300 mg, 1.00 mmol) following general procedure C. R_F 0.4 (50% EtOAc in hexane). δ_H (300 MHz, DMSO-*d*$_6$) 11.36 (1H, br s, NH), 8.07 (1H, d, *J* 8.5, H_8), 7.94 (1H, s, H_5), 7.61 (1H, dd, *J* 8.5, 1.4, H_7), 7.28-7.18 (1H, m, H_3), 6.52 (1H, d, *J* 7.1, H_4); δ_C (75 MHz, $CDCl_3$) 161.4 (C_1), 139.6 (C_q), 130.5 (C_7), 129.2 (C_5), 129.0 (C_8), 128.4 (C_3), 126.3 (C_6), 124.9 (C_q), 103.6 (C_4); HRMS (ESI$^+$): *m/z* calculated for formula $C_9H_6{}^{79}BrNNaO$ [MNa$^+$] 245.9525; found 247.9505; IR (ν_{max}, solid, cm^{-1}): 2735, 1665, 1632, 1239. Spectral data consistent with the literature.[246]

6-Iodoisoquinolin-1(*2H*)-one 175

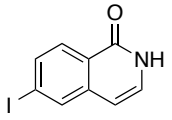

The product was triturated with a 2:1 mixture of Et_2O–MeOH (5 mL) and crystallised from MeOH. The desired compound was isolated as a cream amorphous solid (211 mg, 83%) from 4-iodo-*N*-(pivaloyloxy)-benzamide (347 mg, 1.00 mmol) following general procedure C. M.p. decomposed at 231 °C (MeOH); δ_H (300 MHz, DMSO-*d*$_6$) 11.35 (1H, br s, NH), 8.12 (1H, s, H_5), 7.90 (1H, d, *J* 8.4, H_8), 7.78 (1H, d, *J* 8.2, H_7), 7.20-7.18 (1H, m, H_3), 6.49 (1H, d, *J* 7.1, H_4); δ_C (75 MHz, DMSO-*d*$_6$) 161.6 (C_1), 139.5 (C_q), 134.8 (C_7), 134.5 (C_5), 130.2 (C_8), 128.5 (C_3), 125.1 (C_q), 103.3 (C_4), 100.7 (C_6);

HRMS (ESI$^+$): *m/z* calculated for formula C_9H_7INO [MH^+] 271.9567; found 271.9571; IR (ν_{max}, solid, cm^{-1}): 3012, 2851, 1659, 1633, 1587, 1494, 1237.

tert-Butyl (1-oxo-1,2dihydroisoquinolin-7-yl) carbamate 188a

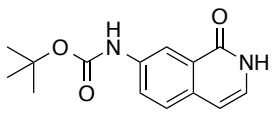

The product was purified by trituration with a 4:1 mixture of pentane–ethanol (5 mL) to afford a colourless amorphous solid (81 mg, 81%) from *tert*-butyl (3-((pivaloyloxy)carbamoyl)phenyl) carbamate (260 mg, 1.00 mmol) following general procedure C. δ_H (300 MHz, DMSO-d_6) 11.10 (1H, br s, NH), 9.61 (1H, s, NH), 8.37 (1H, d, *J* 1.7, H_8), 7.70 (1H, dd, *J* 8.6, 2.2, H_6), 7.54 (1H, d, *J* 8.6, H_5), 7.08-6.97 (1H, m, H_3), 6.45 (1H, d, *J* 7.0, H_4), 1.50 (9H, s, $O(CH_3)_3$); δ_C (75 MHz, DMSO-d_6) 161.6 ($CO_2C(CH_3)_3$), 152.7 (C_1), 137.9 (C_q), 132.6 (C_q), 126.8 (C_3), 126.7 (C_5), 126.6 (C_q), 123.5 (C_6), 114.2 (C_8), 104.4 (C_4), 79.3 ($CO_2C(CH_3)_3$), 28.1 ($CO_2C(CH_3)_3$); HRMS (ESI$^+$): *m/z* calculated for formula $C_{14}H_{16}N_2NaO_3$ [MNa^+] 283.1053; found 283.1054; IR (ν_{max}, solid, cm^{-1}): 3355, 2993, 2980, 2932, 2834, 1694, 1663, 1564, 1522, 1250, 1167.

7-Phenylisoquinolin-1(*2H*)-one 189a

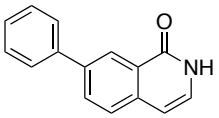

The product was triturated with a 2:1 mixture of Et_2O–MeOH (5 mL) and crystallised from EtOAc–hexane to afford pale yellow crystals (101 mg, 91%) from *N*-(pivaloyloxy)(1,1'-biphenyl)-3-carboxamide (150 mg, 0.50 mmol) following general procedure C. m.p. 223-226 °C (EtOAc–hexane); δ_H (300 MHz, $CDCl_3$) 10.29 (1H, s, NH), 8.66 (1H, d, *J* 2.0, H_8), 7.95 (1H, dd, *J* 8.3, 2.0, H_6), 7.72 (2H, d, *J* 7.1, $H_{2'}$), 7.65 (1H, d, *J* 8.3, H_5), 7.48-7.46 (3H, m, $H_{3'}$ and $H_{4'}$), 7.11 (1H, d, *J 7.4*, H_3), 6.62 (1H, d, *J* 7.4, H_4); δ_C (75 MHz, $CDCl_3$) 164.0 (C_1), 140.0 (C_q), 139.9 (C_q), 137.2 (C_q), 131.8 (C_6), 129.1 ($2C_{3'}$), 127.9 (C_3), 127.5 (C_8 or $C_{4'}$), 127.4 ($2C_{2'}$), 127.0 (C_8 or $C_{4'}$), 126.7 (C_q), 125.5 (C_5), 106.6 (C_4); HRMS (ESI$^+$): *m/z* calculated for formula $C_{15}H_{11}NNaO$ [MNa^+] 244.0733; found 244.0724; IR (ν_{max}, solid, cm^{-1}): 3159, 2907, 1654, 1449, 1223.

7-Bromoisoquinolin-1(*2H*)-one 190a

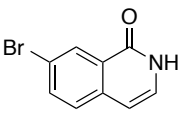

A mixture of regioisomers were isolated from 3-bromo-*N*-(pivaloyloxy)benzamide (300 mg, 1.00 mmol) following general procedure C. The products were isolated as an inseparable mixture of 7- and 5-bromoisoquinolin-1(*2H*)-one, as a yellow amorphous solid, (9:1, 215 mg, 95%) following purification by flash column chromatography using 30% EtOAc in hexane as an eluent. δ_H (500 MHz, DMSO-d_6) δ 11.42 (1H, s, NH), 8.25 (1H, d, *J* 2.1, H_8), 7.84 (1H, dd, *J* 8.5, 2.2, H_6), 7.64 (1H, d, *J* 8.5, H_5), 7.22 (1H, dd, *J* 6.8, 5.7, H_3), 6.56 (1H, d, *J* 7.1, H_4); δ_C (125 MHz, DMSO-d_6)

161.4 (C_1), 139.6 (C_q), 130.7 (C_6), 129.2 (C_3), 129.0 (C_8), 128.4 (C_5), 126.4 (C_q), 124.9 (C_q), 103.6 (C_4); HRMS (ESI^+): *m/z* calculated for formula $C_9H_7{}^{79}BrNO$ [MH^+] 223.9706; found 223.9703; IR (ν_{max}, solid, cm^{-1}): 3152, 3002, 2923, 1660, 1223. Spectral data consistent with literature values.[247]

7-Chloroisoquinolin-1(2*H*)-one 191a

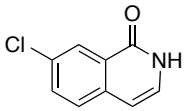

The precipitate was filtered from the reaction and washed with a solution of pentane–MeOH (5 mL, 4:1). The cream amorphous solid was recrystallised from isopropanol to afford a colourless crystalline solid (119 mg, 66%), from 3-chloro-*N*-(pivaloyloxy)benzamide (256 mg, 1.00 mmol) following general procedure C. The regioisomeric ratio of 7-chloroisoquinolin-1-(2*H*)-one compared with 5-chloroisoquinolin-1-(2*H*)-one varied during the purification: crude reaction (4:1, 7-:5-), upon filtration (4:1, 7-:5-) and after crystallisation (98:2, 7-:5-). M.p. decomposed at 190 °C (isopropanol); δ_H (300 MHz, DMSO-d_6) 11.42 (1H, s, NH), 8.11 (1H, d, *J* 0.9, H_7), 7.76-7.68 (2H, m, H_5 and H_6), 7.21 (1H, d, *J* 7.1, H_3), 6.58 (1H, d, *J* 7.2, H_4); δ_C (75 MHz, DMSO-d_6) 160.8 (C_1), 136.6 (C_q), 132.5 (C_6), 130.8 (C_q), 129.5 (C_3), 128.6 (C_5), 127.2 (C_7), 125.7 (C_8), 104.1 (C_4); HRMS (ESI^+): *m/z* calculated for formula $C_9H_7{}^{35}ClNO$ [MH^+] 180.0211; found 180.0208; IR (ν_{max}, solid, cm^{-1}): 2998, 2914, 2855, 2704, 1659, 1632, 1602, 1541, 1493, 1472, 1430, 1344, 1298, 1233, 1152, 1103, 1087, 1060.

5-Chloroisoquinolin-1-(2*H*)-one 191b

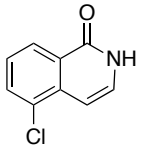

For reference from signals visible in the ^1H NMR: δ_H (300 MHz, DMSO-d_6) 11.42 (1H, s, NH), 8.17 (1H, d, *J* 7.0, H_8), 7.84 (1H, dd, *J* 7.8, 1.1, H_6), 7.47 (1H, t, *J* 8.2, H_7), 7.33 (1H, d, *J* 7.4, H_3), 6.69 (1H, d, *J* 7.4, H_4).

7-Fluoroisoquinolin-1(*2H*)-one 192a and 5-fluoroisoquinolin-1(*2H*)-one 192b

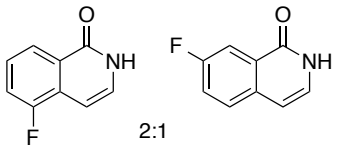

The products were isolated by trituration with a 9:1 mixture of pentane–ethanol (5 mL), the material was then recrystallised from acetone. The desired compounds were isolated, as an inseparable mixture of regioisomers, as a colourless crystalline powder (170 mg, 71%, 2:1, 5-:7) from 3-fluoro-*N*-(pivaloyloxy)benzamide (588 mg, 1.50 mmol) following general procedure C. δ_H (300 MHz, acetone-d_6) 10.35 (1H, br s, NH *major and minor*), 8.12-8.07 (0.66H, m, ArH *major*), 7.90 (0.33H, dd, *J* 9.6, 2.6, H_8 *minor*), 7.74 (0.33H, dd, *J* 8.8, 5.2, H_6 *minor*), 7.55 (0.33H, peak obscured, H_5 *minor*), 7.49 (1.32H, dd, *J* 8.4, 3.7, ArH *major*), 7.33 (0.66H, d, *J* 7.3, H_3 *major*), 7.23 (0.33H, d, *J* 7.4, H_3 *minor*), 6.63 (0.66H, d, *J*, H_4 *major*), 6.58 (0.33H, d, *J* 7.4, H_4 *minor*). ^1H NMR consistent with the literature.[10] δ_H (300 MHz, DMSO-d_6) major signals

only 11.49 (1H, s, NH), 8.01 (1H, d, *J* 7.9, H_8), 7.62-7.53 (1H, m, H_6), 7.48 (1H, td, *J* 8.0, 5.5, H_7), 7.33-7.23 (1H, m, H_3), 6.58 (1H, d, *J* 7.2, H_4); δ_C (75 MHz, DMSO-d_6) 160.7 (d, *J* 2.9, C_q-O), 156.9 (d, *J* 248.6, C-F), 130.1 (C_3), 127.8 (d, *J* 4.0, C_q), 126.9 (C_q), 126.7 (d, *J* 7.9, C_7), 122.7 (d, *J* 3.6, C_8), 117.2 (d, *J* 19.6, C_6), 96.4 (d, *J* 5.7, C_4). HRMS (ESI^+): *m/z* calculated for formula C_9H_6FNNaO [MNa^+] 186.0326; found 186.0318; IR (ν_{max}, solid, cm^{-1}): 3162, 2999, 2861, 1633, 1549, 1480, 1352, 1247.

7-Methoxyisoquinolin-1(*2H*)-one 193a and 5-methoxyisoquinolin-1(*2H*)-one 193b

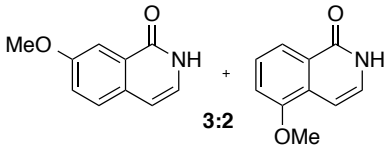

The products were isolated by flash column chromatography using 1% MeOH in EtOAc to afford an amorphous off-white solid containing an inseparable 3:2 mixture of 7-methoxyisoquinolin-1(*2H*)-one **193a** and 5-methoxyisoquinolin-1(*2H*)-one **193b** (172 mg, 98%) from 3-methoxy-*N*-(pivaloyloxy)benzamide (251 mg, 1.00 mmol) following general procedure C. ^{13}C spectral values consistent with the literature[100] in $CDCl_3$ however data reported below for spectra measured in MeOD-d_4, which gave better signal separation. δ_H (500 MHz, MeOD-d_4) missing NH peak, 7.86 (0.4H, d, *J* 8.1, H_6 *minor*), 7.74 (0.6, d, *J* 2.6, H_8 - *major*), 7.59 (0.6H, d, *J* 8.7, H_5 *major*), 7.46 (0.4H, t, *J* 8.1, H_7 *minor*), 7.34 (0.6H, dd, *J* 8.7, 2.7, H_6 *major*), 7.23 (0.4H, d, *J* 8.3, H_8 *minor*), 7.15 (0.4H, d, *J* 7.2, H_3 *minor*), 7.07 (0.6H, d, *J* 7.1, H_3 *major*), 6.96 (0.4H, d, *J* 7.3, H_4 *minor*), 3.97 (1.2H, s, OMe *minor*), 3.91 (1.8H, s, 3H, OMe *major*); δ_C (75 MHz, MeOD-d_4) 164.8 (C_q), 160.3 (C_q), 156.1 (C_q), 134.0 (C_q), 130.8 (C_q), 129.2 (C_5 *major*), 128.3 (C_7 *minor*), 128.2 (C_q), 128.0 (C_3 *minor*), 126.4 (C_3 *major*), 124.3 (C_6 *major*), 119.4 (C_6 *minor*), 113.1 (C_8 *minor*), 107.9 (C_4 *major* and C_8 *major*), 102.2 (C_4 *minor*), 56.4 (OMe), 56.0 (OMe). IR (ν_{max}, solid, cm^{-1}): 2828, 1653, 1258, 1057; HRMS (ESI^+): *m/z* calculated for formula $C_{10}H_{10}NO_2$ [MH^+] 176.0706; found 176.0711.

[1,3]-Dioxolo[4,5-*f*]isoquinolin-6(*7H*)-one 194b

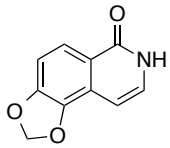

The product was filtered from the cooled reaction mixture and subsequently washed with a 3:7 mixture of MeOH–Et_2O (5 mL). The desired compound was isolated as a cream amorphous solid (101 mg, 53%) from *N*-(pivaloyloxy)benzo[*d*][1,3]dioxole-5-carboxamide (265 mg, 1.00 mmol) following general procedure C. δ_H (300 MHz, $CDCl_3$) 11.04 (1H, s, NH), 7.79 (1H, d, *J* 8.5, H_5), 7.19-7.07 (2H, m, H_4 and H_8), 6.34 (1H, d, *J* 7.2, H_9), 6.22 (2H, s, OCH_2O); δ_C (75 MHz, $CDCl_3$) 161.0 (C_6), 149.1 (C_qO), 140.9 (C_qO), 129.7 (C_8), 121.0 (C_5), 121.6 (C_q), 121.1 (C_q), 108.2 (C_4), 102.3 ($O(CH_2)_2O$), 96.9 (C_9); HRMS ($ESI^{+)}$: *m/z* calculated for formula $C_{10}H_8NO_3$ [MH^+] 190.0499 and $C_{10}H_7NNaO_3$ [MNa^+] 212.0318; found 190.0507 and 212.0315; IR (ν_{max}, solid, cm^{-1}): 3282, 2844, 1688, 1663, 1633, 1442, 1270, 1236, 1048, 944.

2,3-Dihydro-[1,4]dioxino[2,3-f]isoquinolin-7(*8H*)-one 195b

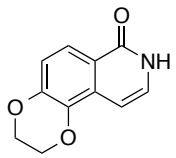

The product was triturated with a 9:1 mixture of pentane–ethanol (5 mL), then crystallised from EtOH. The desired compound was isolated as a tan microcrystalline powder (97 mg, 48%) from *N*-(pivaloyloxy)-2,3-dihydrobenzo[*b*][*1,4*]dioxine-6-carboxamide (279 mg, 1.00 mmol) following general procedure C. M.p. decomposed at 225 °C (EtOH); ^{1}H NMR (300 MHz, DMSO-d_6) δ 11.08 (1H, br s, NH), 7.67 (1H, d, *J* 8.8, H_6), 7.12 (1H, dd, *J* 7.0, 5.6, H_9), 6.99 (1H, d, *J* 8.8, H_5), 6.54 (1H, d, *J* 7.3, H_{10}), 4.42-4.31 (4H, m, O(CH_2)$_2$O); δ_C (75 MHz, DMSO-d_6) 161.2 (C_7), 145.0 (C_qO), 136.5 (C_qO), 129.0 (C_9), 128.9 (C_q), 120.2 (C_q), 119.7 (C_6), 116.5 (C_5), 97.6 (C_{10}), 64.2 (CH_2), 64.1(CH_2); HRMS (ESI$^+$): *m/z* calculated for formula $C_{11}H_{10}NO_3$[MH$^+$] 204.0655; found 204.0649; IR (ν_{max}, solid, cm^{-1}): 3259, 2980, 1655, 1603, 1462, 1286, 1088.

Heterocyclic Pyridones

Thieno[2,3-*c*]pyridin-7(*6H*)-one 204

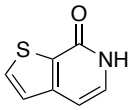

The product was purified by flash column chromatography using a solvent gradient of 10-100% EtOAc in hexane. The desired compound was isolated as a colourless solid (74 mg, 49%) from *N*-(pivaloyloxy)thiophene-2-carboxamide (227 mg, 1.00 mmol) following general procedure C. A sample was taken and crystallised from $CDCl_3$. M.p. 186-189 °C ($CDCl_3$, [lit. value 195 °C][248]); δ_H (300 MHz, $CDCl_3$) 12.68 (1H, s, NH), 7.69 (1H, d, *J* 5.2, H_2), 7.29 (1H, d, *J* 6.9, H_5), 7.21 (1H, d, *J* 5.2, H_3), 6.70 (1H, d, *J* 6.9, H_4); δ_C (75 MHz, $CDCl_3$) 161.4 (C_7), 146.9 (C_q), 133.6 (C_2), 129.5 (C_q), 129.4 (C_5), 124.6 (C_3), 104.0 (C_4); HRMS (ESI^+): *m/z* calculated for formula C_7H_5NNaOS [MNa^+] 173.9984; found 174.0008; IR (ν_{max}, solid, cm^{-1}): 3100, 1627, 1526, 1480.

Benzo[4,5]thieno[2,3-*c*]pyridine-1*(2H)*-one 205

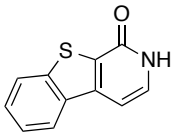

The product was isolated by trituration with MeOH (0.5 mL). The desired compound was isolated as a colourless amorphous solid (23 mg, 64%) from *N*-(pivaloyloxy)-benzo[*b*]thiophene-2-carboxamide (50 mg, 0.18 mmol) following general procedure C. δ_H (300 MHz, DMSO-d_6) 11.87 (1H, br s, NH), 8.33 (1H, d, *J* 7.6, H_8), 8.13 (1H, d, *J* 7.8, H_5), 7.63 (1H, t, *J* 7.8, H_6), 7.54 (1H t, *J* 7.8, H_7), 7.49 (1H, d, *J* 6.8, H_3), 7.20 (1H, d, *J* 6.8, H_4); δ_C (75 MHz, DMSO-d_6) 158.8 (C_qO), 142.1 (SC_q), 140.9 (SC_q), 135.0 (C_q), 131.4 (C_3), 128.4 (C_q), 128.2 (C_6), 125.0 (C_7), 123.9 (C_8), 123.6 (C_5), 100.1 (C_4); HRMS (ESI^+): *m/z* calculated for formula $C_{11}H_8NOS$ [MH^+] 202.0321; found 202.0314; IR (ν_{max}, solid, cm^{-1}): 2949, 1652, 1610, 1464, 1235, 1056.

Benzofuro[2,3-*c*]pyridine-*1(2H)*-one 206

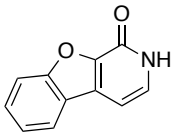

The reaction was heated to 45 °C for **48 hours**, after which time the solvent was removed *in vacuo*. The product was triturated with a 1:4 mixture of MeOH–Et_2O (5 mL) and subsequently crystallised from *sec*-butanol. The desired compound was isolated as a colourless solid (70 mg, 38%) from *N*-(pivaloyloxy)benzo[*b*]furan carboxamide (261 mg, 1.00 mmol) following general procedure C. M.p. decomposed above 260 °C (*sec*-butanol), (literature value 276 °C (ethanol));[249] δ_H (300 MHz, DMSO-d_6) 11.90 (1H, br s, NH), 8.14 (1H, d, *J* 7.8, H_5), 7.80 (1H, d, *J* 8.3, H_8), 7.62 (1H, t, *J* 7.4, H_6), 7.45 (1H, t, *J* 7.7, H_7), 7.36 (1H, d, *J* 6.7, H_3), 6.99 (1H, d, *J* 6.7, H_4); δ_C (75 MHz, DMSO-d_6) 155.7 (C_qO), 153.7 (C_qO), 143.8 (C_qO), 130.2 (C_3), 129.5 (C_q), 129.0 (C_6), 123.7 (C_7), 122.9 (C_q), 122.5 (C_5), 112.5 (C_8), 98.4 (C_4); HRMS (ESI^+): *m/z* calculated for

formula $C_{11}H_7NNaO_2$ [MNa^+] 208.0369; found 208.0363; IR (ν_{max}, solid, cm^{-1}): 2876, 1699, 1572, 1473, 1184.

9-Methyl-2,9-dihydro-*1H*-pyrido[3,4-*b*]indol-1-one 207

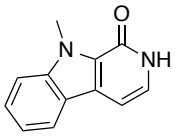

The product was isolated by flash silica chromatography using an eluent of 0-100% EtOAc in hexane then recrystallised from $CDCl_3$–Et_2O. The desired compound was isolated as a colourless solid (17 mg, 11%) from 1-methyl-*N*-(pivaloyloxy)-*1H*-indole-2-carboxamide (214 mg, 0.78 mmol) following general procedure C. M.p. decomposed above 260 °C ($CDCl_3$–Et_2O); δ_H (500 MHz, $CDCl_3$) 11.35 (1H, br s, NH), 7.98 (1H, d, *J* 8.0, H_5), 7.54 (1H, t, *J* 7.5, H_7), 7.48 (1H, d, *J* 8.4, H_8), 7.28 (1H, t, *J* 7.4, H_6), 7.13 (1H, d, *J* 6.8, H_3), 6.99 (1H, d, *J* 6.7, H_4), 4.36 (3H, s, NMe); δ_C (126 MHz, $CDCl_3$) 158.2 (CO), 141.1 (C_q), 127.3 (C_q), 127.1 (C_7), 126.2 (C_q), 124.2 (C_3), 121.7 (C_q), 121.5 (C_5), 120.2 (C_6), 110.2 (C_8), 101.4 (C_4), 31.5 (NMe); HRMS (ESI^+): *m/z* calculated for formula $C_{12}H_{11}N_2O$ [MNa^+] 199.0866; found 199.0861; IR (νmax, solid, cm^{-1}): 3140, 2955, 2854, 1642, 1458, 1351, 1329, 1226.

Benzo[b][1,6]naphthyridin-1(*2H*)-one 208

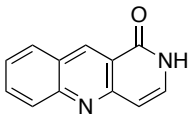

After filtration from the reaction solution the solid precipitate was washed with a 1:4 mixture of EtOH–pentane (1 mL) and subsequently crystallised from isopropanol. The desired compound was isolated as a colourless solid (24 mg, 51%) from *N*-(pivaloyloxy)isoquinoline-3-carboxamide (65 mg, 0.24 mmol) following general procedure C. M.p. 288 °C (isopropanol, [lit. decomposed above 290 °C (DMF)][250]); δ_H (300 MHz, DMSO-d_6) 11.37 (1H, br s, NH), 9.25 (1H, s, H_{10}), 8.24 (1H, d, *J* 7.9, H_9), 8.06 (1H, d, *J* 8.5, H_6), 7.90 (1H, t, *J* 8.5, H_7), 7.63 (1H, t, *J* 7.5, H_8), 7.47 (1H, dd, *J* 7.4, 5.8, H_3), 6.68 (1H, d, *J* 7.5, H_4); δ_C (75 MHz, DMSO-d_6) 162.5 (C_1), 153.2 (C_q), 150.3 (C_q), 137.5 (C_{10}), 133.5 (C_7), 132.4 (C_3), 129.6 (C_9), 128.1 (C_6), 126.0 (C_8), 125.9 (C_q), 120.8 (C_q), 106.1 (C_4); HRMS (ESI^+): *m/z* calculated for formula $C_{12}H_9N_2O$ [MH^+] 197.0709; found 197.0704; IR (ν_{max}, solid, cm^{-1}): 3166, 3029, 2930, 1661, 1614, 1587, 1499, 1202.

Hepatitis C inhibitor intermediates

3-Bromo-4-methoxy-*N*-(pivaloyloxy)benzamide 226

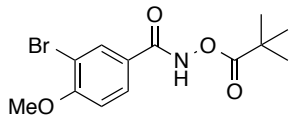

Oxalyl chloride (480 μL, 5.50 mmol) was added to a solution of 3-bromo-4-methoxybenzoic acid (1.16 g, 5.00 mmol) in DCM (25 mL, 0.20 M) with cat. DMF. The mixture was stirred at room temperature for 2 hours, then concentrated *in vacuo* to afford the crude acid chloride. The crude acid chloride was diluted in EtOAc (5 mL) and transferred to a flask containing *O-(*pivaloyl)-hydroxylamine triflic acid[34] (1.47 g, 5.50 mmol) and $NaHCO_3$ (840 mg, 10.0 mmol) dissolved in a 2:1 mixture of EtOAc–H_2O (45 mL, 0.1 M) at 0 °C. After 2 hours the reaction was quenched with sat. $NaHCO_3$ (50 mL) and diluted with EtOAc (50 mL). The two phases were separated and the organic layer was washed with brine (50 mL). The organic layer was dried over $MgSO_4$ and concentrated *in vacuo* to give 3-bromo-4-methoxy-*N*-(pivaloyloxy)benzamide (1.65g, quant.) (>95% pure by ^{1}H NMR). A sample of the crude product (1 g) was purified by crystallisation from Et_2O–pentane, recovery (0.65 g). R_F 0.7 (33% EtOAc in pentane); M.p. 94-96 °C (Et_2O–pentane); δ_H (500 MHz, $CDCl_3$) 9.65 (1H, br s, NH), 7.99 (1H, d, *J* 2.2, H_6), 7.72 (1H, dd, *J* 8.6, 2.2, H_2), 6.86 (1H, d, *J* 8.6, H_3), 3.91 (3H, s, OMe), 1.33 (9H, s, $(CH_3)_3$); δ_C (125 MHz, $CDCl_3$) 177.2 (C_qO), 165.3 (C_4-OMe), 159.3 (C_qO), 132.9 (C_2) 128.5 (C_6), 124.3 (C_1), 112.0 (C_3), 111.5 (C_5), 56.5 (OMe), 38.6 ($C_q(CH_3)_3$), 27.1 ($(CH_3)_3$); HRMS (ESI$^+$): *m/z* calculated for formula $C_{13}H_{17}{}^{79}BrNO_4$ [MH^+] 330.0335; found 330.0335; IR (ν_{max}, solid, cm^{-1}): 3167, 2976, 1772, 1648, 1597, 1560, 1510, 1481, 1461, 1443, 1397, 1370, 1311, 1268.

7-Bromo-6-methoxyisoquinolin-1(2*H*)-one 147

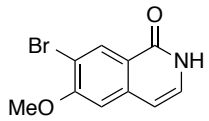

Vinyl acetate (69 μL, 0.75 mmol) was added to a solution of $[Cp^*RhCl_2]_2$ (3 mg, 5 μmol), CsOAc (28 mg, 0.15 mmol) and 3-bromo-4-methoxy-*N*-(pivaloyloxy)benzamide (165 mg, 0.5 mmol) in MeOH (1.25 mL, **0.4 M**) in a vial under a nitrogen atmosphere. The reaction was heated to **30 °C** for 16 hours, after which time the solvent was removed *in vacuo*. The product was triturated with a 1:4 mixture of MeOH–Et_2O (2 mL) to afford a cream amorphous solid (108 mg, 85%). A sample was crystallised from THF to afford colourless crystals. R_F 0.12 (33% EtOAc in pentane); M.p decomposed at 250 °C (THF); δ_H (500 MHz, DMSO-*d*$_6$) 11.23 (1H, br s, NH), 8.26 (1H, s, H_8), 7.29 (1H, s, H_5), 7.18 (1H, dd, *J* 6.7, 6.6, H_3), 6.51 (1H, d, *J* 7.1, H_4), 3.97 (3H, s, OMe); δ_C (125 MHz, DMSO) 160.5 (C_6), 158.0 (C_1), 139.3 (C_q), 131.1 (C_8), 130.2 (C_3), 120.7 (C_q), 110.2 (C_7), 107.6 (C_5), 104.1 (C_4), 56.6 (OMe); HRMS (ESI$^+$): *m/z* calculated for formula

$C_{10}H_9{}^{79}BrNO_2$ [MH^+] 253.9811; found 253.9812; IR (ν_{max}, solid, cm^{-1}): 2896, 2834, 1647, 1631, 1594, 1494, 1464, 1449, 1426, 1381, 1346, 1279, 1256, 1246, 1219.

4-Hydroxyisoquinolin-1(2*H*)-one 217

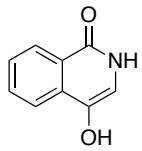

Vinylene carbonate (95 μL, 1.5 mmol) was added to a solution of *N-(*pivaloyloxy)benzamide (221 mg, 1.00 mmol), CsOAc (57 mg, 0.30 mmol) and $[Cp^*RhCl_2]_2$ (6 mg, 0.01 mmol) in MeOH (5 mL, 0.2 M). The solution was heated to 45 °C for 5 hours during which time a pale pink solid precipitated from the reaction. The MeOH was removed *in vacuo* and the solid was triturated with cold EtOH–diethyl ether (9:1, 10 mL) and the solid was filtered and collected under reduced pressure to afford a pale brown amorphous solid (126 mg, 78%). δ_H (300 MHz, DMSO-d_6) 10.65 (1H, s, NH), 9.02 (1H, s, OH), 8.17 (1H, d, *J* 8.0, H_8), 7.84 (1H, d, *J* 8.0, H_5), 7.73 (1H, t, *J* 7.6, H_6), 7.51 (1H, t, *J* 7.9, H_7), 6.63 (1H, s, H_3); δ_C (75 MHz, DMSO) 159.5 (CO), 134.8 (C_q), 133.4 (C_q), 131.7 (C_6), 126.9 (C_8), 126.6 (C_7), 125.9 (C_q), 121.3 (C_5), 109.7 (C_3); LCMS (ESI^+): *m/z* calculated for formula $C_9H_8NO_2$ [MH^+] 162.1; found 161.9; IR (ν_{max}, solid, cm^{-1}): 3279, 2689, 1652, 1505, 1343, 1241, 1083, 907, 821, 773, 675, 613, 555, 469. Spectral data consistent with the literature.[119]

4-Hydroxy-7-chloroisoquinolin-1-(*2*H)-one 235

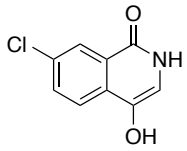

Vinylene carbonate (78 μL, 1.5 mmol) was added to a solution of 3-chloro-*N-(*pivaloyloxy)benzamide (210 mg, 0.82 mmol), CsOAc (47 mg, 0.3 mmol) and $[Cp^*RhCl_2]_2$ (5 mg, 0.01 mmol) in MeOH (4.1 mL, 0.2 M). The solution was heated to 45 °C for 16 hours during which time a pale pink solid precipitated from the reaction. The pink solid was filtered from the reaction, and subsequently washed with a mixture of MeOH−Et_2O (2 mL, 1:1), then ether (2 × 2 mL). The pink solid was dried *in vacuo* at 80 °C to afford the amorphous product (104 mg, 65%). δ_H (300 MHz, DMSO-d_6) 10.86 (1H, br s , NH), 9.17 (1H, s, OH), 8.11 (1H, d, *J* 2.1, H_8), 7.86 (1H, d, *J* 8.7, H_5), 7.77 (1H, dd, *J* 8.7, 2.1, H_6), 6.66 (1H, s, H_3); δ_C (75 MHz, DMSO) 158.4 (C_1), 134.5 (C_q), 132.1 (C_q), 132.0 (C_6), 131.4 (C_q), 127.1 (C_q), 126.0 (C_8), 123.8 (C_5), 110.3 (C_3); LRMS (ESI^+): *m/z* 161.9 [MH^+]; IR (ν_{max}, solid, cm^{-1}): 3100, 2953, 1643, 1602, 1534, 1462, 1437, 1403, 1325, 1276, 1237, 1220, 1102, 1073.

6.6 Deuterated enol carboxylate derivatives

Heptan-1-ol-d_2 246

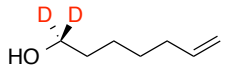

A suspension of $LiAlD_4$ (203 mg, 4.80 mmol) in THF (10 mL) was cooled to 0 °C in a salt/ice bath. 6-Heptenoic acid (541 µL, 4.00 mmol) in THF (10 mL) was added dropwise to the suspension. The reaction was warmed slowly to room temperature and stirred for five hours. The reaction was cooled to 0 °C and quenched with water (5 mL). Diethyl ether (20 mL) and 1N HCl (20 mL) was added and the aqueous layer was extracted twice with diethyl ether (2 x 20 mL). The organic layer was dried with $MgSO_4$ and concentrated *in vacuo* to give a colourless oil (395 mg, 85%, 100% D by ^1H NMR). δ_H (300 MHz, $CDCl_3$) 5.91-5.70 (1H, m, H_6), 5.07-4.89 (2H, m, H_7), 2.13-2.01 (2H, m, H_5), 1.57 (2H, t, *J* 6.9, H_2), 1.49-1.31 (4H, m, H_3 and H_4); δ_C (75 MHz, $CDCl_3$) 138.9 (H*C*=CH_2), 114.3 (HC=*C*H_2), 33.7, 22.4, 28.7, 25.2; IR (ν_{max}, NaCl, film, cm^{-1}) 3337, 2928, 2090, 1640, 1460, 1134, 966, 909, 635; Unable to acquire HRMS for this sample.

N-Methoxy-*N*-methylhept-6-enamide 247[251]

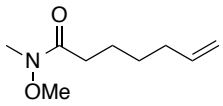

Isobutyl chloroformate (203 µL, 1.56 mmol) was added dropwise to a solution of 6-heptenoic acid (211 µL, 1.56 mmol) in DCM (3 mL) with NEt_3 (658 µL, 4.68 mmol) at -15 °C (EtOH/ice bath). The solution was allowed to stir at 0 °C for 30 minutes to allow the mixed anhydride to form. The reaction was cooled again to – 20 °C (EtOH/ice bath) and *N,O*-dimethylhydroxylamine·HCl (197 mg, 2.03 mmol) was added to the anhydride solution. The reaction was allowed to warm to room temperature overnight. The reaction was quenched with 1N HCl (20 mL) and the organic layer was washed with sat. $NaHCO_3$ (20 mL), brine (20 mL), dried ($MgSO_4$) and concentrated *in vacuo*. The crude material was purified using flash silica chromatography with an EtOAc–hexane eluent (1:1) to afford a colourless oil (256 mg, 96%). δ_H (300 MHz, $CDCl_3$) 5.82 (1H, ddt, *J* 17.0, 10.3, 6.6, H_6), 5.05-4.93 (2H, m, H_7), 3.69 (3H, s, NOCH_3), 3.19 (3H, s, NCH_3), 2.43 (2H, t, H_2), 2.12-2.05 (2H, m, H_5), 1.71-1.61 (2H, m, H_3), 1.50-1.39 (2H, m H_4); δ_C (75 MHz, $CDCl_3$) 174.6 (CO), 138.7 (C_7), 114.5 (C_6), 61.2 (OMe), 33.6 (NMe), 32.2 (C_2), 31.7 (C_5), 28.7 (C_3), 24.1 (C_4); HRMS (ESI^+): *m/z* calculated for formula $C_9H_{17}NNaO_2$ $[MNa]^+$ 194.1151; found 194.1179; IR (ν_{max}, NaCl film, cm^{-1}) 3494, 2937, 1667, 1415, 1177. Spectral data consistent with literature.[251]

Hept-6-enal-d_1 244

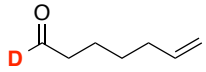

N-Methoxy-*N*-methylhept-6-enamide (267 mg, 1.56 mmol) in THF (10 mL) was added dropwise to a suspension of $LiAlD_4$ (80 mg, 1.87 mmol) in THF (10 mL) at 0 °C. The reaction was monitored by TLC. After the starting material had been consumed (~3 hours) the reaction was quenched with water (5 mL). The reaction was diluted with 1N HCl (20 mL) and extracted with Et_2O (2 x 20 mL) and the organic phases were combined and washed with brine (20 mL), dried (Na_2SO_4) and concentrated *in vacuo* (<10 °C). At this stage an aqueous droplet formed in the solution (from dehydration of the acetal), the reaction was rediluted in Et_2O (10 mL) and dried again using Na_2SO_4. The solution was filtered and concentrated *in vacuo* to give a clear oil (150 mg, 85%, 100% D). δ_H (300 MHz, $CDCl_3$) 5.86-5.71 (1H, m, H_6), 5.06-4.95 (2H, m, H_7), 2.44 (2H, t, *J* 7.3, H_2), 2.12-2.05 (2H, m, H_5), 1.71-1.61 (2H, m, H_3), 1.49-1.39 (2H, m, H_4); δ_C (75 MHz, $CDCl_3$) 202.3 (t, *J 25.9*, OC_q-D), 138.2 (C_7), 114.8 (C_6), 43.4 (C_2), 33.4 (C_5), 28.3 (C_3), 21.5 (C_4); IR (ν_{max}, NaCl film, cm^{-1}) 3077, 2931, 1736, 1641, 1439, 1261, 993, 910. Spectral data matches that of hept-6-enal (aside from the deuterated carbon peak).[252] Unable to obtain a HRMS due to volatility of the sample.

(*E/Z*)-Hepta-1,6-dien-1-yl hexanoate 248

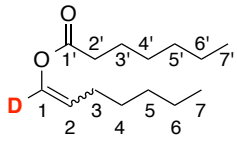

Following a modified procedure by Nishizawa *et al*.,[253] KHMDS (3.3 mL, 0.5 M solution in toluene, 1.66 mmol) was added dropwise to a solution of hept-6-enal-d_1 (170 mg, 1.5 mmol) in THF (15 mL) at -78 °C. Following the addition the reaction was allowed to warm to 0 °C and stirred for a further half an hour. The reaction was cooled again to -78 °C and hexanoyl chloride (230 µL, 1.65 mmol) was added dropwise to the solution. The reaction was monitored by TLC and after 30 minutes the reaction was quenched with $NaHCO_3$ (5 mL) and the aqueous solution was extracted with EtOAc (3 × 10 mL) and dried with $MgSO_4$. The crude reaction mixture was purified using a gradient of 0-5% EtOAc in hexane using flash silica chromatography to afford a colourless oil (100 mg, 32%, *E:Z* 1.8:1). δ_H (300 MHz, $CDCl_3$) 5.86-5.76 (1H, m, H_6), 5.40 (0.64H, t, *J 7.7*, H_2, *E* isomer) 5.04-4.95 (2H, m, *2*H_7), 4.87 (0.36 H, t, *J 7.5*, H_2, *Z* isomer), 2.40 (0.36H, t, *J* 7.5, *2*$H_{2'}$, *Z*-isomer), 2.36 (1.28H, t, *J* 7.5, *2*$H_{2'}$, *E*-isomer), 2.10-2.05 (2H, m, *2*H_5), 2.05-2.00 (1.28H, m, *2*H_3, *E* isomer), 2.16 (0.72H, q, *J 7.3*, *2*H_3, *Z* isomer), 1.69-1.63 (2H, m, *2*$H_{3'}$), 1.49 (2H, q, *J* 7.5, *2*H_4), 1.37-1.30 (4H, m, *2*$H_{4'}$ and *2*H_5'), 0.93-0.89 (3H, m, *3*H_6'); δ_C (75 MHz, $CDCl_3$) 171.1 (C_qO, *E* isomer), 170.9 (C_qO, *Z* isomer), 138.5 (C_6, *Z* isomer), 138.4 (C_6, *E* isomer), 135.4 (C_1D, t, *J* 17.3, *E* isomer), 134.0 (C_1-D, t, *J* 17.3, *Z* isomer), 114.8 (C_7, *E* isomer), 114.6 (C_7, *Z* isomer), 114.3 (C_2, *E* isomer), 113.5 (C_2, *Z* isomer), 34.1 ($C_{2'}$, *Z* isomer), 34.0 ($C_{2'}$, *E* isomer), 33.0 (C_5), 31.2 ($C_{4'}$), 28.7 (C_4), 26.6

(C_3, *E* isomer), 24.4 (C_3, *Z* isomer) 22.3 ($C_{3'}$ and $C_{5'}$) 13.9 ($C_{6'}$); HRMS (ESI^+): *m/z* calculated for formula $C_{13}H_{21}DNaO_2$ $[MNa]^+$ 234.1575; found 234.1565; IR (ν_{max}, NaCl, film, cm^{-1}) 2930, 1751, 1652, 1458, 1160, 1114, 911;

Vinyl *N,N*-diisopropylcarbamate 265

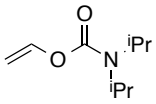

Following a modified procedure by Clayden *et al.,*[142] *n*-butyllithium (2.5 M in hexanes, 6.0 mL, 15 mmol) was added to THF (11 mL, 1.3 M) at room temperature. After 16 hours *N,N*-diisopropyl carbamoyl chloride (1.6 g, 10 mmol) was dissolved in DMPU (11 mL, 0.91 M) and added dropwise to a cooled solution (0 °C) containing the lithium ethenolate. The reaction was warmed to room temperature over four hours. The reaction was quenched with saturated NH_4Cl and extracted with Et_2O (3 x 25 mL). The organic layer was washed with water and dried over Na_2SO_4. The solvent was removed *in vacuo* and purified by flash silica chromatography using 33% EtOAc in hexane to afford a clear oil (1.42 g, 83%). R_F 0.84 (50% EtOAc in hexane); δ_H (300 MHz, $CDCl_3$) 7.26 (1H, dd, *J* 14.7, 5.6, C=C*H*-O), 4.77 (1H, dd, *J* 14.0, 1.4, OC=CH *trans*), 4.43 (1H, dd, *J* 6.3, 1.4, OC=CH *cis*), 4.07 (1H, br s, *C*H-$(Me)_2$), 3.86 (1H, br s, *C*H-$(Me)_2$), 1.25 (12H, d, *J* 6.7, Me); δ_C (75 MHz, $CDCl_3$) 152.7 (*C*O), 142.3 (C=*C*-O), 94.5 (*C*=C-O), 46.7 (*C*$(Me)_2$), 45.8 (*C*$(Me)_2$), 20.4 (Me), 19.4 (Me); IR (ν_{max}, film, cm^{-1}): 3417, 2972, 1713, 1646, 1436, 1371, 1316, 1144, 1048; HRMS (ESI^+): *m/z* calculated for formula $C_9H_{18}NO_2$ $[MH^+]$ 172.1332; found 172.1328. The ^1H NMR spectral data corresponds to the literature values.[254]

Vinyl *N,N*-diisopropylcarmabate-*d*$_1$ 265-*d*$_1$

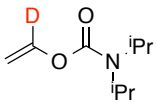

sec-Butyllithium (1.4 M in hexanes, 1.40 mL, 1.90 mmol) was added dropwise to a solution of TMEDA (290 mL, 1.93 mmol) in THF (2 mL) at -78 °C. After ten minutes *O*-vinyl-*N,N*-diisopropylcarbamate (300 mg, 1.75 mmol) was added to the yellow solution. After two hours at -78 °C, the reaction was quenched with DCl in D_2O (35% wt solution, 100 mL, 2.47 mmol) and the solution was allowed to warm to room temperature. The reaction was diluted with water and the product was extracted with Et_2O (3 x 20 mL). The organic layers were combined and washed with brine (30 mL) and dried over Na_2-SO_4. The crude material was passed through a silica plug to remove base line impurities using 50% EtOAc in hexane. The solvent was concentrated *in vacuo* to afford a colourless oil (288 mg, 96%, 87% D by ^1H NMR). R_F 0.84 (50% EtOAc in hexane); δ_H (500 MHz, CD_3CN) 7.20 (0.13 H, dd, *J* 14.1, 6.3 Hz, 1H), 4.75 (1H, s, *H*HC=CD), 4.41 (1H, s, H*H*C=CD), 3.99 (2H, br s, C*H*$(Me)_2$), 1.22 (12H, d, *J* 6.8, CH(*Me*)$_2$); δ_C (126 MHz, CD_3CN) 153.5 (*C*O), 142.9 (t, *J* 16.3, C=*C*D-O), 94.9 (*C*=CDO), 47.6 (*C*$(Me)_2$), 46.8 (*C*$(Me)_2$), 21.7 (Me), 20.7 (Me); IR (ν_{max},

film, cm^{-1}): 2972, 1714, 1622, 1435, 1371, 1314, 1144, 1050. HRMS (ESI^+): *m/z* calculated for formula $C_9H_{16}DNO_2$ [M_2H^+] 345.2748; found 345.2761.

Isoquinolin-1*(2H)*-one-d_1 137-d_1

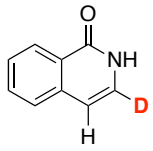

The desired compound was isolated as a crude solid (10 mg, 6%, 85% D by ^1H NMR) containing impurities (<90% pure) from *N*-(pivaloyloxy)benzamide (221 mg, 1.00 mmol) following general procedure C using mesitylene (46 μL, 0.33 mmol) as an internal standard. The ^1H NMR of the crude reaction mixture indicated 10% conversion to the isoquinolone (5aD) (see spectrum). The product was isolated as an amorphous solid (8 mg, 5%) by preparative TLC using 50% EtOAc in hexane. δ_H (500 MHz, $CDCl_3$) 10.68 (1H, s, NH), 8.42 (1H, d, *J* 8.1, ArH), 7.67 (1H, t, *J* 8.1, ArH), 7.56 (2H, d, *J* 7.8, ArH), 7.51 (1H, t, *J* 7.1, ArH), 7.14 (**0.15 H**, d, *J* 7.1, H_3), 6.55 (1H, s, H_4).

***tert*-Butyl 5-oxo-3a,4,5,9b-tetrahydro-*1H*-pyrrolo[2,3-*c*]isoquinoline-3(*2H*)-carboxylate 267**

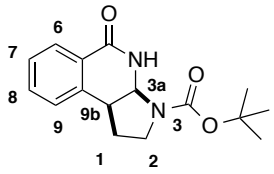

N-Boc-2,3-dihydro-*1H*-pyrrole (172 μL, 1.50 mmol) was added to a solution of [Cp*$RhCl_2$]$_2$ (6 mg, 0.01 mmol), CsOAc (58 mg, 0.3 mmol) and *N*-(pivaloyloxy) benzamide (221 mg, 1.00 mmol) in MeOH (5 mL, 0.2 M) in a vial under a nitrogen atmosphere. The reaction was heated to 45 °C for 16 hours, after which time the solvent was removed *in vacuo*. The crude material was purified by flash silica chromatography using an eluent of 50% EtOAc in hexane then crystallised from EtOAc–pentane to afford pale yellow crystals (131 mg, 45%). M.p. 161-165 °C (DCM–pentane); δ_H (500 MHz, 343K, DMSO-d_6) 7.94 (1H, d, *J* 7.2, H_6), 7.53 (1H, td, *J* 7.3, 1.0, H_8), 7.42-7.38 (2H, m, H_7 and H_9), 7.27 (1H, br s, NH), 5.51 (1H, d, *J* 6.4, H_{3a}), 3.54 (1H, dt, *J* 10.8, 6.7, H_{9b}), 3.46-3.33 (2H, m, $2H_2$), 2.38-2.26 (1H, m, H_1), 2.01-1.91 (1H, m, H_1), 1.47 (9H, s, ^{t}Bu); δ_C (126 MHz, 343K, DMSO-d_6) δ 161.9 (C5), 153.0 ($CO_2{}^t$Bu), 138.3 (C_q), 131.9 (C_8), 127.3 (C_7), 127.0 (C_6), 126.8 (C_9), 126.3 (C_q), 79.3 (OC^tBu), 66.7 (C_{3a}), 44.4 (C_2), 39.5 (C_{9b}) 31.9 (C_1), 27.8 ($C(CH_3)_3$). C_{9b} is obscured by the DMSO signal but can be identified in the HMQC; HRMS (ESI^+): *m/z* calculated for formula $C_{16}H_{21}N_2O_3$ [MH^+] 289.1547; found 289.1542; IR (ν_{max}, solid, cm^{-1}): 3585, 3518, 3199, 2955, 2849, 1705, 1650, 1464, 1387, 1284, 1122.

6.7 Preparation of (*E*)-acetophenone oxime derivatives

General procedure (D) for the synthesis of (*E*)-acetophenone *O*-acetyl oxime derivatives[64]

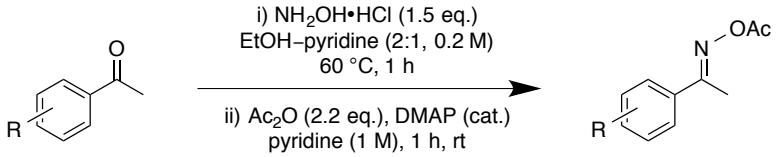

To a stirred solution of hydroxylamine hydrochloride (1.5 eq.) in a pyridine–ethanol (1:2, 0.2 M) solution at 60 °C was added the acetophenone derivative (1 eq.). After one hour the reaction mixture was partitioned between water (25 mL) and EtOAc (25 mL). The aqueous layer was re-extracted with EtOAc (25 mL) and the organic layers were combined and washed with 1 N HCl (25 mL), brine (20 mL) and dried with $MgSO_4$ and filtered. The solvent was removed *in vacuo* to afford the crude oxime. The product was added to a solution of acetic anhydride (2.2 eq.) in pyridine (1 M) with DMAP (cat.) at room temperature. After 2 hours, the reaction was quenched with water (25 mL), extracted with EtOAc (2 × 25 mL). The organic layers were combined and washed with 1 N HCl (25 mL), brine (25 mL) and dried with $MgSO_4$. The solvent was removed *in vacuo* to afford the crude *O*-acetyl oxime, which was purified by crystallisation or flash column chromatography.

(*E*)-Acetophenone *O*-acetyl oxime 271

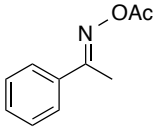

The desired compound was isolated as colourless needles (709 mg, 80%) from acetophenone (583 μL, 5.00 mmol) following general procedure D. The crude material was crystallised from EtOAc–hexane. M.p. 54-55 °C (EtOAc–hexane, [lit. 53-55 °C, EtOAc–hexane][64]); δ_H (300 MHz, $CDCl_3$) 7.74 (2H, d, *J* 8.2, H_2 and H_6), 7.50-7.35 (3H, m, H_3, H_4 and H_5), 2.39 (3H, s, $CNCH_3$), 2.27 (3H, s, $COCH_3$); δ_C (75 MHz, $CDCl_3$) 169.0 ($COCH_3$), 162.5 ($CNCH_3$), 134.9 (C_1), 130.6 (C_4), 128.6 (C_3 and C_5), 127.0 (C_2 and C_6), 20.0 ($COCH_3$), 14.4 ($CNCH_3$); LCMS (ESI^+): *m/z* calculated for formula $C_{10}H_{11}NNaO_2$ [MNa^+] 200.1; found 200.1; IR (ν_{max}, solid, cm^{-1}) 3063, 2629, 1760, 1684, 1599, 1449, 1361, 1267. Spectral data consistent with the literature.[64]

(*E*)-Acetophenone *O*-pivaloyloxime 270

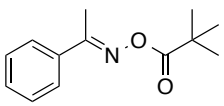

The desired compound was isolated as crystalline needles (745 mg, 68%) from (*E*)-acetophenone oxime (675 mg, 5.00 mmol) and pivalic anhydride (2.33 mL, 11.0 mmol) (instead of acetic anhydride) following general procedure D. The product was purified by flash column chromatography using 0-30% EtOAc

in hexane, followed by crystallisation from EtOAc–pentane. M.p. 51-53 °C (EtOAc–hexane); δ_H (300 MHz, $CDCl_3$) 7.78-7.73 (2H, m, H_2 and H_6, 7.47 (3H, m, H_3, H_4 and H_5), 2.38 (3H, s, $CNCH_3$), 1.34 (9H, s, $CO_2(CH_3)_3$); δ_C (75 MHz, $CDCl_3$) 175.2 ($CO_2(CH_3)_3$), 163.3 ($CNCH_3$), 135.1 (C_1), 130.6 (C_4), 128.7 (C_3 and C_5), 127.2 (C_2 and C_6), 39.0 ($C(CH_3)_3$), 27.5 ($C(CH_3)_3$), 14.5 ($CNCH_3$); LCMS (ESI^+): *m/z* calculated for formula $C_{13}H_{17}NNaO_2$ [MNa^+] 242.1; found 242.1; IR (ν_{max}, solid, cm^1): 2964, 1753, 1481, 1445, 1390, 1366, 1305, 1267, 1110, 1075, 1021. Spectral data consistent with the literature.[34]

(*E*)-1-(4-Nitrophenyl)ethanone *O*-acetyl oxime 273

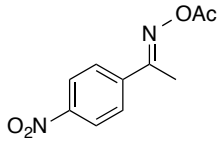

The desired compound was isolated as a brown crystalline solid (1.05 g, 95%) from 4'-nitroacetophenone (825 mg, 5.00 mmol) following general procedure D. The crude material was crystallised from EtOAc–hexane. M.p. 124-128 °C (EtOAc–hexane); δ_H (300 MHz, $CDCl_3$) 8.23 (2H, d, *J* 9.1, H_3 and H_5), 7.91 (2H, d, *J* 9.1, H_2 and H_6), 2.42 (3H, s, $CNCH_3$), 2.27 (3H, s, $COCH_3$); δ_C (75 MHz, $CDCl_3$) 168.3 ($COCH_3$), 160.5 ($CNCH_3$), 149.0 (C_4), 140.9 (C_1), 128.0 (C_2 and C_6), 123.8 (C_3 and C_5), 19.7 ($COCH_3$), 14.4 ($CNCH_3$); HRMS (ESI^+): *m/z* calculated for formula $C_{10}H_{10}N_2NaO_4$ [MNa^+] 245.0533; found 245.0542; IR (ν_{max}, solid, cm^{-1}) 3429, 2304, 1771, 1645, 1517, 1191.

(*E*)-1-(4-(Trifluoromethyl)phenyl)ethanone *O*-acetyl oxime 274

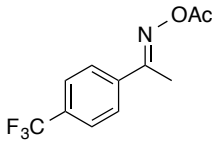

The desired compound was isolated as colourless needles (980 mg, 80%) from 4'-trifluoromethylacetophenone (940 mg, 5.00 mmol) following general procedure D. The crude material was crystallised from EtOAc–hexane. M.p. 43-44 °C (EtOAc–hexane), [lit. 42-44 °C, EtOAc–hexane][64]); δ_H (300 MHz, $CDCl_3$) 7.87 (2H, d, *J* 8.3, H_3 and H_5), 7.67 (2H, d, *J* 8.7, H_2 and H_6), 2.42 (3H, s, $CNCH_3$), 2.28 (3H, s, $COCH_3$); δ_C (75 MHz, $CDCl_3$) 168.6 ($COCH_3$), 161.2 ($CNCH_3$), 138.3 (C_1), 132.3 (q, *J 32.3*, C_4), 127.4 (C_2 and C_6), 125.6 (q, *J* 3.8, C_3 and C_5), 19.8 ($COCH_3$), 14.4 ($CNCH_3$), missing CF_3 quartet; HRMS (ESI^+): *m/z* calculated for formula $C_{11}H_{10}F_3NNaO_2$ [MNa^+] 268.0556; found 268.0564; IR (ν_{max}, solid, cm^{-1}) 3397, 3063, 1773, 1615, 1328, 1200, 1064. Spectral data consistent with the literature.[64]

(*E*)-1-(*p*-Tolyl)ethanone *O*-acetyl oxime 275

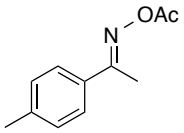

The desired compound was isolated as a pale yellow crystalline solid (787 mg, 82%) from 4'-methylacetophenone (666 μL, 5.00 mmol) following general procedure D. The crude material was crystallised from EtOAc–hexane. M.p. 105-109 °C (EtOAc–hexane); δ_H (300 MHz, $CDCl_3$) 7.64 (2H, d, *J* 8.3, H_2 and H_6), 7.21 (2H, d, *J* 8.5, H_3 and H_5), 2.38 (3H, s, $CNCH_3$), 2.37 (3H, s, Me), 2.27 (3H, s, $COCH_3$); δ_C (75 MHz, $CDCl_3$) 169.1 (*C*OCH_3), 162.4 (*C*NCH_3), 140.9 (C_1), 131.9 (C_4), 129.3 (C_3 and C_5), 126.9 (C_2 and C_6), 21.4 (Me), 19.9 (CO*C*H_3), 14.3 (CN*C*H_3); HRMS (ESI^+): *m/z* calculated for formula $C_{11}H_{13}NNaO_2$ [MNa^+] 214.0838; found 214.0839; IR (ν_{max}, solid, cm^{-1}) 3036, 1756, 1681, 1370, 1200.

(*E*)-1-(2-Fluorophenyl)ethanone *O*-acetyl oxime 276

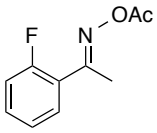

The desired compound was isolated as a colourless crystalline solid (429 mg, 44%) from 2'-fluoroacetophenone (607 μL, 5.00 mmol) following general procedure D. The product was purified by crystallisation from EtOAc–pentane. R_F 0.67 (20% EtOAc in pentane); M.p. 44-47 °C (EtOAc–pentane).; δ_H (300 MHz, $CDCl_3$) 7.55 (1H, td, *J* 7.6, 1.8, H_6), 7.44-7.35 (1H, m, H_4), 7.17 (1H, dd, *J* 7.6, 1.0, H_5), 7.09 (1H, dd, *J* 11.0, 8.5, H_3), 2.38 (3H, d, *J* 2.6, $CNCH_3$), 2.24 (3H, s, $COCH_3$); δ_C (75 MHz, $CDCl_3$) 168.7 (*C*OCH_3), 162.5 (*C*NCH_3), 160.8 (d, *J* 251.0, C_2), 132.0 (d, *J* 8.4, C_4), 130.1 (d, *J* 3.0, C_6), 124.4 (d, *J* 3.5, C_5), 123.8 (d, *J* 12.5, C_1), 116.3 (d, *J* 21.7, C_3), 19.8 (CO*C*H_3), 17.1 (d, *J* 5.3, CN*C*H_3); HRMS (ESI^+): *m/z* calculated for formula $C_{10}H_{11}FNO_2$ [MH^+] 196.0768; found 196.0765; IR (ν_{max}, solid, cm^{-1}): 3068, 2938, 1767, 1615, 1490, 1450, 1366, 1320, 1189.

(*E*)-1-(4-Chlorophenyl)ethanone *O*-acetyl oxime 277

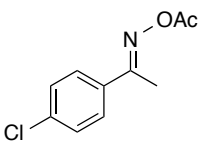

The desired compound was isolated as pale yellow needles (1.07 g, 74%) from 4'-chloroacetophenone (646 μL, 4.18 mmol) following general procedure D. The crude material was crystallised from EtOAc–hexane. M.p. 88-92 °C (EtOAc–hexane); δ_H (300 MHz, $CDCl_3$) 7.70 (2H, d, *J* 8.8, H_2 and H_6), 7.38 (2H, d, *J* 8.8, H_3 and H_5), 2.37 (3H, s, $CNCH_3$), 2.27 (3H, s, $COCH_3$); δ_C (75 MHz, $CDCl_3$) 168.8 (*C*OCH_3), 161.4 (*C*NCH_3), 136.8 (C_4), 133.3 (C_1), 128.9 (C_3 and C_5), 128.3 (C_2 and C_6), 19.8 (CO*C*H_3), 14.3 (CN*C*H_3); HRMS (ESI^+): *m/z* calculated for formula $C_{10}H_{10}{}^{35}ClNNaO_2$ [MNa^+] 234.0292; found 234.0290; IR (ν_{max}, solid, cm^{-1}) 3054, 2987, 2305, 1768, 1617, 1491, 1421, 1204.

(*E*)-1-(4-Bromophenyl)ethanone *O*-acetyl oxime 278[64]

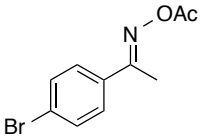

The desired compound was isolated as colourless needles (997 mg, 78%) from 4'-bromoacetophenone (995 mg, 4.18 mmol) following general procedure D. The crude material was crystallised from EtOAc–hexane. M.p. 94-96 °C (EtOAc–hexane, [lit. 95-97 °C, EtOAc–hexane][64]); δ_H (300 MHz, $CDCl_3$) 7.63 (2H, d, *J* 8.8, H_2 and H_6), 7.54 (2H, d, *J* 8.8, H_3 and H_5), 2.37 (3H, s, $CNCH_3$), 2.27 (3H, s, $COCH_3$); δ_C (75 MHz, $CDCl_3$); 168.7 (*C*OCH_3), 161.4 (*C*NCH_3), 133.7 (C_1), 131.8 (C_2 and C_6), 128.5 (C_3 and C_5), 125.2 (C_4), 19.8 (CO*C*H_3), 14.2 (CN*C*H_3); HRMS (ESI^+): *m/z* calculated for formula $C_{10}H_{10}{}^{79}BrNNaO_2$ [MNa^+] 277.9787; found 277.9780; IR (ν_{max}, solid, cm^{-1}) 3054, 2987, 2305, 1767, 1421, 1204. Spectral data consistent with the literature.[64]

(*E*)-1-(4-Iodophenyl)ethanone *O*-acetyl oxime 279

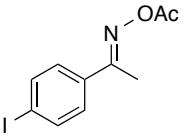

The desired compound was isolated as a brown crystalline solid (1.23 g, 81%) from 4'-iodoacetophenone (1.23 g, 5.00 mmol) following general procedure D. The crude material was crystallised from EtOAc–hexane. M.p. 54-55 °C (EtOAc–hexane); δ_H (300 MHz, $CDCl_3$) 7.75 (2H, d, *J* 8.7, H_2 and H_6), 7.48 (2H, d, *J* 8.7, H_3 and H_5), 2.36 (3H, s, $CNCH_3$), 2.26 (3H, s, $COCH_3$); δ_C (75 MHz, $CDCl_3$) 168.8 (*C*OCH_3), 161.6 (*C*NCH_3), 137.8 (C_3 and C_5), 134.3 (C_1), 129.0 (C_2 and C_6), 97.3 (C_4), 19.8 (CO*C*H_3), 14.2 (CN*C*H_3); HRMS (ESI^+): *m/z* calculated for formula $C_{10}H_{10}INNaO_2$ [MNa^+] 325.9648; found 325.9659; IR (ν_{max}, solid, cm^{-1}) 3420, 3054, 2987, 2305, 1767, 1421, 1274.

(*E*)- and (*Z*)-1-(Naphthalene-1-yl)ethanone *O*-acetyl oxime 280

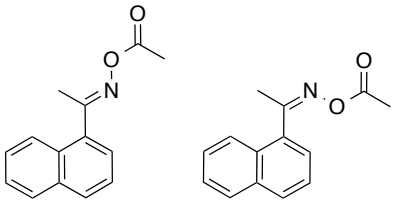

(*E*)-isomer **(*Z*)-isomer**

The desired compound was isolated as a colourless oil (984 mg, 87%) from 1'-acetonaphthone (760 μL, 5.00 mmol) following general procedure D. The product was purified by flash silica chromatography using 0-40% EtOAc in hexane to afford a mixture of the (*E*)- and (*Z*)-isomers (*E:Z*, 3:1). R_F 0.57 (20% EtOAc in pentane); δ_H (300 MHz, $CDCl_3$) 7.98 (1H, dd, *J* 8.1, 1.0, H_2, (*E*)-isomer), 7.78-7.71 (2H, m, ArH), 7.60-7.54 (0.35H, m, ArH (*Z*)-isomer), 7.46 (4H, m, ArH), 7.16 (0.3H, dd, *J* 7.1, 1.1, ArH, (*Z*)-isomer) 2.37 (3H, s, $CNCH_3$ (*E*)-isomer), 2.35 (0.9H, s, $CNCH_3$, (*Z*)-isomer) 2.17 (3H, s, $COCH_3$); δ_C (75 MHz, $CDCl_3$) 168.3 (*C*OCH_3, (*E*)-isomer), 167.9 (*C*OCH_3, (*Z*)-isomer), 164.3 (*C*NCH_3, (*E*)-isomer), 163.9 (*C*NCH_3, (*Z*)-isomer), 133.3 (C_q, (*E*)-isomer), 133.2 (C_q, (*Z*)-isomer), 132.8 (C_q, (*E*)-isomer), 132.8 (C_q, (*Z*)-isomer), 132.8, 130.0 (C_q), 129.6, 128.8, 128.2, 128.1, 128.0 (C_q), 126.5 (C_q), 126.5, 126.0, 125.8, 124.7, 124.6,

124.2, 122.9, 22.4 (CO*C*H$_3$, (*Z*)-isomer), 19.3 (CO*C*H$_3$, (*E*)-isomer), 18.7 (CO*C*H$_3$, (*Z*)-isomer), 18.3 (CO*C*H$_3$, (*E*)-isomer); HRMS (ESI$^+$): *m/z* calculated for formula $C_{14}H_{13}NO_2$ [MNa$^+$] 228.1019; found 228.1013; IR (ν_{max}, film, cm^{-1}): 3061, 2247, 1759, 1627, 1509, 1429, 1366, 1254, 1207, 1188.

(*E*)-1-(2-Methoxyphenyl)ethanone *O*-acetyl oxime 281

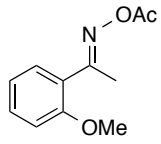

The desired compound was isolated as a colourless oil (850 mg, 82%) from 2'-methoxyacetophenone (690 μL, 5.00 mmol) following general procedure D. The product was purified by flash silica chromatography using 0-40% EtOAc in hexane. R_F 0.64 (20% EtOAc in pentane); δ_H (300 MHz, $CDCl_3$) 7.32-7.21 (2H, m, H_4 and H_6), 6.88-6.77 (2H, m, H_3 and H_5), 3.70 (3H, s, OMe), 2.23 (3H, s, $COCH_3$), 2.12 (3H, s, $CNCH_3$); δ_C (75 MHz, $CDCl_3$) 168.5 (*C*OCH$_3$), 164.4 (C_2), 157.2 (*C*NCH$_3$), 130.9 (C_4), 129.4 (C_6), 124.8 (C_1), 120.2 (C_5), 110.7 (C_3), 55.1 (OMe), 19.4 (CO*C*H$_3$), 17.1 (CN*C*H$_3$); LCMS (ESI$^+$): *m/z* calculated for formula $C_{11}H_{13}NNaO_3$ [MNa$^+$] 230.1; found 230.1; IR (ν_{max}, film, cm^{-1}): 2839, 2247, 1759, 1600, 1492, 1462, 1436, 1366, 1319, 1273, 1246, 1202, 1163, 1127, 1046, 1025. Spectral data consistent with the literature.[64]

(*E*)-1-(4-Methoxyphenyl)ethanone *O*-acetyl oxime 282

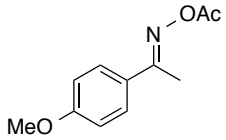

The desired compound was isolated as colourless needles (1.04 g, 80%) from 4'-methoxyacetophenone (750 mg, 5.00 mmol) following general procedure D. The crude material was crystallised from EtOAc–hexane. M.p. 52-54 °C (EtOAc–hexane, [lit. 53-55 °C, EtOAc–hexane][64]); δ_H (300 MHz, $CDCl_3$) 7.70 (2H, d, *J* 8.6, H_2 and H_6), 6.90 (2H, d, *J* 8.6, H_3 and H_5), 3.82 (3H, s, OMe) , 2.34 (3H, s, $CNCH_3$), 2.24 (3H, s, $COCH_3$); δ_C (75 MHz, $CDCl_3$) 169.2 (*C*OCH$_3$), 161.9 (*C*NCH$_3$), 161.6 (C_4), 129.7 (C_2 and C_6), 127.4 (C_1), 113.9 (C_3 and C_5), 55.4 (OMe), 19.9 (CO*C*H$_3$), 14.2 (CN*C*H$_3$); HRMS (ESI$^+$): *m/z* calculated for formula $C_{11}H_{13}NNaO_3$ [MNa$^+$] 230.0788; found 230.0796; IR (ν_{max}, film, cm^{-1}) 3517, 2937, 2840, 2559, 1765, 1604, 1514, 1254, 1180, 834. Spectral data consistent with the literature.[64]

(*E*)-1-(3-Bromophenyl)ethanone *O*-acetyl oxime 293

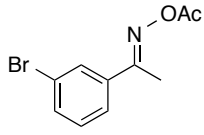

The desired compound was isolated as a colourless oil (1.24 g, 97%) from 3'-bromoacetophenone (661 μL, 5.00 mmol) following general procedure D. The product was purified by flash silica chromatography using 0-40% EtOAc in hexane. R_F 0.59 (20% EtOAc in pentane); δ_H (300 MHz, $CDCl_3$) 7.84 (1H, t, *J* 1.7,

H_2), 7.61 (1H, dd, *J* 7.9, 1.7, H_6), 7.51 (1H, dd, *J* 7.9, 1.7, H_4), 7.22 (1H, t, *J* 8.0, H_5), 2.31 (3H, s, $CNCH_3$), 2.21 (3H, s, $COCH_3$); δ_H (75 MHz, $CDCl_3$) 168.5 (*C*OCH_3), 161.1 (*C*NCH_3), 136.8 (C_1), 133.4 (C_4), 130.1 (C_5), 129.8 (C_2), 125.6 (C_6), 122.7 (C_3), 19.7 (CO*C*H_3), 14.3 (CN*C*H_3); LCMS (ESI^+): *m/z* calculated for formula $C_{10}H_{10}{}^{79}BrNO_2$ [MNa^+] 278.0; found 278.0; IR (ν_{max}, film, cm^{-1}): 3066, 2933, 2250, 1764, 1557, 1418, 1365, 1310, 1297, 1269, 1190, 1070. Spectral data consistent with the literature.[64]

(*E*)-1-(3-Fluorophenyl)ethanone *O*-acetyl oxime 294

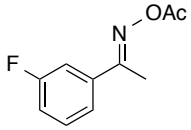

The desired compound was isolated as a colourless crystalline solid (713 mg, 73%) from 3'-fluoroacetophenone (613 μL, 5.00 mmol) following general procedure D. The product was purified by flash silica chromatography using 0-30% EtOAc in hexane and subsequently crystallised from pentane. R_F 0.61 (20% EtOAc in pentane); M.p. 38-41 °C (pentane); δ_H (300 MHz, $CDCl_3$) 7.53-7.42 (2H, m, H_6 and H_2), 7.36 (1H, td, *J* 8.0, 5.8, H_5), 7.12 (1H, tdd, *J* 8.3, 2.5, 0.8, H_4), 2.36 (3H, s, $CNCH_3$), 2.25 (3H, s, $COCH_3$); δ_C (75 MHz, $CDCl_3$) 168.8 (*C*OCH_3), 162.8 (d, *J* 246.5, C_3), 161.4 (d, *J* 2.5, *C*NCH_3), 137.1 (d, *J* 7.8, C_1), 130.3 (d, *J* 8.2, C_5), 122.8 (d, *J* 3.0, C_6), 117.6 (d, *J* 21.3, C_4), 114.1 (d, *J* 23.3, C_2), 19.8 (CO*C*H_3), 14.4 (CN*C*H_3); LCMS (ESI^+): *m/z* calculated for formula $C_{10}H_{11}FNO_2$ [MH^+] 196.0768; found 196.0767; IR (ν_{max}, film, cm^{-1}): 3075, 2937, 2766, 1580, 1435, 1367, 1316, 1210, 1187.

(*E*)-1-(3-Methylphenyl)ethanone *O*-acetyl oxime 295

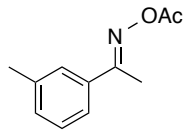

The desired compound was isolated as a colourless oil (857 mg, 90%) from 3'-methylacetophenone (680 μL, 5.00 mmol) following general procedure D. The product was purified by flash silica chromatography using 0-30% EtOAc in hexane. R_F 0.65 (20% EtOAc in pentane); δ_H (300 MHz, $CDCl_3$) 7.58 (1H, s, H_2), 7.51 (1H, d, *J* 7.3, H_6), 7.30-7.24 (2H, m, H_4 and H_5), 2.36 (3H, s, $CNCH_3$), 2.35 (3H, s, Me), 2.25 (3H, s, $COCH_3$); δ_C (75 MHz, $CDCl_3$) 169.0 (*C*OCH_3), 162.6 (*C*NCH_3), 134.7 (C_3), 131.3 (C_4), 129.8 (C_1), 128.4 (C_5), 127.5 (C_2), 124.1 (C_6), 21.3 (Me), 19.7 (CO*C*H_3), 14.3 (CN*C*H_3); LCMS (ESI^+): *m/z* calculated for formula $C_{11}H_{13}NaNO_2$ [MNa^+] 214.1; found 214.1; IR (ν_{max}, film, cm^1): 3412, 3039, 2922, 2251, 1764, 1428, 1366, 1313, 1209, 1193, 1042. Spectral data consistent with the literature.[178]

(*E*)-1-(3-Methoxyphenyl)ethanone *O*-acetyl oxime 296

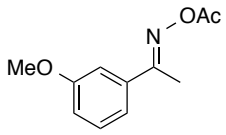

The desired compound was isolated as a colourless oil (969 mg, 94%) from 3'-methoxyacetophenone (686 μL, 5.00 mmol) following general procedure D. The product was purified by flash silica chromatography using 0-40% EtOAc in hexane. R_F 0.52 (20% EtOAc in pentane); δ_H (300 MHz, $CDCl_3$) 7.24-7.20 (3H, m, H_2, H_5 and H_6), 6.93-6.88 (1H, m, H_4), 3.74 (3H, s, OMe), 2.28 (3H, s, $COCH_3$), 2.17 (3H, s, $CNCH_3$); δ_C (75 MHz, $CDCl_3$) 168.8 (*C*OCH_3), 162.2 (C_3), 159.5 (*C*NCH_3), 136.1 (C_1), 129.4 (C_5), 119.3 (C_6), 116.2 (C_4), 112.9 (C_2), 55.2 (OMe), 19.6 (CO*C*H_3), 14.3 (CN*C*H_3); LCMS (ESI^+): *m/z* calculated for formula $C_{11}H_{13}NNaO_3$ [MNa^+] 230.1; found 230.0; IR (ν_{max}, film, cm^{-1}): 2940, 2837, 2251, 1762, 1577, 1428, 1366, 1320, 1236, 1194, 1041. Spectral data consistent with the literature.[64]

(*E*)-1-(Benzo[*d*][1,3]dioxol-5-yl)ethanone *O*-acetyl oxime 297

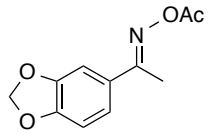

The desired compound was isolated as colourless needles (854 mg, 77%) from 3',4'-(methylenedioxy)acetophenone (810 mg, 5.00 mmol) following general procedure D. The crude material was crystallised from EtOAc–hexane. M.p. 108-110 °C (EtOAc–hexane); δ_H (300 MHz, $CDCl_3$) 7.29 (1H, d, *J* 1.8, H_4), 7.20 (1H, dd, *J* 1.8, 8.2, H_6), 6.80 (1H, d, *J* 8.2, H_7), 5.99 (2H, s, OCH_2O), 2.23 (3H, s, $COCH_3$), 2.24 (3H, s, $CNCH_3$); δ_C (75 MHz, $CDCl_3$) 169.0 (*C*OCH_3), 161.8 (*C*NCH_3), 149.8 (C_qO), 148.0 (C_qO), 128.8 (C_5), 122.1 (C_6), 108.1 (C_4), 107.0 (C_7), 101.6 (OCH_2O), 19.9 (CO*C*H_3), 14.3 (CN*C*H_3); HRMS (ESI^+): *m/z* calculated for formula $C_{11}H_{11}NNaO_4$ [MNa^+] 244.0580; found 244.0588; IR (ν_{max}, solid, cm^{-1}) 1756, 1591, 1439, 1214, 1032.

6.8 Preparation of isoquinoline library

General procedure (E) for the synthesis of isoquinolines

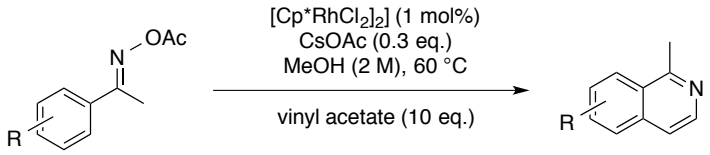

Vinyl acetate (922 μL, 10.0 mmol) was added to a solution of the acetylated oxime (1.00 mmol) in MeOH (0.5 mL, 2 M) with CsOAc (58 mg, 0.30 mmol) and $[Cp^*RhCl_2]_2$ (6 mg, 0.01 mmol) in a septum-topped vial under nitrogen. The reaction vials were sealed and heated to 60 °C for 48 hours. The crude reaction mixture was loaded on to a 5 g SCX column that was subsequently washed with MeOH (2 × 25 mL). The product eluted with the secondary wash using 0.7 M NH_3 in MeOH (2 × 25 mL) to give the clean product (>90% purity). Products containing impurities were purified using flash silica chromatography.

1-Methylisoquinoline 272

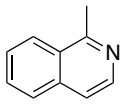

The desired compound was isolated as a brown oil (82 mg, 57%) from (*E*)-acetophenone *O*-acetyl oxime (177 mg, 1.00 mmol) following general procedure E. δ_H (300 MHz, $CDCl_3$) 8.37 (1H, d, *J* 5.7, H_3), 8.08 (1H, d, *J* 7.6, H_8), 7.77 (1H, d, *J* 7.8 Hz, H_5), 7.68-7.60 (1H, m, H_6), 7.60-7.52 (1H, m, H_7), 7.48 (1H, d, *J* 5.8, H_4), 2.94 (3H, s, CH_3); δ_C (75 MHz, $CDCl_3$) 158.6 (C_1), 141.8 (C_3), 135.8 (C_q), 129.9 (C_6), 127.2 (C_8 and C_q), 127.0 (C_7), 125.6 (C_5), 119.3 (C_4), 22.4 (CH_3); LRMS (ESI^+): *m/z* 144.0 [MH^+]; IR (ν_{max}, film, cm^{-1}) 2968, 1623, 1563, 1391. Data consistent with the literature.[255]

1-Methyl-6-nitroisoquinoline 283

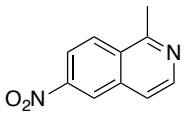

The desired compound was isolated as a brown oil (156 mg, 83%) from (*E*)-1-(4-nitrophenyl)ethanone *O*-acetyl oxime (222 mg, 1.00 mmol) following general procedure E. δ_H (300 MHz, $CDCl_3$) 8.72 (1H, d, *J* 2.0, H_5), 8.56 (1H, d, *J* 5.8, H_3), 8.36-8.24 (2H, m, H_7 and H_8), 7.69 (1H, d, *J* 5.8, H_4), 3.02 (3H, s, CH_3); δ_C (75 MHz, $CDCl_3$) 159.3 (C_1), 148.0 (C_6), 143.9 (C_3), 135.2 (C_q), 129.1 (C_q), 127.8 (C_8), 123.5 (C_5), 120.4 (C_4 and C_7), 22.7 (CH_3); HRMS (ESI^+): *m/z* calculated for formula $C_{10}H_9N_2O_2$ [MH^+] 189.0659; found 189.0660; IR (ν_{max}, solid, cm^{-1}) 3074, 1535, 1344, 906.

1-Methyl-6-(trifluoromethyl)isoquinoline 284

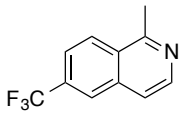

The desired compound was isolated as a brown oil (174 mg, 82%) from (*E*)-1-(4-(trifluoromethyl)phenyl)ethanone *O*-acetyl oxime (245 mg, 1.00 mmol) following general procedure E. δ_H (300 MHz, $CDCl_3$) 8.49 (1H, d, *J* 5.8, H_3), 8.22 (1H, d, *J* 8.8, H_8), 8.09 (1H, dt, *J* 1.9, 1.0, H_5), 7.75 (1H, dd, *J* 8.8, 1.8, H_7), 7.57 (1H, d, *J* 5.8, H_4), 2.99 (3H, s, CH_3); δ_C (75 MHz, $CDCl_3$) δ 158.9 (C_1), 143.2 (C_3), 135.0 (C_q), 131.6 (q, *J* 32.6, C_6), 128.3 (C_q), 126.9 (C_8), 124.9 (q, *J* 4.4, C_5), 123.9 (q, *J* 271.0, *C*F_3), 122.7 (q, *J* 3.1, C_7), 119.6 (C_4), 22.4 (CH_3); HRMS (ESI^+): *m/z* calculated for formula $C_{11}H_9F_3N$ [MH^+] 212.0682; found 212.0690; IR (ν_{max}, solid, cm^{-1}) 3060, 1590, 1574, 1340, 1237, 1127.

1,6-Dimethylisoquinoline 285

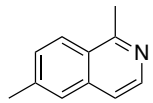

The desired compound was isolated as a brown oil (69 mg, 44%) from (*E*)-1-(*p*-tolyl)ethanone *O*-acetyl oxime (191 mg, 1.00 mmol) following general procedure E. δ_H (300 MHz, $CDCl_3$) 8.32 (1H, d, *J* 5.9, H_3), 8.00 (1H, d, *J* 8.6, H_8), 7.56 (1H, s, H_5), 7.47-7.39 (2H, m, H_4 and H_7), 2.95 (3H, s, 1-Me), 2.53 (3H, s, 6-Me); δ_C (75 MHz, $CDCl_3$) 158.0 (C_1), 141.0 (C_3), 140.6 (C_6), 136.4 (C_7), 129.6 (C_q), 126.2 (C_5), 125.8 (C_q), 125.6 (C_8), 119.2 (C_4), 21.9 (Me) 21.7 (Me); HRMS (ESI^+): *m/z* calculated for formula $C_{11}H_{12}N$ [MH^+] 158.0964; found 158.0962; IR (ν_{max}, solid, cm^{-1}) 1643, 1631, 1403, 1258, 1037.

8-Fluoro-1-methylisoquinoline 286

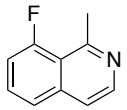

The desired product was isolated as a brown oil (66 mg, 41%) from (*E*)-1-(2-fluorophenyl)ethanone *O*-acetyl oxime (195 mg, 1.00 mmol) following general procedure E. The material was purified by column chromatography using 0-100% EtOAc in hexane without the use of an SCX column. R_F 0.73 (50% EtOAc in pentane); δ_H (300 MHz, $CDCl_3$) 8.37 (1H, d, *J* 5.8, H_3), 7.56-7.52 (2H, m, H_5 and H_6), 7.45 (1H, dd, *J* 5.8, 2.7, H_4), 7.22-7.14 (1H, m, H_7), 3.05 (3H, d, *J* 7.0, Me); δ_C (75 MHz, $CDCl_3$) 160.0 (d, *J* 256.8, C_8), 156.8 (d, *J* 5.9, C_1), 142.3 (d, *J* 1.8, C_3), 138.5 (d, *J* 3.5, C_q), 130.4 (d, *J* 9.3, C_6), 123.3 (d, *J* 4.5, C_5), 118.7 (d, *J* 3.7, C_4), 118.4 (d, *J* 14.1, C_q), 112.4 (d, *J* 23.2, C_7), 26.8 (d, *J* 10.7, Me); HRMS (ESI^+): *m/z* calculated for formula $C_{10}H_9FN$ [MH^+] 162.0714; found 162.0709; IR (ν_{max}, film, cm^{-1}): 2932, 1629, 1565, 1385, 1346, 1325, 1260, 1223, 1118, 1017.

6-Chloro-1-methylisoquinoline 287

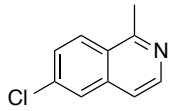

The desired compound was isolated as a brown oil (106 mg, 60%) from (*E*)-1-(4-chlorophenyl)ethanone *O*-acetyl oxime (211 mg, 1.00 mmol) following general procedure E. δ_H (300 MHz, $CDCl_3$) 8.40 (1H, d, *J* 5.8, H_3), 8.04 (1H, d, *J* 9.0, H_8), 7.77 (1H, d, *J* 2.1, H_5), 7.52 (1H, dd, *J* 9.0, 2.1, H_7), 7.41 (1H, d, *J* 5.8, H_4), 2.93 (3H, s, CH_3); δ_C (75 MHz, $CDCl_3$) 158.7 (C_1), 143.0 (C_3), 136.8 (C_q), 136.1 (C_6), 128.0 (C_7), 127.4 (C_8), 125.9 (C_5), 125.7 (C_q), 118.4 (C_4), 22.4 (CH_3); HRMS (ESI^+): *m/z* calculated for formula $C_{10}H_9{}^{35}ClN$ [MH^+] 178.0418; found 178.0421; IR (ν_{max}, solid, cm^{-1}) 3390, 3056, 1616, 1562, 1089.

6-Bromo-1-methylisoquinoline 288

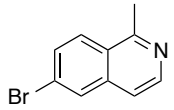

The desired compound was isolated as a brown oil (159 mg, 72%) from (*E*)-1-(4-bromophenyl)ethanone *O*-acetyl oxime (256 mg, 1.00 mmol) following general procedure E. δ_H (300 MHz, $CDCl_3$) 8.38 (1H, d, *J* 5.8, H_3), 7.96-7.90 (2H, m, H_5 and H_8), 7.63 (1H, dd, *J* 9.0, 1.9, H_7), 7.38 (1H, d, *J* 5.8, H_4), 2.91 (3H, s, CH_3); δ_C (75 MHz, $CDCl_3$) 158.8 (C_1), 142.7 (C_3), 137.1 (C_q), 130.6 (C_7), 129.3 (C_5), 127.4 (C_8), 125.9 (C_q), 124.7 (C_6), 118.3 (C_4), 22.3 (CH_3); HRMS (ESI^+): *m/z* calculated for formula $C_{10}H_9{}^{79}BrN$ [MH^+] 221.9913; found 221.9915; IR (ν_{max}, solid, cm^{-1}) 1611, 1560, 1393, 1077.

6-Iodo-1-methylisoquinoline 289

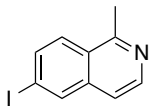

The desired compound was isolated as a tan crystalline solid (172 mg, 64%) from (*E*)-1-(4-iodophenyl)ethanone *O*-acetyl oxime (303 mg, 1.00 mmol) following general procedure E. The product was recrystallized from EtOAc–hexane. M.p. 132-134 °C (EtOAc–hexane); δ_H (300 MHz, $CDCl_3$) 8.41 (1H, d, *J* 5.9, H_3), 8.24 (1H, d, *J* 1.1, H_5), 7.88-7.84 (2H, m, H_7 and H_8), 7.42 (1H, d, *J* 5.8, H_4), 2.96 (3H, s, CH_3); δ_C (75 MHz, $CDCl_3$) 158.8 (C_1), 142.7 (C_3), 137.5 (C_q), 136.1 (C_5), 136.0 (C_7), 127.2 (C_8), 126.3 (C_q), 118.2 (C_4), 97.1 (C_6), 21.6 (CH_3); HRMS (ESI^+): *m/z* calculated for formula $C_{10}H_9IN$ [MH^+] 269.9774; found 269.9774; IR (ν_{max}, solid, cm^{-1}) 1607, 1558, 1392, 1072.

1-Methylbenzo[*h*]isoquinoline 290

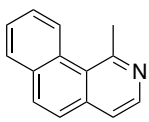

The desired product was isolated as a brown oil (46 mg, 24%) from (*E*)- and (*Z*)-1-(naphthalene-1-yl)ethanone *O*-acetyl oxime (229 mg, 1.00 mmol) (*E:Z*, 3:1) following general procedure E. The material was purified by column chromatography using 0-100% EtOAc in hexane without the use of an SCX column. R_F 0.61

(50% EtOAc in pentane); δ_H (500 MHz, $CDCl_3$) 8.89 (1H, d, *J* 8.5, H_{10}), 8.59 (1H, d, *J* 5.3, H_3), 7.96 (1H, dd, *J* 7.8, 1.5, H_7), 7.91 (1H, d, *J* 8.7, H_5), 7.74 (1H, ddd, *J* 8.6, 7.0, 1.6, H_9), 7.67 (1H, d, *J* 8.7, H_6), 7.67 (1H, ddd, *J* 8.0, 7.1, 1.1, H_8), 7.60 (1H, d, *J* 5.3, H_4), 3.35 (3H, s, Me); δ_C (75 MHz, $CDCl_3$) 157.0 (C_1), 143.1 (C_3), 138.0 (C_q), 133.6 (C_q), 131.9 (C_5), 130.5 (C_q), 129.3 (C_7), 127.2 (C_{10} and C_9), 126.8 (C_6 or C_8), 126.0 (C_6 or C_8), 125.5 (C_q), 120.4 (C_4), 30.3 (Me); HRMS (ESI^+): *m/z* calculated for formula $C_{14}H_{12}N$ [MH^+] 194.0964; found 194.0961; IR (ν_{max}, film, cm^{-1}): 2969, 2929, 1675, 1588, 1448, 1416, 1382, 1248.

8-Methoxy-1-methylisoquinoline 291

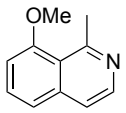

The desired product was isolated as a brown oil (23 mg, 14%) from (*E*)-1-(2-methoxyphenyl)ethanone *O*-acetyl oxime (207 mg, 1.00 mmol) following general procedure E. The material was purified by column chromatography using 0-100% EtOAc in hexane without the use of an SCX column. R_F 0.65 (50% EtOAc in pentane); δ_H (300 MHz, $CDCl_3$) 8.31 (1H, d, *J* 5.7, H_3), 7.53 (1H, t, *J* 8.0, H_6), 7.40 (1H, d, *J* 5.7, H_4), 7.32 (1H, d, *J* 7.6, H_5), 6.88 (1H, d, *J* 7.8, H_7), 3.97 (3H, s, OMe), 3.10 (3H, s, Me); δ_C (75 MHz, $CDCl_3$) 158.6 (C_1 or C_8), 158.2 (C_1 or C_8), 142.1 (C_3), 138.9 (C_q), 130.3 (C_6), 120.6 (C_q), 119.5 (C_5), 119.1 (C_4), 106.4 (C_7), 55.6 (OMe), 28.9 (Me); HRMS (ESI^+): *m/z* calculated for formula $C_{11}H_{12}NO$ [MH^+] 174.0913; found 174.0910; IR (ν_{max}, film, cm^{-1}): 2970, 2934, 1619, 1561, 1457, 1359, 1344, 1327, 1272, 1231, 1067.

6-Methoxy-1-methylisoquinoline 292

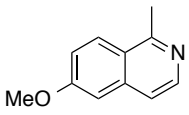

The desired compound was isolated as a brown oil (16 mg, 9%) from (*E*)-1-(4-methoxyphenyl)ethanone *O*-acetyl oxime (207 mg, 1.00 mmol) following general procedure E. δ_H (300 MHz, $CDCl_3$) 8.32 (1H, d, *J* 5.8, H_3), 8.02 (1H, d, *J* 9.2, H_8), 7.44 (1H, d, *J* 5.9, H_4), 7.23 (1H, dd, *J* 9.2, 2.6, H_7), 7.06 (1H, d, *J* 2.5, H_5), 3.95 (3H, s, OMe), 2.92 (3H, s, CH_3); δ_C (75 MHz, $CDCl_3$) 160.9 (C_6), 157.7 (C_1), 141.4 (C_3), 138.2 (C_q), 127.6 (C_8), 120.0 (C_7), 119.0 (C_4), 104.9 (C_5), 55.5 (OMe), 21.6 (CH_3), one C_q not observed; HRMS (ESI^+): *m/z* calculated for formula $C_{11}H_{12}NO$ [MH^+] 174.0913; found 174.0919; IR (ν_{max}, solid, cm^{-1}) 3249, 1619, 1514, 1251, 1179, 1029.

7-Bromo-1-methylisoquinoline 298a and 5-bromo-1-methylisoquinoline 298b

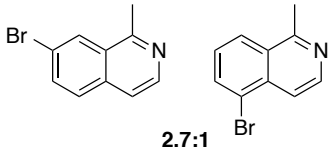

2.7:1

The regioisomeric compounds were isolated as an inseparable 1:2.7 mixture of 5-bromo-1-methylisoquinoline **298b** and 7-bromo-1-methylisoquinoline **298a** in the form of a brown oil

(131 mg, 50%) from (*E*)-1-(3-bromophenyl)ethanone *O*-acetyl oxime (256 mg, 1.00 mmol) following the general procedure. The material was purified by column chromatography using 0-100% EtOAc in hexane without the use of an SCX column. R_F 0.58 (50% EtOAc in pentane); δ_H (300 MHz, $CDCl_3$) 8.38 (1H, d, *J* 5.8, H_3, *major and minor*), 8.20 (0.73H, d *J* 1.7, H_8, *major*), 8.03 (0.27H, dd, *J* 8.4, 0.9, H_8, *minor*), 7.89 (0.27H, dd, *J* 7.5, 0.9, H_6, *minor*), 7.81 (0.27H, d, *J* 6.0, H_4, *minor*), 7.69 (0.73H, dd, *J* 8.7, 1.8, H_6, *major*), 7.61 (0.73H, d, *J* 8.7, H_5, *major*), 7.42 (0.73H, d, *J* 5.8, H_4, *major*), 7.37 (0.27H, t, *J* 8.0, H_7, *minor*), 2.93 (0.81H, s, Me, *minor*), 2.88 (2.19H, s, Me *major*); δ_C (75 MHz, $CDCl_3$) 159.0 (C_1, *minor*), 157.8 (C_1, *major*), 143.0 (C_3, *minor*), 142.1 (C_3, *major*), 135.1 (C_q, *minor*), 134.4 (C_q, *major*), 133.8 (C_6, *minor*), 133.5 (C_6, *major*), 129.0 (C_5, *major*), 128.6 (C_q, *minor*), 128.5 (C_q, *major*), 128.1 (C_8, *major*), 127.4 (C_8, *minor*), 125.4 (C_7, *minor*), 122.3 (C_5, *minor*), 120.8 (C_7, *major*), 119.0 (C_4, *major*), 118.2 (C_4, *minor*), 22.5 (Me, *minor*), 22.3 (Me, *major*); HRMS (ESI^+): *m/z* calculated for formula $C_{10}H_9{}^{79}BrN$ [MH^+] 221.9913; found 221.9912; IR (ν_{max}, film, cm^{-1}): 2919, 1579, 1557, 1488, 1400, 1365, 1346, 1299, 1070.

7-fluoro-1-methylisoquinoline 299a and 5-fluoro-1-methylisoquinoline 299b

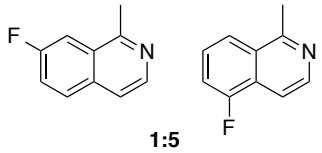

1:5

The regioisomeric compounds were isolated as an inseparable 5:1 mixture of 5-fluoro-1-methylisoquinoline **299b** and 7-fluoro-1-methylisoquinoline **299a** in the form of a brown oil (76 mg, 47%) from (*E*)-1-(3-fluorophenyl)ethanone *O*-acetyl oxime (195 mg, 1.00 mmol) following the general procedure. The material was purified by column chromatography using 0-100% EtOAc in hexane without the use of an SCX column. R_F 0.56 (50% EtOAc in pentane); δ_H (300 MHz, $CDCl_3$) 8.42 (0.83H, d, *J* 5.9, H_3, *major*), 8.35 (0.17H, d, *J* 5.8, H_3, *minor*), 7.85 (0.83H, d, *J* 8.5, H_8, *major*), 7.80-7.74 (0.34H, m, H_5 and H_8, *minor*), 7.71 (0.83H, d, *J* 5.9, H_4, *major*), 7.66 (0.17H, dd, *J* 9.9, 2.4, H_6, *minor*), 7.52-7.44 (0.83H, m, H_7, *major*), 7.43-7.37 (0.17H, m, H_4, *minor*), 7.30 (0.83H, dd, *J* 9.8, 7.8, H_6, *major*), 2.93 (2.49H, s, Me, *major*), 2.88 (0.51H, s, Me, *minor*); δ_C (75 MHz, $CDCl_3$) 160.8 (d, *J* 248.8, C_7, *minor*), 158.4 (d, *J* 2.7, C_1, *major*), 158.0 (d, *J* 5.7, C_1, *minor*), 158.0 (d, *J* 253.3, C_5, *major*), 141.9 (d, *J* 1.7, C_3, *major*), 141.0 (d, *J* 2.6, C_3, *minor*), 133.0 (C_q, *minor*), 129.8 (d, *J* 8.5, C_5, *minor*), 128.3 (d, *J* 7.9, C_q, *minor*), 128.6 (d, *J* 4.6, C_q, *major*), 126.8 (d, *J* 7.9, C_7, *major*), 126.6 (d, *J* 17.5, C_q, *major*), 121.4 (d, *J* 4.4, C_8, *major*), 120.5 (d, *J* 25.3, C_6, *minor*), 119.0 (C_4, *minor*), 113.5 (d, *J* 19.2, C_6, *major*), 111.9 (d, *J* 4.6, C_4, *major*), 109.2 (d, *J* 21.1, C_8, *minor*), 22.5 (Me, *major*), 22.1 (Me, *minor*); HRMS (ESI^+): *m/z* calculated for formula $C_{10}H_9FN$ [MH^+] 162.0714; found 162.0718; IR (ν_{max}, film, cm^{-1}): 2970, 2926, 1632, 1591, 1498, 1414, 1389, 1356, 1237, 1156.

1,7-Dimethylisoquinoline 300a and 1,5-dimethylisoquinoline 300b

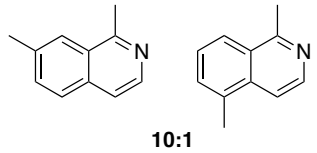

The regioisomeric compounds were isolated as an inseparable 1:10 mixture of 1,5-dimethylisoquinoline **300b** and 1,7-dimethylisoquinoline **300a** in the form of a brown oil (82 mg, 52%) from (*E*)-1-(3-methylphenyl)ethanone *O*-acetyl oxime (193 mg, 1.00 mmol) following the general procedure. The material was purified by column chromatography using 0-100% EtOAc in hexane without the use of an SCX column. R_F 0.56 (50% EtOAc in pentane); δ_H (300 MHz, $CDCl_3$) 8.40 (0.09H, d, *J* 6.0, *H_3 minor*), 8.31 (0.91H, d, *J* 5.8, H_3), 7.96-7.91(0.09H, m, *H_8 minor*), 7.84 (0.91H, d, *J* 1.5, H_8), 7.67 (0.91H, d, *J* 8.3, H_5), 7.60 (0.09H, d, *J* 6.1, *H_4 minor*), 7.47 (1H, dd, J 8.4, 1.5, H_6 and *H_6 or H_7 minor*), 7.44 (1H, d, *J* 5.7, H_4 and *H_6 or H_7 minor*), 2.94 (0.27H, s, *1-Me minor*), 2.91 (2.73H, s, 1-Me), 2.63 (0.27H, s, *5-Me minor*), 2.54 (2.73H, s, 7-Me); δ_C (75 MHz, $CDCl_3$) Signals for major isomer only: 157.8 (C_1), 140.8 (C_3), 137.0 (C_7), 134.2 (C_q), 132.3 (C_6), 127.7 (C_q), 127.1 (C_5), 124.6 (C_8), 119.2 (C_4), 22.2 (1-Me), 22.1 (7-Me); HRMS (ESI^+): *m/z* calculated for formula $C_{11}H_{12}N$ [MH^+] 158.0964; found 158.0961; IR (ν_{max}, film, cm^{-1}): 2919, 1589, 1561, 1434, 1411, 1366, 1309, 1239.

7-Methoxy-1-methylisoquinoline 301a and 5-methoxy-1-methylisoquinoline 301b

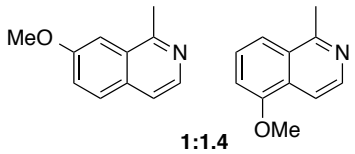

Mixed fractions of 5-methoxy-1-methylisoquinoline **301b** and 7-methoxy-1-methylisoquinoline **301a** (51 mg, 29%, 1:5) and pure fractions of 5-methoxy-1-methylisoquinoline **301b** (49 mg, 29%) were isolated in the form of brown oils (combined yield: 100 mg, 58%, 1.4:1 ratio of 5-:7-) from (*E*)-1-(3-methoxyphenyl)ethanone *O*-acetyl oxime (207 mg, 1.00 mmol) following the general procedure. The material was purified by column chromatography using 0-100% EtOAc in hexane without the use of an SCX column. δ_H (300 MHz, $CDCl_3$) 8.38 (1H, d, *J* 5.9, H_3, *major*), 8.27 (0.8H, d, *J* 5.7, H_3, *minor*), 7.88 (1H, d, *J* 5.9, H_4, *major*), 7.68 (0.8H, d, *J* 8.9, H_5, *minor*), 7.65 (1H, d, *J* 8.5, 0.7, H_8, *major*), 7.47 (1H, t, *J* 8.1, H_7, *major*), 7.41 (0.8H, d, *J* 5.7, H_4, *minor*), 7.30 (0.8H, dd, *J* 8.9, 2.5, H_6, *minor*), 7.25 (0.8H, d, *J* 2.5, H_8, *minor*), 6.97 (1H, dd, *J* 7.7, 0.7, H_6, *major*), 3.98 (3H, s, OMe, *major*), 3.93 (2.4H, s, OMe, *minor*), 2.93 (3H, s, Me, *major*), 2.89 (2.4H, s, Me, *minor*); δ_C (75 MHz, $CDCl_3$) 158.2 (C_1, *minor*), 158.0 (C_1, *major*), 156.9 (C_7, *minor*), 155.0 (C_5, *major*), 141.5 (C_3, *major*), 134.0 (C_3, *minor*), 131.4 (C_q, *minor*), 128.8 (C_5, *minor*), 128.7 (C_q, *major*), 128.6 (C_q, *minor*), 128.3 (C_q, *major*), 127.0 (C_7, *major*), 122.7 (C_6, *minor*), 119.1 (C_4, *minor*), 117.5 (C_8, *major*), 113.6 (C_4, *major*), 107.4 (C_6, *major*), 103.5 (C_8, *minor*), 55.8 (OMe, *major*), 55.5 (OMe, *minor*), 22.8 (Me, *major*), 22.4 (Me, *minor*); HRMS (ESI^+): *m/z* calculated for formula

$C_{11}H_{12}NO$ [MH^+] 174.0913; found 174.0908. IR (ν_{max}, film, cm^{-1}): 2957, 2935, 2836, 1621, 1585, 1495, 1446, 1412, 1389, 1353, 1261, 1248, 1181, 1041.

6-Methyl-[1,3]dioxolo[4,5-*f*]isoquinoline 297b

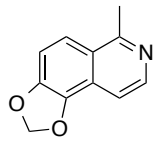

The desired compound was isolated as a brown oil (58 mg, 36%) after column chromatography using 10-30% EtOAc in hexane, from (*E*)-1-(benzo[*d*][1,3]dioxol-5-yl)ethanone *O*-acetyl oxime (221 mg, 1.00 mmol) following general procedure E. δ_H (300 MHz, $CDCl_3$) 8.31 (1H, d, *J* 5.9, H_8), 7.74 (1H, d, *J* 8.7, H_5), 7.47 (1H, d, *J* 5.9, H_9), 7.26 (1H, d, *J* 8.7, H_4), 6.22 (2H, s, OCH_2O), 2.92 (3H, s, CH_3); δ_C (75 MHz, $CDCl_3$) 158.9 (C_6), 146.5 (C_qO), 141.6 (C_8), 140.8 (C_qO), 123.9 (C_q), 122.0 (C_q), 120.6 (C_4), 111.4 (C_5), 110.9 (C_9), 102.3 (OCH_2O), 23.0 (CH_3); HRMS (ESI^+): *m/z* calculated for formula $C_{11}H_{10}NO_2$ [MH^+] 188.0706; found 188.0700; IR (ν_{max}, solid, cm^{-1}) 1646, 1594, 1471, 1428, 1284, 1052.

Decumbenine B intermediate

(*E*)-Benzo[*d*][1,3]dioxole-5-carbaldehyde oxime[256]

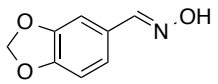

Hydroxylamine hydrochloride (1.73 g, 25.0 mmol) was added to a solution of piperonal (3.0 g, 20 mmol) in a solution of water/ice–EtOH (3:1, 20 mL, 1.0 M) at 0 °C. Sodium hydroxide (1.6 g, 40 mmol) in water (5 mL) was added to the reaction which was left to warm to room temperature. After four hours, the reaction was complete (by TLC). The aqueous layer was extracted with Et_2O (30 mL). The aqueous phase was cooled and acidified to pH 1 using 6 N HCl and extracted with Et_2O (3 × 30 mL). The organic layers were combined, dried with $MgSO_4$, filtered and the solvent was removed *in vacuo* to afford a colourless amorphous solid (3.16 g, 96%) which was not purified further. δ_H (300 MHz, $CDCl_3$) 8.04 (1H, s, HCN), 7.50 (1H, s, OH), 7.17 (1H, d, *J* 1.5, H_4), 6.96 (1H, dd, *J* 8.0, 1.5, H_6), 6.81 (1H, d, *J* 8.0, H_7), 6.00 (2H, s, OCH_2O); δ_C (75 MHz, $CDCl_3$) δ 150.2 (*H*CN), 149.5 (C_qO), 148.4 (C_qO), 126.5 (C_5), 123.1 (C_6), 108.5 (C_7), 105.8 (C_4), 101.6 (C_2); LCMS (ESI^+): *m/z* calculated for formula $C_8H_8NO_3$ [MH^+] 166.0; found 166.0; IR (ν_{max}, solid, cm^{-1}): 3222, 3124, 2998, 2917, 1605, 1497, 1445, 1357, 1317, 1249, 1195, 1124, 1107, 1034. Spectral data consistent with the literature.[256,257]

(*E*)-Benzo[*d*][1,3]dioxole-5-carbaldehyde *O*-acetyl oxime 312

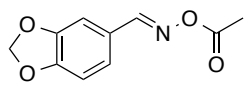

Acetyl chloride (1.85 mL, 15.0 mmol) was added to a solution of (*E*)-benzo[*d*][1,3]dioxole-5-carbaldehyde oxime (1.65 g, 10.0 mmol) in pyridine (10 mL, 2.0 M) with catalytic DMAP (5 mg). After 4 hours,

water (30 mL) was added to quench the reaction and the product was extracted with EtOAc (2 × 50 mL). The organic layers were combined and washed with 1 N HCl (50 mL), brine (50 mL), dried with $MgSO_4$, filtered and concentrated *in vacuo*. The crude material was crystallised from Et_2O–pentane to afford a colourless crystalline solid (1.94 g, 73%). M.p. 107-109 °C (EtOAc–pentane); δ_H (300 MHz, $CDCl_3$) 8.24 (1H, s, HCN), 7.35 (1H, d, *J* 1.6, H_4), 7.08 (1H, dd, *J* 8.0, 1.6, H_6), 6.83 (1H, d, *J* 8.0, H_7), 6.03 (2H, s, OCH_2O), 2.22 (3H, s, COMe); δ_C (75 MHz, $CDCl_3$) 168.9 (*C*OMe), 155.6 (H*C*N), 151.0 (C_qO), 148.6 (C_qO), 125.3 (C_6), 124.4 (C_5), 108.6 (C_7), 106.7 (C_4), 101.9 (C_2), 19.8 (Me); HRMS (ESI^+): *m/z* calculated for formula $C_{10}H_{10}NO_4$ - $[MH^+]$ 208.0604; found 208.0601; IR (ν_{max}, solid, cm^{-1}): 2914, 2855, 1757, 1596, 1508, 1493, 1439, 1359, 1338, 1253, 1209, 1100, 1035, 1001.

[1,3]Dioxolo[4,5-*f*]isoquinoline 310

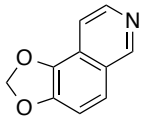

The desired compound was isolated as a brown amorphous solid (45 mg, 26%) from (*E)*-benzo[*d*][1,3]dioxole-5-carbaldehyde *O*-acetyl oxime (207 mg, 1.00 mmol) following general procedure E. δ_H (300 MHz, $CDCl_3$) 9.16 (1H, s, H_6), 8.43 (1H, d, *J* 5.8, H_8), 7.60-7.57 (2H, m, H_5 and H_9), 7.29 (1H, d, *J* 8.7, H_4), 6.23 (2H, s, OCH_2O); δ_C (75 MHz, $CDCl_3$) 152.9 (C_6), 147.1 (C_q-O_3), 142.8 (C_q-O_1), 140.3 (C_q), 125.3 (C_q), 122.9 (C_5), 121.8 (C_q), 112.7 (C_9), 111.8 (C_4), 102.5 (OCH_2O); LRMS (ESI^+): *m/z* 174.1 $[MH^+]$; IR (ν_{max}, solid, cm^{-1}): 2897, 1648, 1549, 1466, 1431, 1369, 1287, 1261, 1070, 1050, 1020. Spectral data consistent with the literature.[173]

Benzo[*d*][1,3]dioxole-5-carbonitrile 313

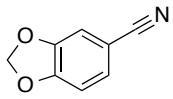

The remaining starting material rearranged to give the benzo[*d*][1,3]dioxole-5-carbonitrile, of which a sample was isolated from the column. For reference: δ_H (300 MHz, $CDCl_3$) 7.13 (1H, dd, *J* 8.1, 1.6, H_6), 6.96 (1H, d, *J* 1.3, H_4), 6.85 (1H, d, *J* 8.4, H_7), 5.99 (2H, s, OCH_2O); δ_C (75 MHz, $CDCl_3$) 151.7 (C_qO), 148.2 (C_qO), 128.3 (C_6), 119.0 (CN), 111.5 (C_7), 109.2 (C_4), 105.1 (C_5), 102.3 (OCH_2O). The ^1H NMR data was consistent with the literature.[258]

6.9 Preparation of imide derivatives

Isoindolo[2,1-*b*]isoquinoline-5,7-dione 143

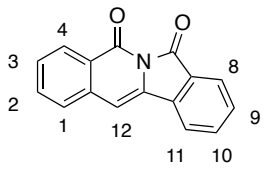

A solution of *N*-methoxybenzamide (302 mg, 2.00 mmol), CsOAc (115 mg, 0.600 mmol), $[Cp^*RhCl_2]_2$ (12 mg, 2.0 mol%) and vinyl acetate (277 μL, 3.00 mmol) in MeOH (5 mL, 0.4 M) was heated for 48 hours at 60 °C. The reaction mixture was concentrated *in vacuo* and subsequently purified by flash silica chromatography using 50% EtOAc in hexane to afford isoindolo[2,1-*b*]isoquinoline-5,7-dione as a bright yellow amorphous solid (28 mg, 6%). R_F 0.33 (1:1 petrol–EtOAc) strong blue fluorescent trace; δ_H (500 MHz, $CDCl_3$) 8.51 (1H, d, *J* 7.9, H_4), 8.02 (1H, d, *J* 7.6, H_8), 7.81 (1H, d, *J* 7.6 H_{11}), 7.74 (1H, t, *J* 7.6, H_{10}), 7.69 (1H, t, *J* 7.9, H_2), 7.58 (1H, t, *J* 7.9, H_9), 7.57 (1H, d, *J* 7.9, H_1), 7.53 (1H, t, *J* 7.6, H_3), 6.98 (1H, s, H_{12}); δ_H (500 MHz, DMF-d_7) 8.36 (1H, d, *J* 6.8, ArH), 8.19 (1H, d, *J* 7.1, ArH), 7.98 (1H, d, *J* 7.5, ArH), 7.91 (1H, t, *J* 7.5, ArH), 7.85-7.77 (2H, m, ArH), 7.71 (1H, t, *J* 7.0, ArH), 7.63 (1H, t, *J* 7.5, ArH), 7.55 (1H, s);[85] δ_C (75 MHz, $CDCl_3$) 165.1 (C_7O), 159.8 (C_5O), 135.6 (C_q), 135.1 (C_q), 134.7 (C_{10}), 134.3 (C_q), 133.9 (C_2), 130.6 (C_1 or C_9), 129.5 (C_4), 128.5 (C_3), 128.3 (C_q), 127.8 (C_q), 127.4 (C_1 or C_9), 125.7 (C_8), 120.5 (C_{11}), 103.6 (C_{12}); HRMS: *m/z* calculated for formula $C_{16}H_9NNaO_2$ [MNa^+]: 270.0525; found 270.0528; IR (ν_{max}, solid, cm^{-1}): 2925, 2852, 1838, 1759, 1682, 1639, 1607, 1520, 1473, 1380, 1340, 1289, 1277, 1178, 1089, 1030, 957, 928, 860, 766, 702; Spectral data consistent with the literature.[85]

General procedure (F) for the synthesis of methyl-2-alkynyl benzoates

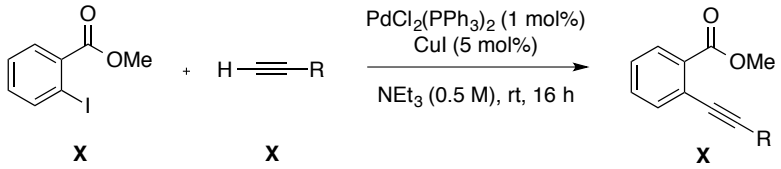

X X X

Following a modified procedure by Larock *et al.,*[209] a nitrogen degassed solution of the terminal alkyne (1.1 eq.), methyl iodobenzoate (1.0 eq.), CuI (0.05 eq.) and $PdCl_2(PPh_3)_2$ (0.01 eq.) in NEt_3 (0.5 M) were stirred for 16 hours at room temperature. The reaction solution was concentrated *in vacuo*, rediluted in DCM, washed with saturated sodium thiosulphate, brine, dried ($MgSO_4$) and concentrated *in vacuo*. The crude material was purified by flash silica chromatography to afford the desired product. The alkynes below are numbered according to the following system:

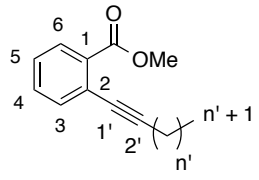

General procedure (G) for the synthesis of tetracyclic imides

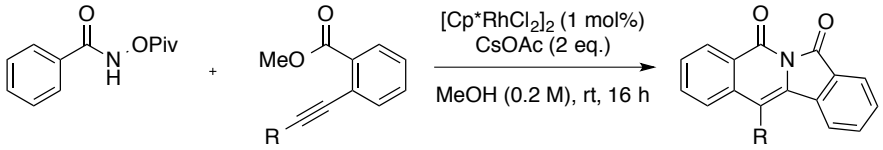

X X X

A solution of $[Cp^*RhCl_2]_2$ (1 mol%), CsOAc (2 eq.), *N*-(pivaloyloxy)benzamide (1 eq.) and the methyl alkynyl benzoate derivative (1.5 eq.) were stirred in MeOH (0.2 M) overnight at room temperature. Upon completion of the reaction, the crude mixture was concentrated *in vacuo*. The crude product was purified by various methods depending on the substrate (see below).

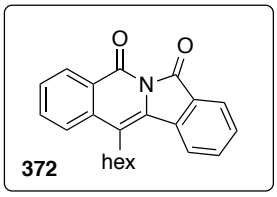

Methyl 2-(oct-1-yn-1-yl)benzoate 370[209]

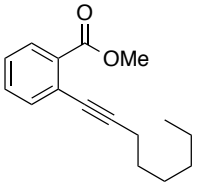

Isolated as a pale yellow oil (3.26 g, 76%) from 1-octyne (3.54 mL, 24.0 mmol) following general procedure F. The product was isolated by flash silica chromatography using 0-5% EtOAc in hexane. R_F 0.4 (10% EtOAc in hexane); δ_H (300 MHz, $CDCl_3$) 7.87 (1H, dd, *J* 7.8, 1.0, H_6), 7.51 (1H, dd, *J* 7.7, 1.0, H_3), 7.41 (1H, td, *J* 7.6, 1.4, H_4), 7.30 (1H, td, *J* 7.7, 1.4, H_5), 3.91 (3H, s, OMe), 2.47 (2H, t, *J* 7.0, $H_{3'}$), 1.68-1.57 (2H, m, $H_{4'}$), 1.48-1.46 (2H, m, $H_{5'}$), 1.38-1.28 (4H, m, $H_{6'}$ and $H_{7'}$), 0.90 (3H, t, *J* 6.8, $H_{8'}$); δ_C (75 MHz, $CDCl_3$) 167.2 (CO_2Me), 134.4 (C_3), 132.1 (C_q), 131.6 (C_4), 130.3 (C_6), 127.2 (C_5), 124.7 (C_q), 96.2 ($C_{2'}$), 79.3 ($C_{1'}$), 52.2 (OMe), 31.6 ($C_{3'}$), 28.8 ($C_{4'}$), 28.8 ($C_{5'}$), 22.7 ($C_{6'}$), 20.0 ($C_{7'}$), 14.2 ($C_{8'}$); HRMS (ESI^+): *m/z* calculated for formula: $C_{16}H_{21}O_2$ [MH^+] 245.1536; found 245.1534; IR (ν_{max}, solid, cm^{-1}): 2952, 2857, 2227, 1732, 1484, 1447, 1291, 1247, 1128, 1081. Spectral data was consistent with the literature.[209]

Purification of the parent imide 372

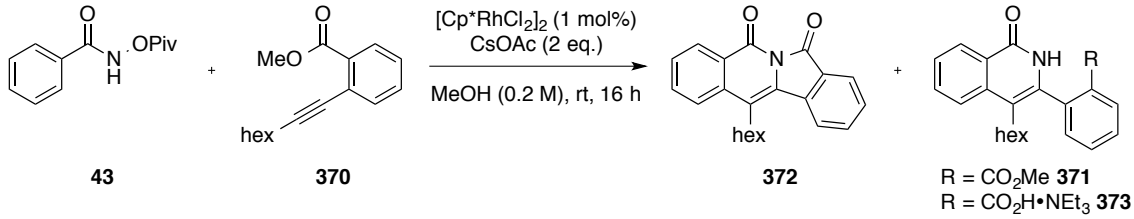

N-(Pivaloyloxy)benzamide (221 mg, 1.00 mmol), $[Cp^*RhCl_2]_2$ (6 mg, 0.01 mmol), CsOAc (382 mg, 2.00 mmol) and methyl 2-(1-octynyl)benzoate (366 mg, 1.50 mmol) were dissolved in MeOH (5 mL, 0.2 M). The reaction was stirred at room temperature for 16 hours and concentrated *in vacuo*. The reaction was initially purified by flash silica chromatography (A), however, due to the poor recovery an alternative precipitation and crystallisation work up (B) was employed.

(A) Purification using flash silica chromatography:

The crude material was purified by flash silica chromatography using 0-40% EtOAc in hexane (0-40%) with triethylamine (2.5% v/v), followed by a 10% MeOH in DCM flush to afford three

products: 12-hexylisoindolo[2,1-*b*]-isoquinoline-5,7-dione **372** as a yellow amorphous solid (11 mg, 3%); methyl 2-(4-hexyl-1-oxo-1,2-dihydroisoquinolin-3-yl)benzoate **371** (69 mg, 19%) as a colourless amorphous solid; and 2-(4-hexyl-1-oxo-1,2-dihydroisoquinolin-3-yl)benzoic acid, triethylamine salt **373** as an orange amorphous solid (121 mg, 27%).

(B) Purification using precipitation and crystallisation:

The crude reaction was suspended in cold ether (0 °C) and 2M HCl in ether (5 mL) was added to the solution to precipitate the product. The solid was filtered and redissolved in $CHCl_3$. CsOAc was filtered off from the solution, which was concentrated *in vacuo* and the crude product was crystallised from EtOAc. The desired imide **372** was isolated as yellow needles (176 mg, 53%).

12-Hexylisoindolo[2,1-*b*]isoquinoline-5,7-dione 372

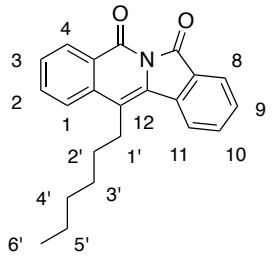

R_F 0.33 (50% EtOAc in hexane); M.p. 172-175 °C (EtOAc); δ_H (300 MHz, $CDCl_3$) 8.56 (1H, d, *J* 7.9, H_4), 8.07 (1H, d, *J* 7.6, H_8), 7.90 (1H, d, *J* 7.9, H_1 or H_{11}), 7.80-7.71 (3H, m, H_3 and ArH), 7.58-7.52 (2H, m, ArH), 3.19-3.08 (2H, m, $H_{1'}$), 1.75 (2H, dt, *J* 10.9, 7.3, $H_{2'}$), 1.67-1.54 (2H, m, $H_{3'}$), 1.49-1.31 (4H, m, $H_{4'}$ and $H_{5'}$), 0.94 (3H, t, *J* 7.0, $H_{6'}$); δ_C (75 MHz, $CDCl_3$) 165.4 (C_7O), 159.9 (C_5O), 136.6 (C_q) 135.4 (C_q), 135.0, 134.0 (C_3), 131.1 (C_q), 129.8 (C_4), 129.7, 128.7 (C_q), 128.5, 128.4 (C_q), 126.0 (C_8), 124.1, 123.8, 119.9 (C_q), 31.8 ($C_{4'}$), 29.9 ($C_{3'}$), 29.2 ($C_{2'}$), 26.8 ($C_{1'}$), 22.8 ($C_{5'}$), 14.2 ($C_{6'}$); HRMS (ESI^+): *m/z* calculated for formula: $C_{22}H_{22}NO_2$ [MH^+] 332.1645; found 332.1635; IR (ν_{max}, solid, cm^{-1}): 3080, 2952, 2851, 1758, 1673, 1599, 1472, 1293, 1157, 1097, 1034.

Methyl 2-(4-hexyl-1-oxo-1,2-dihydroisoquinolin-3-yl)benzoate 371

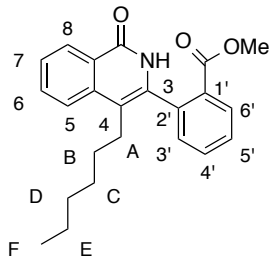

R_F 0.2 (50% EtOAc in hexane); δ_H (500 MHz, $CDCl_3$) 10.08 (1H, s, NH), 8.43 (1H, d, *J* 8.0, H_8), 8.13 (1H, dd, *J* 7.9, 1.3, $H_{6'}$), 7.72-7.71 (2H, m, H_6 and H_5), 7.63 (1H, td, *J* 7.5, 1.5, $H_{4'}$), 7.58 (1H, td, *J* 7.6, 1.3, $H_{5'}$), 7.52-7.47 (1H, m, H_7), 7.40 (1H, dd, *J* 7.3, 1.2, $H_{3'}$), 3.62 (3H, s, OMe), 2.51-2.33 (2H, m, H_A), 1.46-1.37 (2H, m, H_B), 1.21-1.08 (6H, m, H_C, H_D and H_E), 0.80 (3H, t, *J* 7.2, H_F); δ_C (125 MHz, $CDCl_3$) 166.4 (CO_2Me), 162.8 (C_1O), 138.1 (C_q), 136.7 (C_q), 135.7 (C_q), 132.7 ($C_{4'}$), 132.4 (C_5 or C_6), 131.6 ($C_{3'}$), 131.1 ($C_{6'}$), 130.5 (C_q), 129.5 ($C_{5'}$), 128.2 (C_8), 126.2 (C_7), 125.6 (C_q), 123.7 (C_5 or C_6), 114.5 (C_q), 52.3 (OMe), 31.5 (C_D), 29.8 (C_C), 29.5 (C_B), 27.6 (C_A), 22.6 (C_E), 14.1 (C_F); HRMS (ESI^+): *m/z*

calculated for formula: $C_{23}H_{25}NNaO_3$ [MNa^+] 386.1727; found 386.1737; IR (ν_{max}, solid, cm^{-1}): 2978, 2602, 2496, 1647, 1605, 1552, 1445, 1474, 1376, 1172, 1036.

2-(4-Hexyl-1-oxo-1,2-dihydroisoquinolin-3-yl)benzoic acid, triethylamine salt 373

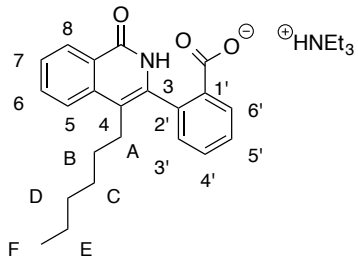

δ_H (300 MHz, $CDCl_3$) 9.50 (2H, br s, NH and $HNEt_3$), 8.37 (1H, d, *J* 8.0, $H_{6'}$), 7.86 (1H, dd, *J* 7.3, 1.6, H_8), 7.67-7.66 (2H, m, $H_{3'}$ and H_5), 7.44-7.33 (3H, m, $H_{4'}$, $H_{5'}$ and H_6), 7.28-7.24 (1H, m, H_7), 2.48-2.33 (2H, m, H_A), 2.91 (6H, q, *J* 7.2, $N(CH_2CH_3)_3$) 1.55-1.42 (2H, m, H_B), 1.40-1.23 (2H, m, H_C), 1.15-1.13 (13H, m, H_D, H_E and $N(CH_2CH_3)_3$), 0.76 (3H, t, *J* 6.9, H_F); δ_C (75 MHz, $CDCl_3$) 172.0 (CO_2^-), 162.1 (C_1O), 138.4 (C_q), 138.4 (C_q), 137.2 (C_q), 133.7 (C_q), 132.3 ($C_{3'}$ or C_5), 130.4 (C_8), 130.0 (C_7), 129.5, 129.1, 127.8 ($C_{6'}$), 125.6 (ArH and C_q), 123.5 ($C_{3'}$ or C_5), 114.1 (C_q), 45.4 ($N(CH_2CH_3)_3$), 31.4 (C_D), 29.9 (C_C), 29.4 (C_B), 27.6 (C_A), 22.5 (C_E), 14.0 (C_F), 8.40 ($N(CH_2CH_3)_3$); HRMS (ESI^+): *m/z* calculated for formula: $C_{22}H_{24}NO_3$ [MH^+] 350.1751; found 350.1758; IR (ν_{max}, solid, cm^{-1}): 2978, 2602, 2496, 1647, 1605, 1552, 1445, 1474, 1376, 1172, 1036.

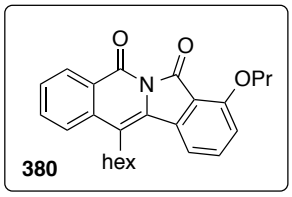

380

Methyl 2-iodo-6-propoxybenzoate 385

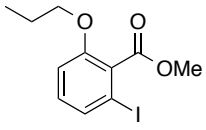

Following a modified procedure by Taylor *et al.*,[213] *s*-BuLi (7.5 mL, 11 mmol, 1.4 M in cyclohexane) was added to a solution of TMEDA (1.57 mL, 10.5 mmol) in THF (20 mL). The resultant yellow solution was cooled to −100 °C (ethanol–N_2 bath) and 2-propoxybenzoic acid (800 mg, 4.44 mmol) in THF (9 mL) was added *via* a syringe pump over 30 minutes. After a further 30 minutes at −100 °C, the orange/brown solution was warmed to −78 °C. Iodine (4.41 g, 17.4 mmol) in THF (5 mL) was added dropwise to the stirred solution at −78 °C, and the reaction mixture was subsequently stirred for another hour after the addition was complete. The reaction was quenched with saturated ammonium chloride solution (5 mL) and the solution was warmed to room temperature. The unreacted iodine was quenched with saturated sodium thiosulphate solution (40 mL). The phases were separated and the aqueous phase was extracted with Et_2O (30 mL) and the organic phase was re-extracted with 2N NaOH (10 mL). The aqueous phases were combined and acidified to pH 2 with 4N HCl. The aqueous phase was extracted with DCM (4 × 50 mL) and dried over $MgSO_4$. The reaction was filtered and concentrated *in vacuo* to afford an oily yellow solid. The crude residue was rediluted in DCM (10 mL) with catalytic DMF (10 μL) and oxalyl chloride (300 μL, 3.54 mmol). The reaction mixture was concentrated *in vacuo* and methanol was added to the residue. The solvent was removed *in vacuo* and the crude material was purified by flash silica chromatography, using 10-30% EtOAc in hexane to afford a clear oil (454 mg, 32%). R_F 0.71 (50% EtOAc in hexane); δ_H (300 MHz, $CDCl_3$) 7.37 (1H, d, *J* 7.9, H_3), 7.02 (1H, t, *J* 8.1, H_4), 6.88 (1H, d, *J* 8.4, H_5), 3.98-3.87 (5H, m, OMe and OCH_2), 1.80-1.71 (2H, m, OCH_2CH_2), 0.99 (3H, t, *J* 7.4, $O(CH_2)_2CH_3$); δ_C (75 MHz, $CDCl_3$) 168.1 (CO_2Me), 156.5 (C_6), 131.6 (C_3), 130.8 (C_4), 120.2 (C_1), 112.0 (C_5), 92.4 (C_2), 70.7 (OCH_2), 52.8 (OMe), 22.5 (OCH_2CH_2), 10.5 ($O(CH_2)_2CH_3$); HRMS (ESI^+): *m/z* calculated for formula $C_{11}H_{14}IO_3$ [MH^+]: 320.9982; found 320.9985; IR (ν_{max}, solid, cm^{-1}): 2966, 2877, 1753, 1583, 1567, 1443, 1391, 1265, 1190, 1151, 1106, 1062, 1014.

Methyl 2-(oct-1-yn-1-yl)-6-propoxybenzoate 386

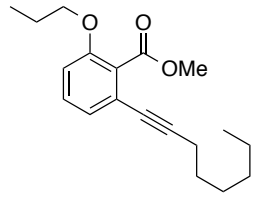

The desired compound was isolated as a brown oil (382 mg, 90%) from methyl 2-iodo-6-propoxybenzoate (454 mg, 1.41 mmol) and 1-octyne (230 μL, 1.56 mmol) following general procedure F. The product was isolated by flash silica chromatography using 0-10% EtOAc in hexane. R_F 0.49 (10% EtOAc in hexane); δ_H (500 MHz, $CDCl_3$) 7.23 (1H, t, *J* 8.1, H_4), 6.99 (1H, d, *J* 7.7, H_3), 6.83 (1H, d, *J* 8.4, H_5), 3.94 (2H, t, *J* 6.4, OCH_2), 3.90 (3H, s, *J* 3.2, OMe), 2.38 (2H, t, *J* 7.1, $H_{3'}$), 1.81-1.72 (2H, m, OCH_2CH_2), 1.61-1.53 (2H, m, $H_{4'}$), 1.43 (2H, q, *J* 7.8, $H_{5'}$), 1.36-1.26 (4H, m, $H_{6'}$ and $H_{7'}$), 1.00 (3H, t, *J* 7.4, $O(CH_2)_2CH_3$), 0.90 (3H, t, *J* 7.0, $3H_{8'}$); δ_C (125 MHz, $CDCl_3$); 167.9 (CO_2Me), 155.8 (C_6), 130.3 (C_4), 126.8 (C_1), 124.4 (C_3), 123.0 (C_2), 111.9 (C_5), 94.4 ($C_{2'}$), 77.7 ($C_{1'}$), 70.5 (OCH_2), 52.4 (OMe), 31.5 ($C_{6'}$), 28.8 ($C_{5'}$), 28.7 ($C_{4'}$), 22.7 ($C_{7'}$), 22.6 (OCH_2CH_2), 19.6 ($C_{3'}$), 14.2 ($O(CH_2)_2CH_3$), 10.5 ($C_{8'}$); HRMS (ESI^+): *m/z* calculated for formula: $C_{19}H_{27}O_3$ [MH^+] 303.1955; found 303.1959; IR (ν_{max}, solid, cm^{-1}): 2933, 2875, 2859, 2246, 1737, 1594, 1574, 1456, 1430, 1390, 1302, 1278, 1261, 1117, 1090, 1067.

12-Hexyl-8-propoxyisoindolo[2,1-*b*]isoquinoline-5,7-dione 387

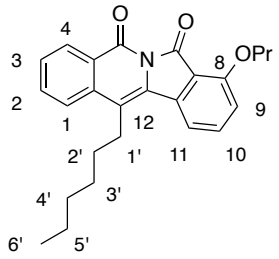

The desired compound was isolated as yellow needles (106 mg, 32%) from methyl 2-(oct-1-yn-1-yl)-6-propoxybenzoate (290 mg, 0.960 mmol, **1.10 eq**.) and *N*-(pivaloyloxybenzamide) (192 mg, 0.870 mmol) following general procedure G. The crude reaction mixture was treated with 2N HCl in ether (1 mL) and stirred for 2 hours to convert the methyl ester to the imide. The solvent was removed *in vacuo* and the product was crystallised from cold MeOH. R_F 0.3 (33% EtOAc in hexane); M.p. 142-144 °C (MeOH); δ_H (500 MHz, $CDCl_3$) 8.55 (1H, dd, *J* 7.9, 0.8, H_4), 7.76-7.69 (2H, m, H_1 and H_2), 7.63 (1H, t, *J* 8.1, H_{10}), 7.51 (1H, ddd, *J* 8.1, 6.7, 1.5, H_3), 7.43 (1H, d, *J* 7.8, H_{11}), 6.97 (1H, d, *J* 8.3, H_9), 4.13 (2H, t, *J* 6.4, OCH_2), 3.13-3.05 (2H, m, $H_{1'}$), 2.00-1.87 (2H, m, OCH_2CH_2), 1.72 (2H, ddd, *J* 11.6, 10.4, 6.4, $H_{2'}$), 1.64-1.54 (2H, m, $H_{3'}$), 1.47-1.31 (4H, m, $H_{4'}$ and $H_{5'}$), 1.13 (3H, t, *J* 7.4, $O(CH_2)_2CH_3$), 0.93 (3H, t, *J* 7.1, $H_{6'}$); δ_C (126 MHz, $CDCl_3$) 163.2 (C_5O), 159.7 (C_7O), 159.2 (C_8), 137.6 (C_q), 136.6 (C_q), 136.4 (C_{10}), 133.7 (C_2 or C_1), 130.8 (C_q), 129.7 (C_4), 128.7 (C_q), 128.2 (C_3), 123.9 (C_2 or C_1), 119.3 (C_q), 115.7 (C_q), 115.6 (C_{11}), 113.3 (C_9), 70.8 (OCH_2), 31.8 ($C_{4'}$), 29.9 ($C_{3'}$), 29.1 ($C_{2'}$), 26.7 ($C_{1'}$), 22.8 (OCH_2CH_2), 22.7 ($C_{5'}$), 14.2 ($C_{6'}$), 10.6 ($O(CH_2)_2CH_3$); HRMS (ESI^+): *m/z* calculated for formula $C_{25}H_{27}NNaO_3$ [MNa^+]: 412.1883 found 412.1890; IR (ν_{max}, solid, cm^{-1}): 2959, 2921, 2860, 1759, 1667, 1626, 1601, 1590, 1485, 1472, 1350, 1319, 1282, 1255, 1196, 1099, 1076, 1043.

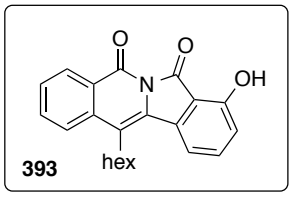

393

5-Hydroxy-2,2-dimethyl-*4H*-benzo[*d*][1,3]dioxin-4-one 389[215]

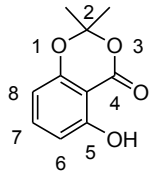

Thionyl chloride (1.0 mL, 14 mmol) in DME (0.5 mL) was added dropwise to a solution of 2,6-dihydroxybenzoic acid (1.5 g, 10 mmol) in DME (3 mL) with DMAP (61 mg, 0.50 mmol) and acetone (1 mL). After four hours the solvents were removed *in vacuo* and the residue was filtered through a silica plug (1:1 DCM-cyclohexane, 50 mL). The solvent was removed *in vacuo* and the residue was diluted in hexane and cooled to 0 °C. The product began to crystallise out and the resulting solid was collected by vacuum filtration to afford a colourless crystalline solid (1.10 g, 56%). M.p. 65-66 °C ([lit.[215] 59-61 °C] hexane); δ_H (300 MHz, $CDCl_3$) 10.32 (1H, s, OH), 7.40 (1H, t, *J* 8.3, H_7), 6.62 (1H, d, *J* 8.4, H_8), 6.43 (1H, d, *J* 8.1, H_6), 1.74 (6H, s, $(Me)_2$); δ_C (75 MHz, $CDCl_3$) 165.6 (C_4O), 161.6 (C_qO_1), 155.7 (C_5), 138.0 (C_7), 110.9 (C_8), 107.4 (C_6), 107.3 (C_2), 99.5 (C_q-C_4), 25.8 ($(Me)_2$); LRMS (ESI^+): *m/z* 195.0 [MH^+]; IR (ν_{max}, film, cm^{-1}): 3203, 3000, 1687, 1629, 1584, 1486, 1470, 1390, 1379, 1346, 1272, 1199, 1151, 1074, 1054. Spectral data match the literature.[215]

Trifluoromethanesulfonic acid 2,2-dimethyl-4-oxo-*4H*-1,3-benzodioxin-5-yl ester 390[215]

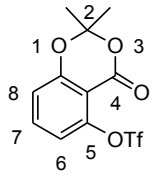

Triflic anhydride (780 μL, 4.64 mmol) was added dropwise to a cooled solution (0 °C) of 5-hydroxy-2,2-dimethyl-*4H*-benzo[*d*][1,3]dioxin-4-one (750 mg, 3.87 mmol) in DCM (0.5 M) with pyridine (1.13 mL, 13.9 mmol). After one hour, the reaction was diluted with 0.1 M HCl (30 mL) and the aqueous phase was extracted three times with diethyl ether (3 × 30 mL). The organic phases were combined and dried over $MgSO_4$. The solvent was removed *in vacuo* and purified by flash silica chromatography using 25% EtOAc in hexane to afford colourless needles (1.01 g, 87%) which were subsequently recrystallised from hexane. M.p. 112-114 °C ([lit.[215] 115-117 °C], hexane); δ_H (300 MHz, $CDCl_3$) 7.60 (1H, t, *J* 8.4, H_7), 7.05 (1H, d, *J* 8.5, H_6), 7.00 (1H, d, *J* 8.3, H_8), 1.76 (6H, s, $(Me)_2$); δ_C (75 MHz, $CDCl_3$) 157.6 (C_4), 157.2 (C_5), 148.8 (C_q-O_1), 136.4 (C_7), 118.9 (q, *J* 320, CF_3), 118.0 (C_6), 116.7 (C_8), 108.5 (C_q-C_4), 107.0 (C_2), 25.6 ($(Me)_2$); LRMS (ESI^+): *m/z* 326.9 [MH^+]; IR (ν_{max}, film, cm^{-1}): 1744, 1621, 1474, 1430, 1323, 1293, 1138, 1074. Spectral data match the literature.[215]

2,2-Dimethyl-5-(oct-1-yn-1-yl)-*4H*-benzo[*d*][1,3]dioxin-4-one 391

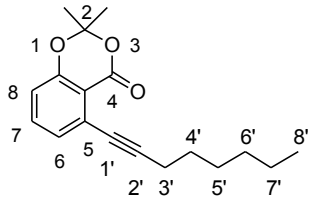

Following a modified procedure by Sakamoto *et al.,*[215] octyne (130 μL, 0.86 mmol) was added to a degassed solution of 2,2-dimethyl-4-oxo-*4H*-benzo[*d*][1,3]dioxin-5-yl trifluoromethane sulfonate (254 mg, 0.780 mmol), $PdCl_2(PPh_3)_2$ (30 mg, 0.040 mmol), copper(I) iodide (23 mg, 0.12 mmol) and diethylamine (120 μL, 1.17 mmol) in MeCN (16 mL, 0.05 M). The yellow solution was heated to 70 °C for three hours. The reaction solvent was removed *in vacuo* and the crude mixture was partitioned between EtOAc (25 mL) and water (25 mL). The two phases were separated, and then the aqueous phase was extracted with EtOAc (25 mL). The organic extracts were combined and washed with water (25 mL), brine (25 mL), dried over $MgSO_4$ and concentrated *in vacuo*. The crude oil was purified using flash silica chromatography using 10-30% EtOAc in hexane to afford a brown oil (138 mg, 62%). δ_H (500 MHz, $CDCl_3$) 7.40 (1H, t, *J* 7.9, H_7), 7.19 (1H, dd, *J* 7.7, 0.9, H_6), 6.86 (1H, dd, *J* 8.2, 0.9, H_8), 2.51 (2H, t, *J* 7.2, $H_{3'}$), 1.71 (6H, s, $(Me)_2$), 1.66 (2H, app q, *J* 7.5, $H_{4'}$), 1.53-1.45 (2H, m, $H_{5'}$), 1.37-1.30 (4H, m, $H_{6'}$ and $H_{7'}$), 0.90 (3H, t, *J* 7.0 Hz, $H_{8'}$); δ_C (75 MHz, $CDCl_3$); ^{13}C NMR (126 MHz, $CDCl_3$) δ 159.1 (C_4), 156.7 (C_q-O_1), 134.9 (C_7), 129.0 (C_6), 126.6 (C_5), 116.5 (C_8), 114.3 (C_q-C_4), 105.6 (C_2), 98.8 ($C_{2'}$), 78.8 ($C_{1'}$), 31.6 ($C_{4'}$), 28.8 ($C_{5'}$), 28.6 ($C_{6'}$), 25.9 ($(Me)_2$), 22.7 ($C_{7'}$), 20.2 ($C_{3'}$), 14.2 ($C_{8'}$); HRMS (ESI^+): *m/z* calculated for formula $C_{18}H_{23}O_3$ [MH^+] 287.1641: found 287.1642; IR (ν_{max}, solid, cm^{-1}): 2998, 2931, 2587, 2228, 1748, 1593, 1578, 1475, 1437, 1389, 1316, 1293, 1271, 1255, 1232, 1205, 1169, 1085, 1039.

3-(2,2-Dimethyl-4-oxo-4*H*-benzo[*d*][1,3]dioxin-5-yl)-4-hexylisoquinolin-1(*2H*)-one 392

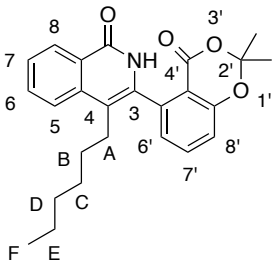

2,2-Dimethyl-5-(oct-1-yn-1-yl)-*4H*-benzo[*d*][1,3]dioxin-4-one (138 mg, 0.480 mmol) was added to a solution of *N*-(pivaloyloxy)-benzamide (110 mg, 0.500 mmol), CsOAc (30 mg, 0.30 mmol) and $[Cp^*RhCl_2]_2$ (3 mg, 0.005 mmol) in MeOH (2.5 mL, 0.20 M). After 16 hours consumption of the starting material was observed by TLC. The reaction was concentrated *in vacuo* and purified by flash silica chromatography using 8% isopropanol in toluene to afford an orange-brown solid (195 mg, 96%). The solid was triturated with cold Et_2O (3 × 5 mL) to afford a colourless solid (143 mg, 71%). A sample was taken and recrystallised from $CHCl_3$ and pentane using a vapour diffusion to afford colourless cubic crystals. M.p. 231-234 °C ($CHCl_3$–pentane); δ_H (500 MHz, $CDCl_3$) 10.25 (1H, s, NH), 8.27 (1H, d, *J* 8.2, H_8), 7.71-7.65 (2H, m, H_6 and H_5), 7.63 (1H, t, *J* 7.5, $H_{7'}$), 7.43 (1H, ddd, *J* 8.1, 5.9, 2.3, H_7), 7.15 (1H, dd, *J* 8.0, 0.7, $H_{8'}$), 7.10 (1H, dd, *J* 7.5, 0.9, $H_{6'}$), 2.51 (1H, ddd, *J* 14.4, 10.0, 6.4, H_A), 2.39 (1H, ddd, *J* 14.3, 9.9, 6.6, H_a), 1.81 (3H, s, Me), 1.74 (3H, s, Me),

1.53-1.43 (2H, m, H_B), 1.25-1.11 (6H, m, H_C, H_D and H_E), 0.82 (3 H, t, *J* 7.0, H_F); δ_C (125 MHz, $CDCl_3$) 162.8 (C_1), 158.4 ($C_{4'}$), 157.3 (*C*-$O_{1'}$), 138.2 (C_q), 137.4 (C_q), 135.6 ($C_{7'}$), 135.5 (C_q), 132.4 (C_6), 128.0 (C_8), 126.0 (C_7 and $C_{6'}$), 123.8 (C_5), 118.9 ($C_{8'}$), 114.0 (C_q), 113.0 (C_q), 106.1 ($C_{2'}$), 31.6 (C_A), 29.9 (C_B), 29.7 (C_C), 27.9 (C_D), 26.2 (Me), 25.6 (Me), 22.7 (C_E), 14.1 (C_F), one quaternary carbon was not observed; HRMS (ESI^+): *m/z* calculated for formula $C_{25}H_{28}NO_4$ - $[MH^+]$ 406.2013: found 406.2023; IR (ν_{max}, solid, cm^{-1}): 2952, 2926, 2856, 1742, 1647, 1602, 1583, 1478, 1381, 1311, 1276, 1202, 1044.

12-Hexyl-8-hydroxyisoindolo[2,1-*b*]isoquinoline-5,7-dione 393

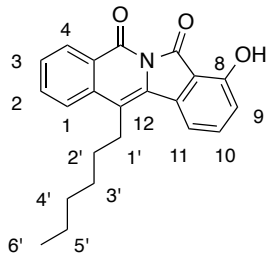

Sodium hydride (100 mg, 2.50 mmol, 60% dispersion in oil) was triturated with petrol (2 × 5 mL) under nitrogen and diluted in THF (10 mL). In a separate flask, 3-(2,2-dimethyl-4-oxo-*4H*-benzo[*d*][1,3]-dioxin-5-yl)-4-hexylisoquinolin-1(*2H*)-one (100 mg, 0.250 mmol) was dissolved in THF (5 mL) and cooled to 0 °C. An aliquot of the sodium hydride solution (1.00 mL, 0.250 mmol) was added dropwise to the reaction. The homogeneous solution changed colour from pale yellow to bright orange, indicating formation of the phenolate ion. An additional aliquot of the sodium hydride solution (1.00 mL, 0.25 mmol) was added in order to achieve full conversion. The reaction mixture was quenched with acetic acid (0.5 mL), at which point the solution changed colour from orange to bright yellow. The reaction was concentrated *in vacuo* and the residue was rediluted in acetic acid (1 mL). The resultant solid was filtered and washed with Et_2O (2 mL) to afford an amorphous yellow solid (55 mg, 63%). The solid was recrystallised from AcOH. M.p. 215-218 °C (AcOH); δ_H (500 MHz, $CDCl_3$) 8.69 (1H, s, OH), 8.56 (1H, d, *J* 7.9, H_4), 7.77-7.76 (2H, m, H_2 and H_1), 7.63 (1H, t, *J* 8.0, H_{10}), 7.58-7.55 (1H, m, H_3), 7.37 (1H, d, *J* 7.7, H_{11}), 7.00 (1H, d, *J* 8.2, H_9), 3.14-3.07 (2H, m, $H_{1'}$), 1.77-1.70 (2H, m, $2H_{2'}$), 1.59 (2H, q, *J* 7.5, $2H_{3'}$), 1.45-1.33 (4H, m, $2H_{4'}$ and $2H_{5'}$), 0.94 (3H, t, *J* 7.0, $H_{6'}$); δ_C (126 MHz, $CDCl_3$) 168.2 (C_7O), 159.7 (C_5O), 158.2 (C_8O), 137.4 (C_{10}), 136.5 (C_q), 135.2 (C_q), 134.2 (C_1 or C_2), 131.0 (C_q), 129.9 (C_4), 128.7 (C_3), 128.1 (C_q), 124.2 (C_1 or C_2), 121.4 (C_q), 117.2 (C_9), 115.6 (C_{11}), 112.8 (C_q), 31.8 ($C_{4'}$), 29.9 ($C_{3'}$), 29.1 ($C_{2'}$), 26.9 ($C_{1'}$), 22.8 ($C_{5'}$), 14.2 ($C_{6'}$); HRMS (ESI^+): *m/z* calculated for formula $C_{22}H_{22}NO_3$ $[MH^+]$: 348.1594; found 348.1590; IR (ν_{max}, solid, cm^{-1}): 3220, 2959, 2919, 2854, 1743, 1665, 1612, 1589, 1474, 1458, 1445, 1354, 1341, 1294, 1212, 1189, 1177, 1159, 1117, 1081, 1064, 1038.

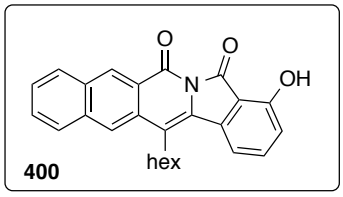

400

_N_-(pivaloyloxy)-2-naphthamide 396[259]

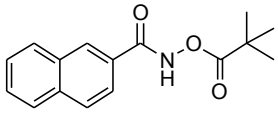

Oxalyl chloride (480 μL, 5.50 mmol) was added to a solution of 2-naphthoic acid (860 mg, 5.00 mmol) in DCM (25 mL, 0.2 M) with DMF (2 drops). The mixture was stirred at room temperature for 2 hours, then concentrated *in vacuo*. The crude acid chloride was diluted in EtOAc (5 mL) and transferred to a flask containing *O-(*pivaloyl)-hydroxylammonium triflate[34] (1.34 g, 5.00 mmol) and $NaHCO_3$ (840 mg, 10.0 mmol) dissolved in a 2:1 mixture of EtOAc–H_2O (45 mL, 0.1 M) at 0 °C. After 2 hours the reaction was quenched with saturated aqueous $NaHCO_3$ (50 mL) and diluted with EtOAc (50 mL). The two phases were separated and the organic phase was washed with brine (50 mL). The organic phase was dried over $MgSO_4$ and concentrated *in vacuo.* The solid was crystallised from Et_2O–pentane to afford colourless crystals (901 mg, 66%). M.p. 110-113 °C (Et_2O–pentane); δ_H (300 MHz, $CDCl_3$) 9.80 (1H, br s, NH), 8.31 (1H, s, H_1), 7.90-7.74 (4H, m, ArH), 7.62-7.44 (2H, m, ArH), 1.36 (9H, s, $(CH_3)_3$); δ_C (75 MHz, $CDCl_3$) δ 177.3 (C_qO), 167.0 (C_qO), 135.3 (C_q), 132.5 (C_q), 129.2, 128.8, 128.6, 128.3, 128.1 (C_q), 127.9, 127.0, 123.5, 38.6 ($C(CH_3)_3$), 27.2 ($CH_3)_3$); HRMS (ESI^+): *m/z* calculated for formula $C_{16}H_{18}NO_3$ [M-H^+]: 272.1281; found 272.1281; IR (ν_{max}, solid, cm^{-1}): 3146, 2967, 2938, 1782, 1644, 1627, 1600, 1505, 1479, 1462, 1435, 1387, 1369, 1298, 1269, 1236, 1145, 1117, 1071, 1035, 1012. The spectral data was consistent with the literature.[259]

3-(2,2-Dimethyl-4-oxo-4H-benzo[*d*][1,3]dioxin-5-yl)-4-hexylbenzo[*g*]isoquinolin-1(2*H*)-one 397

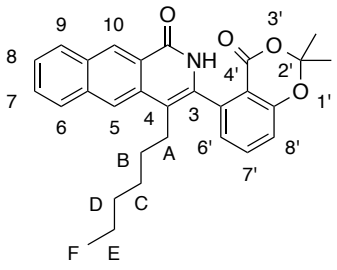

2,2-Dimethyl-5-(oct-1-yn-1-yl)-*4H*-benzo[*d*][1,3]dioxin-4-one (315 mg, 1.10 mmol) was added to a solution of *N*-(pivaloyloxy)-2-napthamide (271 mg, 1.00 mmol), CsOAc (384 mg, 2.00 mmol) and $[Cp^*RhCl_2]_2$ (6 mg, 0.01 mmol) in MeOH (5 mL, 0.2 M). After 2 hours the reaction was concentrated *in vacuo* and a ^1H NMR of the crude reaction mixture indicated a mixture of regioisomers. The crude material was purified by flash silica chromatography using 50% EtOAc in pentane to afford an orange-brown solid (231 mg, 51%) and mixed fractions containing a mixture of regioisomers (5:2, **397**:**398**, 124 mg, 27%). A sample from the pure fractions were removed and crystallised from slow mixing of THF and pentane to afford

colourless crystals. M.p. 194-197 °C (THF– pentane); δ_H (500 MHz, $CDCl_3$) 9.77 (1H, s, NH), 8.89 (1H, s, H_{10}), 8.12 (1H, s, H_5), 8.02 (1H, d, *J* 8.2, H_9), 7.97 (1H, d, *J* 8.3, H_6), 7.64 (1H, dd, *J* 8.3, 7.6, $H_{7'}$), 7.58 (1H, ddd, *J* 8.2, 6.8, 1.2, H_7), 7.51 (1H, ddd, *J* 8.0, 6.8, 1.1, H_8), 7.18-7.15 (2H, m, $H_{6'}$ and $H_{8'}$), 2.66-2.57 (1H, m, H_A), 2.55-2.46 (1H, m, H_A), 1.80 (3H, s, Me), 1.75 (3H, s, Me), 1.60-1.52 (2H, m, H_B), 1.31-1.15 (6H, m, H_C, H_D and H_E), 0.84 (3H, t, *J* 7.0, H_F); δ_C (126 MHz, $CDCl_3$) 163.3 ($C_{4'}$), 158.4 (C_1), 157.3 (C-O), 137.7 (C_q), 135.7 ($C_{7'}$), 135.6 (C_q), 134.2 (C_q), 134.1 (C_q), 131.3 (C_q), 129.4 (C_9), 129.2 (C_{10}), 128.1 (C_6 and C_7), 126.2 ($C_{8'}$), 126.0 (C_8), 124.7 (C_q), 122.4 (C_5), 118.9 ($C_{6'}$), 113.7 (C_q), 113.0 (C_q), 106.1 (C_q), 31.6 (C_D), 29.7 (C_B), 29.7 (C_C), 28.2 (C_A), 26.0 (Me), 25.7 (Me), 22.7 (C_E), 14.2 (C_F); HRMS (ESI^+): *m/z* calculated for formula $C_{29}H_{30}NO_4$ [MH^+]: 456.2169; found 456.2172; IR (ν_{max}, solid, cm^{-1}): 2927, 2857, 1746, 1737, 1650, 1622, 1597, 1581, 1476, 1442, 1381, 1362, 1314, 1273, 1240, 1200, 1149, 1096, 1040.

14-Hexyl-4-hydroxybenzo[*g*]isoindolo[2,1-*b*]isoquinoline-5,7-dione 400

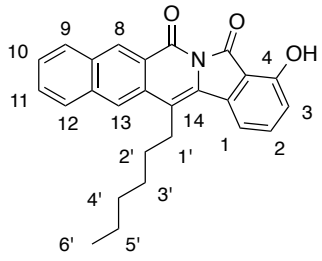

Sodium hydride (19 mg, 0.81 mmol, 60% dispersion in oil) was triturated with pentane (2 × 1 mL) under nitrogen and diluted in THF (0.5 mL). In a separate vial, 3-(2,2-dimethyl-4-oxo-4*H*-benzo[*d*][1,3]dioxin-5-yl)-4-hexylbenzo[*g*]isoquinolin-1(*2H*)-one (88 mg, 0.19 mmol) was dissolved in THF (3 mL, 0.06 M) and cooled to 0 °C. The sodium hydride solution was added dropwise to the reaction. The homogeneous solution changed colour from pale yellow to bright orange, indicating formation of the phenolate ion. After 30 minutes the reaction was quenched with acetic acid (0.5 mL), at which point the solution changed colour from orange to bright yellow. The reaction mixture was concentrated *in vacuo* and the residue was triturated with water (1 mL) and dissolved into DCM (15 mL), dried ($MgSO_4$), filtered and concentrated *in vacuo* to afford a yellow amorphous solid (52 mg, 69%). The solid was crystallised by slow evaporation of $CHCl_3$ to afford yellow needles. M.p. 244-246 °C ($CHCl_3$); δ_H (500 MHz, $CDCl_3$) 9.04 (1H, s, H_8), 8.73 (1H, s, OH), 8.14 (1H, s, H_{13}), 8.00 (1H, d, *J* 8.2, H_9), 7.97 (1H, d, *J* 8.3, H_{12}), 7.65-7.61 (2H, m, H_2 and H_{11}), 7.55 (1H, ddd, *J* 8.0, 6.8, 1.1, H_{10}), 7.38 (1H, d, *J* 7.8, H_1), 6.96 (1H, d, *J* 8.3, H_3), 3.24-3.17 (2H, m, $H_{1'}$), 1.82-1.76 (2H, m, $H_{2'}$), 1.68-1.61 (2H, m, $H_{3'}$), 1.49-1.35 (4H, m, $H_{4'}$ and $H_{5'}$), 0.95 (3H, t, *J* 7.2, $H_{6'}$); δ_C (126 MHz, $CDCl_3$) δ 167.9 (C_qO), 159.9 (C_qO), 157.9 (C_qO), 137.1 (C_8), 135.9 (C_q), 135.0 (C_q), 132.2 (C_q), 131.7 (C_9), 130.0 (C_q), 129.5 (C_2), 129.3 (C_{11}), 128.4 (C_{12}), 127.6 (C_{10}), 125.0 (C_q), 124.0 (C_{13}), 121.9 (C_q), 116.7 (C_3), 115.5 (C_1), 112.9 (C_q), 31.7 ($C_{1'}$), 29.8 ($C_{2'}$), 28.9 ($C_{3'}$), 26.9 ($C_{4'}$), 22.7 ($C_{5'}$), 14.1 ($C_{6'}$), missing a quaternary carbon. HRMS (ESI^+): *m/z* calculated for formula $C_{26}H_{23}NNaO_3$ [MNa^+]: 420.1570; found 420.1571; IR

(ν_{max}, solid, cm^{-1}): 3243, 2950, 2923, 2873, 2854, 1742, 1664, 1619, 1596, 1567, 1490, 1464, 1440, 1347, 1324, 1308, 1277, 1259, 1232, 1209, 1178, 1164, 1076, 1055, 1015.

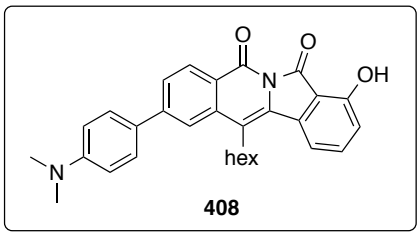

408

Ethyl 4'-(dimethylamino)-[1,1'-biphenyl]-4-carboxylate 403

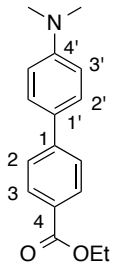

Following a modified procedure by Buchwald *et al.*,[217] palladium acetate (25 mg, 0.11 mmol) and SPhos (130 mg, 0.320 mmol) were charged into an oven-dried Schlenk flask and evacuated and refilled with nitrogen (×3). Degassed THF (5 mL) was added to the flask and the solution was allowed to stir at room temperature for 30 minutes. In a separate Schlenk flask, 4-(dimethylamino)-phenylboronic acid (2.62 g, 15.9 mmol) and potassium phosphate tribasic (6.74 g, 31.8 mmol) and ethyl 4-bromobenzoate (1.73 mL, 10.6 mmol) were charged into a flask which was evacuated and refilled with nitrogen (×3). Degassed THF (15 mL) was added followed by the palladium acetate/SPhos solution. The reaction mixture was stirred for 16 hours at room temperature. The reaction mixture was diluted with water (100 mL) and the aqueous phase was extracted with DCM (3 × 75 mL). The organic extracts were recombined and washed with brine (50 mL), dried over Na_2SO_4 and concentrated *in vacuo*. The crude material was purified by flash silica chromatography using 10% EtOAc in pentane to afford a colourless solid (2.24 g, 79%). A sample was taken and recrystallized from EtOAc. R_F 0.66 (20% EtOAc in hexane); M.p. 180-182 °C (EtOAc); δ_H (300 MHz, $CDCl_3$) 8.06 (2H, d, *J* 8.3, H_3), 7.62 (2H, d, *J* 8.3, H_4), 7.56 (1H, d, *J* 8.8, $H_{2'}$), 6.84 (1H, d, *J* 8.6, $H_{3'}$), 4.39 (2H, q, *J* 7.1, OCH_2CH_3), 3.02 (6H, s, NMe_2), 1.41 (3H, t, *J* 7.1, OCH_2CH_3); δ_C (75 MHz, $CDCl_3$) 166.9 (CO_2Et), 150.6 (C_q), 145.6 (C_q), 130.2 ($C_{2'}$), 128.1 (C_2), 128.0 ($2C_q$), 125.9 (C_3), 113.0 ($C_{3'}$), 60.9 (OCH_2CH_3), 40.8 (NMe_2), 14.5 (OCH_2CH_3); LRMS (ESI^+): *m/z* 270.1 [MH^+]; found 270.1; IR (ν_{max}, solid, cm^{-1}): 2981, 1702, 1603, 1536, 1500, 1467, 1444, 1402, 1365, 1313, 1280, 1221, 1184, 1169, 1106, 1064, 1026. The spectral data corresponds to the literature values.[260]

4'-(Dimethylamino)-[1, 1'-biphenyl]-4-carboxylic acid 404

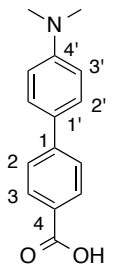

The biphenyl ester (**X**) (2.24 g, 8.30 mmol) was heated to reflux in a solution of ethanol–water (2:1, 60 mL, 0.1 M) with KOH (1.0 g, 18 mmol) for 16 hours, after which time the reaction solution was neutralised with sat. NH_4Cl solution. The resulting precipitate was filtered and washed with water. The amorphous solid was dried at 70 °C *in vacuo* to afford a brown solid (2.00 g, quant.). δ_H (300 MHz, DMSO-d_6) 7.93 (2H, d, *J* 7.9, H_3), 7.68 (2H, d, *J* 8.0, H_2), 7.59 (2H, d, *J* 8.3, $H_{2'}$), 6.81 (2H, d, *J* 8.6, $H_{3'}$), 3.55 (1H, br s, OH), 2.95 (6H, s, NMe_2); δ_C (75 MHz, DMSO) 167.6 (*C*.O_2H), 150.3 (C_q), 143.8 (C_q), 129.9 ($C_{2'}$), 127.4 (C_2), 126.2 (C_q), 126.1 (C_q), 125.0 (C_3), 112.5 ($C_{3'}$), 39.9 (NMe_2); LRMS (ESI^+): *m/z* 242.1 [MH^+]; found 242.0. The spectral data was consistent with the literature.[260]

4'-(Dimethylamino)-*N*-(pivaloyloxy)-[1, 1'-biphenyl]-4-carboxamide 405

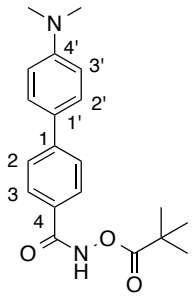

Oxalyl chloride (1.31 mL, 15.0 mmol) was added to a solution of the biphenyl acid **X** (2.0 g, 8.3 mmol) in DCM (50 mL, 3.3 M) with cat. DMF (10 μL). After two hours the reaction was concentrated *in vacuo* to afford the crude acid chloride. The crude intermediate was transferred to a separate flask containing *N*-(pivaloyl)ammonium triflate (2.94 g, 11.0 mmol) in a biphasic solution of EtOAc–water (2:1, 100 mL, 0.1 M) with $NaHCO_3$ (1.68 g, 20.0 mmol) at 0 °C. After 16 hours the reaction mixture was diluted with EtOAc (100 mL) and the phases were separated. The organic phase was washed with brine (50 mL) and dried over Na_2SO_4 and concentrated *in vacuo*. The crude material was purified by flash silica chromatography using 10-50% EtOAc in hexane to afford an orange solid (1.10 g, 39%). A sample was recrystallized from EtOAc. R_F 0.9 (50% EtOAc in hexane); M.p. 90-92 °C (EtOAc); δ_H (300 MHz, $CDCl_3$) 9.36 (1H, s, NH), 7.84 (2H, d, *J* 8.3, H_3), 7.64 (2H, d, *J* 8.2, H_2), 7.54 (2H, d, *J* 8.9, $H_{2'}$), 6.80 (2H, d, *J* 8.8, $H_{3'}$), 3.02 (6H, s, NMe_2), 1.38 (9H, s, $(CH_3)_3$); δ_C (75 MHz, $CDCl_3$) 177.3 ($CO_2{}^tBu$), 167.1 (*C*ONH), 150.7 (C_q), 145.8 (C_q), 128.1 ($C_{2'}$ and C_2), 128.0 (C_q), 127.3 (C_q), 126.3 (C_3), 112.8 ($C_{3'}$), 40.6 (NMe_2), 38.6 ($C(CH_3)_3$), 27.1 ($C(CH_3)_3$); HRMS (ESI^+): *m/z* calculated for formula $C_{20}H_{24}N_2NaO_3$ [MNa^+] 363.1679; found 363.1685; IR (ν_{max}, solid, cm^{-1}): 3187, 2959, 2933, 2904, 1779, 1734, 1697, 1653, 1598, 1535, 1501, 1478, 1397, 1361, 1269, 1220, 1168, 1142, 1075, 1028.

3-(2,2-Dimethyl-4-oxo-4*H*-benzo[*d*][1,3]dioxin-5-yl-)-6-(4-dimethylamino)phenyl)-4-hexylisoquinolin-1(2*H*)-one 406 – major regioisomer

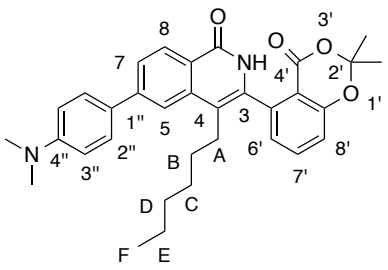

2,2-Dimethyl-5-(oct-1-yn-1-yl)-*4H*-benzo[*d*][1,3]dioxin-4-one (315 mg, 1.10 mmol) was added to a solution of 4'-(dimethylamino)-*N*-(pivaloyloxy)-[1,1'-biphenyl]-4-carboxamide (340 mg, 1.00 mmol), CsOAc (382 mg, 2.00 mmol) and $[Cp^*RhCl_2]_2$ (6 mg, 0.01 mmol) in MeOH (5.0 mL, 0.2 M). After 16 hours the reaction mixture was concentrated *in vacuo* and a ^{1}H NMR of the crude reaction mixture indicated a 4:1 mixture between the major regioisomer **X** and the minor regioisomer **X**. The crude material was purified by flash silica chromatography using 50% EtOAc in pentane to afford the minor regioisomer **X** as an amorphous tan solid (63 mg, 12%) and the major regioisomer as a tan amorphous solid **X** (222 mg, 42%) (combined yield: 54%, ratio 3.5:1). A sample from the pure fractions of the major regioisomer were removed and crystallised from slow mixing of THF and pentane to afford colourless crystals. M.p. 247-248 °C (THF–pentane); δ_H (300 MHz, $CDCl_3$) 10.04 (1H, s, NH), 8.28 (1H, d, *J* 8.0, H_8), 7.82 (1H, s, H_5), 7.66-7.58 (4H, m, H_7, $H_{7'}$ and $H_{2''}$), 7.15 (1H, d, *J* 7.7, $H_{8'}$), 7.11 (1H, d, *J* 7.7, $H_{6'}$), 6.84 (2H, d, *J* 8.7, $H_{3''}$), 3.03 (6H, s, NMe_2), 2.63-2.35 (2H, m, H_A), 1.82 (3H, s, Me), 1.75 (3H, s, Me), 1.59-1.46 (2H, m, H_B), 1.33-1.10 (6H, m, H_C, H_D and H_E), 0.83 (3H, t, *J* 6.5, H_F); δ_C (75 MHz, $CDCl_3$) 162.7 ($C_{4'}$), 158.4 (C_q-$O_{1'}$), 157.2 (C_1), 150.6 ($C_{4''}$-NMe_2), 145.2 (C_q), 138.5 (C_q), 137.5 (C_q), 135.6 (C_7), 128.5 (C_8), 128.3 ($C_{2''}$), 126.1 ($C_{6'}$), 124.7 ($C_{7'}$), 123.9 (C_q), 120.7 (C_5), 118.8 ($C_{8'}$), 114.1 (C_q), 113.1 (C_q), 112.8 ($C_{3''}$), 106.1 (C_q), 40.6 (NMe_2), 31.5 (C_D), 29.9 (C_C), 29.7 (C_B), 27.9 (C_A), 26.2 (Me), 25.6 (Me), 22.7 (C_E), 14.2 (C_F), two quaternary carbons were obscured; HRMS (ESI$^+$): *m/z* calculated for formula $C_{33}H_{37}N_2O_4$ [MH^+] 525.2748; found 525.2758; IR (ν_{max}, solid, cm^{-1}): 2926, 2856, 1746, 1647, 1601, 1584, 1546, 1503, 1478, 1444, 1361, 1330, 1309, 1279, 1201, 1044.

4-(2,2-Dimethyl-4-oxo-4*H*-benzo[*d*][1,3]dioxin-5-yl)-6-(4-dimethylamino)phenyl-3-hexylisoquinoline-1-(2*H*)-one 407 – minor regioisomer

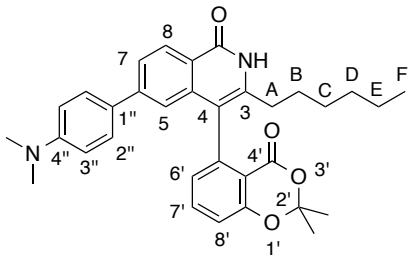

M.p. >250 °C (DCM–pentane); δ_H (300 MHz, $CDCl_3$) 10.32 (1H, s, NH), 8.43 (1H, d, *J* 8.4, H_8), 7.62 (1H, t, *J* 7.9, $H_{5'}$), 7.58 (1H, dd, *J* 8.2, 1.8, H_7), 7.34 (2H, d, *J* 8.8, $H_{2''}$), 7.09 (1H, dd, *J* 8.2, 0.8, $H_{6'}$), 7.02 (1H, dd, *J* 7.5, 0.8, $H_{4'}$), 6.95 (1H, d, *J* 1.4, H_5), 6.70 (2H, d, *J* 8.8, $H_{3''}$), 2.96 (6H, s, NMe_2), 2.47-2.24 (2H, m, H_A), 1.75 (3H, s, Me), 1.74 (3H, s, Me), 1.65-1.55 (2H, m, H_B), 1.38-1.11 (6H, m, H_C, H_D and H_E), 0.84 (3H, t, *J* 6.6, H_F); δ_C (75 MHz, $CDCl_3$) 163.8

($C_{4'}$), 158.5 (C_q-$O_{1'}$), 157.3 (C_1), 150.4 ($C_{4''}$), 145.3 (C_q), 140.0 (C_q), 139.3 (C_q), 137.8 (C_q), 135.6 ($C_{5'}$), 128.4 (C_q), 128.2 ($C_{2''}$), 128.0 ($C_{4'}$), 127.9 (C_8), 124.5 (C_7), 122.6 (C_q), 121.1 (C_5), 117.6 ($C_{6'}$), 114.9 (C_q), 114.5 (C_q), 112.6 ($C_{3''}$), 105.5 (C_q), 40.5 (NMe_2), 31.8 (C_D), 31.4 (C_C), 29.3 (C_B), 28.5 (C_A), 25.9 (Me), 25.9 (Me), 22.6 (C_E), 14.2 (C_F); HRMS (ESI^+): *m/z* calculated for formula $C_{33}H_{37}N_2O_4$ [MH^+] 525.2748; found 525.2765; IR (ν_{max}, solid, cm^{-1}): 2924, 2854, 2806, 1738, 1647, 1626, 1597, 1578, 1544, 1530, 1504, 1475, 1459, 1435, 1358, 1315, 1271, 1205, 1167, 1111, 1042.

2-(4-(Dimethylamino)phenyl-12-hexyl-8-hydroxyisoindolo[2,1–*b*]isoquinoline-5,7-dione 408

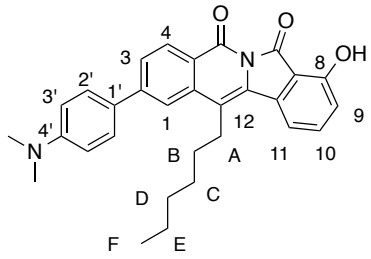

Sodium hydride (19 mg, 0.81 mmol, 60% dispersion in oil) was triturated with pentane (2 × 1 mL) under nitrogen and diluted in THF (1 mL). In a separate vial, 4-(2,2-dimethyl-4-oxo-4*H*-benzo[*d*][1,3]dioxin-5-yl)-6-(4-dimethylamino)-phenyl-3-hexylisoquinoline-1-(2*H*)-one (X) (100 mg, 0.190 mmol) was dissolved in THF (5 mL, 0.04 M) and cooled to 0 °C. The sodium hydride solution was added to the reaction solution, which was allowed to warm to room temperature and stirred overnight. The reaction was acidified with 2N HCl in ether (2 mL) and the solvents were removed *in vacuo*. The crude reaction mixture was dissolved in DCM (5 mL) and the solid was filtered from the reaction. The filtrate was concentrated *in vacuo* and precipitated using diethyl ether (2 mL) to afford a red amorphous solid (49 mg, 50%). The solid was crystallised from DMSO. M.p. >250 °C; δ_H (500 MHz, DMSO-d_6, 343 K) 8.33 (1H, d, *J* 8.3, H_4), 7.96 (1H, s, H_1), 7.82 (1H, d, *J* 8.3, H_3), 7.72 (2H, d, *J* 8.7, $H_{2'}$), 7.65 (1H, t, *J* 7.9, H_{10}), 7.46 (1H, d, *J*, 7.7, H_{11}), 7.14 (1H, d, *J* 8.2, H_9), 7.04 (2H, d, *J* 7.7, $H_{3'}$), 3.22-3.15 (2H, m, H_A), 3.02 (6H, s, NMe_2), 1.75-1.66 (2H, m, H_B), 1.63-1.54 (2H, m, H_C), 1.44-1.36 (2H, m, H_D), 1.36-1.27 (2H, m, H_E), 0.89 (3H, t, *J* 7.1, H_F); δ_C (126 MHz, DMSO-d_6, 343 K) 162.9 (C_7O), 158.2 (C_5O), 157.5 (C_8O), 145.2 (C_q), 136.4 (C_q), 136.3 (C_{10}), 135.8 (C_q), 128.7 (C_4), 127.6 ($C_{2'}$), 125.4 (C_3), 125.1 (C_q), 120.4 (C_1), 118.4 (C_q), 117.6 (C_9), 114.4 (C_{11}), 113.7 ($C_{3'}$), 112.5 (C_q), 40.4 (NMe_2), 30.7 (C_D), 28.3 (C_C), 28.1 (C_B), 25.2 (C_A), 21.6 (C_E), 13.4 (C_F), three quaternary carbons obscured; HRMS (ESI^+): *m/z* calculated for formula $C_{30}H_{30}N_2NaO_3$ [MNa^+] 489.2149; found 489.2151; IR (ν_{max}, solid, cm^{-1}): 3309, 2951, 2921, 2853, 1743, 1592, 1530, 1486, 1450, 1356, 1311, 1168, 1084, 1068, 1043.

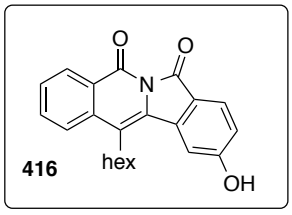

416

2-Iodo-4-methoxy benzoic acid 410[214]

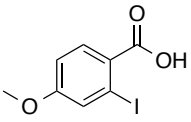

s-BuLi (20 mL, 28 mmol, 1.4 M in hexane) was added to a cooled solution (−78 °C) of TMEDA (4.14 mL, 27.7 mmol) in THF (60 mL). The yellow solution was stirred for 30 minutes at −78 °C. *p*-Anisic acid (2.0 g, 13 mmol), dissolved in THF (15 mL) was added dropwise to the *s*-BuLi/TMEDA solution whilst keeping the temperature of the reaction mixture at −70 °C. The solution was stirred at −78 °C for 2 hours, then the mixture was treated with an excess of iodine (10.0 g, 20.0 mmol) dissolved in THF (10 mL) after which the reaction was stirred for a further 30 minutes. The resulting solution was then allowed to warm to ambient temperature and saturated NH_4Cl (50 mL) was added to the reaction. The aqueous phase was treated with saturated sodium thiosulphate (50 mL) and washed with diethyl ether (2 × 30 mL). The aqueous layer was acidified to pH 1 using 2 M HCl. The aqueous phase was then extracted with diethyl ether (4 × 100 mL) and the organic phases were combined and dried over $MgSO_4$. The solution was concentrated *in vacuo* and the crude product was crystallised from $CHCl_3$–Et_2O to afford a colourless crystalline solid (1.54 g, 78%). δ_H (300 MHz, $CDCl_3$) 8.05 (1H, d, *J* 8.8, H_6), 7.58 (1H, d, *J* 2.5, H_3), 6.95 (1H, dd, *J* 8.8, 2.5, H_5), 3.86 (3H, s, OMe); δ_C (75 MHz, $CDCl_3$) 170.2 (CO_2H), 162.8 (C_4), 133.9 (C_6), 132.6 (C_1), 127.8 (C_3), 113.8 (C_5), 96.5 (C_2), 55.9 (OMe); LRMS (ESI^-): *m/z* 276.9 [$M-H^-$]; found 276.7. Spectral data consistent with the literature.[214]

Methyl 2-iodo-4-(methoxymethoxy)benzoate 413

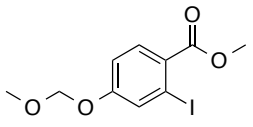

Boron tribromide (1 M solution in DCM, 4.3 mL, 4.3 mmol) was added dropwise to a solution of 2-iodo-4-methoxy benzoic acid (400 mg, 1.44 mmol) in DCM (15 mL, 0.10 M) at 0 °C. After 16 hours, the reaction was cooled to 0 °C and quenched by the dropwise addition of MeOH (20 mL). The solvents were removed *in vacuo*. To achieve full conversion to the methyl ester from the benzoic acid, conc. HCl (5 mL) was added to the crude material in a solution of MeOH (15 mL) and the reaction was heated to reflux for a further 24 hours. The reaction was concentrated *in vacuo* and the reaction was rediluted with DCM (30 mL). The organic layers were combined and washed with water (25 mL) and brine (25 mL), dried with $MgSO_4$ and concentrated *in vacuo*. The solid was washed with cold DCM–pentane (1:4, 30 mL) to give

methyl 2-iodo-4-hydroxybenzoate as a colourless amorphous solid (300 mg, 76%). δ_H (500 MHz, $CDCl_3$) 7.84 (1H, d, *J* 8.6, H_6), 7.51 (1H, d, *J* 2.6, H_3), 6.86 (1H, dd, *J* 8.6, 2.6, H_5), 5.35 (1H, s, OH), 3.89 (3H, s, OMe). Methyl 2-iodo-4-hydroxybenzoate (300 mg, 1.08 mmol) was dissolved in THF (10 mL, 0.10 M) with triethylamine (2.8 mL, 20 mmol). The solution was cooled to 0 °C and chloromethylmethyl ether (800 mL, 10.5 mmol) was added dropwise to the solution, which was allowed to stir for one hour. Water (5 mL) was added to quench the reaction and the THF was removed *in vacuo*. The residue was redissolved in EtOAc (30 mL), washed with 1N HCl (20 mL), water (20 mL), brine (20 mL), dried over $MgSO_4$ and concentrated *in vacuo* to afford a crude oil which was purified by flash silica chromatography using 0-50% EtOAc in hexane to give a colourless oil (273 mg, 79%). δ_H (500 MHz, $CDCl_3$) 7.83 (1H, d, *J* 8.7, H_6), 7.68 (1H, d, *J* 2.5, H_3), 7.04 (1H, dd, *J* 8.7, 2.5, H_5), 5.19 (2H, s, OCH_2O), 3.90 (3H, s, OMe), 3.47 (3H, s, OCH_2OCH_3); δ_C (125 MHz, $CDCl_3$) 166.2 (CO_2Me), 159.8 (C_4), 132.6 (C_6), 131.7 (C_1), 129.3 (C_3), 115.5 (C_5), 95.4 (C_2), 94.4 (OCH_2O), 56.5 (OCH_2OCH_3), 52.4 (OMe); HRMS (ESI^+): *m/z* calculated for formula $C_{10}H_{12}IO_4$ [MH^+]: 322.9775; found 322.9775; IR (ν_{max}, film, cm^{-1}): 2951, 2904, 2828, 1725, 1590, 1559, 1486, 1433, 1292, 1258, 1229, 1195, 1152, 1115, 1083.

Methyl 4-(methoxymethoxy)-2-(oct-1-yn-1-yl)benzoate 414

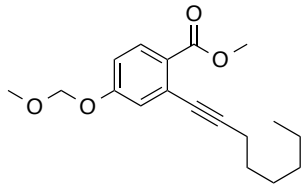

The desired compound was isolated as a colourless oil (206 mg, 67%) from methyl 2-iodo-4-(methoxymethoxy)benzoate (278 mg, 1.00 mmol) and 1-octyne (221 mL, 1.50 mmol) following general procedure F. The product was isolated by flash silica chromatography using 10-40% EtOAc in hexane. R_F 0.68 (50% EtOAc in hexane); δ_H (300 MHz, $CDCl_3$) 7.87 (1H, d, *J* 8.8, H_6), 7.14 (1H, d, *J* 2.6, H_3), 6.95 (1H, dd, *J* 8.8, 2.6, H_5), 5.20 (2H, s, OCH_2O), 3.88 (3H, s, OMe), 3.47 (3H, s, OCH_2OCH_3), 2.47 (2H, t, *J* 7.1, $H_{3'}$), 1.69-1.57 (2H, m, $H_{4'}$), 1.52-1.41 (2H, m, $H_{5'}$), 1.36-1.29 (4H, m, $H_{6'}$ and $H_{7'}$), 0.90 (3H, t, *J* 6.9, $H_{8'}$); δ_C (75 MHz, $CDCl_3$) 166.6 (CO_2Me), 159.7 (C_4), 132.5 (C_6), 126.7 (C_2), 125.3 (C_1), 121.3 (C_3), 115.3 (C_5), 96.4 ($C_{2'}$), 94.3 (OCH_2O), 79.4 ($C_{1'}$), 56.4 (OCH_2OCH_3), 52.0 (OMe), 31.6 ($C_{6'}$), 28.8 ($C_{5'}$ and $C_{4'}$), 22.7 ($C_{7'}$), 20.0 ($C_{3'}$), 14.2 ($C_{8'}$); HRMS (ESI^+): *m/z* calculated for formula $C_{18}H_{25}O_4$ [MH^+]: 305.1747; found 305.1750; IR (ν_{max}, film, cm^{-1}): 2952, 2930, 2858, 2230, 1730, 1712, 1598, 1563, 1491, 1434, 1318, 1287, 1256, 1217, 1180, 1154, 1140, 1093, 1080, 1016.

12-Hexyl-10-(methoxymethoxy)isoindolo[2,1-*b*]isoquinoline-5,7-dione 415

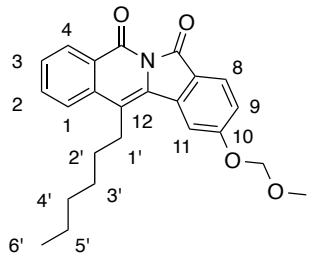

The desired compound was isolated as a colourless crystalline solid (138 mg, 40%) from methyl 4-(methoxymethoxy)-2-(oct-1-yn-1-yl)benzoate (345 mg, 1.13 mmol) following general procedure G. After 16 hours the reaction was concentrated *in vacuo* and THF (5 mL) was added to dissolve the product and precipitate the CsOAc. The solid was removed by filtration and the filtrate was cooled to 0 °C and acidified with 2N HCl in ether (5.0 mL, 2.5 mmol). After one hour the solid, which had precipitated from the solution, was collected by filtration to afford a cream amorphous solid (138 mg, 35%). A sample was taken and recrystallized from slow diffusion of pentane into a solution of the compound in DMF. M.p. 149-151 °C (DMF–pentane); δ_H (500 MHz, $CDCl_3$) 8.56 (1H, d, *J* 7.3, H_4), 7.97 (1H, d, *J* 8.5, H_8), 7.78-7.72 (2H, m, H_1 and H_2), 7.58 (1H, d, *J* 2.0, H_{11}), 7.54 (1H, ddd, *J* 8.1, 6.6, 1.7, H_3), 7.18 (1H, dd, *J* 8.4, 2.0, H_9), 5.32 (2H, s, OCH_2O), 3.54 (3H, s, OCH_2OCH_3), 3.12-3.06 (2H, m, $H_{1'}$), 1.78-1.71 (2H, m, $H_{2'}$), 1.66-1.58 (2H, m, $H_{3'}$), 1.47-1.34 (4H, m, $H_{4'}$ and $H_{5'}$), 0.94 (3H, t, *J* 7.1, $H_{6'}$); δ_C (125 MHz, $CDCl_3$) 164.9 (C_7), 163.1 (C_{10}), 159.8 (C_5), 137.4 (C_q), 136.5 (C_q), 133.9 (C_1 or C_2), 130.9 (C_q), 129.8 (C_4), 128.6 (C_q), 128.5 (C_3), 127.5 (C_8), 124.0 (C_1 or C_2), 122.2 (C_q), 120.0 (C_q), 118.4 (C_9), 110.9 (C_{11}), 94.9 (OCH_2O), 56.6 (OCH_2OCH_3), 31.9 ($C_{4'}$), 29.8 ($C_{3'}$), 29.3 ($C_{2'}$), 26.8 ($C_{1'}$), 22.8 ($C_{5'}$), 14.2 ($C_{6'}$); HRMS (ESI^+): *m/z* calculated for formula $C_{24}H_{26}NO_4$ $[MH^+]$: 392.1856; found 392.1855; IR (ν_{max}, solid, cm^{-1}): 2954, 2922, 2857, 1751, 1669, 1618, 1600, 1479, 1347, 1299, 1274, 1255, 1242, 1229, 1152, 1109, 1076, 1032, 1016.

12-Hexyl-10-hydroxyisoindolo[2,1-*b*]isoquinoline-5,7-dione 416

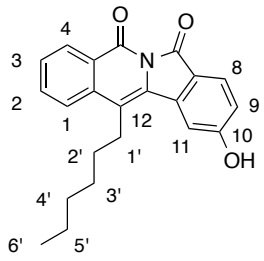

12-Hexyl-10-(methoxymethoxy)isoindolo[2,1-*b*]-isoquinoline-5,7-dione (140 mg, 0.35 mmol) was dissolved in MeCN (2.5 mL) and cooled to 0 °C. 2 N HCl in ether (5 mL) was added to the reaction mixture, which was stirred overnight. The solvents were removed *in vacuo* and the remaining solid was washed with THF–Et_2O (5 mL) to afford the desired product (76 mg, 62%). A sample was recrystallized from (DMF–pentane) to afford colourless crystals. M.p. >270 °C (DMF–pentane); δ_H (500 MHz, DMSO-d_6) 10.92 (1H, s, OH), 8.33 (1H, dd, *J* 7.9, 1.3, H_4), 7.95 (1H, d, *J* 8.1, H_1), 7.86 (1H, t, *J* 7.6, H_2), 7.81 (1H, d, *J* 8.3, H_8), 7.62 (1H, t, *J* 7.2, H_3), 7.36 (1H, d, *J* 1.8, H_{11}), 7.03 (1H, dd, *J* 8.4, 1.9, H_9), 3.11-3.04 (2H, m, $H_{1'}$), 1.68 (4H, m, $H_{2'}$ and $H_{3'}$), 1.42-1.29 (4H, m, $H_{4'}$ and $H_{5'}$), 0.90 (3H, t, *J* 7.1, $H_{6'}$); δ_C (125 MHz, DMSO-d_6) 164.0 (C_7 and C_{10}), 158.5 (C_5), 137.0 (C_q), 136.0 (C_q), 134.2 (C_2), 130.5 (C_q), 128.5 (C_3), 128.4 (C_4), 127.7 (C_q), 127.2 (C_8), 124.6

(C_1), 119.0 (C_q), 118.7 (C_q), 117.8 (C_9), 110.1 (C_{11}), 31.2 ($C_{4'}$), 28.8 ($C_{3'}$), 28.7 ($C_{2'}$), 25.6 ($C_{1'}$), 22.1 ($C_{5'}$), 13.9 ($C_{6'}$); HRMS (ESI^+): *m/z* calculated for formula $C_{22}H_{22}NO_3$ [MH^+]: 348.1594; found 348.1593; IR (ν_{max}, film, cm^{-1}): 2959, 2924, 2853, 1741, 1667, 1640, 1628, 1592, 1475, 1433, 1416, 1391, 1352, 1322, 1295, 1277, 1262, 1239, 1204, 1153, 1089, 1032, 1010.

6.10 Imide stability studies

372 **371**

A solution of the imide **372** in MeOD-d_6 (0.5 mL, 0.2 M) was monitored over six hours (at 30 minute intervals) at room temperature (23 °C, 296 K) and 50 °C (323 K) to compare the rate of alcoholysis of the imide.

6.11 Absorbance and fluorescent studies

UV-Vis absorbance measurements were recorded on a Perkin-Elmer UV/VIS/NIR Spectrometer Lambda 900. Fluorescence measurements were performed using Jobin Yvon Horiba FluoroMax-3 in a 1 cm-pathlength cell without an incident ray filter and the Xenon lamp calibrated to 467 nm and water peak to 397 nm. The excitation and emission slit widths were set to 1 nm. Spectrophotometric grade solvents were purchased from Sigma-Aldrich. Solvents were undegassed during the measurements. 9,10-Diphenylanthracene (97%) was purchased from Sigma-Aldrich and subsequently recrystallised from toluene to afford yellow needles. Solutions for absorbance and fluorescence studies were prepared prior to the experiment and used within 8 hours. The solutions were stored at 0 °C in the dark to prevent photodegradation.

Solvent correction

9,10-Diphenylanthracene was selected as a reference compound, based on the absorbance and fluorescence within the same region as the imide **372**. The literature value for 9,10-diphenylanthracene is specified in cyclohexane ($\Phi_F = 0.9$[233]), therefore a correction for measurements performed in DCM was required. Absorbance and fluorescence data for 9,10-diphenylanthracene in DCM and cyclohexane were recorded using solutions prepared from serial dilutions using stock solutions in the corresponding solvent (4.33×10^{-6} M). The emission for 9,10-diphenylanthracene in DCM and cyclohexane (Cy) was integrated from 363-552 nm, with excitation at 375 nm. The relative slope gradients, obtained from a plot of absorbance *versus* integrated fluorescence, were used to calculated the quantum yield of 9,10-diphenylanthracene in DCM (Φ_F) using the following equation:

$$\phi_{DCM} = \phi_{Cy}\left(\frac{Gradient_{DCM}}{Gradient_{Cy}}\right)\left(\frac{\eta^2_{DCM}}{\eta^2_{Cy}}\right)$$

$$\phi_{DCM} = 0.90\left(\frac{2.55\times10^8}{2.37\times10^8}\right)\left(\frac{1.424^2}{1.426^2}\right)$$

$$\phi_{DCM} = 0.97$$

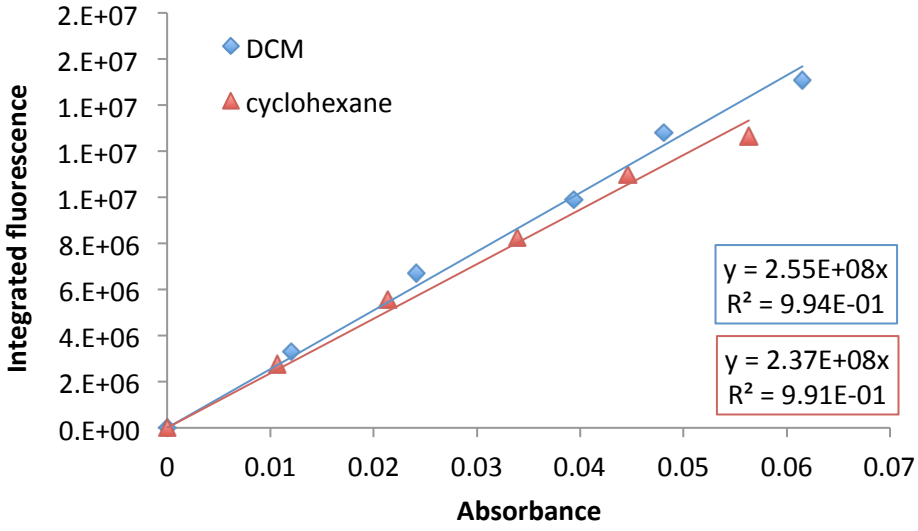

Quantum yield of 12-hexylisoindolo[2,1-*b*]isoquinoline-5,7-dione 372

The quantum yield of fluorescence was determined by comparison of the integrated area of the corrected emission spectrum of the imide **372** to that of 9,10-diphenylanthracene as a standard fluorescence reference. Absorbance and fluorescence data for 9,10-diphenylanthracene and the imide **372** were recorded using solutions in DCM prepared from serial dilutions from stock solutions (Standard: 5.19×10^{-6} M; imide: 4.33×10^{-6} M). The emission for 9,10-diphenylanthracene and 12-hexylisoindolo-[2,1-*b*]isoquinoline-5,7-dione **372** was integrated from 380-545 nm with excitation at 383 nm and 375 nm, respectively.

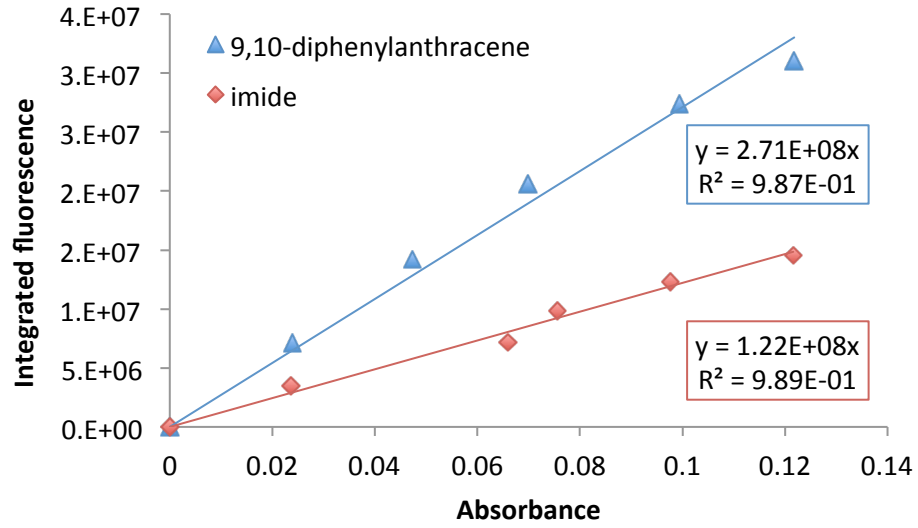

$$\phi_X = 0.97\left(\frac{1.22\times10^8}{2.71\times10^8}\right)$$

$$\phi_X = 0.44$$

6.12 Cyclic voltammetry

Electrochemical measurements were conducted using an Autolab PGSTAT20 voltammetric analyser under an argon atmosphere, solvated in pre-dried CH_3CN containing 0.10 M $[^nBu_4N]BF_4$ as supporting electrolyte. Voltammetric experiments utilised a Pt disk working electrode, a Pt rod auxiliary electrode and an Ag/AgCl reference electrode. All potentials quoted are referenced to an internal ferrocene/ferrocenium standard and were obtained at various scan rates (v) of 10-1000 mVs^{-1}. The ferrocene/ferrocenium couple under these conditions was observed at $+ 0.45 \leq E_{1/2} \leq 0.47$ V *vs* Ag/AgCl.

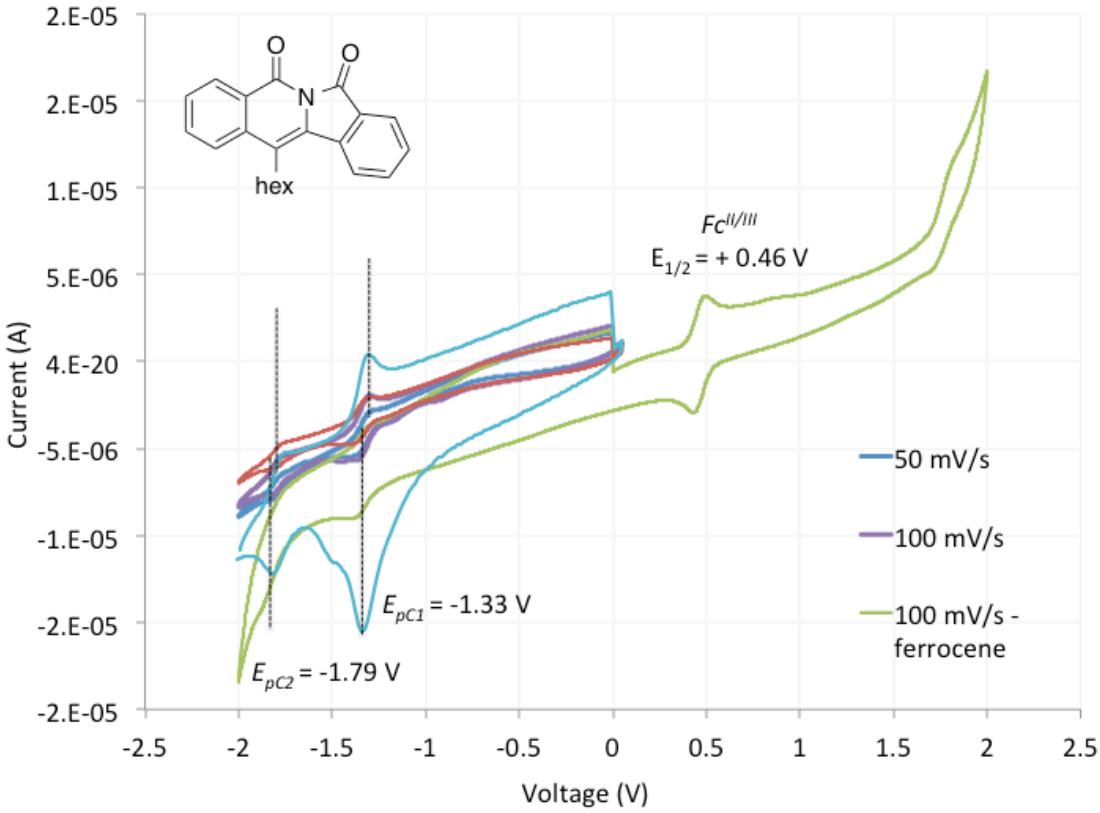

Cyclic voltammogram of ***372*** *(1.0 mM) in non-aqueous media ($CH_3CN/[^nBu_4N]BF_4$ 0.10 M), T = 298 K, [Fc] = 1.0 mM.*

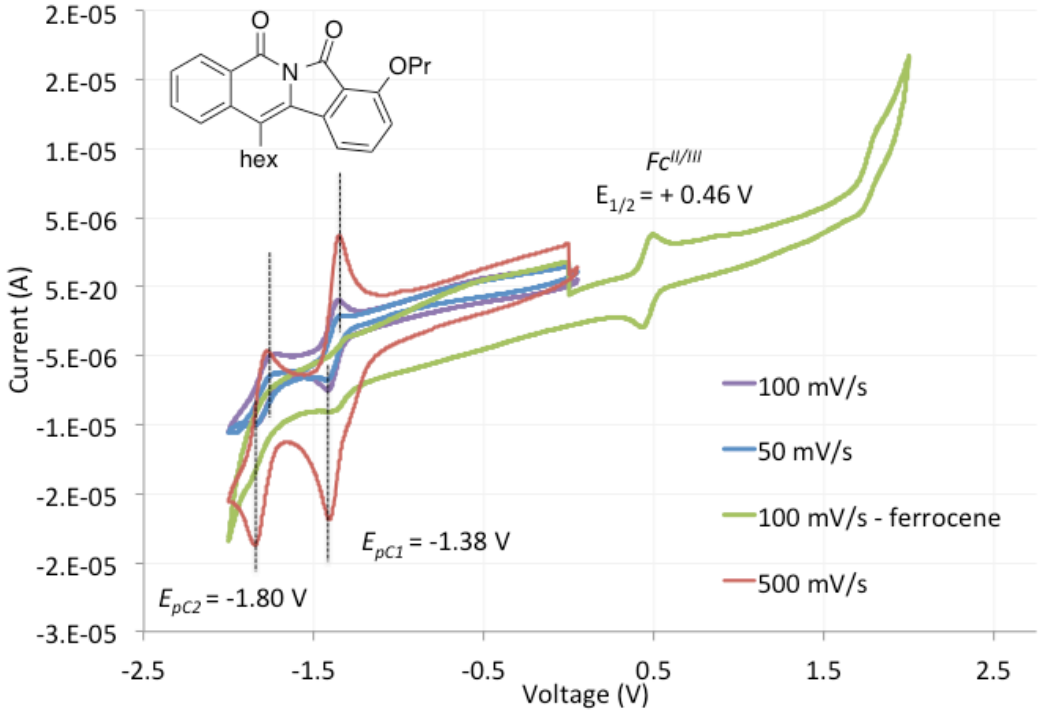

*Cyclic voltammogram of **387** (1.0 mM) in non-aqueous media ($CH_3CN/[^nBu_4N]BF_4$ 0.10 M), T = 298 K, [Fc] = 1.0 mM.*

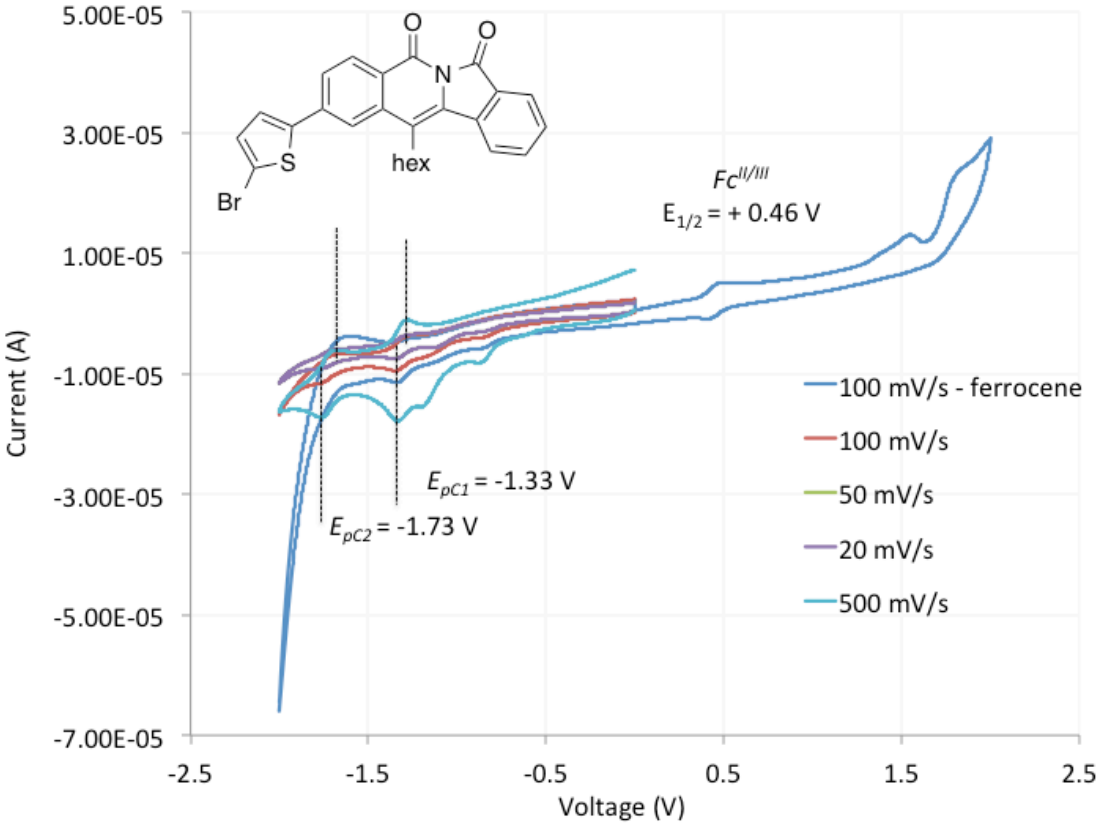

*Cyclic voltammogram of **423** (1.0 mM) in non-aqueous media ($CH_3CN/[^nBu_4N]BF_4$ 0.10 M), T = 298 K, [Fc] = 1.0 mM.*

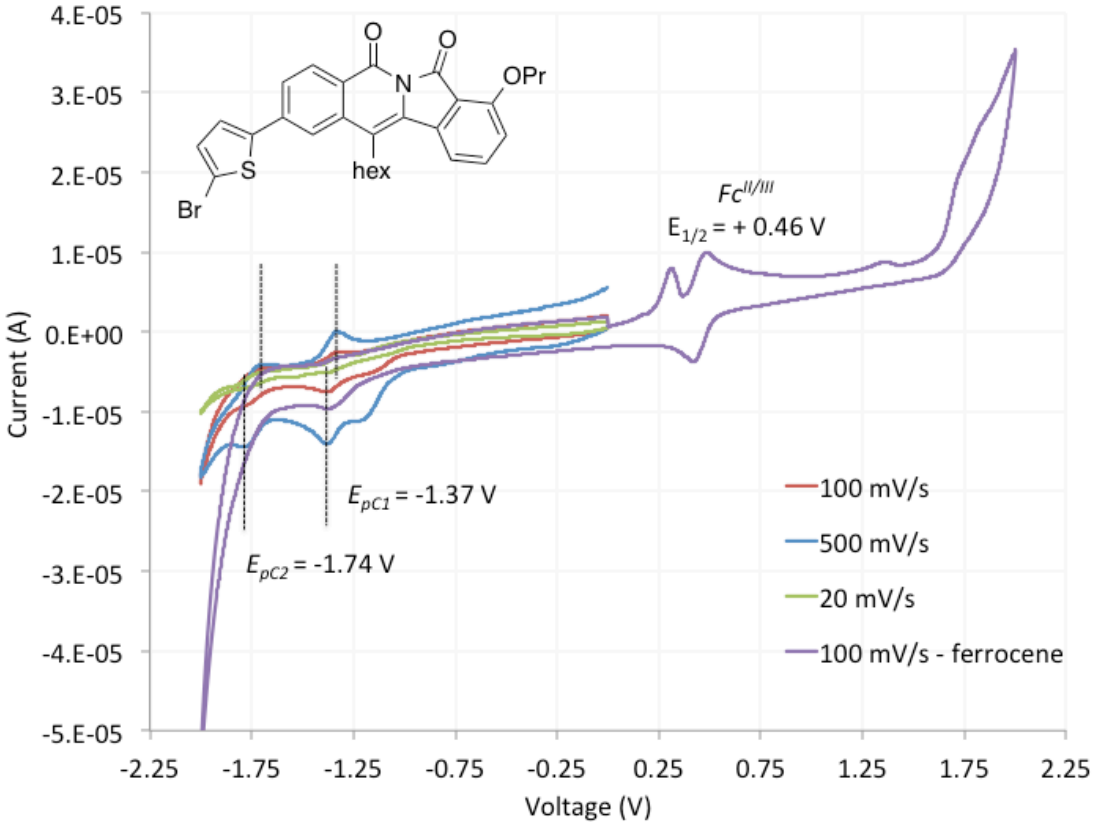

*Cyclic voltammogram of **424** (1.0 mM) in non-aqueous media ($CH_3CN/[^nBu_4N]BF_4$ 0.10 M), T = 298 K, [Fc] = 1.0 mM.*

References

1 N. Miyaura and A. Suzuki, *J. Chem. Soc. Chem. Commun.*, 1979, 866–867.

2 N. Miyaura, K. Yamada and A. Suzuki, *Tetrahedron Lett.*, 1979, **20**, 3437–3440.

3 A. O. King, N. Okukado and E. Negishi, *J. Chem. Soc. Chem. Commun.*, 1977, 683–684.

4 E. Negishi, A. O. King and N. Okukado, *J. Org. Chem.*, 1977, **42**, 1821–1823.

5 S. Baba and E. Negishi, *J. Am. Chem. Soc.*, 1976, **98**, 6729–6731.

6 R. F. Heck and J. P. Nolley, *J. Org. Chem.*, 1972, **37**, 2320–2322.

7 R. F. Heck, *J. Am. Chem. Soc.*, 1968, **90**, 5518–5526.

8 M. S. Kharasch, R. C. Seyler and F. R. Mayo, *J. Am. Chem. Soc.*, 1938, **60**, 882–884.

9 I. Moritani and Y. Fujiwara, *Tetrahedron Lett.*, 1967, **8**, 1119–1122.

10 Y. Fujiwara, I. Noritani, S. Danno, R. Asano and S. Teranishi, *J. Am. Chem. Soc.*, 1969, **91**, 7166–7169.

11 R. S. Shue, *J. Chem. Soc. D*, 1971, 1510–1511.

12 C. Jia, W. Lu, T. Kitamura and Y. Fujiwara, *Org. Lett.*, 1999, **1**, 2097–2100.

13 H. Grennberg, A. Gogoll and J. E. Baeckvall, *Organometallics*, 1993, **12**, 1790–1793.

14 D. Lapointe and K. Fagnou, *Chem. Lett.*, 2010, **39**, 1118–1126.

15 F. W. Patureau and F. Glorius, *J. Am. Chem. Soc.*, 2010, **132**, 9982–9983.

16 M. D. K. Boele, G. P. F. van Strijdonck, A. H. M. de Vries, P. C. J. Kamer, J. G. de Vries and P. W. N. M. van Leeuwen, *J. Am. Chem. Soc.*, 2002, **124**, 1586–1587.

17 T. Yamada, A. Sakakura, S. Sakaguchi, Y. Obora and Y. Ishii, *New J. Chem.*, 2008, **32**, 738–742.

18 H. Horino and N. Inoue, *J. Org. Chem.*, 1981, **46**, 4416–4422.

19 F. W. Patureau, J. Wencel-Delord and F. Glorius, *Aldrichimica Acta*, 2012, **45**, 31–41.

20 F. W. Patureau, T. Besset and F. Glorius, *Angew. Chem. Int. Ed.*, 2011, **50**, 1064–1067.

21 T. K. Hyster and T. Rovis, *J. Am. Chem. Soc.*, 2010, **132**, 10565–10569.

22 D. R. Stuart, M. Bertrand-Laperle, K. M. N. Burgess and K. Fagnou, *J. Am. Chem. Soc.*, 2008, **130**, 16474–16475.

23 S. Rakshit, F. W. Patureau and F. Glorius, *J. Am. Chem. Soc.*, 2010, **132**, 9585–9587.

24 N. Guimond and K. Fagnou, *J. Am. Chem. Soc.*, 2009, **131**, 12050–12051.

25 T. Fukutani, N. Umeda, K. Hirano, T. Satoh and M. Miura, *Chem. Commun.*, 2009, 5141–5143.

26 X. Wei, M. Zhao, Z. Du and X. Li, *Org. Lett.*, 2011, **13**, 4636–4639.

27 G. Song, F. Wang and X. Li, *Chem. Soc. Rev.*, 2012, **41**, 3651–3678.

28 J. Wencel-Delord, T. Dröge, F. Liu and F. Glorius, *Chem. Soc. Rev.*, 2011, **40**, 4740–4761.

29 M. Zhang, Y. Zhang, X. Jie, H. Zhao, G. Li and W. Su, *Org. Chem. Front.*, 2014, **1**, 843–895.

30 D. A. Colby, A. S. Tsai, R. G. Bergman and J. A. Ellman, *Acc. Chem. Res.*, 2012, **45**, 814–825.

31 D. A. Colby, R. G. Bergman and J. A. Ellman, *Chem. Rev.*, 2010, **110**, 624–655.

32 N. Kuhl, M. N. Hopkinson, J. Wencel-Delord and F. Glorius, *Angew. Chem. Int. Ed.*, 2012, **51**, 10236–10254.

33 J. Wu, X. Cui, L. Chen, G. Jiang and Y. Wu, *J. Am. Chem. Soc.*, 2009, **131**, 13888–13889.

34 N. Guimond, S. I. Gorelsky and K. Fagnou, *J. Am. Chem. Soc.*, 2011, **133**, 6449–6457.

35 N. Guimond, C. Gouliaras and K. Fagnou, *J. Am. Chem. Soc.*, 2010, **132**, 6908–6909.

36 S. Rakshit, C. Grohmann, T. Besset and F. Glorius, *J. Am. Chem. Soc.*, 2011, **133**, 2350–2353.

37 L. Xu, Q. Zhu, G. Huang, B. Cheng and Y. Xia, *J. Org. Chem.*, 2012, **77**, 3017–3024.

38 L. Li, W. W. Brennessel and W. D. Jones, *Organometallics*, 2009, **28**, 3492–3500.

39 R. K. Chinnagolla, S. Pimparkar and M. Jeganmohan, *Org. Lett.*, **14**, 3032–3035.

40 K. Parthasarathy, M. Jeganmohan and C.-H. Cheng, *Org. Lett.*, 2007, **10**, 325–328.

41 L. Ackermann and S. Fenner, *Org. Lett.*, **13**, 6548–6551.

42 B. Ye and N. Cramer, *Science*, 2012, **338**, 504–506.

43 T. K. Hyster, L. Knörr, T. R. Ward and T. Rovis, *Science*, 2012, **338**, 500–503.

44 B. Ye, P. A. Donets and N. Cramer, *Angew. Chem. Int. Ed.*, 2014, **53**, 507–511.

45 C. M. Thomas and T. R. Ward, *Chem. Soc. Rev.*, 2005, **34**, 337–346.

46 M. Zhao, H.-B. Wang, L.-N. Ji and Z.-W. Mao, *Chem. Soc. Rev.*, 2013, **42**, 8360–8375.

47 R. K. Friedman and T. Rovis, *J. Am. Chem. Soc.*, 2009, **131**, 10775–10782.

48 T. K. Hyster, D. M. Dalton and T. Rovis, *Chem. Sci.*, 2015, Advance Article DOI: 10.1039/C4SC02590C.

49 T. K. Hyster and T. Rovis, *Chem. Commun.*, 2011, 11846–11848.

50 H. Wang and F. Glorius, *Angew. Chem. Int. Ed.*, 2012, **51**, 7318–7322.

51 G. Song, X. Gong and X. Li, *J. Org. Chem.*, 2011, **76**, 7583–7589.

52 J. R. Huckins, E. A. Bercot, O. R. Thiel, T.-L. Hwang and M. M. Bio, *J. Am. Chem. Soc.*, 2013, **135**, 14492–14495.

53 J. P. Michael, *Nat. Prod. Rep.*, 2008, **25**, 139–165.

54 J. P. Michael, *Nat. Prod. Rep.*, 2007, **24**, 191–222.

55 R. Zeng, S. Wu, C. Fu and S. Ma, *J. Am. Chem. Soc.*, 2013, **135**, 18284–18287.

56 E. M. Woerly, J. Roy and M. D. Burke, *Nat. Chem.*, 2014, **6**, 484–491.

57 M. Presset, D. Oehlrich, F. Rombouts and G. A. Molander, *Org. Lett.*, 2013, **15**, 1528–1531.

58 S. Ide, B. Şener, H. Temizer and S. Könükol, *Cryst. Res. Technol.*, 1996, **31**, 617–624.

59 T. K. Hyster, K. E. Ruhl and T. Rovis, *J. Am. Chem. Soc.*, 2013, **135**, 5364–5367.

60 Z. Shi, C. Grohmann and F. Glorius, *Angew. Chem. Int. Ed.*, 2013, **52**, 5393–5397.

61 S. Cui, Y. Zhang, D. Wang and Q. Wu, *Chem. Sci.*, 2013, **4**, 3912–3916.

62 T. Hyster and T. Rovis, *Synlett*, 2013, **24**, 1842–1844.

63 D.-G. Yu, F. de Azambuja, T. Gensch, C. G. Daniliuc and F. Glorius, *Angew. Chem. Int. Ed.*, 2014, **53**, 9650–9654.

64 P. C. Too, Y.-F. Wang and S. Chiba, *Org. Lett.*, 2010, **12**, 5688–5691.

65 G. Liu, Y. Shen, Z. Zhou and X. Lu, *Angew. Chem. Int. Ed.*, 2013, **52**, 6033–6037.

66 Y. Shen, G. Liu, Z. Zhou and X. Lu, *Org. Lett.*, 2013, **15**, 3366–3369.

67 X. Huang, J. Huang, C. Du, X. Zhang, F. Song and J. You, *Angew. Chem. Int. Ed.*, 2013, **52**, 12970–12974.

68 C. Wang and Y. Huang, *Org. Lett.*, 2013, **15**, 5294–5297.

69 B. Liu, C. Song, C. Sun, S. Zhou and J. Zhu, *J. Am. Chem. Soc.*, 2013, **135**, 16625–16631.

70 D. Zhao, Z. Shi and F. Glorius, *Angew. Chem. Int. Ed.*, 2013, **52**, 12426–12429.

71 S.-C. Chuang, P. Gandeepan and C.-H. Cheng, *Org. Lett.*, 2013, **15**, 5750–5753.

72 C. Grohmann, H. Wang and F. Glorius, *Org. Lett.*, 2013, **15**, 3014–3017.

73 J. Y. Kim, S. H. Park, J. Ryu, S. H. Cho, S. H. Kim and S. Chang, *J. Am. Chem. Soc.*, 2012, **134**, 9110–9113.

74 T. L. Lemke and D. A. Williams, *Foye's Principles of Medicinal Chemistry, 5th Edition*, Lippincott Williams and Wilkins, USA, 2002.

75 G. R. Pettit, Q. Zhang, V. Pinilla, D. L. Herald, D. L. Doubek and J. A. Duke, *J. Nat. Prod.*, 2004, **67**, 983–985.

76 I. T. Harrison, B. Lewis, P. Nelson, W. Rooks, A. Roszkowski, A. Tomolonis and J. H. Fried, *J. Med. Chem.*, 1970, **13**, 203–205.

77 P. Dubé, N. F. F. Nathel, M. Vetelino, M. Couturier, C. L. Aboussafy, S. Pichette, M. L. Jorgensen and M. Hardink, *Org. Lett.*, 2009, **11**, 5622–5625.

78 H. L. Yale, *Chem. Rev.*, 1943, **33**, 209–256.

79 L. Bauer and O. Exner, *Angew. Chem. Int. Ed.*, 1974, **13**, 376–384.

80 L. Jašíková, E. Hanikýřová, A. Škríba, J. Jašík and J. Roithová, *J. Org. Chem.*, 2012, **77**, 2829–2836.

81 A. Vannini, C. Volpari, G. Filocamo, E. C. Casavola, M. Brunetti, D. Renzoni, P. Chakravarty, C. Paolini, R. De Francesco, P. Gallinari, C. Steinkühler and S. Di Marco, *Proc. Natl. Acad. Sci. U. S. A.*, 2004, **101**, 15064–15069.

82 D. P. Dowling, S. L. Gantt, S. G. Gattis, C. A. Fierke and D. W. Christianson, *Biochemistry*, 2008, **47**, 13554–13563.

83 L. Ducháčková and J. Roithová, *Chemistry*, 2009, **15**, 13399–13405.

84 J. Ephraim, *Ber. Dtsch. Chem. Ges.*, 1891, **24**, 2820–2827.

85 J. Dusemund, *Arch. Pharm. (Weinheim)*, 1977, **310**, 846–850.

86 V. Scartoni, R. Fiaschi, S. Catalano, I. Morelli and A. Marsili, *J. Chem. Soc., Perkin Trans. 1*, 1979, **1**, 1547–1551.

87 S. Wawzonek, J. K. Stowell and R. E. Karll, *J. Org. Chem.*, 1966, **31**, 1004–1006.

88 J. Dusemund and E. Kröger, *Arch. Pharm. (Weinheim)*, 1984, **317**, 2–9.

89 J. Willwacher, S. Rakshit and F. Glorius, *Org. Biomol. Chem.*, 2011, **9**, 4736–4740.

90 J. C. Godfrey, *J. Org. Chem.*, 1959, **24**, 581.

91 T. Matsui, T. Sugiura, H. Nakai, S. Iguchi, S. Shigeoka, H. Takada, Y. Odagaki, Y. Nagao and Y. Ushio, *J. Med. Chem.*, 1992, **35**, 3307–3319.

92 C. Xie, N. C. Veitch, P. J. Houghton and M. S. J. Simmonds, *Phytochemistry*, 2004, **65**, 3041–3047.

93 P. T. Sunderland, E. C. Y. Woon, A. Dhami, A. B. Bergin, M. F. Mahon, P. J. Wood, L. A. Jones, S. R. Tully, M. D. Lloyd, A. S. Thompson, H. Javaid, N. M. B. Martin and M. D. Threadgill, *J. Med. Chem.*, 2011, **54**, 2049–2059.

94 S. A. Busby, N. Kumar, D. S. Kuruvilla, M. A. Istrate, J. J. Conkright, Y. Wang, T. M. Kamenecka, M. D. Cameron, W. R. Roush, T. P. Burris and P. R. Griffin, *ACS Chem. Biol.*, 2011, **6**, 618–627.

95 Y.-L. Yang, F.-R. Chang and Y.-C. Wu, *Tetrahedron Lett.*, 2003, **44**, 319–322.

96 C. Xie, N. C. Veitch, P. J. Houghton and M. S. J. Simmonds, *Phytochemistry*, 2004, **65**, 3041–3047.

97 M. T. Rudd, J. A. McCauley, J. W. Butcher, J. J. Romano, C. J. McIntyre, K. T. Nguyen, K. F. Gilbert, K. J. Bush, M. K. Holloway, J. Swestock, B.-L. Wan, S. S. Carroll, J. M. DiMuzio, D. J. Graham, S. W. Ludmerer, M. W. Stahlhut, C. M. Fandozzi, N. Trainor, D. B. Olsen, J. P. Vacca and N. J. Liverton, *ACS Med. Chem. Lett.*, 2011, **2**, 207–212.

98 N. Briet, M. H. Brookes, R. J. Davenport, F. C. Galvin, P. J. Gilbert, S. R. Mack and V. Sabin, *Tetrahedron*, 2002, **58**, 5761–5766.

99 K. Hirao, R. Suchiya, Y. Yanu and H. Tsue, *Heterocycles*, 1996, **42**, 415–422.

100 T.-H. Chuang and P.-L. Wu, *J. Chin. Chem. Soc.*, 2006, **53**, 413–420.

101 S. W. Li, M. G. Nair, D. M. Edwards, R. L. Kisliuk, Y. Gaumont, I. K. Dev, D. S. Duch, J. Humphreys, G. K. Smith and R. Ferone, *J. Med. Chem.*, 1991, **34**, 2746–2754.

102 A. S. Kiselyov, *Tetrahedron Lett.*, 1995, **36**, 493–496.

103 M. Alvarez and J. A. Joule, *Sci. Synth.*, 2005, **15**, 839–906.

104 P. Thansandote, D. G. Hulcoop, M. Langer and M. Lautens, *J. Org. Chem.*, 2009, **74**, 1673–1678.

105 C.-C. Liu, K. Parthasarathy and C.-H. Cheng, *Org. Lett.*, 2010, **12**, 3518–3521.

106 T. Miura, K. Hiraga, T. Toyoshima, M. Yamauchi and M. Murakami, *Chem. Lett.*, 2012, **41**, 798–800.

107 F. Wang, H. Liu, H. Fu, Y. Jiang and Y. Zhao, *Org. Lett.*, 2009, **11**, 2469–2472.

108 G. Song, D. Chen, C.-L. Pan, R. H. Crabtree and X. Li, *J. Org. Chem.*, 2010, **75**, 7487–7490.

109 S. Mochida, N. Umeda, K. Hirano, T. Satoh and M. Miura, *Chem. Lett.*, 2010, **39**, 744–746.

110 N. J. Webb, S. P. Marsden and S. A. Raw, *Org. Lett.*, 2014, **16**, 4718–4721.

111 A. Vilsmeier and A. Haack, *Ber. Dtsch. Chem. Ges.*, 1927, **60**, 119–122.

112 V. D. Geffken, *Chemiker-Zeitung.*, 1986, **10**, 377–379.

113 W. B. Renfrow and C. R. Hauser, *J. Am. Chem. Soc.*, 1937, **59**, 2308–2314.

114 R. D. Bright and C. R. Hauser, *J. Am. Chem. Soc.*, 1939, **61**, 618–629.

115 A. D. Selmeczy, W. D. Jones, M. C. Partridge and R. N. Perutz, *Organometallics*, 1994, **13**, 522–532.

116 K. J. T. Carr, D. L. Davies, S. A. Macgregor, K. Singh and B. Villa-Marcos, *Chem. Sci.*, 2014, **5**, 2340–2346.

117 A. Berkessel, M. L. Sebastian-Ibarz and T. N. Müller, *Angew. Chem. Int. Ed.*, 2006, **45**, 6567–6570.

118 M. Jean, J. Renault, P. Uriac, M. Capet and P. van de Weghe, *Org. Lett.*, 2007, **9**, 3623–3625.

119 K. A. B. Austin, E. Herdtweck and T. Bach, *Angew. Chem. Int. Ed.*, 2011, **50**, 8416–8419.

120 *WHO Wkly. Epidemiol. Rec.*, 1999, **74**, 425–427.

121 Z. J. Song, D. M. Tellers, P. G. Dormer, D. Zewge, J. M. Janey, A. Nolting, D. Steinhuebel, S. Oliver, P. N. Devine and D. M. Tschaen, *Org. Process Res. Dev.*, 2014, **18**, 423–430.

122 P. M. Scola, L. Sun, A. X. Wang, J. Chen, N. Sin, B. L. Venables, S. Sit, Y. Chen, A. Cocuzza, D. M. Bilder, S. V. D. Andrea, B. Zheng, P. Hewawasam, Y. Tu, J. Friborg, P. Falk, D. Hernandez, S. Levine, C. Chen, F. Yu, A. K. Shea, G. Zhai, D. Barry, J. O. Knipe, Y. Han, R. Schartman, M. Donoso, K. Mosure, M. W. Sinz, T. Zvyaga, A. C. Good, R. Rajamani, K. Kish, H. E. Klei, Q. Gao, L. Mueller, R. J. Colonno, D. M. Grasela, S. P. Adams, J. Loy, P. C. Levesque, H. Sun, H. Shi, L. Sun, W. Warner, D. Li, J. Zhu, N. A. Meanwell and F. Mcphee, *J. Med. Chem.*, 2014, **57**, 1730–1752.

123 S. A. Springfield, W. W. Doubleday, F. Buono, M. A. Couturier, Y. Lear, D. Favreau, K. Levesque, P. S. Manchand, M. Frieser, A. J. Cocuzza, H. Kim, S.-S. Lee, C. Kim, S. Yang and E. Choi, 2010, WO2010/027889.

124 L.-Q. Sun and P. M. Scola, 2012, WO2012/166459.

125 W. J. Bartley, S. Jobson, G. G. Harkreader, M. Kitson and F. Lemanski, 1993, US005185308A.

126 Y.-F. Han, D. Kumar, C. Sivadinarayana and D. W. Goodman, *J. Catal.*, 2004, **224**, 60–68.

127 A. M. Sladkov and G. S. Petrov, *Zhurnal Obs. Khimii.*, 1954, **24**, 450–454.

128 J. S. Clark and J. G. Kettle, *Tetrahedron*, 1999, **55**, 8231–8248.

129 O. Fujimura, G. C. Fu and R. H. Grubbs, *J. Org. Chem.*, 1994, **59**, 4029–4031.

130 J. D. Rainier, J. M. Cox and S. P. Allwein, *Tetrahedron Lett.*, 2001, **42**, 179–181.

131 A. Okada, T. Ohshima and M. Shibasaki, *Tetrahedron Lett.*, 2001, **42**, 8023–8027.

132 M. Arisawa, C. Theeraladanon, A. Nishida and M. Nakagawa, *Tetrahedron Lett.*, 2001, **42**, 8029–8033.

133 A. J. Giessert, L. Snyder, J. Markham and S. T. Diver, *Org. Lett.*, 2003, **5**, 1793–1796.

134 D. B. Dess and J. C. Martin, *J. Org. Chem.*, 1983, **48**, 4155–4156.

135 K. Omura and D. Swern, *Tetrahedron*, 1978, **34**, 1651–1660.

136 S. Hilf and A. F. M. Kilbinger, *Nat. Chem.*, 2009, **1**, 537–546.

137 P. E. Standen and M. C. Kimber, *Tetrahedron Lett.*, 2013, **54**, 4098–4101.

138 P. E. Standen, D. Dodia, M. R. J. Elsegood, S. J. Teat and M. C. Kimber, *Org. Biomol. Chem.*, 2012, **10**, 8669–8676.

139 N. A. Petasis and S.-P. Lu, *Tetrahedron Lett.*, 1995, **36**, 2393–2396.

140 W. Giersch and F. Naef, *Helv. Chim. Acta*, 2004, **87**, 1697–1703.

141 P. Heretsch, S. Rabe and A. Giannis, *Org. Lett.*, 2009, **11**, 5410–5412.

142 A. M. Fournier and J. Clayden, *Org. Lett.*, 2012, **14**, 142–145.

143 F. G. Kathawala, G. M. Coppola and H. F. Schuster, *The Chemistry of Heterocyclic Compounds, Part 3, Volume 38, 2nd Ed. Isoquinolines*, John Wiley & Sons, Inc., 2009.

144 M. D. Rozwadowska, *Heterocycles*, 1994, **39**, 903–931.

145 J. A. Joule and K. Mills, *Heterocyclic Chemistry, 4th Ed.*, Blackwell Science Ltd.: Cambridge MA, 2000.

146 M. Chrzanowska and M. D. Rozwadowska, *Chem. Rev.*, 2004, **104**, 3341–3370.

147 K. W. Bentley, *Nat. Prod. Rep.*, 2006, **23**, 444–463.

148 V. Andrushko and N. Andrushko, *Stereoselective Synthesis of Drugs and Natural Products*, John Wiley & Sons, Inc., 2013.

149 K. Bhadra and G. S. Kumar, *Med. Res. Rev.*, 2011, **31**, 821–862.

150 A. Bischler and B. Napieralski, *Ber. Dtsch. Chem. Ges.*, 1893, **26**, 1903–1908.

151 A. Pictet and T. Spengler, *Ber. Dtsch. Chem. Ges.*, 1911, **44**, 2030–2036.

152 A. Pictet and A. Gams, *Ber. Dtsch. Chem. Ges.*, 1909, **42**, 2943–2952.

153 C. Pomeranz, *Monatsh Chem.*, 1893, **14**, 116–119.

154 P. Fritsch, *Ber. Dtsch. Chem. Ges.*, 1893, **26**, 419–422.

155 S. Obika, H. Kono, Y. Yasui, R. Yanada and Y. Takemoto, *J. Org. Chem.*, 2007, **72**, 4462–4468.

156 B. W.-Q. Hui and S. Chiba, *Org. Lett.*, 2009, **11**, 729–732.

157 D. Yang, S. Burugupalli, D. Daniel and Y. Chen, *J. Org. Chem.*, 2012, **77**, 4466–4472.

158 D. Fischer, H. Tomeba, N. K. Pahadi, N. T. Patil, Z. Huo and Y. Yamamoto, *J. Am. Chem. Soc.*, 2008, **130**, 15720–15725.

159 Y.-N. Niu, Z.-Y. Yan, G.-L. Gao, H.-L. Wang, X.-Z. Shu, K.-G. Ji and Y.-M. Liang, *J. Org. Chem.*, 2009, **74**, 2893–2896.

160 K. Parthasarathy and C.-H. Cheng, *J. Org. Chem.*, 2009, **74**, 9359–9364.

161 D. Zheng, S. Li and J. Wu, *Org. Lett.*, 2012, **14**, 2655–2657.

162 K. R. Roesch and R. C. Larock, *J. Org. Chem.*, 2002, **67**, 86–94.

163 K. R. Roesch and R. C. Larock, *Org. Lett.*, 1999, **1**, 553–556.

164 C. D. Gilmore, K. M. Allan and B. M. Stoltz, *J. Am. Chem. Soc.*, 2008, **130**, 1558–1559.

165 Y.-Y. Yang, W.-G. Shou, Z.-B. Chen, D. Hong and Y.-G. Wang, *J. Org. Chem.*, 2008, **73**, 3928–3930.

166 S. Gupta, J. Han, Y. Kim, S. W. Lee, Y. H. Rhee and J. Park, *J. Org. Chem.*, 2014, **79**, 9094–9103.

167 P. C. Too, S. H. Chua, S. H. Wong and S. Chiba, *J. Org. Chem.*, 2011, **76**, 6159–6168.

168 Y.-F. Wang, K. K. Toh, J.-Y. Lee and S. Chiba, *Angew. Chem. Int. Ed.*, 2011, **50**, 5927–5931.

169 L. Zheng, J. Ju, Y. Bin and R. Hua, *J. Org. Chem.*, 2012, **77**, 5794–800.

170 B. Liu, F. Hu and B.-F. Shi, *Adv. Synth. Catal.*, 2014, **356**, 2688–2696.

171 J. Jayakumar, K. Parthasarathy and C.-H. Cheng, *Angew. Chem. Int. Ed.*, 2012, **51**, 197–200.

172 X.-Y. Xu, G.-W. Qin, R.-S. Xu and X.-Z. Zhu, *Tetrahedron*, 1998, **54**, 14179–14188.

173 Y. Wada, N. Nishida, N. Kurono, T. Ohkuma and K. Orito, *Eur. J. Org. Chem.*, 2007, 4320–4327.

174 T. Oishi, K. Yamaguchi and N. Mizuno, *Angew. Chem. Int. Ed.*, 2009, **48**, 6286–6288.

175 E. Choi, C. Lee, Y. Na and S. Chang, *Org. Lett.*, 2002, **4**, 2369–2371.

176 K. Tambara and G. D. Pantoş, *Org. Biomol. Chem.*, 2013, **11**, 2466–2472.

177 H. S. Kim, S. H. Kim and J. N. Kim, *Tetrahedron Lett.*, 2009, **50**, 1717–1719.

178 S. R. Neufeldt and M. S. Sanford, *Org. Lett.*, 2010, **12**, 532–535.

179 X.-Y. Ma, Y. He, T.-T. Lu and M. Lu, *Tetrahedron*, 2013, **69**, 2560–2564.

180 K. Ishihara, Y. Furuya and H. Yamamoto, *Angew. Chem. Int. Ed.*, 2002, **41**, 2983–2986.

181 K. Yamaguchi, H. Fujiwara, Y. Ogasawara, M. Kotani and N. Mizuno, *Angew. Chem. Int. Ed.*, 2007, **46**, 3922–3925.

182 R. M. Denton, J. An, P. Lindovska and W. Lewis, *Tetrahedron*, 2012, **68**, 2899–2905.

183 B. R. Cho, W. J. Jang, J. T. Je and R. A. Bartsch, *J. Org. Chem.*, 1993, **58**, 3901–3904.

184 J. L. Vennerstrom and D. L. Klayman, *J. Med. Chem.*, 1988, **31**, 1084–1087.

185 M. D. Watson, A. Fechtenkötter and K. Müllen, *Chem. Rev.*, 2001, **101**, 1267–1300.

186 J. E. Anthony, *Angew. Chem. Int. Ed.*, 2008, **47**, 452–483.

187 U. Mitschke and P. Bäuerle, *J. Mater. Chem.*, 2000, **10**, 1471–1507.

188 T. Oyamada, H. Sasabe, Y. Oku, N. Shimoji and C. Adachi, *Appl. Phys. Lett.*, 2006, **88**, 093514.

189 F. Cicoira and C. Santato, *Adv. Funct. Mater.*, 2007, **17**, 3421–3434.

190 D. Qin and Y. Tao, *J. Appl. Phys.*, 2005, **97**, 044505.

191 D. Qin and Y. Tao, *Appl. Phys. Lett.*, 2005, **86**, 113507.

192 Y. Sagara, T. Mutai, I. Yoshikawa and K. Araki, *J. Am. Chem. Soc.*, 2007, **129**, 1520–1521.

193 T. Oyamada, H. Uchiuzou, S. Akiyama, Y. Oku, N. Shimoji, K. Matsushige, H. Sasabe and C. Adachi, *J. Appl. Phys.*, 2005, **98**, 074506.

194 Y. Li, *Acc. Chem. Res.*, 2012, **45**, 723–733.

195 C.-G. Zhen, Z.-K. Chen, Q.-D. Liu, Y.-F. Dai, R. Y. C. Shin, S.-Y. Chang and J. Kieffer, *Adv. Mater.*, 2009, **21**, 2425–2429.

196 M.-C. Hung, J.-L. Liao, S.-A. Chen, S.-H. Chen and A.-C. Su, *J. Am. Chem. Soc.*, 2005, **127**, 14576–14577.

197 A. W. Grice, D. D. C. Bradley, M. T. Bernius, M. Inbasekaran, W. W. Wu and E. P. Woo, *Appl. Phys. Lett.*, 1998, **73**, 629.

198 K. L. Chan, M. J. McKiernan, C. R. Towns and A. B. Holmes, *J. Am. Chem. Soc.*, 2005, **127**, 7662–7663.

199 J. Liu, Q. G. Zhou, Y. X. Cheng, Y. H. Geng, L. X. Wang, D. G. Ma, X. B. Jing and F. S. Wang, *Adv. Mater.*, 2005, **17**, 2974–2978.

200 D. J. Stephens and V. J. Allan, *Science*, 2003, **300**, 82–86.

201 I. Johnson, *The Molecular Probes Handbook: A Guide to Fluorescent Probes and Labeling Technologies, 11th Edition*, Life Technologies Corporation, 2010.

202 J. Jayakumar, K. Parthasarathy, Y.-H. Chen, T.-H. Lee, S.-C. Chuang and C.-H. Cheng, *Angew. Chem. Int. Ed.*, 2014, **53**, 9889–9892.

203 N. Umeda, H. Tsurugi, T. Satoh and M. Miura, *Angew. Chem.*, 2008, **120**, 4083–4086.

204 X. Tan, B. Liu, X. Li, B. Li, S. Xu, H. Song and B. Wang, *J. Am. Chem. Soc.*, 2012, **134**, 16163–16166.

205 J.-R. Huang, L. Dong, B. Han, C. Peng and Y.-C. Chen, *Chem. Eur. J.*, 2012, **18**, 8896–8900.

206 G. Song, D. Chen, C.-L. Pan, R. H. Crabtree and X. Li, *J. Org. Chem.*, 2010, **75**, 7487–7490.

207 F. Wang, G. Song, Z. Du and X. Li, *J. Org. Chem.*, 2011, **76**, 2926–2932.

208 J. Wang, G. Zhang, Z. Liu, X. Gu, Y. Yan, C. Zhang, Z. Xu, Y. Zhao, H. Fu and D. Zhang, *Tetrahedron*, 2013, **69**, 2687–2692.

209 T. Yao and R. C. Larock, *J. Org. Chem.*, 2003, **68**, 5936–5942.

210 W. J. Coates, B. Connolly, D. Dhanak, S. T. Flynn and A. Worby, *J. Med. Chem.*, 1993, **36**, 1387–1392.

211 B. Bennetau, J. Mortier, J. Moyroud and J.-L. Guesnet, *J. Chem. Soc. Perkin Trans. 1*, 1995, 1265–1271.

212 T.-H. Nguyen, A.-S. Castanet and J. Mortier, *Org. Lett.*, 2006, **8**, 765–768.

213 A. Lewis, I. Stefanuti, S. A. Swain, S. A. Smith and R. J. K. Taylor, *Org. Biomol. Chem.*, 2003, **1**, 104–116.

214 T.-H. Nguyen, N. T. T. Chau, A.-S. Castanet, K. P. P. Nguyen and J. Mortier, *J. Org. Chem.*, 2007, **72**, 3419–3429.

215 M. Uchiyama, H. Ozawa, K. Takuma, Y. Matsumoto, M. Yonehara, K. Hiroya and T. Sakamoto, *Org. Lett.*, 2006, **8**, 5517–5520.

216 B. Valeur, *Molecular Fluorescence: Principles and Applications, Wiley-VCH Verlag GmbH, Weinheim*, 2001.

217 T. E. Barder, S. D. Walker, J. R. Martinelli and S. L. Buchwald, *J. Am. Chem. Soc.*, 2005, **127**, 4685–4696.

218 C. Schotten, *Ber. Dtsch. Chem. Ges.*, 1886, **17**, 2544–2547.

219 E. Baumann, *Ber. Dtsch. Chem. Ges.*, 1886, **19**, 3218–3222.

220 L.-M. Chen, Z. Xu, Z. Hong and Y. Yang, *J. Mater. Chem.*, 2010, **20**, 2575–2598.

221 G. Li, V. Shrotriya, J. Huang, Y. Yao, T. Moriarty, K. Emery and Y. Yang, *Nat. Mater.*, 2005, **4**, 864–868.

222 C. Li and H. Wonneberger, *Adv. Mater.*, 2012, **24**, 613–636.

223 B. S. Ong, Y. Wu, Y. Li, P. Liu and H. Pan, *Chem. Eur. J.*, 2008, **14**, 4766–4778.

224 E. Amir, K. Sivanandan, J. E. Cochran, J. J. Cowart, S.-Y. Ku, J. H. Seo, M. L. Chabinyc and C. J. Hawker, *J. Polym. Sci. Part A Polym. Chem.*, 2011, **49**, 1933–1941.

225 J. R. Holst, E. Stöckel, D. J. Adams and A. I. Cooper, *Macromolecules*, 2010, **43**, 8531–8538.

226 M. Horie, L. A. Majewski, M. J. Fearn, C.-Y. Yu, Y. Luo, A. Song, B. R. Saunders and M. L. Turner, *J. Mater. Chem.*, 2010, **20**, 4347–4355.

227 Y. Liu, X. Chen, J. Qin, G. Yu and Y. Liu, *Polymer (Guildf).*, 2010, **51**, 3730–3735.

228 T. Yokozawa, H. Kohno, Y. Ohta and A. Yokoyama, *Macromolecules*, 2010, **43**, 7095–7100.

229 R. M. Walczak, R. N. Brookins, A. M. Savage, E. M. van der Aa and J. R. Reynolds, *Macromolecules*, 2009, **42**, 1445–1447.

230 M. Mushrush, A. Facchetti, M. Lefenfeld, H. E. Katz and T. J. Marks, *J. Am. Chem. Soc.*, 2003, **125**, 9414–9423.

231 D. J. Schipper and K. Fagnou, *Chem. Mater.*, 2011, **23**, 1594–1600.

232 G. Gauglitz and T. Vo-Dinh, *Handbook of Spectroscopy*, WILEY-VCH Verlag GmbH & Co. KGaA, Weinheim, 2003.

233 S. R. Meech and D. Phillips, *J. Photochem.*, 1983, **23**, 193–217.

234 A. Gilbert and J. Baggott, *Essentials of Molecular Photochemistry, 1st edition*, Blackwell Scientific Publications, 1991.

235 W. E. Piers and J. F. Araneda, 2014, US2014/0206870.

236 H. Wynberg, H. Van Driel, R. M. Kellogg and J. Buter, *J. Am. Chem. Soc.*, 1967, **89**, 3487–3494.

237 I. B. Berlman, *Handbook of Fluorescence Spectra of Aromatic Molecules*, Academic Press, N.Y., 1971.

238 G. A. Mabbott, *J. Chem. Educ.*, 1983, **60**, 697–701.

239 P. T. Kissinger and W. R. Heineman, *J. Chem. Educ.*, 1983, **60**, 702–706.

240 S. Dey, A. Efimov and H. Lemmetyinen, *European J. Org. Chem.*, 2012, **2012**, 2367–2374.

241 D. W. Domaille, E. L. Que and C. J. Chang, *Nat. Chem. Biol.*, 2008, **4**, 168–175.

242 E. J. Corey and F. J. Hannon, *Tetrahedron Lett.*, 1987, **28**, 5237–5240.

243 R. Petrus and P. Sobota, *Dalton Trans.*, 2013, **42**, 13838–13844.

244 Z. Zhang, Y. Yu and L. S. Liebeskind, *Org. Lett.*, 2008, **10**, 3005–3008.

245 K. D. Hesp, R. G. Bergman and J. A. Ellman, *J. Am. Chem. Soc.*, 2011, **133**, 11430–11433.

246 G. A. Gfesser, D. Whittern, M. A. Cowart and R. Faghih, *Heterocycles*, 2008, **75**, 1199–1203.

247 S. Shkavrov, S. Popov, D. Kravchenko and M. Krasavin, *Synth. Commun.*, 2005, **35**, 725–730.

248 M. Farnier, S. Soth and P. Fournari, *Can. J. Chem.*, 1976, **54**, 1066–1073.

249 J. N. Chatterjea, R. P. Sahai, B. B. Swaroopa, C. Bhakta, H. C. Jha and F. Zilliken, *Chem. Ber.*, 1980, **113**, 3656–3661.

250 C. Rivalle and E. Bisagni, *J. Heterocycl. Chem.*, 1980, **17**, 245–248.

251 F. A. Davis and N. Theddu, *J. Org. Chem.*, 2010, **75**, 3814–3820.

252 T. R. Hoye, M. E. Danielson, A. E. May and H. Zhao, *Angew. Chem. Int. Ed.*, 2008, **47**, 9743–9746.

253 H. Imagawa, H. Saijo, T. Kurisaki, H. Yamamoto, M. Kubo, Y. Fukuyama and M. Nishizawa, *Org. Lett.*, 2009, **11**, 1253–1255.

254 M. Siemer, R. Fröhlich and D. Hoppe, *Synthesis (Stuttg).*, 2008, **14**, 2264–2270.

255 R. J. Abraham and M. Reid, *J. Chem. Soc. Perkin Trans. 2*, 2002, 1081–1091.

256 R. S. Ramón, J. Bosson, S. Díez-González, N. Marion and S. P. Nolan, *J. Org. Chem.*, 2010, **75**, 1197–1202.

257 N. Jain, A. Kumar and S. M. S. Chauhan, *Tetrahedron Lett.*, 2005, **46**, 2599–2602.

258 P. Y. Yeung, C. M. So, C. P. Lau and F. Y. Kwong, *Org. Lett.*, 2011, **13**, 648–651.

259 C. Grohmann, H. Wang and F. Glorius, *Org. Lett.*, 2012, **14**, 656–659.

260 C. Miura, M. Kiyama, S. Iwano, K. Ito, R. Obata, T. Hirano, S. Maki and H. Niwa, *Tetrahedron*, 2013, **69**, 9726–9734.

Appendix

A1. NMR Studies

Appendix 1.1

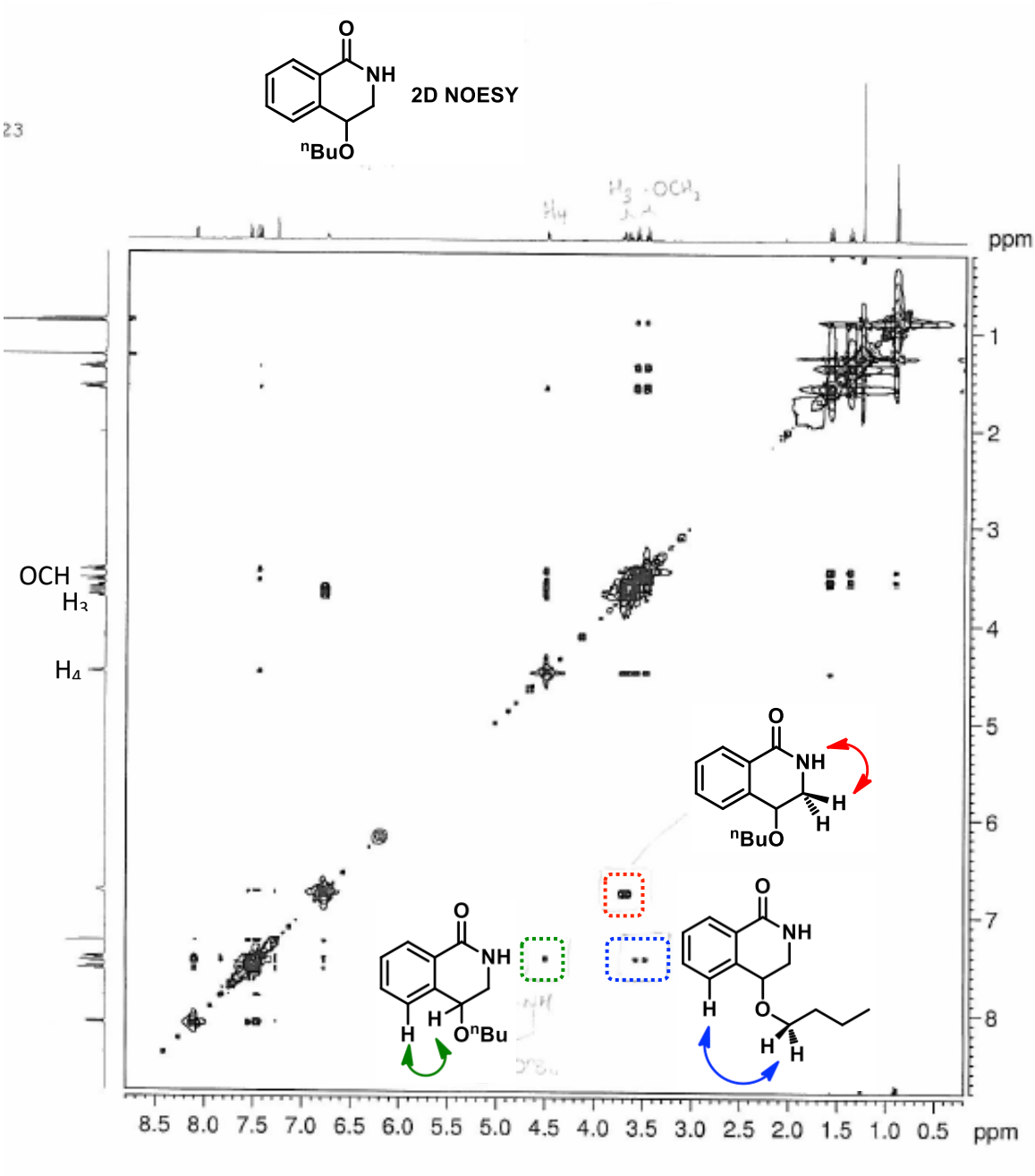

*500 MHz ^{1}H NMR NOESY of **130** in deuterated $CDCl_3$.*

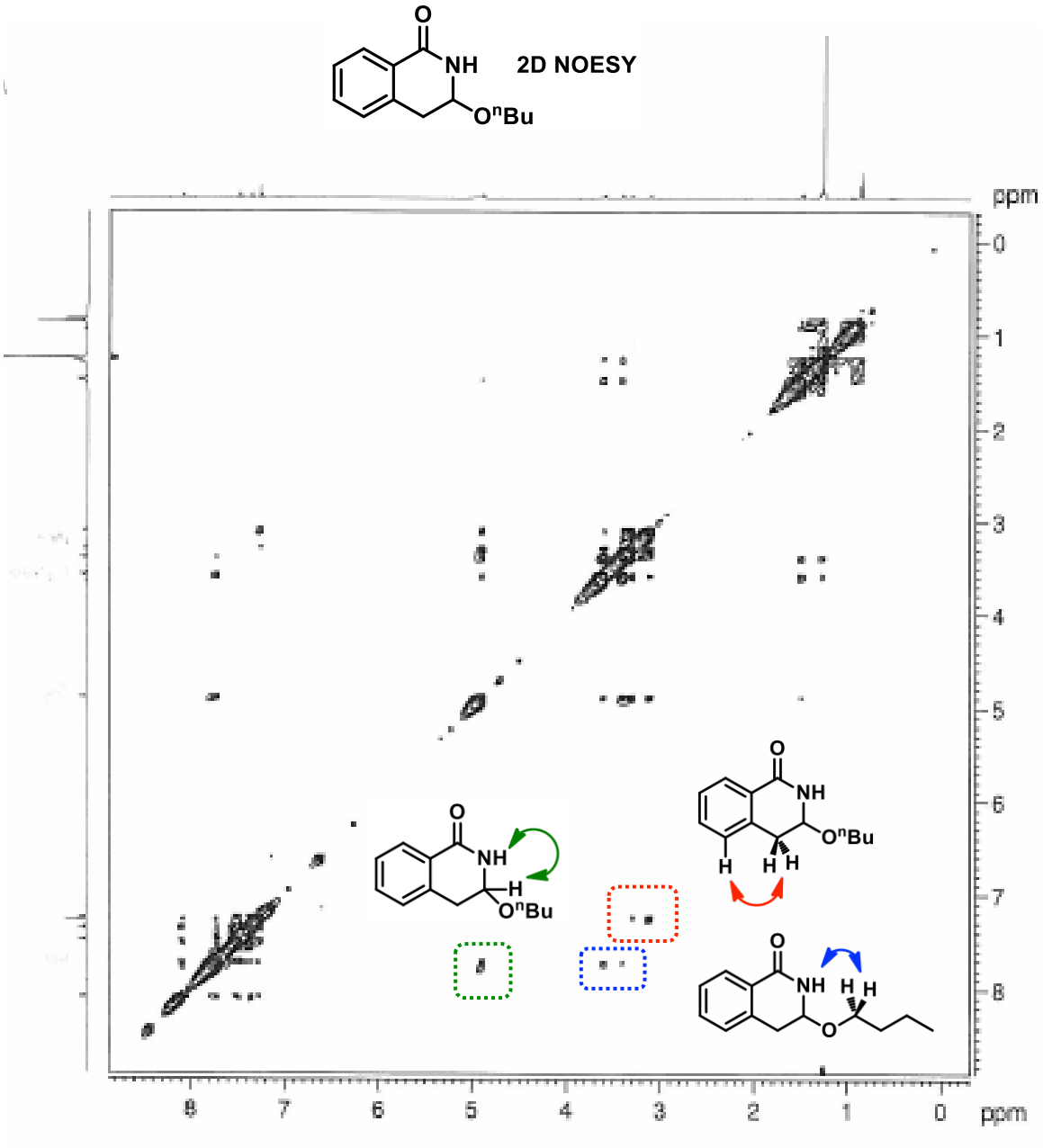

*500 MHz ^{1}H NMR NOESY of **131** in deuterated $CDCl_3$.*

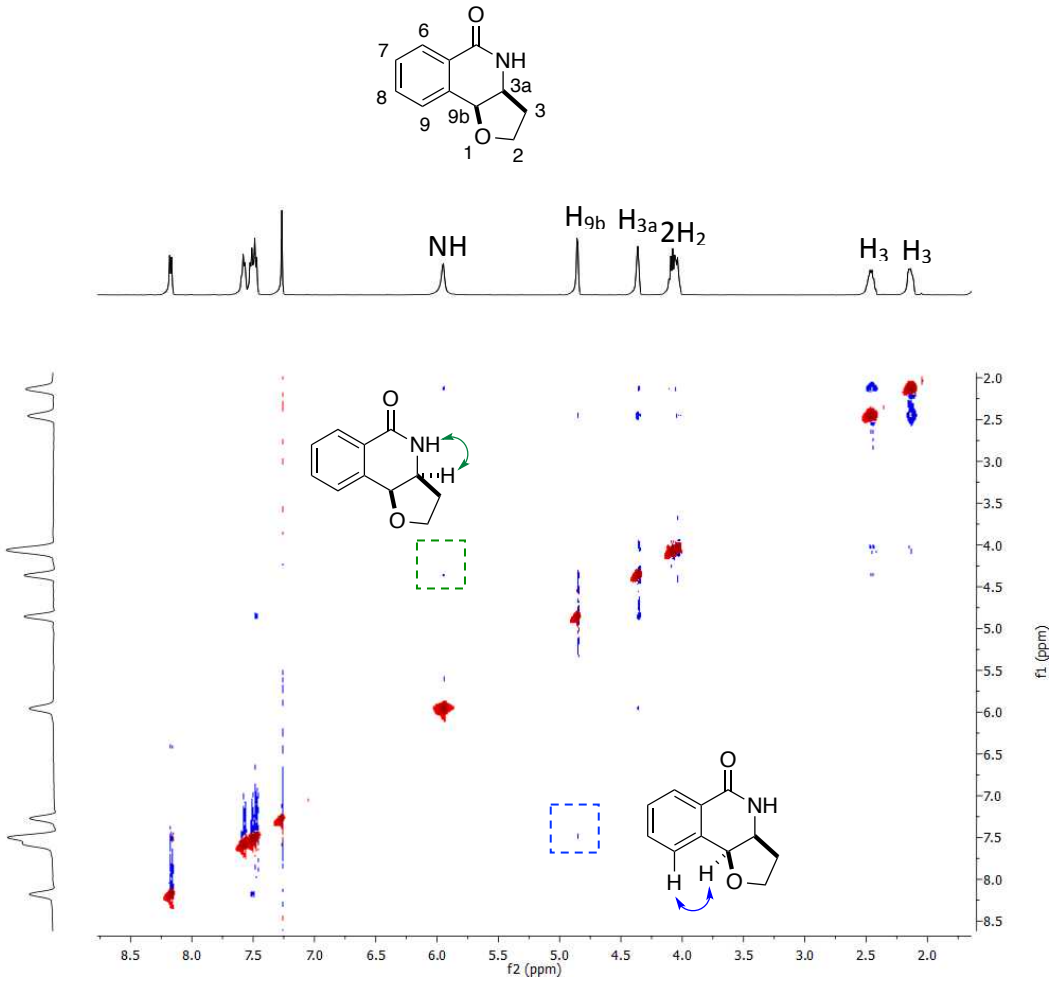

*500 MHz ^{1}H NMR NOESY of **123** in deuterated $CDCl_3$.*

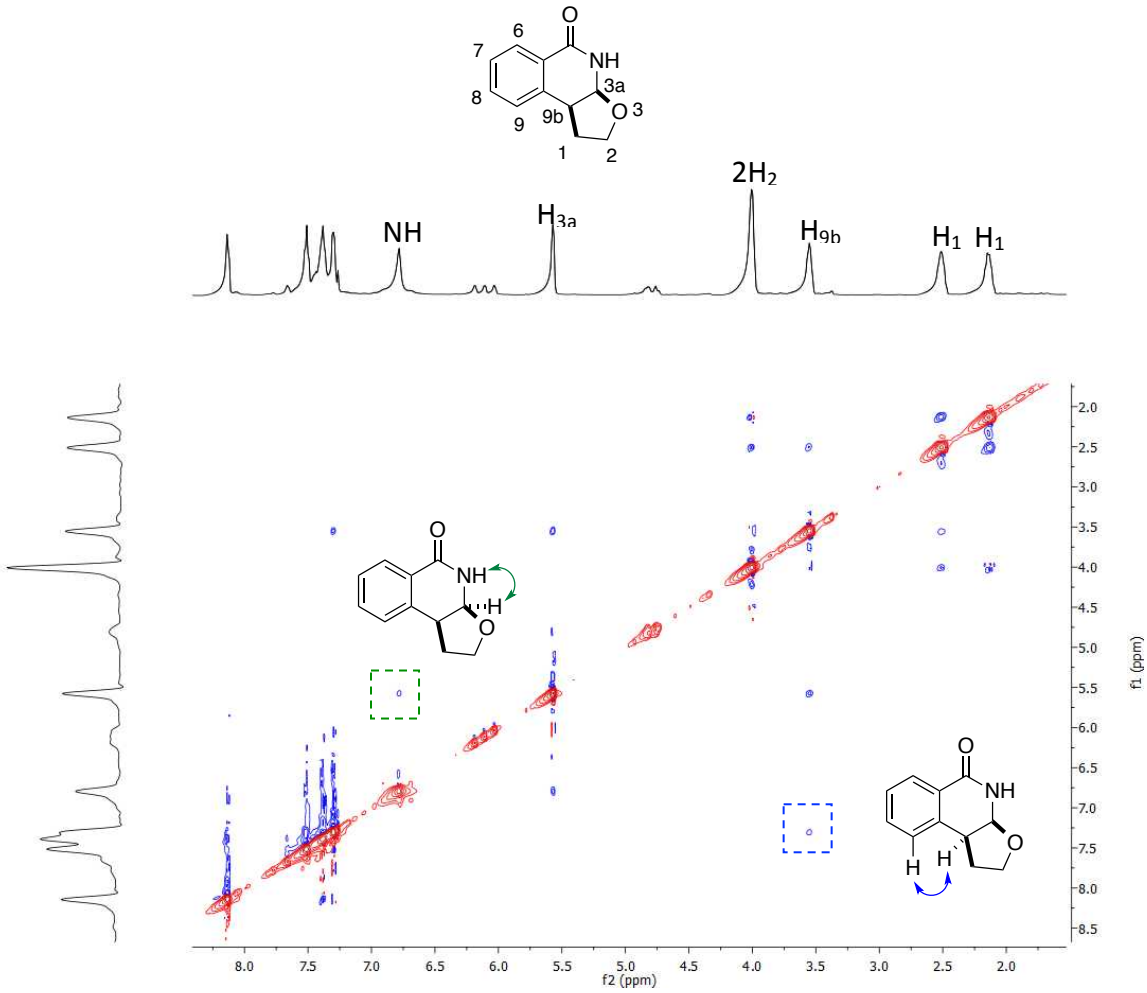

*500 MHz ^{1}H NMR NOESY of **122** in deuterated $CDCl_3$.*

A2. X-ray crystal structures

Appendix 2.1

Compound 123

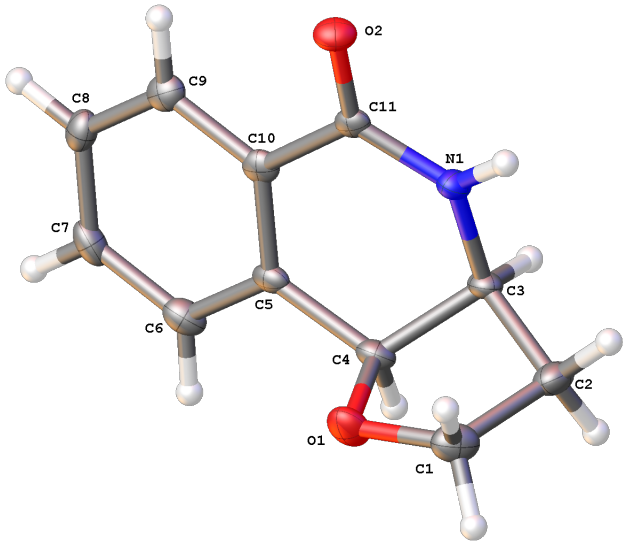

Crystal data and structure refinement.

Identification code	Compound **123**	
Formula	$C_{11}H_{11}NO_2$	
Formula weight	189.21	
Size	0.5284 x 0.2603 x 0.1529 mm	
Crystal morphology	Colourless block	
Temperature	100.00(10) K	
Wavelength	0.7107 Å [Mo -K_a]	
Crystal system	Orthorhombic	
Space group	$Pna2_1$	
Unit cell dimensions	a = 7.2675(4) Å	a = 90°
	b = 12.9319(6) Å	b = 90°
	c = 9.6419(5) Å	g = 90°
Volume	906.18(8) Å^3	
Z	4	
Density (calculated)	1.387 Mg/m^3	
Absorption coefficient	0.096 mm^{-1}	
F(000)	400	
Data collection range	3.15 ≤ q ≤ 26.35°	
Index ranges	-7 ≤ h ≤9, -16 ≤ k ≤ 15, -12 ≤ l ≤ 10	

Reflections collected	3228
Independent reflections	1560 [R(int) = 0.0632]
Observed reflections	1315 [I >2s(I)]
Absorption correction	multi-scan
Max. and min. transmission	1 and 0.46407
Refinement method	Full
Data / restraints / parameters	1560 / 1 / 127
Goodness of fit	1.07
Final R indices [I >2s(I)]	R_1 = 0.0529, wR_2 = 0.1146
R indices (all data)	R_1 = 0.0661, wR_2 = 0.1307
Largest diff. peak and hole	0.235 and -0.27e.Å^{-3}
Absolute structure parameter	-1(2)

Appendix 2.2

Compound 267

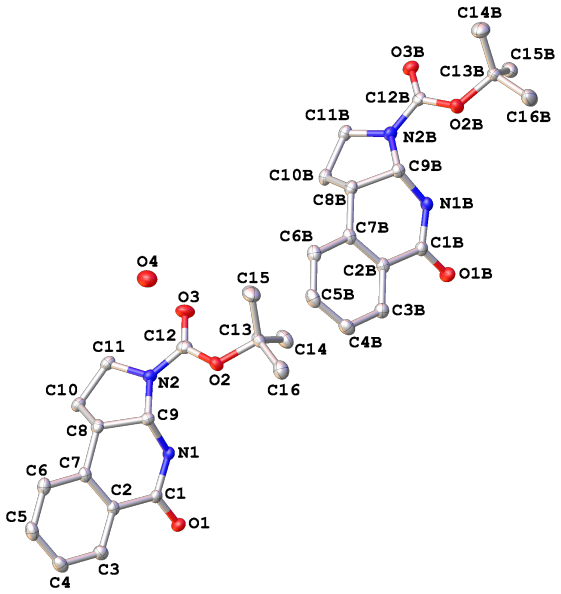

Identification code	Compound **267**	
Formula	$C_{32}H_{41}N_4O_{6.50}$	
Formula weight	585.69	
Size	0.3092 x 0.2031 x 0.1568 mm	
Crystal morphology	Colourless block	
Temperature	100.00(10) K	
Wavelength	0.7107 Å [Mo -K_a]	
Crystal system	Monoclinic	
Space group	$P2_1/n$	
Unit cell dimensions	a = 10.1273(5) Å	a = 90°
	b = 12.4095(5) Å	b = 91.343(4)°
	c = 24.1328(9) Å	g = 90°
Volume	3032.0(2) Å^3	
Z	4	
Density (calculated)	1.283 Mg/m^3	
Absorption coefficient	0.09 mm^{-1}	
F(000)	1252	
Data collection range	1.85 ≤ q ≤ 29.88°	
Index ranges	-10 ≤ h ≤14, -16 ≤ k ≤ 14, -32 ≤ l ≤ 32	
Reflections collected	18513	

Independent reflections	7396 [R(int) = 0.034]
Observed reflections	6032 [I >2s(I)]
Absorption correction	multi-scan
Max. and min. transmission	1 and 0.87787
Refinement method	Full
Data / restraints / parameters	7396 / 0 / 551
Goodness of fit	1.016
Final R indices [I >2s(I)]	R_1 = 0.0461, wR_2 = 0.1063
R indices (all data)	R_1 = 0.0594, wR_2 = 0.1149
Largest diff. peak and hole	0.295 and -0.275e.Å^{-3}

Appendix 2.3

Compound 372

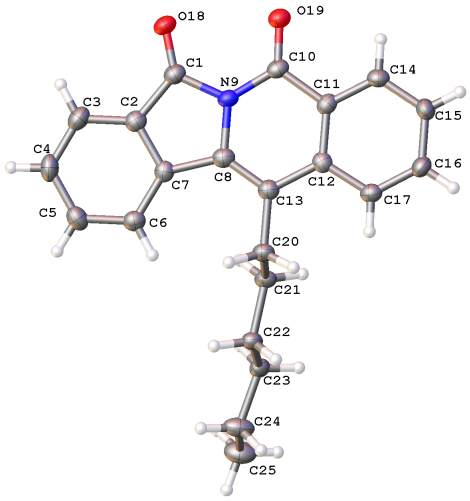

Identification code	Compound **372**	
Formula	$C_{22}H_{21}NO_2$	
Formula weight	331.4	
Size	0.16 x 0.07 x 0.03 mm	
Crystal morphology	Colourless plate	
Temperature	99.9(5) K	
Wavelength	1.54184 Å [Cu-K_α]	
Crystal system	Monoclinic	
Space group	*P*2(1)/*c*	
Unit cell dimensions	*a* = 4.90124(14) Å	α = 90°
	b = 21.2010(5) Å	β = 93.043(2)°
	c = 16.3443(4) Å	γ = 90°
Volume	1695.96(8) Å^3	
Z	4	
Density (calculated)	1.298 Mg/m^3	
Absorption coefficient	0.654 mm^{-1}	
F(000)	704	
Data collection range	3.42 ≤ θ ≤ 66.6°	
Index ranges	-5 ≤ *h* ≤5, -25 ≤ *k* ≤ 25, -19 ≤ *l* ≤ 19	
Reflections collected	11979	
Independent reflections	2989 [*R*(int) = 0.0348]	
Observed reflections	2590 [*I* >2σ(*I*)]	
Absorption correction	analytical	

Max. and min. transmission	0.981 and 0.947
Refinement method	Full
Data / restraints / parameters	2989 / 0 / 227
Goodness of fit	1.045
Final *R* indices [$I > 2\sigma(I)$]	$R_1 = 0.0417$, $wR_2 = 0.0994$
R indices (all data)	$R_1 = 0.0497$, $wR_2 = 0.1044$
Largest diff. peak and hole	0.439 and -0.197e.Å^{-3}

Appendix 2.4

Compound 440

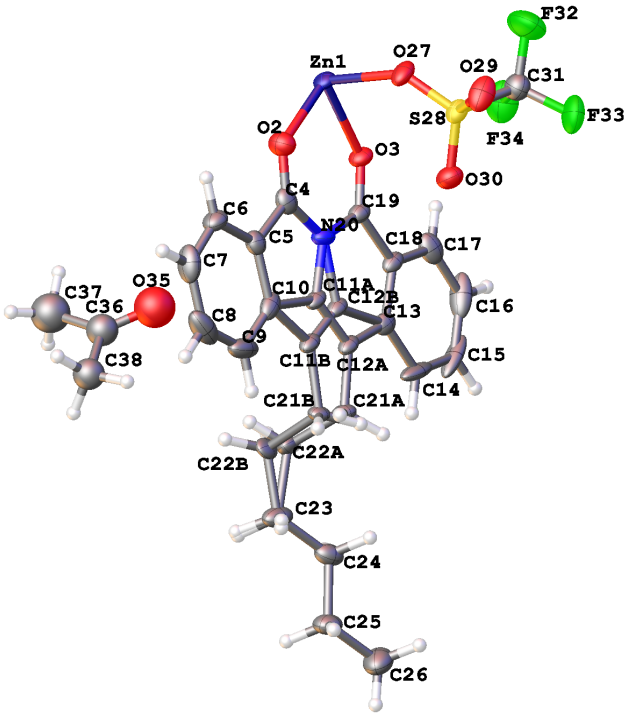

Identification code	Compound **440**	
Formula	$C_{49}H_{48}F_6N_2O_{11}S_2Zn$	
Formula weight	1084.38	
Size	0.16 x 0.1 x 0.07 mm	
Crystal morphology	Yellow Fragments	
Temperature	120.01(13) K	
Wavelength	0.71073 Å [Mo-K_α]	
Crystal system	Triclinic	
Space group	$P\bar{1}$	
Unit cell dimensions	a = 6.6901(4) Å	α = 78.707(4)°
	b = 12.7594(7) Å	β = 84.883(4)°
	c = 14.8752(6) Å	γ = 75.297(5)°
Volume	1203.36(10) Å^3	
Z	1	
Density (calculated)	1.496 Mg/m^3	
Absorption coefficient	0.683 mm^{-1}	
F(000)	560	
Data collection range	3.15 ≤ θ ≤ 26.37°	

Index ranges	$-8 \leq h \leq 8$, $-15 \leq k \leq 15$, $-18 \leq l \leq 17$
Reflections collected	13053
Independent reflections	4910 [R(int) = 0.0451]
Observed reflections	3789 [$I > 2\sigma(I)$]
Absorption correction	analytical
Max. and min. transmission	0.965 and 0.94
Refinement method	Full
Data / restraints / parameters	4910 / 1 / 341
Goodness of fit	1.052
Final R indices [$I > 2\sigma(I)$]	$R_1 = 0.0479$, $wR_2 = 0.0976$
R indices (all data)	$R_1 = 0.0713$, $wR_2 = 0.1077$
Largest diff. peak and hole	0.724 and -0.462e.Å^{-3}